The Cloning and Functional Characterisation of Murine Phosphatidylinositol 3-kinase gamma

By

Sumone Chakravarti B.Sc (Hons)

Department of Molecular Biosciences

Discipline of Microbiology & Immunology

Adelaide University, Australia

A thesis submitted to Adelaide University in fulfilment of the requirements for the degree of Doctor of Philosophy

August 2001

To the woman who has given so much of her life to others,

and through her most difficult times continued to support my dreams.

Her generosity, and her strength will be an inspiration for a lifetime.

To my Mother

ABSTRACT

The family of PI3-kinases are an important group of lipid kinases involved in cellular signalling. All members of the family are responsible for phosphorylating the 3-hydroxyl groups of inositol phospholipids. Their structural conformation and substrate specificity separates members into three distinct classes, these being the Class I, II and III PI3-kinases. The Class I family is the best-characterised of all the members and can be further subdivided into 2 groups, the Class IA and Class IB PI3-kinases. The Class IA PI3-kinases are activated through the downstream recruitment of protein tyrosine kinases. In contrast, the Class IB PI3-kinases are dependent on heterotrimeric G proteins for their activation. This study focuses on the only known member of the Class IB PI3-kinases, PI3kγ.

The chemokine gene superfamily is a group of chemotactic cytokines originally identified on their ability to directly recruit distinct and overlapping subsets of leukocytes, and therefore has a critical role in the maintenance, activation and regulation of the immune system. To date, all chemokine receptors are G protein-coupled receptors. Activation of chemotactic receptors results in a transient increase in the level of 3-phosphorylated phospholipids, products of the PI3kinase family. More recently, this increase has been attributed to PI3kγ.

The present study addresses the role of PI3kγ in lymphocyte migration *in vitro* and *in vivo*, in response to chemotactic factors. A novel isoform of PI3kγ, MmPI3kγ1111, was isolated from a murine macrophage cDNA library. Comparison of the sequence of MmPI3kγ1111 with the previously cloned human and porcine

orthologues demonstrated above 90% identity. Consistent with the human and porcine PI3kγs, MmPI3kγ1111 possesses all four conserved domains common to the Class IB subfamily. Uniquely, MmPI3kγ1111 contained an additional 11 amino acids in the catalytic domain. During the latter stages of this study a murine orthologue of PI3kγ, MmPI3kγ1100, was independently cloned. MmPI3kγ1100 did not contain the additional 11 amino acids found in MmPI3kγ1111.

MmPI3kγ1111 was over-expressed in HEK 293 cells and examined for lipid and protein kinase activity. Consistent with MmPI3kγ1100, MmPI3kγ1111 produced PI 3 P *in vitro*, hence lipid kinase activity. MmPI3kγ1111 also demonstrated autophosphorylation, a characteristic common to all known Class IB PI3-kinases. Furthermore, phosphorylation of MmPI3kγ1111 downregulated the ability of MmPI3kγ1111 to act as a lipid kinase.

Mutation of the lysine residue (position 833) critical for the activation of all Class I PI3-kinases resulted in a loss of both the lipid and protein kinase activities of MmPI3kγ1111. The catalytically-inactive form of MmPI3kγ1111 was stably transfected into a B lymphocyte cell line (B300.19) expressing the CCR6 chemokine receptor. B300.19-huCCR6 cells expressing the catalytically-inactive form of MmPI3kγ1111, MmPI3kγKR, demonstrated a marked decrease in the ability to migrate towards huMIP-3α, the ligand for huCCR6, in an *in vitro* chemotaxis assay. Subcutaneous air pouches were used to examine the role of MmPI3kγ1111 in *in vivo* B lymphocyte migration. However, in contrast to the *in vitro* data obtained, the *in vivo* model did not provide clear support for a role for MmPI3kγ1111 in lymphocyte

migration. The biological significance of these data, and future research directions are addressed in this thesis.

DECLARATION OF ORIGINALITY

This thesis contains no material which has been accepted for any other degree or diploma in any university or other tertiary institution and, to the best of my knowledge, contains no material previously published or written by another person, except where due reference has been made.

I give consent to my thesis, when in the University Library, being available for loan and photocopying.

Sumone Chakravarti, B.Sc. (Hons)

ACKNOWLEDGEMENTS

I would firstly like to thank my supervisor, Dr Shaun McColl, for enabling me to undertake this PhD within his laboratory. I am deeply grateful for your guidance and support over the many years. Thank you also for the amount of time you have dedicated to the editing of this thesis. I would also like to thank my colleagues in Canada, Professor Paul Naccache, and Sylvain Levasseur for their assistance in various aspects of this work. A special thank you must also go to Professor Paul Nacacche's family for their hospitality and kindness during my visit to his laboratory. I would also like to thank Professor Graham Mayrhofer for his encouragement in every facet of my PhD.

A big thank you to all members of the McColl lab. Over the years I have enjoyed our many comic moments, daily conversations and outings. A special thank you must go to Dr Nicholas Coates for being primarily responsible for the development of my strong foundations in molecular biology, and also for our useful discussions of my ideas in their infancy. Rachel Kohler for being a wonderful lab friend, her patience during my introduction to animal work also deserves a special mention. Thanks to Lisa Ebert for her expertise in flow cytometry. A final thank you to everyone for their help and laughs during the last few months – Fsssssssss to you all!

The work carried out in this thesis has involved the expertise of many people over the years. I would like to thank Assoc. Professor Sharad Kumar and Professor Angel Lopez and their respective laboratories for the generous donation of reagents and expertise in mammalian over-expression systems and PI3-kinase assays. I also acknowledge Professor Reinhard Wetzker for the kind donation of the monoclonal PI3kγ antibody, and Dr Matthias Wymann for insightful discussions about PI3kγ, and his generous donation of constructs.

During the mid stages of my studies I was fortunate to join Dr Grant Booker and his laboratory in their weekly "signalling" meetings. It was a pleasure to present and discuss my work with a group of enthusiastic peers whose interests were common to

mine. I would like to thank Dr Grant Booker for providing an alternative perspective for the study of signalling systems and for creating an environment where the opinion and ideas of students were encouraged and so openly received.

To "my girls", Rebecca Lunn, Miriam Boxer and Jo Willmott, thank you for your love and support over the years – it's finally over! Thank you also to Kathryn Hudson, Rachel Kohler and Stephen Rodda for their friendship and care, especially during the past months.

Thank you to the Harvey family for their continuous interest and encouragement towards achieving my goals.

To my greatest critics and, my greatest supporters - my family. To Mum, Dad, and Dolone, thank you for teaching me, by example, how to fight the difficult times with strength and determination. I am grateful for all your support in every aspect of my 25 years.

To my best friend, Kieran Harvey, it is difficult to express how grateful I am to have your support. Thank you for your fresh ideas and your willingness to help with every facet of my work. I have enjoyed all our scientific discussions and am most thankful for your continuous encouragement, support, laughter and unconditional love. Most importantly, thank you for teaching me how to "smell the flowers along the way".

LIST OF ABBREVIATIONS

µCI	microcurie
µg	microgram
µF	microfaraday
µL	microlitre
µmol	micromole
%	percentage
Amp	ampicillin
APC	antigen presenting cell
APS	ammonium persulfate
ATP	adenosine 5'-triphosphate
bp	base pair
BSA	Bovine serum albumin
°C	degrees Celcius
CIP	calf intestinal phosphatase
cm	centimetre
DC	dendritic cell
DMEM	Dulbecco's Modified Eagle Medium
DNA	deoxyribonucleic acid
dNTP	deoxyribonucleotide triphosphate
DTT	dithiothreitol
ECL	enhanced chemiluminescence
EDTA	ethylene-diamine-tetra-acetic acid

ELISA	enzyme-linked immunosorbent assay
FCS	foetal calf serum
hr	hour
IPTG	isopropylthio-b-D-galactoside
i.v.	intravenous
kD	kilodalton
M	molar
mA	milliampere
mAb	monoclonal antibody
mg	milligram
min	minute
mL	millilitre
mM	millimolar
mRNA	messenger ribonucleic acid
MW	molecular weight
ng	nanogram
nm	nanometre
NP-40	nonidet-P40-detergent
NRS	normal rabbit serum
OD	optical density
ORF	open reading frame
PAGE	polyacrylamide gel electrophoresis
PBS	phosphate buffered saline
PCR	polymerase chain reaction

RT	room temperature
RNA	ribonucleic acid
rpm	revolutions per minute
SDS	sodium dodecyl sulfate
sec	seconds
X-gal	5-bromo-4-chloro-3-indolyl-b-D-galactopyranoside

ABSTRACT

DECLARATION OF ORIGINALITY

ACKNOWLEDGMENTS

LIST OF ABBREVIATIONS

CHAPTER 1: INTRODUCTION

CHAPTER 5: THE ROLE OF MmPI3kγ1111 IN LYMPHOCYTE MIGRATION *IN VITRO* AND *IN VIVO*

CHAPTER 7: BIBLIOGRAPHY

AMENDMENT

- Abstract, second paragraph, line 6 should read: .....PI3-kinase.....
- Page 4, second paragraph, line 9 should read: ...were possibly considered to be...
- Page 5, second paragraph, line 2 should read: ...SH3 domain-containing proteins (Figure 1.3).
- Page 7, second paragraph, line 9 should read: ...for the inter-SH2 antibody...
- Page 9, end of first paragraph,
- Page 20, second paragraph, line 5 should read: ...PI3-kinase...
- Page 23, first line should read: ...proliferation...;second paragraph, line 11 should read: ...hypothesised...
- Page 26, second paragraph, last reference should read: ...(Toker & Cantley, 1997).
- Page 31, last line should read: (Figure 1.7, Gale & McColl, 1999).
- Page 32, first paragraph, last line should read: (Figure 1.7).
- Page 39, first line should read: ...to bind to...
- Page 42, first line should read: ...later...
- Figure legend 1.7 should read: ...delayed type hypersensitivity (DTH)...
- Page 50, second paragraph, line 3 should read: ... (3,700 rpm)...
- Page 56, line 3 should read: ...standard saline citrate (SSC; 3M NaCl, 0.3M Na Citrate and 1mM EDTA)....
- Page 57, line 1 should read: ...SSPE (150mM NaCl, 10mM $NaPO_4$ and 1mM EDTA)...; and second paragraph should read:...DEPC-treated water (diethylene pyrocarbonate; 0.05% in MQ water incubated for 12-16 hours at 37°C and heat inactivated prior to use)..
- Page 62, sentences 2 to 5 should read: .....cDNA library.
- Page 68, line 4 should read: ...14 000rpm...
- Page 94, first line should read: .....phosphatidylinositol (PI).
- Page 95, last paragraph, line 2 should read: ...activity, MmPI3kγ1111 and MmPI3kγ1100 were...
- Page 100, line 6/7 should read: ...[reviewed in (Vanhaesebroeck *et al.*, 2001)].
- Figure legend 4.7 should read: C. ...5μL..
- Page 111, last two lines and page 112, first line should read: ...μg
- Page 122, second paragraph, line 8 should read: ...activities...
- Figure legend 5.8, line 2 should read: Forty eight...
- Figure legend 5.10, line 4 should read: ...and chemotaxis...
- Page 131, second paragraph, line 1 should read: In view of this...
- Page 143, reference Cook et al., should read: ...Lipp M., and Lira S. A.
- Page 157, reference Traynor-Kaplan should read: Traynor-Kaplan A., Thompson B. L. ...
- Page 158, reference Vanhaesebroeck should read: ...Parker P., and Waterfield M. D.

Chapter One

Introduction

1.1 History of the Phosphatidylinositol 3-kinase family

In the early 1980s, an observation that a transient accumulation of highly polar inositol lipids occurred following cellular stimulation, established inositol phospholipids as potential signalling mediators. It was subsequently discovered that the activation of phospholipase C resulted in the hydrolysis of cellular phosphatidylinositol 4,5 bisphosphate (PI 4,5 P_2) to produce two major second messengers, inositol (1,4,5) trisphosphate (IP_3), which was found to mobilise Ca^{2+} from intracellular stores, and diacylglycerol (DAG), which was an activator of Protein Kinase C (Berridge & Irvine, 1989). At around the same time, Whitmann and co-workers demonstrated that a PI-kinase activity was associated with oncoproteins from the polyoma middle T antigen, $pp60^{v\text{-}src}$ and $pp68^{v\text{-}ras}$ complex (Whitman *et al.*, 1985). This activity was found to directly phosphorylate the D3 hydroxyl group of the inositol head group, a novel type of phosphorylation (Whitman *et al.*, 1988). Hence these inositides were subsequently referred to as D3 phosphoinositides, and the enzymes responsible for this hydrolysis were referred to as phosphatidylinositol 3-kinases (PI3-kinases).

1.1.2 The Phosphatidylinositol 3-kinase Family

Immunoprecipitates of activated PDGF receptors and middle T-$pp60^{c\text{-}src}$ complexes that illicit PI3-kinase activity consistently showed the presence of an 81-85kD protein (Whitman *et al.*, 1988). The subsequent isolation and cloning of the PI3-kinase revealed the existence of an 85kD protein that was found to be ultimately associated with another protein of 110kD. Initially, 2 closely related isoforms of the

85kD protein were isolated, cloned and termed p85α and p85β (Escobedo *et al.*, 1991b; Otsu *et al.*, 1991; Skolnik *et al.*, 1991). Structurally, both p85 isoforms were able to bind proteins containing phospho-tyrosine sequences consistent with observations in assays of purified p85, however, neither appeared to possess intrinsic PI3-kinase activity and hence have subsequently been termed adaptor molecules (Escobedo *et al.*, 1991b; Otsu *et al.*, 1991). Experiments then focussed on the p110kD protein that had been found to be associated with the p85 subunit. Otsu and colleagues utilised the *in vitro* baculovirus expression system to express and study the 110kD protein. These experiments revealed that the 110kD protein possessed PI3-kinase activity, and hence p110 was designated the catalytic subunit. Moreover, *in vitro* assays illustrated that PI3-kinase activity could only associate with a receptor complex if a both p85 and p110 subunits were present (Otsu *et al.*, 1991). Therefore, it was concluded that the active PI3-kinase enzyme is a heterodimeric complex consisting of an adaptor protein and a catalytic subunit. To date 5 adaptor subunits have been cloned and termed p85α, p85β (Escobedo *et al.*, 1991b; Otsu *et al.*, 1991; Skolnik *et al.*, 1991), p50α, p55α (Pons *et al.*, 1995) and p55γ (Dey *et al.*, 1998) and 4 p110 subunits have been cloned, and termed α, β , γ (Stephens *et al.*, 1997), and δ (Vanhaesebroeck *et al.*, 1997b).

The PI3-kinase family of enzymes is primarily responsible for the transfer of a phosphate group to the 3-hydroxyl position of the inositol headgroup (Figures 1.1 and 1.2), resulting in a transient increase in 3-phosphorylated inositol lipids within the cell. As indicated above, numerous members of this family have been cloned and characterised, and based on their structure and *in vitro* substrate specificities, have

been catergorised into 3 classes: Class I PI3-kinases that appear to be heterodimers composed of a catalytic and an adaptor subunit (Figure 1.3), and have a preference to phosphorylate PI 4,5 P_2 *in vitro*; in contrast, Class II PI3-kinases that are monomeric proteins with C2 domains (Figure 1.3) and an *in vitro* substrate specificity restricted to PI and PI 4 P; finally, Class III PI3-kinases that are homologues of *Saccharomyces cerevisiae* (*S. cerevisiae*) Vps34p (vacuolar protein sorting mutant; Figure 1.3), and whose activity appears to be limited to phosphorylation of PI. This study primarily focuses on a member of the Class I PI3-kinases therefore for the purposes of this review Class II and Class III PI3-kinases will not be discussed in any further detail.

1.1.3 Class I Phosphatidylinositol 3-kinases

The group of Class I PI3-kinases can be further subdivided based on the way in which their activity is regulated. Those members that rely on recruitment by protein tyrosine kinases constitute the Class IA PI3-kinases, and those that are recruited through their interaction with heterotrimeric G proteins are classified as the Class IB PI3-kinases.

1.1.4 Class IA Phosphatidylinositol 3-kinases

1.1.4.1 Structure of the Class IA Regulatory Subunits

The Class IA PI3-kinases are the most well-characterised family members with regards to their structure, regulation and potential functions. This subfamily presently consists of the regulatory subunits p85α, p85β, p50α and p55α, p55γ and the catalytic subunits p110α, p110β, and p110δ. The regulatory p85 α and β subunits share above

85% identity at the nucleotide level and therefore have a similar general structure consisting of 2 *Src* homology 2 (SH2) domains, one *Src* homology 3 (SH3) domain and a breakpoint cluster region homology domain (BH) (reviewed in (Wymann & Pirola, 1998)). Flanking the BH domain are two proline-rich motifs (Figure 1.3) (Escobedo *et al.*, 1991b; Otsu *et al.*, 1991; Skolnik *et al.*, 1991). The smaller adaptor proteins p50α, p55α (Pons *et al.*, 1995), and p55γ (Dey *et al.*, 1998) share 79% identity at the nucleotide level with the p85 proteins but lack the N-terminal SH3 domain, the BH domain and a proline-rich motif. Structurally, p85 is considered the prototypic regulatory subunit.

The SH3 domain was originally identified on the basis of sequence similarity between protein tyrosine kinases $pp60^{c\text{-}src}$ and PLCγ (Mayer *et al.*, 1988), and is now recognised as a motif present in many cellular proteins that mediates protein-protein interactions. The p85 SH3 domain structure conforms to the NMR solution structure previously determined (reviewed in (Fry *et al.*, 1993)) and is described as a hydrophobic region noted for its cluster of conserved tyrosine and tryptophan residues, typically surrounded by charged loops (Cohen *et al.*, 1995). In order to address the function of the SH3 domain, GST-SH3 domain fusion proteins were made and used to screen expression libraries. Although the initial results were possibly considered possibly to be specific for the particular SH3 domain used, common themes emerged from the results of that study (Cicchetti *et al.*, 1992). These centred around the realisation that the SH3 domain fusion protein associated with regions in other proteins that displayed a high number of proline residues. Furthermore, deletion studies in conjunction with a biased peptide library approach identified two putative proline-rich consensus sequences, RXLPPRPXX and XXXPPXPXX that bound SH3

domains, where X corresponds to any amino acid except cysteine (Yu *et al.*, 1994). The proline residues form the basis of the interaction, and the surrounding amino acids contribute to the specificity and strength of the interaction. Thus the role of the SH3 domain revolves around protein-protein interactions and these appear to be mediated through regions in the binding partner that are rich in proline residues.

Proline-rich sequences 1 and 2 of p85, flank the BH domain, and, act as ligands for SH3 domain-containing proteins. Extensive immunoprecipitation studies of whole cell lysates, in conjunction with studies using recombinant proteins have shown that these proline-rich sequences associate with various non-receptor protein tyrosine kinases (PTK), such as *v-src* (Liu *et al.*, 1993), Lyn (Prasad *et al.*, 1993), Fyn (Pleiman *et al.*, 1993), Abl and Lck (Kapeller *et al.*, 1994). It is also possible that the existence of an SH3 domain with proline-rich sequences may enable self-association of p85 subunits, and this may play an important role in the regulation of activity of the p110kD catalytic subunit.

The BH domain of p85 is highly homologous to the GTPase activating protein (GAP) domain of the breakpoint cluster gene product (Diekmann *et al.*, 1991). However this is the region demonstrating least similarity between the p85 isoforms. The crystal structure of this protein consists of a 4 helix bundle with an additional projection of multiple helices (Musacchio *et al.*, 1996). The BH domain interacts with members of the Rho protein family, in particular Cdc42 and Rac1 (Ahmed *et al.*, 1994; Musacchio *et al.*, 1996). However, initiation of GTPase activity following this interaction has not yet been detected, suggesting that this interaction does not

contribute substantially to the signalling pathway (Tolias *et al.*, 1995; Zhang *et al.*, 1999).

All PI3-kinase Class IA regulatory subunits consist of an N-terminal and a C-terminal SH2 domain. SH2 domains were originally identified as protein modules located within non-catalytic regions of tyrosine kinases (Koch *et al.*, 1991; Pawson & Gish, 1992; Sadowski *et al.*, 1986). These domains are approximately 100 amino acids in length, and appear to act in two different manners: firstly as protein-protein interaction domains, or secondly, as enzymes. As for SH3 domains, the SH2 domains in p85 are primarily responsible for mediating protein-protein interactions (Koch *et al.*, 1991; Pawson & Gish, 1992), however in contrast to SH3 domains, their association is not dependent upon proline-rich sequences, but is reliant on phosphotyrosine-containing motifs (reviewed in Koch *et al.*, 1991). SH2 domains recognise a canonical selection of phosphotyrosine motifs, the best-characterised being PYXXM, where the tyrosine residue (Y) must be phosphorylated (Songyang *et al.*, 1993). These SH2 domains possess reduced affinity towards motifs that vary slightly from the PYXXM order (Ponzetto *et al.*, 1993). The solution of the crystal structure of SH2 domains has confirmed the reliance on such a canonical motif. Peptide recognition occurs on the flat surface of the molecule, with a small pocket to house the phosphotyrosine residue. A second pocket is thought to provide the binding site for the conserved methionine residue of the motif (Waksman *et al.*, 1992; Waksman *et al.*, 1993). This is clearly a simplification of SH2-protein interactions as the SH2 domains of the p85 regulatory subunit demonstrate a high degree of specificity for different tyrosines of the PDGF receptor; where the N-terminal SH2 domain of p85 has affinity for the Y751 phosphotyrosine motif, and has no affinity for

the Y740 phosphotyrosine motif in the PDGF receptor. In contrast, the C-terminal SH2 domain has the ability to bind both regions (Panayotou *et al.*, 1993). Further information is clearly required in order to understand the depth of the specificity that a nominal SH2 domain has for its target.

Development of monoclonal antibodies against various portions of the p85 regulatory subunit has illustrated that the region between the N- and C-terminal SH2 domains (inter-SH2 domain) is responsible for the interaction between the regulatory and catalytic subunits. Antibodies that recognise epitopes within the inter-SH2 region were unable to immunoprecipitate active complexes of p85 and p110 in COS-7 cells, whereas antibodies recognising other epitopes of the p85 subunit such as the BH domain were able to precipitate complexes that demonstrated PI3-kinase activity. These results suggested that the inter-SH2 domain was bound to the p110 catalytic subunit and therefore the epitope was not available for the SH2 antibody to recognise and precipitate an active complex (End *et al.*, 1993). Furthermore, the use of recombinant domains and truncation mutants have shown that the inter-SH2 domain was able to bind equivalent amounts of recombinant p110 compared to native p85, and that this directly correlated to the level of PI3-kinase activity. Epitope mapping deciphered amino acids 478-492 as the most important in mediating the interaction with the catalytic subunit (Dhand *et al.*, 1994a; Dhand *et al.*, 1994b; Klippel *et al.*, 1992).

1.1.4.2 Structure of the Class IA Catalytic Subunits

Sequence analysis of lipid kinase catalytic subunits and all members of the PI3-kinase family revealed the existence of four homology regions. These regions have been termed homology regions 1, 2, 3 and 4 (HR1, HR2, HR3, and HR4).

The C-terminally-located HR1 is the most highly-conserved domain in the PI3-kinases. It contains an ATP-binding site at lysine 802 and kinase motifs responsible for the coordination of the phosphate transfer reaction. Site-directed mutagenesis of lysine 802 caused a loss of p85/p110 protein kinase and lipid kinase activity, demonstrating its importance in the activity of this enzyme (Dhand *et al.*, 1994a; Wymann *et al.*, 1996).

HR2, also known as the PI kinase (PIK) domain, is conserved amongst all lipid kinases. To date, no direct function has been attributed to this region, however, deletion of this region in Vps34, the *S. Cerevisiae* PI3-kinase, removes all lipid kinase activity (Molendijk & Irvine, 1998).

HR3 is found in all PI3-kinases while HR4 is only located in Class I PI3-kinases. No specific functions have yet been assigned to these homology regions. Upstream of HR4 lies the ras-binding domain. As its name suggests, this domain mediates the association of GTP-loaded ras with the catalytic subunit (Kodaki *et al.*, 1994; Rodriguez Viciana *et al.*, 1994; Vanhaesebroeck *et al.*, 1997a). Homology regions 2 and 3 flank a leucine zipper motif in p110δ with an additional proline-rich region upstream of HR4. It is postulated that these domains may facilitate a unique

regulatory pathway for p110δ, mediated through protein-protein interactions (Vanhaesebroeck *et al.*, 1997b). These potential protein targets have yet to be identified. Located at the extreme N-terminal end of the p110 subunit is a binding domain for the p85 regulatory subunit. This is thought not only to mediate the interaction with the Class IA kinases but also to assist in the stabilisation of p110 within the cell (Wymann & Pirola, 1998).

1.1.4.3 Activity and Regulation of the Class IA Phosphatidylinositol 3-kinases

Class I PI3-kinases are able to phosphorylate the 3 substrates: PI, PI 4 P, and PI 4,5 P_2, *in vitro*. However, upon cellular stimulation, they display an *in vivo* specificity for PI 4 P and PI 4,5 P_2. All possess intrinsic protein kinase activity specifically targeting serine residues in either the regulatory or catalytic subunit. The catalytic subunit p110α phosphorylates p85α at serine residue 608 which results in a downregulation of its lipid kinase activity (Carpenter *et al.*, 1993; Dhand *et al.*, 1994b). In contrast, p110δ autophosphorylates causing a similar downregulation of lipid kinase activity. Furthermore, removal of the observed protein kinase activity by a point mutation results in the removal of lipid kinase activity of the enzyme (Vanhaesebroeck *et al.*, 1997b).

Since the cloning of the first p85 and p110 subunits a wealth of information regarding the structural aspects of class I PI3-kinases has been generated. In contrast, detailed knowledge pertaining to the factors that regulate the activity of these enzymes is lacking. It is most likely that the regulation of PI3-kinase activity involves the integration of multiple signals ranging from activation by translocation, activation

through interactions with protein tyrosine kinases, and activation through phosphorylation.

1.1.4.3.1 Activation by Translocation

The major cellular sources of substrate for PI3-kinases are the cytoplasmic and nuclear membranes. Thus, it seems feasible that the translocation of these enzymes toward their substrates would play a role in the regulation of their activity. Susa and colleagues demonstrated an increase in total cellular PI3-kinase activity following PDGF stimulation of NIH-3T3 fibroblasts, and upon fractionation showed a 30-50% decrease in activity in the cytosol. The levels of p85 were found to increase in the membrane fraction, however these levels did not directly correlate with changes in enzyme activity (Susa *et al.*, 1992). At present, it is considered that induction of lipid kinase activity involves translocation within the cell, however there is still a large degree of conjecture regarding the need for translocation for the activation of protein kinase activity.

1.1.4.3.2 Interactions with Protein Tyrosine Kinases

Class IA PI3-kinases interact with a large number of receptor and non-receptor protein tyrosine kinases. It has been traditionally thought that these interactions would primarily be mediated through SH2 domains, however recent data indicate that the SH3 domains also play an important role. The most well-characterised protein tyrosine kinases that interact with PI3-kinases are the PDGF and insulin receptors.

Of all the receptors that SH2 domain-containing proteins bind, the PDGFβ receptor is the best characterised. It has been consistently shown that anti-phosphotyrosine immunoprecipitates from PDGF-stimulated cells display a 50-fold increase in PI3-kinase activity (Kaplan *et al.*, 1987). The association between PDGF receptor and Class IA PI3-kinases is mediated through the kinase insert region of the receptor (Coughlin *et al.*, 1989). The direct association and subsequent activation of Class IA PI3-kinases is mediated by two tyrosine phosphorylation sites, these being tyrosine 740 and tyrosine 751 (Escobedo *et al.*, 1991a). It is believed that the N-terminal SH2 domain interacts through Y751 while the C-terminal SH2 domain binds via Y740 (Panayotou *et al.*, 1993).

The insulin receptor differs from that of the PDGF receptor in that Class IA PI3-kinases have not been shown to directly couple to the receptor. Rather, the kinase is recruited through a phosphorylated docking protein known as insulin receptor substrate-1 (IRS-1). IRS-1 is a minor cytosolic protein which remarkably contains 10 tyrosine phosphorylation sites that are phosphorylated upon insulin stimulation (Sun *et al.*, 1991). This provides the basis of the model of insulin receptor stimulation resulting in the activation of insulin receptor kinase and phosphorylation of IRS-1, which subsequently mediates the association with the SH2 domains of Class IA PI3-kinases.

The EGF receptor, a protein tyrosine kinase, has also been shown to associate with PI3-kinase activity (Bjorge *et al.*, 1990; Cochet *et al.*, 1991). Unusually, the C-terminal tail of the receptor lacks any recognisable PYXXM motifs for the association of the p85 SH2 domains (End *et al.*, 1993). This implies that the interaction between

Class IA PI3-kinases and the EGF receptor involves domains other than PYXXM motifs and SH2 domains. Details regarding the domains important for this association remain unclear.

1.1.4.3.3 Protein Phosphorylation

Phosphorylation of protein residues is a well-established way in which protein function is modulated within cells. To date, the majority of work on phosphorylation of the family of PI3-kinases has focussed on the p85 subunit. Initial observations detected serine phosphorylation of the p85 regulatory subunit before and after growth factor stimulation (Cohen *et al.*, 1990a; Cohen *et al.*, 1990b). Following this observation a Mn^{2+}-dependent protein serine kinase activity was co-purified with PI3-kinase, and phosphorylation of the p85 serine residue was found to downregulate the lipid kinase activity (Carpenter *et al.*, 1993). This downregulation in activity was recovered upon treatment with serine phosphatases (Carpenter *et al.*, 1993; Dhand *et al.*, 1994b). Mutational analysis of bovine p110α suggested that this serine kinase activity was inherent to the catalytic subunit (Dhand *et al.*, 1994b), and has been mapped to the serine 608 residue. This is thought to be a major route of downregulation of activity of the enzyme. The mechanism involved in phosphorylation of serine 608 is not yet known.

The basal level of tyrosine phosphorylation within a cell is less than 1% of total phosphorylation. Following activation of the cell, tyrosine phosphorylation can rapidly increase, however it still only contributes to less than 5% of the total phosphorylation in the cell. These characteristics, along with the knowledge that Class

IA PI3-kinases interact extensively with PTKs provided the impetus to examine the role of tyrosine phosphorylation in the activation and regulation of PI3-kinase activity. To date, it is contentious whether tyrosine phosphorylation of p85 occurs, and it has not yet been detected for the p110 catalytic subunit. However, the interaction with receptor and non-receptor PTKs discussed in section 1.1.4.3.2, in conjunction with studies utilising tyrosine phosphorylation inhibitors suggest that tyrosine phosphorylation does play an important but indirect role in the activation of Class IA PI3-kinases.

More recently, Gout and colleagues have identified the existence of a negative regulatory protein known as Ruk. Ruk forms complexes with p85/p110 *in vitro* and *in vivo*, through the interaction with the SH3 domain of p85 and the proline-rich region of Ruk. This interaction substantially inhibits the lipid kinase activity of the enzyme. Over-expression of Ruk was found to induce premature apoptosis which was rescued with the over-expression of p110α or its downstream effector protein kinase B. This is the first known example of a protein that is a negative regulator of Class IA PI3-kinases (Gout *et al.*, 2000).

1.1.5 History of the Class IB Phosphatidylinositol 3-kinases

In the mid-to-late 1980s there was increasing evidence that PI3-kinases could be regulated in two different fashions, or alternatively that an isoform of PI3-kinase existed that was regulated in a tyrosine kinase-independent manner. Observations by Traynor-Kaplan showed that ligands that are known to directly couple and recruit G proteins were able to stimulate a transient increase in PI 3,4,5 P_3 following receptor

ligation (Traynor-Kaplan *et al.*, 1989). Furthermore, this increase, a result of fMLP stimulation, was insensitive to protein tyrosine kinase inhibitors, and sensitive to pre-treatment with pertussis toxin, an established inhibitor of $G_{i\alpha}$ activation (Stephens *et al.*, 1993b). Although evidence began mounting towards the existence of an isoform regulated through G proteins, the experimental data was not conclusive considering that downstream tyrosine phoshorylation was subsequent to all the stimuli utilised above. In 1995, Stoyanov and colleagues reported the cloning, expression and purification of a novel isoform of PI3-kinase (Stoyanov *et al.*, 1995). A human bone marrow cDNA library was screened using a probe generated by degenerate PCR. Examination of hybridising clones identified one large open reading frame encoding 1050 amino acids with three potential methionine start codons. At the time, the predicted amino acid sequence displayed 28-36% identity to other known PI3-kinases. The N-terminus of this putative protein showed little similarity to other cloned catalytic subunits while significant conservation at the C-terminus was observed. This isoform of the PI3-kinase family was termed p110γ (herein referred to as PI3kγ) (Stoyanov *et al.*, 1995). Soon after, a revised sequence revealed an increase in the level of identity to other PI3-kinases (Stephens *et al.*, 1997). However, it was still apparent that the N-terminal portion of PI3kγ was significantly different in comparison to other known PI3-kinases.

1.1.5.1 The Class IB Catalytic subunit- PI3Kγ

As with the Class IA p110 subunits, PI3Kγ contains all four homology regions of the PI-kinases. The extreme C-terminal end consists of a catalytic domain which shares high identity with its counterparts, p110α, β, and δ (Figure 1.3). The PI3Kγ also shares a PIK domain, and a ras-binding domain with other Class I PI3-kinases. Further sequence analysis of the N-terminal region of PI3Kγ suggested the existence of a putative PH domain (Stephens *et al.*, 1997; Stoyanov *et al.*, 1995). Such domains consist of stretches of approximately 100 amino acids, which share greater similarity of hydrophobicity/ hydrophilicity between domains rather than a particular motif conservation. Of greater relevance to this PI3-kinase isoform is the known interaction between PH domains and G protein subunits, particularly the βγ subunits, and the ability of PH domains to bind phospholipids. The existence of a PH domain suggested that PI3Kγ might be activated and regulated in a manner that is different from the Class IA PI3-kinases (Stephens *et al.*, 1996; Stephens *et al.*, 1994b; Stephens *et al.*, 1997; Stoyanov *et al.*, 1995). More recently, the crystal structure of PI3Kγ was solved, the first time any of the PI3-kinases has been crystallised (Walker *et al.*, 1999). The results of this study confirmed the arrangement of motifs and domains that had previously been determined based on sequence homologies and functional assays. Remarkably though, as shown in Figure 1.4, the crystal structure indicated the presence of a C2 domain flanked by the ras-binding and PIK domain. Sequence and functional analysis had not indicated the existence of such a domain, which is traditionally involved in the recruitment of proteins to phospholipid membranes in a Ca^{2+} dependent manner. PI3Kγ is now known to consist of a helical spine with the C2

domain and catalytic domains positioned to allow interaction with the cell membrane, while the ras-binding domain lies in close proximity to the catalytic site (Figure 1.4) (Walker *et al.*, 1999).

Baculovirus expression systems have been extensively employed to study the substrate specificity and interactions of PI3Kγ in comparison to other known mammalian PI3-kinases. A PI3Kγ-GST fusion protein was generated and shown to possess PI3-kinase activity, utilising similar substrates with a similar efficiency as the p85/p110 complex. Co-expression of PI3Kγ and p110α with p85α and β showed that p110α copurified with p85α and β, whereas PI3Kγ failed to associate with either protein, a finding consistent with the lack of a p85-binding domain in PI3Kγ (Stephens *et al.*, 1997; Stoyanov *et al.*, 1995). In summary, the results of these studies indicated that PI3kγ displayed some structural and functional characteristics of the classical PI3-kinases, however it did not appear to be regulated in the same manner as Class IA PI3-kinases.

1.1.5.2 Activity and Regulation of Class IB Phosphatidylinositol 3-kinases

Although PI3Kγ does not physically associate with p85 adaptor subunits Stephens and colleagues found that PI3-kinase activity was associated with an additional protein of 101kDa (Stephens *et al.*, 1997) and because of this it was suggested that PI3kγ function might be regulated by a second protein analogous to the p85α/β subunits. Therefore, in its native state PI3Kγ may also exist as a heterodimer. This putative regulatory protein was subsequently cloned and termed p101 based on

molecular weight (Stephens *et al.*, 1997). Presently, very little is known about p101 as it shares no homology with any previously identified proteins including other well known adaptor proteins in the PI3 kinase family. Baculovirus expression systems have been utilised to show a 100-fold increase in the activity of PI3kγ in the presence of p101 *in vitro* (Stephens *et al.*, 1997). In contrast, data generated by Bondev *et al.*, once again using baculovirus expression of signalling components, demonstrated only a minor increase in PI3kγ activity in the presence of p101 (Bondev *et al.*, 1999). Krugmann and colleagues generated panels of p101 and PI3Kγ truncation and deletion mutants in order to identify protein motifs and regions responsible for an interaction between these two proteins, as well as to examine a potential regulatory role of Gβγ subunits. These studies suggested that both the N-terminal and C-terminal regions of p101 were necessary for binding the N-terminal portion of PI3Kγ, and that this interaction was indispensable for Gβγ binding and activation (Krugmann *et al.*, 1999). Taken together, these studies illustrate, quite clearly, the controversy surrounding the importance of p101 in the activity of PI3kγ. This inconsistency in results may arise from the *in vitro* experimental systems and methods chosen for the analysis of this interaction. However, it is worth bearing in mind that if p101 molecules are required for translocation of PI3kγ to cell membranes where lipid substrates are available, an *in vitro* assay consisting of freely available substrate would not demonstrate this. Another consideration when examining the data generated from Stephens *et al.*, versus Bondev *et al.*, using baculovirus expression of proteins may arise from simple assay differences in the lipid kinase assays. Although studies by Krugmann *et al.*, suggested that p101 binds the N-terminal portion of PI3kγ and was essential for its activity they did not address the potential loss of the quaternary structure of the PI3kγ

protein and the subsequent loss of binding and activation domains when creating truncation mutants. The development of reagents that recognise and bind p101, and more specific reagents for PI3Kγ will be necessary for elucidating the nature and depth of this interaction.

As for Class IA PI3-kinases, the PI3Kγ recombinant protein is able to phosphorylate PI, PI 4 P, and PI 4,5 P_2 *in vitro* (Stoyanov *et al.*, 1995), however it displays an *in vivo* preference for PI 4,5 P_2. PI3Kγ exhibits dual protein and lipid kinase activity, both of which are dependent upon the ATP transfer site of the catalytic subunit. Mutation of lysine 832, an essential amino acid for the ATP transfer reaction, to arginine renders the PI3Kγ protein catalytically inactive (Stoyanova *et al.*, 1997). As for p110δ, PI3Kγ, possesses the capacity to autophosphorylate which results in a downregulation of its lipid kinase activity (Stoyanova *et al.*, 1997).

The predictions made by Stephens in 1994 (Stephens *et al.*, 1994a) regarding the possibility of an isoform of PI3-kinase being regulated in a tyrosine kinase-independent manner, were realised when preliminary studies following the cloning of PI3Kγ, illustrated the necessity of Gβγ subunits for the activation of the novel isoform (Stoyanov *et al.*, 1995; Stoyanova *et al.*, 1997). Stephens *et al.*, confirmed these results when they independently showed that the addition of Gβγ *in vitro* to recombinant PI3Kγ increased activity significantly (Stephens *et al.*, 1997). In order to determine whether PI3Kγ was directly regulated by heterotrimeric G proteins, reconstitution assays and deletion studies were conducted. These showed that Gβγ subunits are critical for the activation of PI3Kγ. This interaction between Gβγ and

PI3Kγ was mapped to 2 binding sites, one located at the N-terminus of PI3Kγ and the other at the C-terminus. This suggested that PI3Kγ activation involved adoption of a horseshoe conformation (Leopoldt *et al.*, 1998). A model of G protein-coupled receptor activation was developed based on these results, which theorised that following receptor ligation, activated Gβγ subunits bind to PI3Kγ and create a conformational change that leads to activation of the enzyme (Leopoldt *et al.*, 1998).

To examine the regulation of the dual kinase activity of PI3Kγ, a system utilising hybrid PI3Kγ proteins was used. Putative lipid-binding sites were exchanged with putative headgroup interaction sites from Class II and III PI3-kinases. This generated PI3Kγ mutants fostering an altered or aborted lipid kinase activity and yet retained protein kinase activity. In this study, transfection of COS-7 cells with a membrane-targeted wild-type PI3Kγ showed constitutive lipid kinase activity, producing PI 3,4,5 P_3 and activating protein kinase B (also known as Akt). Hybrids that had aborted lipid kinase activity failed to produce PI 3,4,5 P_3 but were protein kinase active and stimulated the MAP kinase pathway in COS-7 cells. From these studies, it was concluded that when PI3Kγ was active as a lipid kinase, protein kinase activity was suppressed and *vice versa*. It is still not known what extracellular or intracellular signals dictate the initiation of one activity over the other (Bondeva *et al.*, 1998).

In summary results presented from a variety of groups indicate that the Class IB PI3-kinase, PI3Kγ, has dual kinase activity that is regulated by G protein subunits,

particularly Gβγ. It is still not known whether a putative adaptor subunit of PI3Kγ, p101, is essential for activation of the PI3kγ *in vitro* or *in vivo*.

1.1.6 Cellular Role of PI3-kinases and their Lipid Products

Since the discovery of PI3-kinases, various approaches have been undertaken to examine the roles that they play in cell function. These approaches include the use of phosphopeptide- and antibody-based inhibitors, synthetic inhibitors, dominant-negative overexpression of PI3-kinase subunits, and the use of mice in which components of the PI3kinase system have been "knocked out" by homologous recombination. All approaches have unique limitations regarding the accuracy and interpretation of the data obtained from their use. However, such studies have provided a strong foundation towards the understanding of the biological role of PI3-kinase activation. Discussed below are the most extensively used, and more successful, approaches to delineate PI3Kγ cellular function that have been undertaken to date.

1.1.6.1 Chemical Inhibitors

In the late 1980s, Vlahos and colleagues led the way in the development of synthetic inhibitors of the family of PI3-kinases. Wortmannin, a fungal metabolite was the first such inhibitor, followed by a bioflavoid derivative of quercetin known as LY294002. Both wortmannin and LY294002 bind to the ATP transfer site in the catalytic subunit of PI3-kinases. Wortmannin binds covalently rendering the kinase permanently inactive, whereas LY294002 binds in a competitive manner (Matter *et*

al., 1992; Vlahos *et al.*, 1994). Advantageous to cellular work is the ability of these low molecular weight compounds to permeate the cytoplasmic membrane. They have therefore been used extensively since their discovery in an attempt to decipher the role of the PI3-kinase family in cellular functions *in vitro* and using this approach, important roles in cytoskeletal rearrangement, cellular motility, cytokine gene expression (Pan *et al.*, 1999), antigen presentation (Song *et al.*, 1997) and cell-cycle control have been determined. However, there are several significant limitations to these studies. As outlined previously, the catalytic subunit (HR1) is highly conserved between all classes and isoforms of PI3-kinases and some PI4-kinases, therefore inhibitory drugs targeted to this region are capable of inhibiting all members of the PI3-kinase family. Therefore, the resultant data generated using these molecules provides little information regarding the role of specific PI3-kinase isoforms in signal transduction and cellular effector functions. Moreover, each member of the PI3-kinase family displays varying levels of inhibition by these compounds at nanomolar concentrations (reviewed in Vanhaesebroeck *et al.*, 2001), and it is still not clear whether other signalling mediators within the cell (for instance other PI-kinases) are affected simultaneously, potentially obscuring the precise role that the PI3-kinase family plays.

1.1.6.2 Dominant-negative Over-Expression

This approach has been most extensively used in the analysis of the function of Class IA PI3-kinases, more specifically, of the p85 regulatory subunit. In 1994, Dhand and colleagues found that the removal of 35 amino acids in the inter-SH2 region of p85α (Δp85α) prevented binding of the p110 catalytic subunit to p85. Furthermore,

Δp85α was able to interact with phosphotyrosine molecules as efficiently as wild-type p85α in COS-7-transfected cells. Overexpression of Δp85α in COS-7 cells effectively blocked the recruitment of the endogenous PI3-kinase active heterodimer to membrane receptor proteins (Dhand *et al.*, 1994a). The use of Δp85 has been expanded to many cellular systems to illustrate the importance of the p85/p110 heterodimer in effector functions ranging from cell-cycle progression and survival of NIH-3T3 fibroblasts, and gene expression (Pan *et al.*, 1999).

Over-expression of catalytically-inactive p110 subunits has been far less informative. This is possibly due to an inherent lack of stability of the p110 subunit in the absence of sufficient levels of the p85 regulatory subunits. To date, the only successful experimentation using this approach has been achieved using a catalytically in active PI3kγ. The results of this study showed that its lipid kinase activity was essential for PKB activation and that its protein kinase activity was important for MAP kinase activation (Bondeva *et al.*, 1998).

1.1.6.3 Gene Knockout Animal Models

The method of gene disruption is arguably one of the more precise ways to understand the biological roles of specific proteins. The use of wortmannin, LY294002, and dominant-negative studies indicated that members of the family of PI3-kinases were potentially involved in functions including the proliferation and maturation of cells, and programmed cell death and in the case of dominant-negative over-expression, provided information regarding specific PI3-kinase isoforms. The

fact that these experiments pointed towards roles for PI3-kinases in prliferation, cell maturation and apoptosis implied the possibility that embryological development may be dependent upon their expression. In light of these factors one of the hypotheses proposed was that a homozygous knockout of the members of the PI3-kinase family would potentially be fatal.

In early 1988, the targeted gene disruption of p110α showed that PI3-kinase p110α $^{-/-}$ embryos are developmentally delayed at embryonic day 9.5 and that death regularly occurred between embryonic days 9.5 and 10.5. Moreover, they were found to have a proliferative defect with little change in the rate of apoptosis (programmed cell death) (Bi *et al.*, 1999). The time of death corresponded to the period of accelerated organogenesis and placentation. Disruption of the p110β gene proved to be fatal at the same embryonic stage as the p110α $^{-/-}$ mice. Disruption of the p85α gene led to a similar phenotype to that observed in the p110α knockout mouse (Fruman *et al.*, 1999). Interruption of the first exon of p85α gave rise to viable mice, however, these mice showed impared B lymphocyte differentiation further supporting the hyothesised role of Class IA PI3-kinases in cellular development (Terauchi *et al.*, 1999).

In complete contrast, the disruption of the PI3kγ gene, the only Class IB isoform identified to date, gave rise to phenotypically healthy PI3Kγ$^{-/-}$ mice (Hirsch *et al.*, 2000a; Li *et al.*, 2000; Sasaki *et al.*, 2000). This categorically displayed for the first time the biological functions of the multiple isoforms of this family were non-

redundant. The experimental data generated using the PI3k$\gamma^{-/-}$ mouse will be discussed in more detail in section 1.2.5.

1.1.6.4 Cellular Role of Phosphatidylinositol 3-kinase Lipid Products

Lipids acting as signalling molecules as opposed to structural components in a cell is a relatively recent concept although now there is a considerable body of evidence supporting this notion. This raises the question as to the role of the 3-phosphorylated lipid products within the cell. Due to the low basal level, and transient nature of these products, it is unlikely that a major structural or homeostatic role is played by these products. Rather, evidence suggests that these lipid products are able to act as second messengers themselves and contribute to the stimulation of various effector functions of the cell. Some specific examples of this are described below.

1.1.6.5 Phosphatidylinositol 3 Phosphate

Phosphatidylinositol 3-phosphates (PI 3 P) are only present in eukaryotic cells (Auger *et al.*, 1989). Their production involves the phosphorylation of phosphoinositide (PI) by Class I, II, or III PI3-kinases, however the majority is produced by Class III enzymes (Vanhaesebroeck *et al.*, 1997a). The prototype PI3-kinase used for understanding the role of PI 3 P is the Class III PI3kinase, yeast Vps34p which has been shown to play a role in chemotaxis in yeast (Figure 1.5). The central focus of this thesis is on the Class I PI3-kinases, therefore the production and role of PI 3 P in cellular function will not be discussed in any further detail.

1.1.6.6 Phosphatidylinositol 3,4 bisphosphate

Consistent with an important role in signal transduction rather than homeostatic function, PI 3,4 P_2 production is regulated by extracellular stimuli. Stimulation of NIH 3T3 fibroblasts by PDGF, and of neutrophils with fMLP, results in a transient increase in PI 3,4 P_2 within the cells (Auger *et al.*, 1989; Hawkins *et al.*, 1992; Stephens *et al.*, 1991). It was originally thought that the production of PI 3,4 P_2 was due to the dephosphorylation of PI 3,4,5 P_3, however it has since been demonstrated that Class II PI3-kinases can phosphorylate PI 4 P independently of PI 3,4,5 P_3 synthesis (Rameh *et al.*, 1997).

Protein kinase B (PKB)/Akt is the most well-characterised target of PI 3,4,5 P_2. While PKB contains a PH domain that is able to bind all PIs *in vitro*, it shows a bias for PI 3,4 P_2 and binding of PI 3,4 P_2 results in an increase in PKB activity. This is thought to be mediated by the binding of PKB kinase to the phospholipid following its association with PKB (Franke *et al.*, 1997; Frech *et al.*, 1997). The proposed model of activation involves PI 3,4 P_2 stimulating translocation of PKB and associated kinases from the cytoplasm to cell membranes, promoting conformational changes to expose serine and threonine residues for phosphorylation (Alessi *et al.*, 1996).

The activation of PKB increases cell survival signals (Figure 1.5) which include the phosphorylation and inactivation of BAD, a pro-apoptotic protein. PKB could feasibly interact with other proteins, both pro- and anti-apoptotic, considering cells lacking BAD but possessing PKB also demonstrate increase cell survival (Franke *et al.*, 1997). Glycogen synthase kinase 3 and phosphofructokinase are also substrates

for PKB, implicating PI3-kinase lipid products particularly PI 3,4 P_2 in gluconeogenesis and glycolysis. (Cross *et al.*, 1995)

1.1.6.7 Phosphatidylinositol 3,4,5 Trisphosphate

To date, two separate pathways have been delineated in the regulation of PI 3,4,5 P_3 production. The first involves extracellular stimuli increasing the production of PI 3,4,5 P_3 through the use of Class I PI3-kinases (Hawkins *et al.*, 1992) and recently, suggestions of the existence of a PI 4,5 P_2-independent pathway have arisen. These revolve around PIP5-kinases utilising PI 3 P to produce PI 3,4,5 P_3 by phosphorylating the hyroxyl groups at positions 4 and 5 (Tolias *et al.*, 1998; Zhang *et al.*, 1998). At present the *in vivo* significance of this is not known. Regulation may also involve dephosphorylation at the 3 position of the inositol headgroup by PTEN, a tumour suppressor protein. The production of PI 3,4,5 P_3 potentially induces effector functions such as actin rearrangement, cell growth, and adhesion (Figure 1.5) however, these pathways are still poorly understood (Toker & Cantley., 1997).

1.1.7 Summary of the phosphatidylinositol 3-kinases

Transmission of information from the extracellular environment to the nucleus of any cell requires the coordinated action of many molecules at many levels. The prominence of lipids as signalling molecules acting downstream of cell surface receptor ligation has increased since the discovery of PLC, PLA_2 and the family of PI3-kinases. The PI3-kinase family is an extensive family of lipid kinases with members being found in organisms ranging from mammalian cells, yeast, plant cells,

D. melanogaster, and *C. elegans*. The family is subdivided into 3 classes (class I, II, and III) based upon their structure and *in vitro* substrate specificity. The focus of this review has been on the well-characterised Class I PI3-kinases. The Class I subfamily in general, consists of heterodimers that are able to 3-phosphorylate the lipids PI, PI 4 P and PI 4,5 P_2 *in vitro*, while *in vivo* they display a preference for PI 4,5 P_2. Members of the subfamily can be further divided in two groups, these being the Class IA and the Class IB PI3-kinases.

The Class IA PI3-kinases were the first identified, and are the best-characterised members of the PI3-kinase family. They consist of an 85kD regulatory/adaptor subunit and a 110kD catalytic subunit. Activation of the Class IA enzymes is dependent upon tyrosine phosphorylation and thus upon the activity of protein tyrosine kinases. The model of activation involves the stimulation of cell surface receptors which have inherent PTK activity or recruit PTK activity immediately downstream of ligand binding (Figure 1.6). The 3-phosphorylated lipids generated by the activation of Class IA PI3-kinases, are able to bind to second messengers containing PH domains. In general, this in turn activates various proteins such as small GTPases, and protein kinases such as phosphoinositide dependent kinase (PDK). The associated protein kinase activity may also activate phospholipases involved in the generation of IP_3 and DAG (Figure 1.6). Although, activation of Class IA PI3kinases are associated with resultant effector functions such as secretion and cytoskeletal rearrangement, the precise signalling pathways pathways involved are presently incomplete.

The Class IB PI3-kinases share many characteristics with the Class IA PI3-kinases. Their greatest similarity is displayed in their *in vitro* and *in vivo* lipid substrate specificity. The structure of the Class IB catalytic subunit shares many of the motifs and domains of the Class IA enzymes with a high degree of conservation in the C-terminal catalytic domain, C2 and ras-binding domains. The differences between the 2 subclasses become more apparent when comparing the N-terminal portions of the catalytic subunits and the functional consequences of these differences. Sequence analysis illustrates very little identity between the Class IA and Class IB catalytic subunits at the N terminus. Consistent with this finding Class IB PI3-kinases do not associate with any p85 subunits of the Class IA subfamily. A putative adaptor for the Class IB PI3-kinases has been cloned and termed p101. In contrast to the Class IA, the Class IB catalytic subunit demonstrates PI3-kinase activity independently of the presence of an adaptor protein and therefore the association of p101 with PI3kγ has not yet been proven to be essential. PI3-kinase activity is abolished with pretreatment of cells with pertussis toxin and insensitive to tyrosine kinase inhibitors. At present, the theorised model of PI3kγ activation involves the ligation of GPCRs with a concomitant activation of Gβγ (Figure 1.6). The production of 3-phosphorylated lipids, like Class IA PI3-kinases, results in the activation of various second messengers via the release of activated G protein subunits and production of 3-phosphorylated lipids (Figure 1.6). Although it has been demonstrated that several effector functions are activated upon stimulation of PI3kγ, the precise pathway of signals that separate these from the Class IA signalling pathways are presently unclear.

1.2 The Chemokine Gene Superfamily

Regulation of biological systems in the mammalian body is maintained by the coordinated expression of various extracellular messengers. The chemokine (chemotactic cytokine) gene superfamily is one large family of such messengers. The chemokine superfamily is now accepted as an essential component of leukocyte recruitment and trafficking within the immune system. While chemokines have also been implicated in the regulation of a wide range of physiological systems of the body, examples include embryonic development, haematopoiesis and angiogenesis, this review will focus on the data established on the function of this superfamily in the immune system with particular emphasis on leukocyte trafficking.

1.2.1 Structure and Function of members of the Chemokine Superfamily

Genes are assigned to the chemokine gene superfamily on the basis of both structure and function. Structurally, chemokines can be subdivided into 4 groups. These assignments are based on the nature and form of a cysteine signature motif in the primary amino acid structure. The subfamilies are termed C-X-C, C-C, C and C-X_3-C (where X denotes an intervening amino acid between the first two cysteines in the motif) or alternatively as α, β, γ and δ respectively. Depending on the presence or absence of an ELR (glutamine-leucine-arginine) motif prior to the first cysteine, the C-X-C chemokines can be further divided into ELR and non-ELR chemokines (as reviewed in (Baggiolini, 1998; Gale & McColl, 1999). Functionally, the chemokines can be broadly divided into two categories: the inflammatory/inducible chemokines and the constitutive/homeostatic chemokines. Data to date indicate that most

chemokines involved in innate immunity and that affect myeloid cell migration and function fall into the former category, whereas chemokines in both of these categories are involved in adaptive immunity, particularly with respect to lymphocyte movement.

1.2.1.1 Chemokines involved in myeloid cell trafficking and function.

The majority of members of the chemokine superfamily are inducible chemokines that are rapidly upregulated during inflammation in response to a range of extracellular stimuli. Inducible chemokines are secreted by resident cells at the site of inflammation as well as by infiltrating leukocytes in response to inflammatory mediators such as lipopolysaccharide (LPS), tumour necrosis factor alpha (TNFα) and interleukin-1. The upregulated expression of inflammatory chemokines acts to recruit cells such as monocytes, granulocytes and effector T cells to peripheral organs. IL-8 and MCP-1 were the first chemokines identified based on their ability to induce migration of neutrophils and monocytes, respectively (Walz *et al.*, 1989; Yoshimura *et al.*, 1995). Although most inflammatory chemokines display activity towards myeloid cells the potency of these factors suggests that their primary biological role is in the rapid promotion of myeloid cell accumulation during protective inflammation. However, the detection of high levels of expression of these chemokines in various chronic inflammatory disorders has also been associated with infiltration of leukocytes and subsequent host tissue damage. The presence of IL-8 and MCP-1 has been documented in the synovial fluid from the joints of patients suffering from rheumatoid arthritis (Koch *et al.*, 1992). The use of antibodies against IL-8 in a rabbit model of lung reperfusion led to a marked decrease in the migration of neutrophils into the site as well as a decrease in tissue damage (Sekido *et al.*, 1993). In addition, neutralising

antibodies against inflammatory/inducible chemokines as well as antagonists against inflammatory/inducible chemokine receptors has been shown to inhibit myeloid cell recruitment to peripheral sites of inflammation (Coates & McColl, 2001; McColl & Clark-Lewis, 1999; Tessier *et al.*, 1997; Tessier *et al.*, 1998).

Inflammatory/inducible chemokines as a family have also been implicated in recruitment/activation of all other cells of myeloid origin, including eosinophils, basophils, mast cells and dendritic cells. The cell specificity of these chemokines is illustrated in Table 1.1.

1.2.1.2 Chemokines involved in lymphoid cell trafficking and function.

Adaptive immunity in higher organisms is maintained by lymphocytes which fundamentally differ from other cells of the immune system in that they recirculate. Lymphocyte recirculation enables the adaptive immune system to achieve three critical functions: retention of the cells that provide the T and B cell receptor repertoires that are critical for the ability of the adaptive immune system to protect higher organisms from a diverse range of microbial antigens; localisation of lymphocytes to centres of antigen-presentation; and a distinction between naïve and memory/activated lymphocytes that enables secondary immune responses to occur rapidly in peripheral tissues outside secondary lymphoid organs. For this system to function effectively, lymphocytes must be able to migrate to correct locations. This phenomenon, known as lymphocyte homing, is controlled by an intricate molecular network that involves both inflammatory/inducible chemokines and the constitutive/homeostatic chemokines (Figure 1.8 Gale & McColl, 1999).

Generation of an adaptive response requires recirculation of naïve lymphocytes from the peripheral blood through the secondary lymphoid organs. Similarly, the movement of antigen-presenting cells (APCs) bearing antigen from peripheral sites to secondary lymphoid organs is also required. It is in the T cell zones of these secondary lymphoid organs that naive T lymphocytes are able to encounter APCs presenting cognate antigen resulting in the generation of effector T lymphocytes that then migrate out of secondary lymphoid organs to peripheral tissues. Recent data indicate that circulation and recirculation of naive and memory/activated lymphocytes clearly requires alterations in the ability of these cells to respond to chemokines in the two functional categories (Figure 1.8).

The constitutive/homeostatic chemokines appear to fulfil a critical "housekeeping" role within the body, particularly in the recirculation of naive lymphocytes through secondary lymphoid organs. Members of the constitutive chemokine family include SDF-1α, -1β, MDC, TARC, ELC, SLC and BCA-1 (Table 1.1).

Studies *in vitro* have shown that naïve T and B lymphocytes express chemokine receptors CXCR4 (Oberlin *et al.*, 1996) and CCR7 (Bleul *et al.*, 1996) and therefore migrate towards the ligands SDF-1 and, SLC and ELC, respectively. Naïve B cells also express CXCR5 and respond to BCA-1. These chemokines are expressed constitutively in secondary lymphoid organs and act to recruit naïve T and B cells to the T cell zones and follicular B cell zones, respectively. Mice in which the SDF-1 gene has been disrupted survive only a few days post birth. Within this period of time

it is clear that both myelopoiesis and lymphopoiesis are severely restricted (Nagasawa *et al.*, 1996). In light of the latter observations it has been suggested that the constitutive chemokine SDF-1 is also associated with the development of myeloid and lymphoid precursors in addition to having an important role in the recirculation of lymphocytes in the periphery. A pivotal role for the chemokine receptor CCR7 and its ligands SLC and ELC has been demonstrated *in vivo* in the mutant plt (paucity of lymphoid tissues) mouse. These mice exhibit a genetic defect that results in no production of SLC and dramatically reduced production of ELC in secondary lymphoid tissues. As a consequence there is reduced movement of T cells into peripheral secondary lymphoid organs (Gunn *et al.*, 1999; Ngo *et al.*, 1999). Consistent with this, mice lacking CCR7, the receptor for SLC and ELC, also show reduced numbers of T cells in secondary lymphoid tissues, and a loss of secondary lymphoid structure. No difference in the B cell compartment was observed in either the plt or $CCR7^{-/-}$ mice (Forster *et al.*, 1999).

Naïve T cells also express a receptor for DC-CK1, a chemokine that is produced by follicular and interdigitating dendritic cells (Adema *et al.*, 1997; Hieshima *et al.*, 1997). This chemokine is thought to enhance the activation of naïve T cells during the initiation of an immune response by directing their migration towards APCs in the T cell zone.

Once naïve T cells have encountered the antigen-MHC complex in the T cell zones, they migrate towards the border of the T cell zone and B cell zone (Garside *et al.*, 1998). It is here that some T cells are believed to encounter antigen-primed B cells to complete their activation. As mentioned above, this movement appears to be

controlled by the expression of CXCR5 on T cells and B cells and the expression of its ligand, BCA-1, by stromal cells in the B cell follicles (Ansel *et al.*, 2000). Mice deficient in CXCR5, show a lack of B cell migration toward the primary follicles and germinal centres within the spleen and Peyers Patches, even though the B cells are able to enter the T cell areas of these organs (Forster *et al.*, 1996). The lymphoid organs were notably lacking germinal centres in secondary follicles and a low number of Peyers Patches were also observed in these mice. Together these data support an essential role for this non-ELR CXC chemokine (BCA-1) and its cognate receptor, CXCR5, in the homing of T and B lymphocytes to specific anatomical sites as well as in the formation of functional zones within the lymphoid organs.

Several other chemokines have also been associated with roles in lymphocytic homeostasis as well as in DC trafficking. For instance, Langerhans cells and epithelial dendritic cells express CCR6. As the ligand for CCR6, MIP-3α, appears to be constitutively-expressed in the dermis and epithelium, and CCR6 expression on these cells is believed to regulate the movement of DC precursors towards the epidermis in the skin and into epithelium in other tissues. Maturation of such cells results in downregulation of CCR6 and upregulation of CCR7. This is thought to allow DCs to migrate out of peripheral tissue, laden with antigen and migrate towards T cell compartments of secondary lymphoid organs in response to SLC and ELC (Dieu *et al.*, 1998).

During activation and maturation, naïve T cells are exposed to a milieu of cytokines, and it is the cytokine profiles that appear to drive and polarise of the effector T cell response. Recently, chemokine receptor expression following

activation has been studied with a particular focus on the expression patterns of Th1 verses Th2 effector cells. Overall, these patterns suggest that T cell activation in secondary lymphoid organs results in downregulation of chemokine receptors for constitutive/homeostatic chemokines and an upregulation of receptors for inflammatory/inducible chemokines. This presumably enables activated and memory T cells to adopt additional migratory patterns into and through peripheral tissues where inflammatory/inducible chemokines are being expressed (Moser & Loetscher, 2001).

Th1 effector cells, in general, secrete IL-12 and IFNγ. These cells promote a cell-mediated immune response toward intracellular pathogens. Th1 effector cells preferentially express CXCR3, the receptor for IP-10, Mig, and I-TAC, as well as CCR5, the receptor for MIP-1α, MIP-1β and RANTES. All three CXCR3 ligands are upregulated by IFNγ (Cole *et al.*, 1998; Farber, 1997; Luster & Rothenberg, 1997), while the CCR5 ligands are expressed predominantly in response to agents such as LPS, IL-1 and TNFα. The neurodegenerative disease, multiple sclerosis (MS), is a characteristic Th1 inflammatory disorder. Lesions in the CNS have been reported to show production of RANTES, and MIP-1α, MIP-1β and IP-10 (Godiska *et al.*, 1995; Karpus & Kennedy, 1997) in both MS and experimental autoimmune encephalomyelitis (EAE), the murine model of MS. Moreover, CCR5- and CXCR3-positive T cells have been found in inflammatory lesions in human MS (Balashov *et al.*, 1999; Simpson *et al.*, 2000). T lymphocytes expressing these receptors have also been found in other Th1 inflammatory diseases, including rheumatoid arthritis (RA) and psoriasis (Gerard & Rollins, 2001; Schon & Ruzicka, 2001). In an allogeneic

transplant model, another Th1-mediated response, carried out in mice deficient for CCR5, a 3-fold increase in graft survival time was observed. Furthermore, permanent engraftment was observed in $CXCR3^{-/-}$ mice treated with low doses of cyclosporin A (ref). Taken together, these findings suggest that CCR5, and CXCR3 expression may correlate with a Th1 phenotypic response (Hancock *et al.*, 2000a; Hancock *et al.*, 2000b).

Activated T cells selectively expressing chemokine receptors CCR3 and -4, when cultured *in vitro*, demonstrate secretion of cytokines IL-4 and IL-5. These cytokines, especially the secretion of IL-4, define the generation of a Th2 type response. The initiation of a Th2 response results in humoral or antibody-mediated immune responses that characterise immune responses to parasites and allergens. Th2 cells, or at least subsets of Th2 cells, are able to migrate towards chemokines such as eotaxin, eotaxin-2, and RANTES (ligands for CCR3), TARC and MDC (ligands for CCR4) (Bonecchi *et al.*, 1998; Sallusto *et al.*, 1998a; Sallusto *et al.*, 1998b) and I-309 (ligand for CCR8) (Napolitano & Santoni, 1999). CCR3 is the chemokine receptor whose expression has been most closely associated with a Th2 phenotype *in vitro*, and T cells bearing the CCR3 receptor have been localised with eosinophils in allergic inflammation (Gutierrez-Ramos *et al.*, 1999). While *in vitro* data indicate that Th2 lymphocytes migrate in response to MDC and TARC, a role for CCR4 in Th2 cell migration and activation *in vivo* has also recently been called into question. Mice deficient in CCR4 develop normal bronchial hyperresponsiveness to OVA challenge (a Th2-dependent immune responses) (Chvatchko *et al.*, 2000). It is of course possible that like CCR3, CCR4 plays a subtle role in Th2-mediated immune responses, or that it plays no role in the OVA-challenge model (Chensue *et al.*, 2001;

Gerard & Rollins, 2001). In contrast to the above data, mice deficient in CCR8 show reduced ability to mount Th2-dependent immune responses (*Schistosoma mansoni* soluble egg antigen granuloma formation as well as OVA and cockroach antigen-induce allergic airway inflammation) (Chensue *et al.*, 2001). Considerably more study is required to verify or refute the importance of these receptors for inflammatory/inducible chemokines in Th2-dependent immune responses.

In summary, while the constitutive chemokines maintain a basal level of T cell trafficking and recirculation, as well movement of surveillance cells such as macrophages and dendritic cells from the systemic circulation into tissues, the inducible chemokines collectively play an important role in the migration of activated/memory T lymphocytes as well as in the rapid recruitment of myeloid cells to peripheral tissues.

1.2.2 Chemotactic Factor Receptors

All chemokine receptors are G protein-coupled receptors (GPCR). GPCRs constitute a family of integral membrane proteins, characterised by seven hydrophobic membrane-spanning domains, also commonly referred to as serpentine or seven transmembrane receptors. The expression of these receptors is extensive throughout all biological systems including both plants and animals. Their diverse range of ligands include taste and odourant molecules, hormones and neurotransmitters, and chemotactic factors including chemokines (Gerard & Gerard, 1994; Murphy, 1994).

As with all receptor proteins, the primary function of GPCRs lies in the transmission of information from the extracellular environment to the interior of the cell. Unlike many other cytokine receptors, seven transmembrane receptors do not possess intrinsic protein kinase activity or the ability to recruit such activity immediately downstream of ligand binding. Uniquely, the downstream transmission of signals post-receptor activation is mediated through the interaction between these integral membrane proteins and heterotrimeric G proteins.

G proteins are a trimeric complex comprising α, β and γ subunits. Molecular cloning has revealed the existence of 17 Gα genes, these have been further subdivided into four classes G_i, G_s, G_q and G_{12}. Adding to this diversity are the multiple genes that give rise to at least 4β subunits and 7γ subunits. The ability of these proteins to form different heterotrimers provides the opportunity to create a vast repertoire of G protein complexes that mediate signalling events downstream from the various GPCRs (Birnbaumer., 1992).

In the resting state within the cell, GPCRs lie independently of the G protein complex. At this stage GDP is associated with the α subunit. Upon ligand binding, the receptor undergoes a conformational change and through its cytoplasmic tail and the second intracellular loop associates with the G protein. This interaction leads to the dissociation of GDP from the α subunit, and the subsequent association of GTP. The resultant activation of the G protein induces a conformational change in the α subunit that is thought to mediate the dissociation of the G protein complex from the receptor and of the α subunit from the βγ subunit. These subsequently act as intracellular

second messengers via their ability tot bind to, and activate other enzyme systems including PI3kγ. The dissociation of the G protein subunits returns the receptor to a resting state. The receptor is now able to repeat the cyclic activation (Birnbaumer., 1992; Bourne *et al.*, 1991).

1.2.3 The Chemokine Receptors

All the presently cloned chemokine receptors are GPCRs. Many of these chemokine receptors specifically exhibit the DRYLAIV sequence, a region involved in G protein binding, particularly Giα in the second intracellular loop (Gerard & Gerard, 1994; Murphy, 1994). Examination of the association of chemokine receptors with G proteins shows a bias toward coupling to the $G_{i\alpha}$ subunit, a subunit sensitive to inhibition by pertussis toxin. As a consequence, many of the functions attributed to the chemokines *in vitro* and *in vivo* are inhibited by pertussis toxin.

1.2.4 Chemotactic Factor Receptor Signalling

Only a very schematic view of chemokine receptor signalling is available at present. Much of what is understood is based on studies of signal transduction occurring in response to other chemoattractants such as fMLP, LTB_4, PAF and C5α. Following chemoattractant ligation to its receptor, various second messenger systems are activated. These include the mobilisation of intracellular calcium induced following the activation of phospholipase C, arachidonic acid metabolism which occurs following the activation of phospholipase A_2, phospholipase D activation and

extensive activation of protein and lipid kinases including the PI3-kinases (McColl & Neote, 1996).

Most chemotactic factors have been shown to stimulate the production of rapid increases in intracellular free calcium. The use of agents that directly stimulate G proteins such as various GTP analogues and fluoride, and an inhibitor of G protein activation, pertussis toxin, have illustrated the link between GPCRs and the mobilisation of calcium and the subsequent stimulation of effector functions (Brandt *et al.*, 1985). PLC is responsible for the metabolism of PIP_2 to IP_3 and DAG. IP_3 is able to bind specific receptors within the cell and release calcium which in turn stimulates the translocation of protein kinase C to the plasma membrane, where it is activated by DAG. Other calcium-dependent protein kinases are also activated, and together, this plays a critical role in leukocyte effector function (Berridge & Irvine, 1989).

The transient increase in intracellular calcium also activates PLA_2. The liberation of arachadonic acid and lyso-PAF as a result of PLA_2 activation leads to the formation of prostaglandins and leukotrienes, or PAF respectively (McColl *et al.*, 1991; McDonald *et al.*, 1993). This can subsequently generate a range of chemotactic factors, and vasoactive lipids. This system is also capable of autocrine amplification (McDonald *et al.*, 1993). The latter may suggest that this amplification can serve a dual purpose in not only increasing the chemotactic factor gradient but also maintaining the activation of the cells producing these factors.

1.2.5 Chemotactic factor signalling and PI3kγ activation

The PI3-kinase family is one of the more recently-identified downstream second messenger systems of chemotactic factor signalling. Originally, a great deal of attention focussed on the Class IA enzymes due to the knowledge that tyrosine phosphorylation occurred rapidly following GPCR activation, and that pretreatment with wortmannin inhibited several well-established chemotactic factor-induced effector functions (Vlahos *et al.*, 1995). However, the use of tyrosine kinase inhibitors failed to inhibit chemotactic factor-induced PI3-kinase activation, suggesting that PI3-kinase activation was not dependent on tyrosine phosphorylation. Futhermore, pertussis toxin completely blocked PI3-kinase activity induced by chemotactic factors (Stephens *et al.*, 1996; Stephens *et al.*, 1994b). These characteristics moved attention more towards a possible involvement of other PI3-kinase isoforms or an alternate regulatory pathway for known PI3-kinase isoforms in chemotactic factor signalling. The search for another isoform led to the cloning and isolation of human PI3Kγ (as described in section 1.1.5). The use of chemical inhibitors and dominant-negative expression systems support the involvement of PI3Kγ in GPCR signalling. Al-Aoukaty and coworkers subsequently showed a physical association between Gβγ subunits, pleckstrin and PI3Kγ following natural killer (NK) cell activation with chemokines. Microinjection of polyclonal anti-PI3Kγ antibodies into NK cells inhibited their ability to migrate in response to various chemokines (al-Aoukaty *et al.*, 1999). This was the first cellular system that illustrated PI3Kγ to be a key enzyme involved in leukocyte chemotaxis following chemotactic factor receptor ligation.

During the latter stages of the present study, three groups independently published data generated using mice in which the PI3kγ gene had been disrupted (Hirsch *et al.*, 2000a; Li *et al.*, 2000; Sasaki *et al.*, 2000). Remarkably, in contrast to the observations made upon disruption of various Class IA PI3-kinase genes, all three types of PI3kγ knockout mice were phenotypically normal, fertile and demonstrated life spans comparable to wild-type mice. Studies by Sasaki and Hirsch initially characterised the leukocyte compartments of the PI3kγ$^{+/-}$ mice in comparison to PI3kγ$^{-/-}$ mice. Knockout mice generated by Sasaki and colleagues showed significant increases in the number of neutrophils, monocytes and eosinophils in both the spleen and peripheral circulation. However, thymocyte numbers were significantly reduced in these mice. In contrast, the PI3kγ knockout mice generated by Hirsch and colleagues only demonstrated a difference in the number of circulating neutrophils which were two-fold higher in comparison with wild-type mice. Neutrophils from all three PI3kγ$^{-/-}$ mice were unable to generate PI 3,4,5 P_3, the main cellular product of PI3kγ activation, following chemotactic factor stimulation of GPCRs. *In vitro* assays examining PI3kγ–deficient neutrophil motility in response to fMLP, C5α, and IL-8 demonstrated a significant decrease in migration. Consistent with this *in vitro* observation, recruitment of neutrophils into the peritoneal cavity in response to bacteria and thioglycollate was also impaired (Hirsch *et al.*, 2000a; Li *et al.*, 2000). Neutrophils from wild-type and PI3kγ$^{-/-}$ mice adhered to fibronectin as strongly as each other suggesting that the lack of migration was due to the inability of these cells to rearrange their cytoskeleton rather than an inability to adhere to endothelial cells. Chemotaxis of PI3kγ–deficient macrophages towards the chemokines RANTES, SDF-1, and MDC was also reduced (Hirsch *et al.*, 2000a). Lymphocytic

choriomeningitis virus (LCMV)-induced swelling of the footpad was used to examine functional responses of the T cell compartment. Wild-type mice developed effective footpad swelling following infection with LCMV, however, the PI3kγ-/- mice displayed reduced footpad swelling at the similar time points suggesting a role for PI3kγ in the generation of Th1 immunity. In contrast, cytotoxic responses of these T cells towards LCMV *in vitro* were normal in the PI3kγ-/- mice. Immunisation with the hapten NIP coupled to ovalbumin suggested that PI3kγ was important in the generation of T helper cell-dependent responses to haptens *in vivo* (Sasaki *et al.*, 2000). It is important to note that interpretation of all of studies on T cell-mediated immunity outlined above may be meaningless because these experiments were carried out in knockout mice that displayed developmental defects in the thymic compartment, therefore possibly biasing the true T cell response to antigen load.

In summary, these PI3kγ–deficient mice, while displaying significant differences in their leukocyte compartments, confirmed a critical link between GPCR stimulation and chemotaxis. The inability of neutrophils and macrophages to migrate and induce the respiratory burst in response to chemotactic factors indicates a clear role for PI3kγ in chemotactic factor signalling and the reduced thymic cellularity observed in PI3kγ-/- mice imply a role for PI3kγ in T cell development. However, further studies are required to determine whether the T and B cell responses to antigen and T and B cell migration *in vivo* is dependent on PI3kγ.

1.3 Rationale, Hypothesis and Aims

Rationale

The present study commenced soon after the cloning of the human and porcine orthologues of PI3kγ (Stephens *et al.*, 1997; Stoyanov *et al.*, 1995). At this time very little was understood regarding the *in vivo* importance of this enzyme. Functional and structural studies had emphasised the probable importance of G protein subunits in PI3kγ activation and therefore its involvement in leukocyte effector function downstream of GPCR signalling.

All aspects of the immune system require the continuous regulation of cellular movement. The chemokines have been shown to be an important family of molecules that mediate the recruitment of cells of the immune system to various compartments throughout the body. The chemokine receptors fall into the well-characterised group of integral membrane proteins known as GPCRs. Recent data have clearly implicated PI3kγ in chemotactic factor-induced leukocyte migration *in vitro* (ref) and, studies using mice genetically-deficient in PI3kγ have illustrated the involvement of PI3kγ in the ability of cells of the innate immune system to migrate in response to chemotactic factors *in vitro* and to extravasate from the peripheral circulation into tissues during inflammation *in vivo*. However, there is still very little understanding of the influence that this lipid kinase has on the migration of cells of the adaptive immune system, especially lymphocytes. Furthermore, because of the developmental defects observed in the lymphocyte compartment in PI3kγ$^{-/-}$ mice, the physiological impact that PI3kγ has on mounting an effective adaptive immune response has not yet been elucidated.

Hypothesis

The central hypothesis of this study is that PI3kγ is essential for the migration of lymphocytes *in vitro* and *in vivo*.

Aims

In order to address this hypothesis, four broad aims were generated:

1. To clone the murine orthologue of PI3kγ.
2. To characterise the clone *in vitro* by examining its expression patterns, lipid and protein kinase activities.
3. To generate a catalytically-inactive form of PI3kγ and, using this, develop a mammalian dominant-negative over-expression system.
4. To use this expression system to examine the impact of PI3kγ on migration of lymphocytes *in vitro* and *in vivo*.

Figure 1.1 The general structure of phosphoinositide lipids

All Phosphoinositide lipids demonstrate a general structure consisting of an inositol ring with 5 hydroxyl groups (-OH) attached at positions 2-6. A phosphodiester bond (P) is located at position 1 on the inositol ring. The inositol headgroup is attached via the phosphodiester bond to a phospholipid tail.

Figure adapted from Fruman *et al*, 1999.

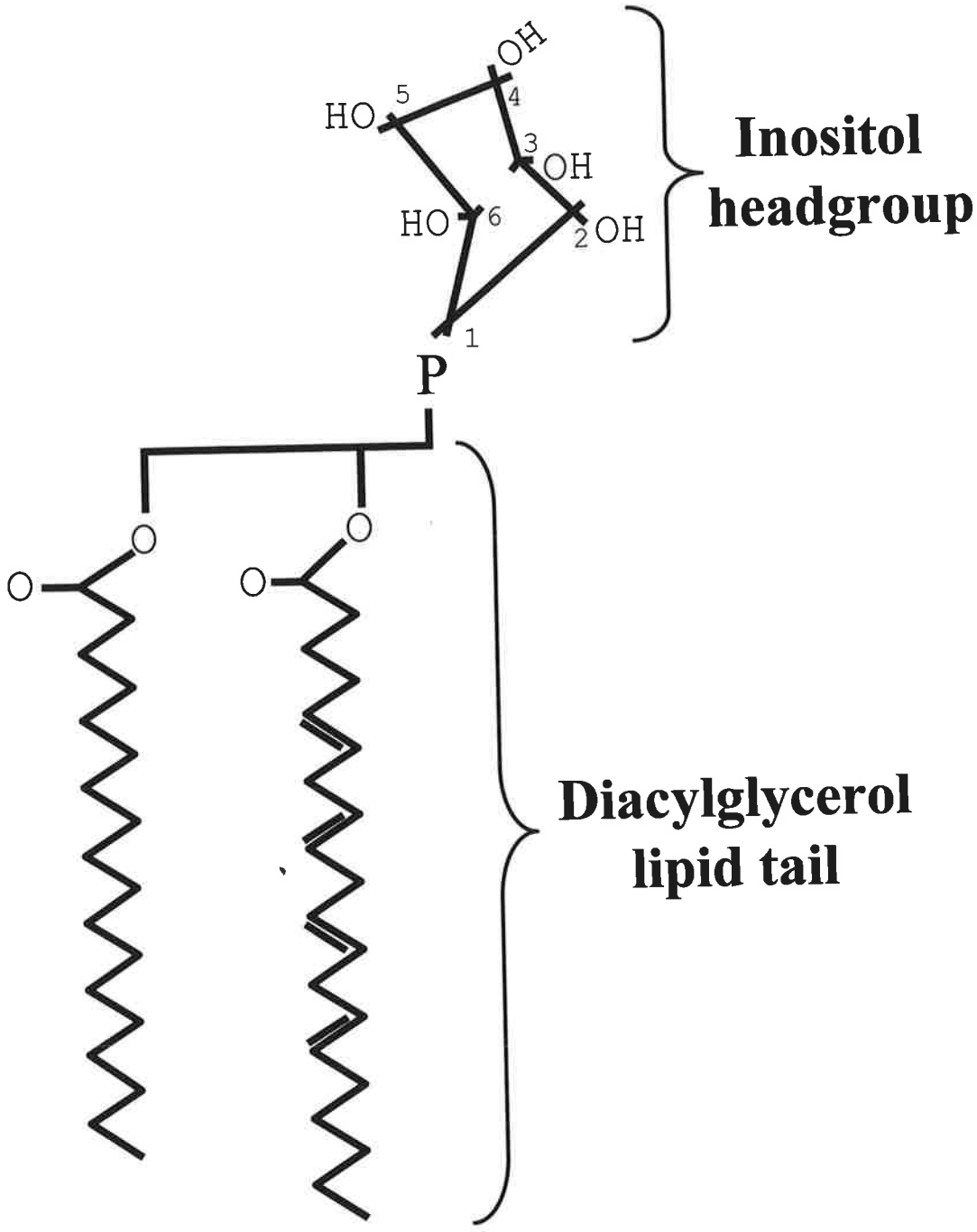
OH
HO
5
4
3
OH
HO
6
2
OH
1
Inositol
headgroup
P
O
O
O
O
Diacylglycerol
lipid tail

Figure 1.2 Substrates and phosphorylated products of the PI3-kinase family

The PI3-kinase family are responsible for phosphorylating phospholipids at the 3-OH position of the inositol ring. The inositol headgroups of the 3 lipid substrates, PI, PI 4 P and PI 4,5 P_2, are illustrated on the left and their phosphorylated products PI 3 P, PI 3,4 P_2 and PI 3,4,5 P_3 are respectively indicated on the right. Phosphorylated hydroxyl groups are represented by red (filled) circles. PTD – phospholipid tail.

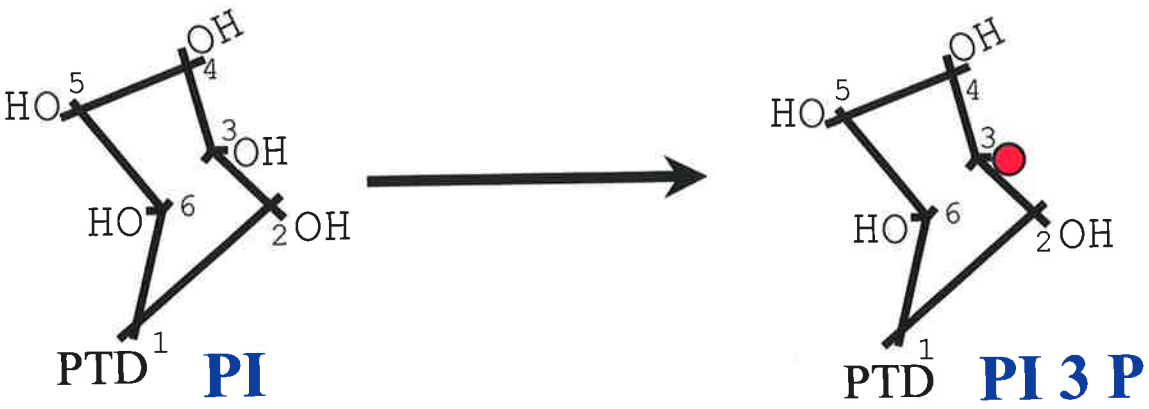
HO
5
OH
4
3
OH
HO
6
2
OH
PTD
1
PI
HO
5
OH
4
3
HO
6
2
OH
PTD
1
PI 3 P

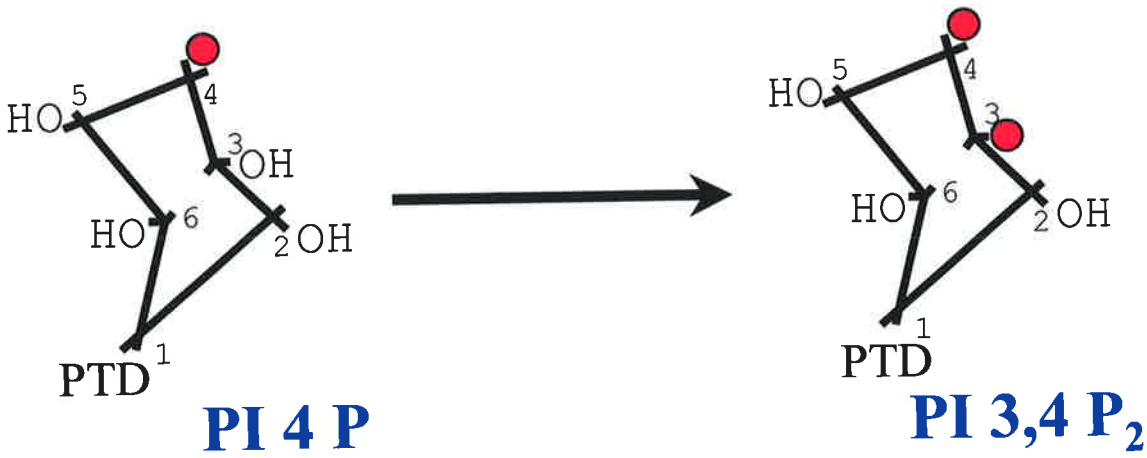
HO
5
4
3
OH
HO
6
2
OH
PTD
1
PI 4 P
HO
5
4
3
HO
6
2
OH
PTD
1
PI 3,4 P2

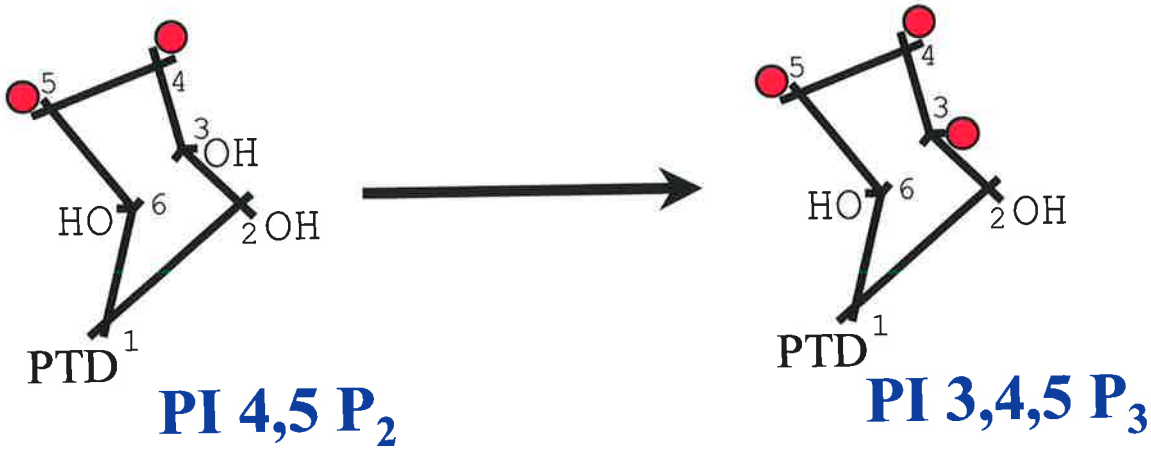
5
4
3
OH
HO
6
2
OH
PTD
1
PI 4,5 P2
5
4
3
HO
6
2
OH
PTD
1
PI 3,4,5 P3

Figure 1.3 Modular structure of representative members of the PI3-kinase family

The family of PI3-kinases share a great degree of conservation across the functional domains present in each subfamily. Presented are the representative members of the regulatory and catalytic subunits of each subfamily. The protein domains for the subunits are as follows: solid rectangles – catalytic domain; solid ovals – PI-kinase domain; open ovals – ras-binding domain; hatched oval - BH homology domain; hatched rectangle – SH2 domain; hatched circle – SH3 domain; solid diamonds – proline-rich motif; hatched diamonds – C2 domain; open diamond – PX domain; saw-toothed line – p85 interaction domain.

Figure taken from Fruman *et al,* 1999.

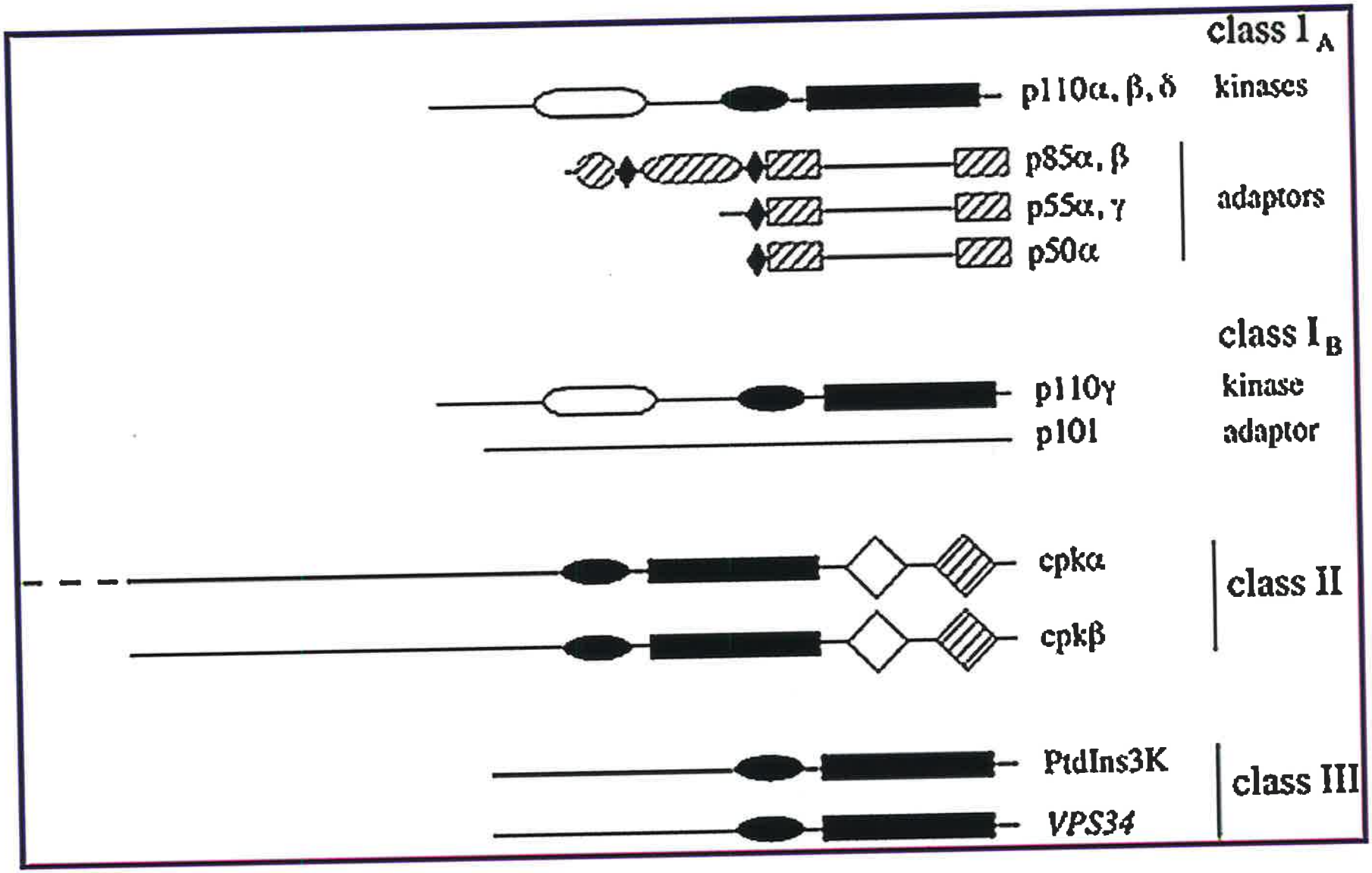
class I A
p110α, β, δ
kinases
p85α, β
p55α, γ
p50α
adaptors
class I B
p110γ
kinase
p101
adaptor
cpkα
cpkβ
class II
PtdIns3K
VPS34
class III

Figure 1.4 Ribbon diagram of the structure of PI3kγ

Based on the crystallographic structure of porcine PI3kγ the ribbon structure of PI3kγ is presented (Walker *et al.,* 1999). PI3kγ contains all 4 homology regions found in all Class I PI3-kinases. The structure consists of 4 domains : a ras-binding domain, a C2 domain, a helical domain and a catalytic domain.

Ribbon diagram taken from Walker *et al.,* 1999.

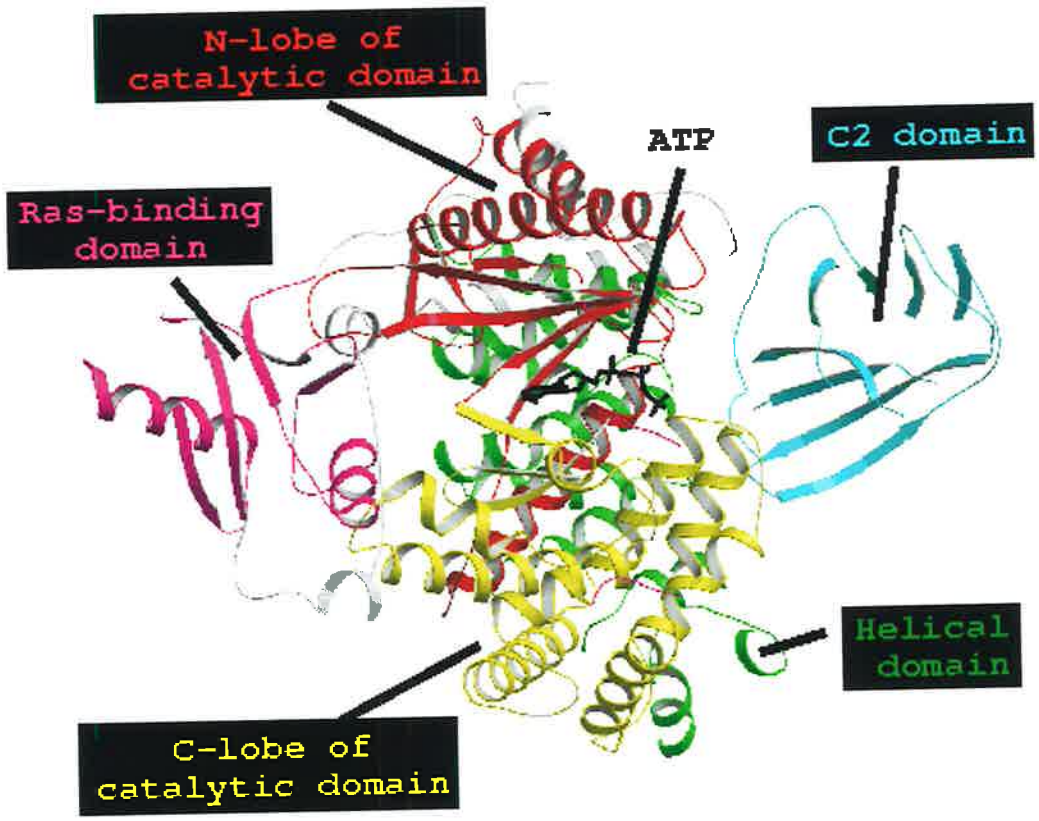
N-lobe of catalytic domain
ATP
C2 domain
Ras-binding domain
Helical domain
C-lobe of catalytic domain

Figure 1.5 Cellular responses downstream of 3-phosphorylated lipid production

The diagram represents the proteins that have been shown to bind 3-phosphorylated lipids *in vitro*. Production of PI 3 P (Ptd Ins (3) P), PI 3,4 P_2 (Ptd Ins (3,4) P), and /or PI 3,4,5 P_3 (Ptd Ins (3,4,5) P) is likely to result in the recruitment of several signalling molecules and the activation of downstream secondary messenger systems. The cellular responses that may be activated are represented in red at the base of the pathways.

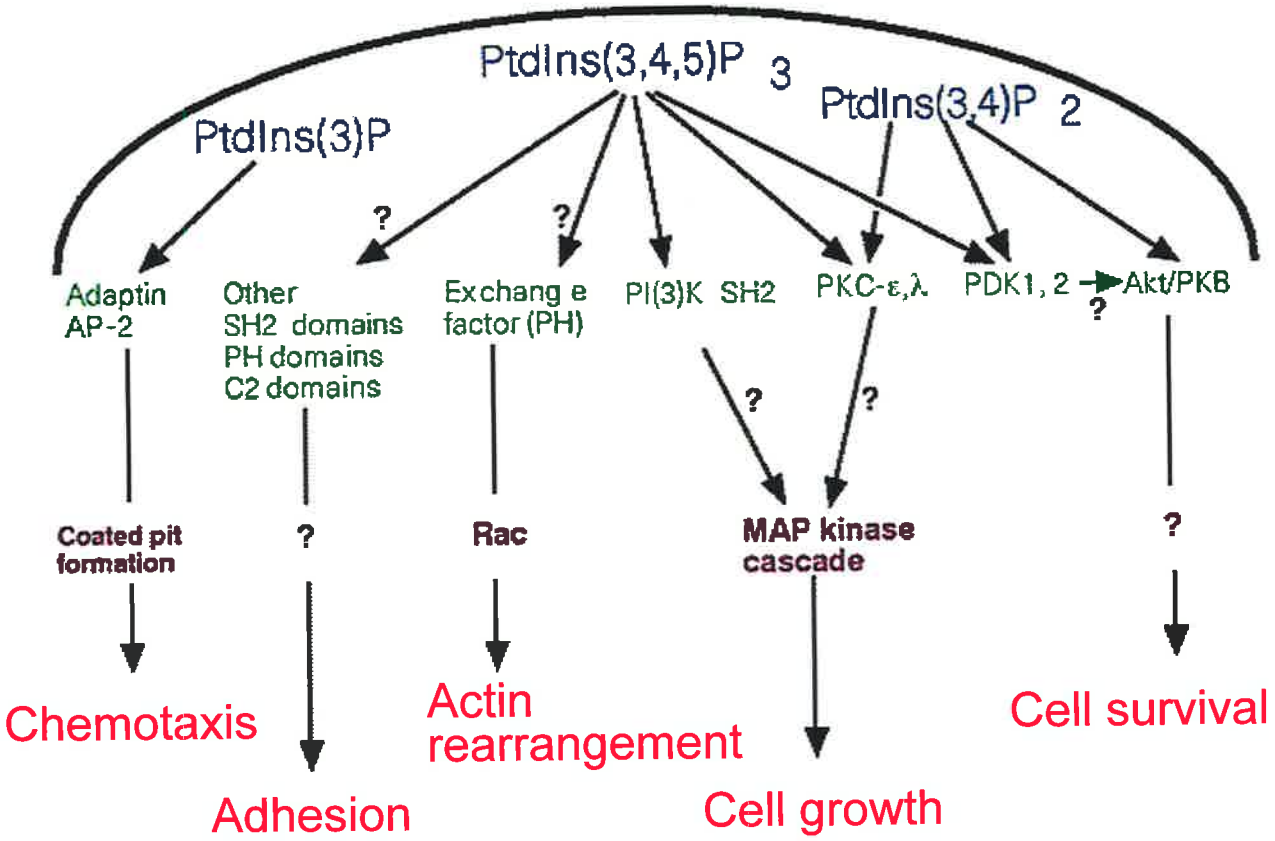
PtdIns(3,4,5)P 3
PtdIns(3)P
PtdIns(3,4)P 2
?
?
Adaptin AP-2
Other SH2 domains PH domains C2 domains
Exchang e factor (PH)
PI(3)K SH2
PKC-ε,λ
PDK1, 2
Akt/PKB
?
?
?
?
Coated pit formation
?
Rac
MAP kinase cascade
?
Chemotaxis
Adhesion
Actin rearrangement
Cell growth
Cell survival

Figure 1.6 Signalling pathways downstream of Class IA and Class IB PI3-kinase activation

Leukocytes are known to possess both Class IA and IB PI3-kinases. Class IB PI3-kinases are activated by G protein-coupled receptors such as chemokine receptors, while PTK's activated downstream of Fc receptors, C3b and most cytokine receptors stimulate the Class IA PI3-kinases. The phospholipid products of these enzymes are generally considered to bind PH domain-containing proteins and activate various second messengers. Some of these include small GTPases such as RAC which is involved in membrane ruffling, the respiratory burst and chemotaxis in granulocytes. Increases in intracellular calcium and the production of diacylglycerol (DAG) are involved in the respiratory burst, but not chemotaxis. The pathways linking proteins such as PKC, PKB and other PTKs with leukocyte functions such as actin polymerisation and secretion are not as well-understood in these cells.

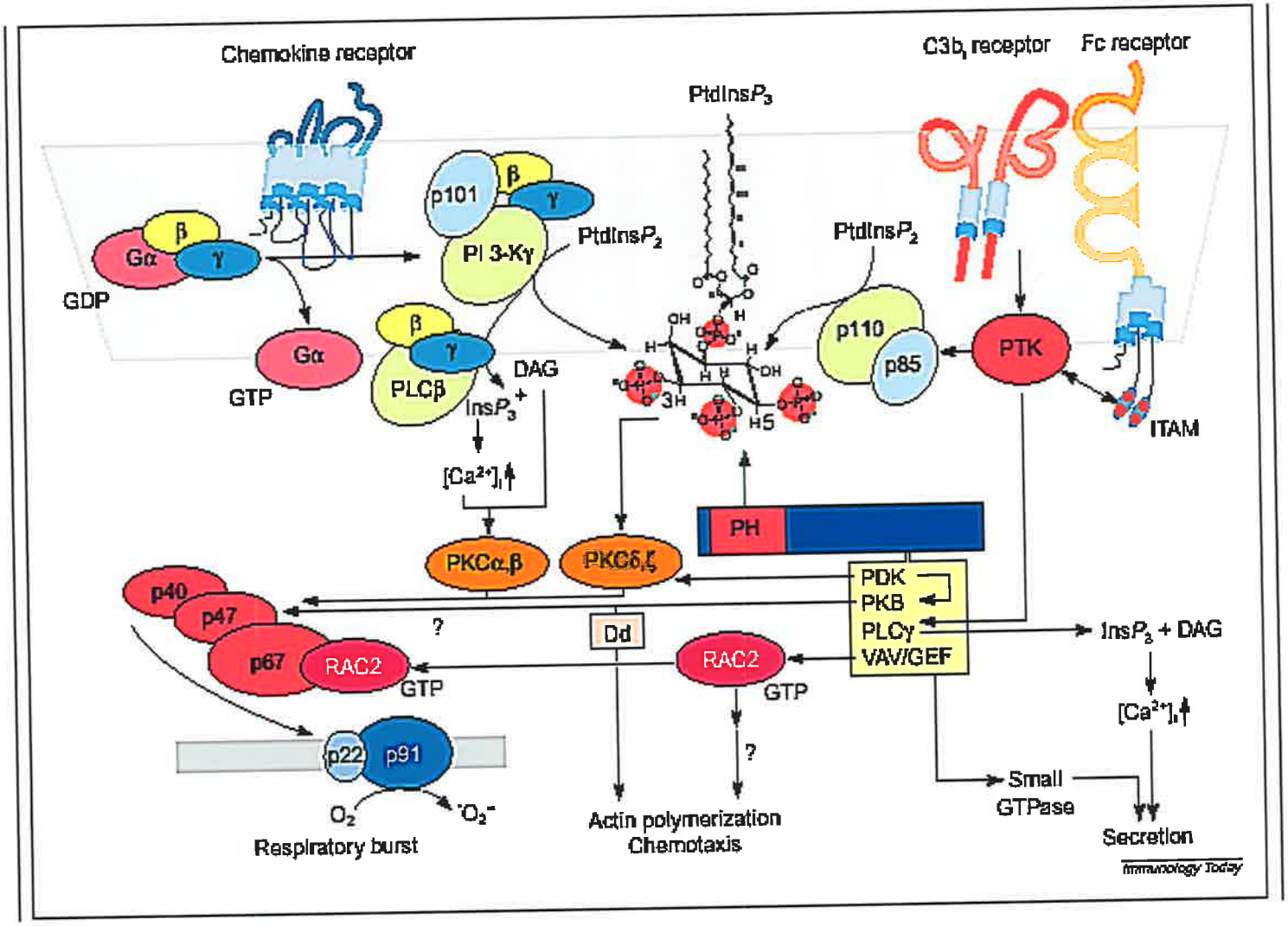
Chemokine receptor
C3b, receptor
Fc receptor
PtdInsP3
p101
β
γ
Gα
GDP
PI 3-Kγ
PtdInsP2
PtdInsP2
p110
p85
PTK
ITAM
GTP
PLCβ
DAG
InsP3 +
[Ca2+]i
3H
H5
PH
PKCα,β
PKCδ,ζ
PDK
PKB
PLCγ
VAV/GEF
InsP3 + DAG
p40
p47
p67
RAC2
GTP
?
Dd
RAC2
GTP
[Ca2+]i
p22
p91
O2
·O2-
Respiratory burst
Actin polymerization
Chemotaxis
?
Small
GTPase
Secretion
Immunology Today

Table 1.1 Functional classification of chemokines and chemokine receptors into inducible/inflammatory and constitutive/homeostatic subfamilies.

Inducible/inflammatory chemokines and their cognate receptor(s) are represented in blue. The constitutive/homeostatic chemokines and their cognate receptor(s) are represented in pink. Chemokines and their receptor(s) belonging to both subfamilies are represented in green.

Table adapted from Moser and Loetscher, 2001.

	CHEMOKINES	RECEPTOR/S	FUNCTIONS
INDUCIBLE/ INFLAMMATORY	I-TAC, MIG, IP-10	CXCR3	Effector T cells
	CXCL16	CXCR6	Effector T cells
	RANTES, MIP-1α	CCR1	Effector T cells
	MCP-1, MCP-2, MCP-3, MCP-4	CCR2	Effector T cells
	Eotaxin-1, -2, -3, RANTES, MCP-2, MCP-3, MCP-4, MEC	CCR3	Effector T cells
	RANTES, MIP-1α, MIP-1β	CCR5	Effector T cells
	I-309	CCR8	Effector T cells
	Fractalkine	CX_3CR1	Effector T cells
	MDC, TARC	CCR4	Effector and memory T cells
	MIP-3α	CCR6	Effector and memory T cells, B cells
CONSTITUTIVE/ HOMEOSTATIC	CTACK, MEC, CCL28	CCR10	Memory T cells
	SDF-1	CXCR4	Naïve, memory T cells, B cells, thymocytes
	BCA-1	CXCR5	Follicular B helper T cells, B cells
	SLC, ELC	CCR7	Naïve, central memory T cells, B cells
	TECK	CCR9	Memory T cells, B cells, immature thymocytes
	DC-CK1	unknown	Naïve T cells

Figure 1.7 Selective expression of chemokines and chemokine receptors during the generation of the adaptive immune response

(1)Monocytes and immature DCs are recruited to sites of antigen challenge. (2) Pathogen-induced signals induce the maturation of DCs and and associated switch in receptor expression. (3) DCs migrate to T cells zones in secondary lymphoid tissues via afferent lymphatics. (4) Naïve T and B cells migrate to the B and T cell areas of the lymph node via high endothelial venules (HEVs). (5) T cells interact with the mature DCs and become activated. (6) Effector T cells are then able to migrate to B cell areas where stimulation of antigen specific B cells takes place. (7) and (8) Th1 or Th2 cells migrate to peripheral sites of DTH and allergic reactions.

Figure taken from Sallusto *et al.,* 1998.

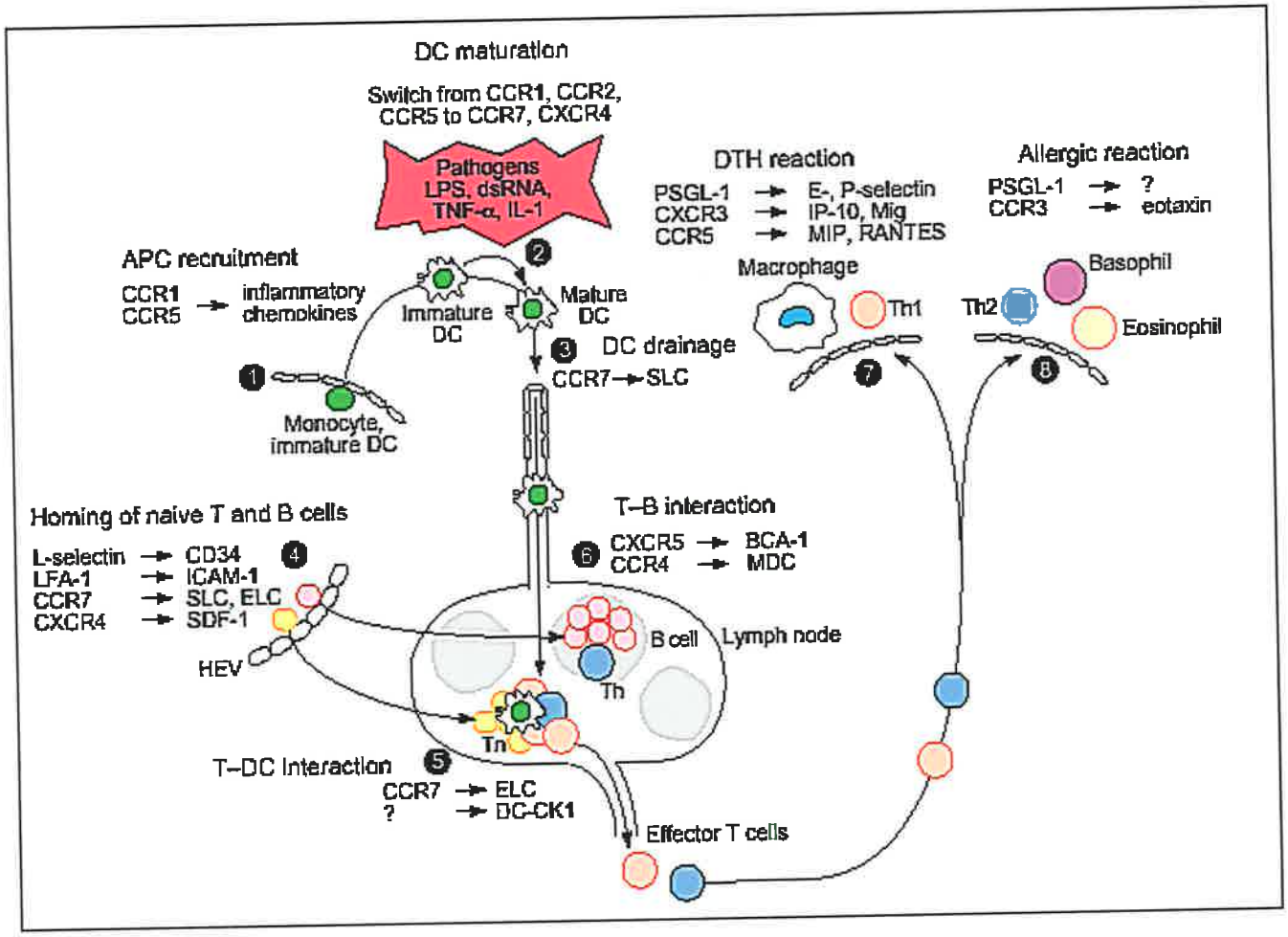
DC maturation
Switch from CCR1, CCR2, CCR5 to CCR7, CXCR4
Pathogens LPS, dsRNA, TNF-α, IL-1
APC recruitment
CCR1
CCR5
inflammatory chemokines
Immature DC
Mature DC
Monocyte, immature DC
DC drainage
CCR7 → SLC
DTH reaction
PSGL-1 → E-, P-selectin
CXCR3 → IP-10, Mig
CCR5 → MIP, RANTES
Macrophage
Th1
Allergic reaction
PSGL-1 → ?
CCR3 → eotaxin
Basophil
Th2
Eosinophil
Homing of naive T and B cells
L-selectin → CD34
LFA-1 → ICAM-1
CCR7 → SLC, ELC
CXCR4 → SDF-1
HEV
T–B interaction
CXCR5 → BCA-1
CCR4 → MDC
B cell
Lymph node
Th
Tn
T–DC Interaction
CCR7 → ELC
? → DC-CK1
Effector T cells

Chapter Two

Reagents and Techniques

2.1 MOLECULAR TECHNIQUES

2.1.1 Bacterial strains, growth media and buffers

***E.coli* DH5α** - F'*/endA1 hsdR17*($r_K^- m_K^+$) sup*E44 thi-1 recA1 gyrA* (Nal^R) *relA1 a(lacZYA-argF)*$_{U169}$*(m801acZμM15)*

XL1-Blue - *endA1 hsdR17*($r_K^- m_K^+$) sup*E44 thi-1 recA1 lambda*$^-$ *gyrA96 relA1 lac*$^-$ *[F', proAB, lac19 ZμM15 Tn10(tet*^{R}*)]*

Luria Bertani (LB) Broth: 10 g Bacto-tryptone (Difco Laboratories, MI, USA), 10 g NaCl and 5g Bacto-yeast (Difco Laboratories) were dissolved in MQ water. The pH was adjusted to 7.0 with 1M NaOH and the volume adjusted to 1L prior to autoclaving.

TAE: 40 mM Tris-acetate and 1mM EDTA in MQ water. Prepared as a 50x stock solution consisting of 242 g Tris Base (Astral Scientific, N.S.W, Australia), 57.1 mL glacial acetic acid and 100 mL 0.5M EDTA pH 8.0. Solution was autoclaved and diluted to 1x in MQ water prior to use in agarose gel electrophoresis.

Orange G Loading Dye: Loading dye was prepared as a 6x stock solution. Seventy mg Orange G (Sigma, St Louis, USA) was dissolved in 30% sucrose (w/v in MQ water) and filter sterilised. Aliquots were stored at 4°C.

Chemicals: All chemicals used in this study were obtained from BDH AnalaR Merck, Victoria, Australia, unless otherwise stated.

2.1.2 Preparation of Competent Cells

To prepare competent cells for bacterial transformation, a single colony of *E.coli* DH5α from a luria bertani (LB) agar plate was inoculated into 10mL of LB broth and grown at 37°C for 16 hours with agitation. This was added to 100 mL LB broth and incubated for a further $1^{1/2}$-2 hours until an OD_{600} of 0.3-0.4 was obtained. The culture was immediately chilled on ice and centrifuged at 3750 rpm (Beckman Benchtop Centrifuge, GS-6R) for 10 min. Following the complete removal of supernatant, the pellet was resuspended in 10 mL Solution A (KAc 30mM, KCl 100mM, $CaCl_2$ 10mM, $MnCl_2$ 50mM, Glycerol 15%) and incubated on ice for 10 min. After centrifugation the pellet was resuspended in 1mL of Solution B (MOPS 10mM, $CaCl_2$ 75mM, KCl 10mM, Glycerol 15%), and incubated on ice for a minimum of 4 hours. One hundred µL aliquots were snap frozen and stored at -70°C until further use.

2.1.3 Preparation of Phenol

Crystallized phenol was melted at 65°C and 8-hydroxyquinoline was added to a final concentration of 0.1%. Phenol was equilibrated with an equal volume of 0.5M Tris-Base buffer followed by repeated washes in 50mM Tris-HCl pH 8.0 until the pH of the aqueous phase reached 8.0. The equilibrated phenol was stored in 50mM Tris-HCl pH 8.0 buffer at 4°C.

2.1.4 Phenol/Chloroform extraction

DNA solutions were extracted using equal volumes of phenol and chloroform (200 µL for small scale plasmid preparations and 300 µL for larger scale preparations). Solutions were mixed vigorously by shaking and the phases separated by centrifugation at 14,000 rpm, for 5 min at RT. The upper aqueous phase containing the DNA was removed and placed into a sterile 1.5 mL eppendorf tube (Treff Lab, Switzerland) followed by the addition of 2.5 -3 volumes of 100% ethanol. This was then incubated at -20°C for a minimum of 30 min. DNA was pelleted by centrifugation at 14,000 rpm for 20-30 min at -9°C. The pellet was washed carefully with 70% ethanol (w/v) and dried *in vacuo*, prior to being dissolved in the required volume of MQ water.

2.1.5 Agarose Gel Electrophoresis

Electrophoresis of DNA was carried out using 1.2% agarose (w/v in TAE) for product sizes of ~1kb and higher, while 2.0% agarose (w/v in TAE) for products smaller than ~1kb. Agarose gels were run in 1x TAE at 100 mA in a horizontal gel apparatus. Gels were stained in ethidium bromide solution (2 µg/mL in 1x TAE) for 5 min, briefly destained and visualised by 254 nm short wave UV light and photographed using Tracktel GDS-2 gel documentation system (Vision Systems, Australia).

2.1.6 Bacterial Transformation

A frozen aliquot of competent cells was allowed to defrost on ice for 10 min prior to the addition of 500 ng recombinant plasmid or a ligation reaction in a volume <30 µL. These were mixed gently and incubated on ice for a further 30-45 min. Cells were then heat shocked at 37°C for precisely 3 min and immediately placed on ice. One mL of LB Broth was added to the cells and incubated with agitation for 30-45 min at 37°C for the induction of the relevant antibiotic resistance gene. Cells were centrifuged at 5,000 rpm (Eppendorf Centrifuge, 5417R) for 7 min. The pellet was resuspended in 100 µL of LB broth and spread onto the appropriate LB agar plate. Plates were incubated in an inverted position for 16-20 hours at 37°C.

2.1.7 Mini-Preparation (small scale) of Plasmid DNA

The following procedure gave sufficient quantity and quality of plasmid DNA for several restriction analyses and sequencing reactions from 1.5 mL of a stationary phase culture. All centrifugation in this protocol was carried out in an Eppendorf Refrigerated Centrifuge, 5417R.

A single colony of bacteria containing plasmid was inoculated in 10mL LB broth and grown overnight at 37°C with the required antibiotic selection. One and a half mL of stationary phase bacteria was centrifuged (14,000 rpm, 2 min, RT) and the pellet resuspended in 100 µL of TES (25 mM Tris-HCl pH8.0, 10 mM EDTA, 15% w/v sucrose). After 5 min incubation on ice, 200 µL of freshly prepared 0.2M NaOH 1%

SDS were added and the tube gently inverted 4-5 times followed by a further 5 min incubation on ice. 3M Na Acetate, pH 4.6 (150 µL) were added and once again mixed gently and placed on ice for 10 min. This mixture was centrifuged (14,000 rpm, 5 min, 4°C) to remove chromosomal DNA. The plasmid DNA was then thoroughly extracted using phenol chloroform (see 2.1.4) and the phases separated by centrifugation (14,000 rpm, 5 min, RT). The plasmid DNA was then precipitated by the addition of 2.5 volumes of 100% ethanol (see 2.1.4). The pellet was washed using 70% ethanol (w/v in MQ water), dried *in vacuo* and redissolved in 20 µL MQ water. RNase A (final concentration 50µg/mL) was added, and the solution incubated for 30 min at RT.

2.1.8 Medium - Scale Preparation of Plasmid DNA

A single colony of bacteria containing plasmid was inoculated in 50mL LB broth containing the required antibiotics and grown overnight at 37°C. Bacteria were pelleted by centrifugation (3,750rpm, 10 min) and the pellet resuspended in 2.5mL TES (25mM Tris-HCl pH 8.0, 10mM EDTA, 15% sucrose). Five mL of freshly prepared 0.2M NaOH, 1% SDS were added and mixed gently by inversion and the tube placed on ice for 10 min. The mixture was then centrifuged at 15,000 rpm for 15 min at 4°C (JA-20 rotor) to remove the chromosomal DNA. The supernatant was placed in a fresh tube, 50 µL of 10mg/mL RNase A, and 20 µL of 10mg/mL proteinase K were added and incubated at 37°C for 60 min. The DNA was precipitated by the addition of 6mL isopropanol and the DNA pelleted by centrifugation at 10,000 rpm, for 15 min at 4°C (Beckman JA-20 rotor). The DNA

was dissolved in 300 µL of 0.3M NaAc pH 5.2, thoroughly phenol/chloroform-extracted twice and the phases separated by centrifugation (14,000rpm, 5 min, RT). Plasmid DNA was then precipitated by the addition of 2.5 volumes of 100% ethanol. The pellet was washed with 70% ethanol, dried *in vacuo* and dissolved in 50 µL MQ water. DNA was incubated at RT for 30 min prior to quantitation.

2.1.9 Restriction Endonuclease Digestion

DNA was digested with the desired restriction endonucleases (New England Biolabs, MA, USA) in a 10-50 µL volume comprising DNA, 5-10 Units of restriction enzyme/µg of DNA, 1x restriction enzyme buffer (specific for each restriction enzyme) and sterile water for 1-12 hours at the appropriate temperature. Reactions were terminated either by heat inactivation at 65°C for 10 min, BRESA-Clean, or by the addition of DNA loading dye which was added immediately prior to analysis by gel electrophoresis.

2.1.10 Dephosphorylation of vector DNA

To prevent self-ligation of the vector 5'-terminal phosphate groups were removed by incubation with calf intestinal alkaline phosphatase (CIP, Boehringer Mannheim, Germany). In a standard reaction 0.5 µg DNA were incubated with 0.5 units of CIP and 1x CIP buffer (50mM Tris-HCl pH 9.0, 1mM $MgCl_2$, 0.1mM $ZnCl_2$). The reaction was carried out in a final volume of 100 µL at 37°C for 30 min. The CIP was inactivated prior to ligation by heating the reaction to 75°C for 10 min.

2.1.11 DNA Ligations

Restricted, phosphatased plasmid vector (50-100ng) was ligated with the DNA fragment to be cloned in a 3:1 molar ratio of insert:vector. Ligations were carried out in a volume <30 µL, containing 50mM Tris-HCl pH 7.5, 10mM $MgCl_2$, 10mM DTT, 1mM rATP, and T4 DNA ligase (1-2 Units). The mixture was incubated at 4°C overnight prior to transformation in the appropriate bacterial strain.

2.1.12 BRESA-Clean™

This procedure was carried out as per manufacturers protocol (Geneworks, Australia). In the case of DNA in solution, 3 volumes of BRESA-SALT solution were added and mixed by inversion. In the case of DNA that was excised from agarose, the weight of the excised band was measured and a volume of BRESA-SALT solution corresponding to 3 volumes of the gel fragment was added. The agarose was dissolved at 55°C for 5 min.

Following vigorous resuspension of BRESA-BIND by vortexing, 5 µL BRESA-BIND were added to the DNA solution and incubated for 5 min at RT. Regular inversion was maintained to ensure an even suspension. Following a short centrifugation the supernatant was removed and the BRESA-BIND/DNA complex washed with 1mL of BRESA-WASH. This mixture was centrifuged and the pellet air-dried. DNA was eluted by the addition of a volume of MQ water equivalent to twice the volume of the

BRESA-BIND matrix used earlier, and incubated at 50°C for 5 min. Following a short centrifugation the supernatant containing the DNA was collected whilst carefully avoiding the matrix.

2.1.13 Mutagenesis

Site directed mutagenesis of plasmid template was carried out based on the Quikchange Mutagenesis Kit (Stratagene, La Jolla, CA, USA).

2.1.13.1 Primer design

Mutagenic primers were designed based on the following considerations:

- both mutagenic primers contained the desired mutation and annealed to the same sequence on opposite strands of the plasmid;
- primers were between 25 and 45 bases in length;
- Tm of primers were ~10°C above the extension temperature of 68°C using the following formula to calculate Tm:
  - Tm = 81.5 + 0.41(%GC) - 675/N - %mismatch
  - N = primer length in base pairs
  - the desired mutation (insertion, deletion or change) was ideally in the middle of the primer with a minimum of 10 bases on either side;
- primers optimally had a minimum GC content of 40% and terminated in one or more C or G bases;
- primers were of the highest synthesized purity.

2.1.13.2 Mutagenesis Reaction

Plasmid DNA template for mutagenesis was amplified in a 50 µL reaction comprising 1x reaction buffer (10mM KCl, 10mM NH_4SO_4, 20mM Tris-HCl pH 8.8, 2mM $MgSO_4$, 0.1% Triton X-100, 0.1 mg/mL BSA), 50 ng plasmid DNA template, 125 ng of each mutagenic primer, 2mM dNTP mix, 2.5 Units PFU DNA polymerase and sterile water. Reactions were conducted in a thermal cycler according to the following parameters: 30 sec at 95°C, followed by 16 cycles of 30 sec at 95°C, 1 min at 55°C, 2 min/kb of plasmid at 68°C. Reactions were cooled to 4°C prior to the addition of 10 Units of *Dpn*I restriction endonuclease, and incubated overnight. A further 10 Units of *Dpn*I were added, incubated for another 3 hours, and 10 µL of the final reaction were used to transform DH5α competent bacterial cells.

2.1.14 cDNA Library Screening

2.1.14.1 Preparation of Host cells

E.coli XL-1 Blue bacterial cells were streaked out onto LB agar plates containing tetracycline (20 µg/ml). These plates were only kept for a maximum of 5 days, after which a fresh streak plate was prepared. Plating cultures were prepared by inoculating a single colony into 10 mL LB broth supplemented with 0.2% maltose and 10mM $MgSO_4$ at 37°C overnight with vigorous agitation. Cells were centrifuged at 1,000g for 10 min and the pellet gently resuspended in 0.5 volumes of 10mM $MgSO_4$. Just prior to use, cells were diluted to OD_{600} 0.5 with 10mM $MgSO_4$.

2.1.14.2 Library Plating

Nutrient agar plates for this procedure were made 2 days in advance to allow adequate removal of excess moisture. Five hundred µL of XL-1 blue bacteria were gently mixed with 100 µL of phage dilution and incubated at 37°C for 30 min. This mixture was then transferred to 12mL (150mm agar plates) or 7mL (70mm agar plates) of top agarose (0.7% agarose, 10mM $MgSO_4$, 0.2% maltose) and cooled to 48°C. The tube was gently and efficiently inverted to mix, and poured evenly over the bottom agar. Once the top agarose had set, plates were incubated in an inverted position at 37°C for 6-8 hours. Plates were refrigerated (4°C) for a minimum of 2 hours to prevent the top agar sticking to Hybond filters during plaque lifts.

2.1.14.3 Plaque Lifts

Hybond N^+ filters (Amersham Pharmacia Biotech, NJ, USA) were labelled with a ballpoint pen in 2 areas, and placed face down (ink side up) on cold LB plates. Filters were placed in one smooth movement to prevent any bubbles forming between the filter and the agarose. The original filter was left on the plate for 7 min whereas duplicate filters were placed on the plate for 10 min to ensure adequate transfer of plaques. Filters were removed from plates and placed DNA side up on 3mm Whatmann paper to air dry for a minimum of 10 min.

2.1.14.4 DNA Denaturation and Fixing

Separate containers were lined with 3mm Whatmann paper. The first container was saturated with 0.2M NaOH/1.5M NaCl, the second with 0.4M Tris-HCl, pH 7.6/2x SSC, and the third with 2x SSC. Filters, DNA side up, were placed in each container (in order) for 2 min. Filters were subsequently dried in a vacuum oven at 80°C for 90-120 min. Filters were stored between Whatmann paper at RT until used for hybridisation.

2.1.14.5 Radiolabelling DNA probes

DNA probes for library screening were made according to manufacturer's instructions using the Megaprime DNA labelling System (Amersham Pharmacia Biotech). Briefly, the required DNA was diluted to 5 ng/μL in distilled water. Template DNA (25 ng) was mixed with 5 μL of primers, and denatured at 95°C for 5 min. At RT, 4 μL of each unlabelled nucleotide, 5 μL of 10x reaction buffer, 2 μL enzyme and water for a final volume of 45 μL were added. Finally, α-P^{32}dNTP (5 μL, 3000Ci/mmol) was added and mixed gently. This mixture was incubated at 37°C for 10 min. The reaction was terminated by the addition of 5 μL of 0.2M EDTA. Removal of unincorporated nucelotides was carried out using a Sephadex G-50 spin column. The labelled probe was stored at -20°C until required and denatured at 95°C for 5 min prior to use in hybridisation.

2.1.14.6 Hybridisation

Filters were soaked in prehybridisation solution (5x SSPE, 5x Denhardts, 0.5% SDS, 100 µg/mL denatured, sonicated salmon sperm DNA) and incubated at 65°C in siliconised glass bottles for a minimum of 4 hours. Following prehybrisation, the denatured labelled probe was added to the pre-hybridisation solution and incubated overnight at 65°C in a hybridisation oven. Filters were transferred to a sealed container and washed in 0.2 x SSC/0.1% SDS at 65°C for 1 hr. Wet filters were covered in plastic wrap and positive plaques detected by autoradiography (exposed overnight at -70°C).

2.1.15 RNA Isolation

RNA was isolated using the recommended protocol accompanying the Trizol reagent (Gibco BRL Life Technologies, Rockville, MD, USA). In the case of RNA extraction from tissues, 50 g of tissue was homogenised in 1 mL of Trizol. RNA extraction from cells in suspension (5-10x10^6cells) involved centrifugation of the cells and resuspension of the pellet in 1 mL Trizol. The cell/trizol mixture was incubated at RT for 5 min prior to the addition of 200 µL chloroform. After vigorous shaking, the mixture was incubated for a further 2-3 minutes at RT. Centrifugation at 12,000g for 15 min at 4°C generated 2 phases. The upper aqueous phase was transferred to a clean 1.5 mL eppendorf tube and the extraction of phases was repeated with 400 µL of DEPC water. RNA from both extractions was precipitated separately by the addition of 500 µL of isopropanol, followed by a 10 min incubation at RT. The precipitate was

then centrifuged at 12,000g for 10 min at 4°C. The pellet was washed carefully in 70% ethanol and semi-dried. RNA was dissolved in 20 µL of DEPC-treated water and incubated at 55°C for 10 min for complete resuspension. RNA purity was determined by measuring optical density at 260nm and 280nm, and calculated using the formula below:

$$\text{Purity} = OD_{260}/OD_{280}$$

$$\text{concentration of RNA (µg/µL)} = OD_{260} \times \text{dilution factor} \times 0.04$$

2.1.16 Generation of First Strand cDNA - Reverse Transcription

Generation of first strand cDNA from RNA was conducted using 'Superscript II' reverse-transcriptase (GibcoBRL, Life Technologies). One µL of random hexamer primers (500 µg/ml; Amersham Pharmacia Biotech) was combined with 2.5 µg of total RNA. The volume was adjusted to 12 µL with DEPC-treated MQ H_2O, and heated to 70°C for 10 min followed by incubation on ice. While still at 4°C, the following were added: 4 µL first strand buffer (5x stock), 2 µL DTT (0.1 M), 1 µL 10 mM dNTP mix (10 mM each dATP, dTTP, dCTP, dGTP diluted in DEPC-treated sterile MQ H_2O). The contents of the tube were mixed gently, centrifuged briefly and incubated for 2 min at 42°C. Finally, 1 µL of 'Superscript II' (200 U/µL) was added and mixed. The reaction was incubated at 42°C for 50 min and terminated by heating to 70°C for 15 min. The cDNA products were stored at –20°C until further use.

2.1.17 PCR - Taq Polymerase Based Amplification

In a standard PCR amplification, cDNA was synthesised in a 25 µL volume comprising DNA template (1.25 µL first strand synthesised cDNA, or 100ng plasmid DNA), 1x amplification buffer, 2.5mM $MgCl_2$, 25 pmol of both the forward and reverse primer, 200µM dNTPs, 0.25 µL Amplitaq GOLD (Perkin Elmer) and sterile water. Reactions were initiated in a hot-bonnet thermal cycler (MJ Research, Geneworks, Adelaide, S. Australia). In general, reactions were denatured at 95°C for 12 min, then subjected to 30-35 cycles of denaturation at 95°C for 30 sec, primer annealing at 55-70°C (specific for each primer set) for 1 min, and primer extension at 72°C for 1 min/kb DNA to be amplified. A final 10 min extension at 72°C was performed. Following this, reactions were held at 4°C.

2.1.18 PCR - Amplification using PFU polymerase

Pfu DNA polymerase was employed for amplification of DNA when high fidelity was required. DNA was amplified in a 25 µL reaction comprising DNA template (1.25 µL of first strand synthesis cDNA or 100 ng plasmid DNA), 30 pM each forward and reverse primer, 300 µM dNTPs, 1x Pfu reaction buffer (20mM Tris-HCl pH 8.75, 10mM KCl, 10mM $(NH_4)_2SO_4$, 2mM $MgCl_2$, 0.1% Triton X-100, 0.1mg/mL BSA) and 2.5 units Pfu polymerase (Stratagene, La Jolla, CA, USA). Reactions were generally denatured for 2 min, and then subjected to 35 cycles of denaturation at 95°C for 30 sec, primer annealing at 55-70°C (specific for each primer set) for 45 sec and

primer extension at 72°C for 1.5 min/kb of DNA to be amplified. Reactions were held at 4°C prior to analysis or manipulation.

2.1.19 DNA Sequencing -Dye Terminator Sequencing

The ABIPRISM Dye Terminator Cycle sequencing reaction kit (Applied Biosystems, Roche, NJ, USA) was used to sequence alkaline lysis purified plasmid DNA. In a sequencing reaction, 8 µL terminator ready reaction mix (A, C, G, T-Dye terminator, dITP, dATP, dCTP, dTTP, Tris-HCl pH9.0, $MgCl_2$, thermal stable pyrophosphatase, Amplitaq polymerase) were added to 500 ng plasmid template and 3.2 pmol sequencing primer. The volume was adjusted to 20 µL using sterile water. The reaction was placed in a thermal cycler for 25 cycles of 96°C for 10 sec, 50°C for 5 sec, 60°C for 4 min. DNA was precipitated by the addition of 2 µL 3M NaAc pH4.6 and 50 µL 95% ethanol and incubated on ice for a minimum of 10 min. DNA was pelleted by centrifugation at 14,000 rpm for 25 min at -9°C. The pellet was gently washed in 70% ethanol and dried in vacuum. DNA was sequenced using a Perkin Elmer automated sequencer. IMVS sequencing facility, IMVS Adelaide, South Australia).

2.1.20 Primer design

Primers were, in general, designed to be 15-35bp in length (according to type of reaction) and to have a 50-55% GC content, ideally with high GC regions at the 3' end. Primer designer software (version 2.0; Scientific and Educational Software) was

utilised to analyse primer pairs for complementarity and melting temperatures. Primers were manufactured by Geneworks (Australia) and purified using reverse phase chromatography. Primers were received in a lyophilised form and diluted in sterile water and all stocks stored at -20°C.

2.1.21 Primers

NAME	SEQUENCE (5' to 3')	APPLICATION
p110γNA-519	CTTCTGAGGAGACCTTGGCT	Sequencing
p110γNB-603	GGACCACGAGAGTGTGTTCA	Sequencing
p110γNC-460	CCGCAACCAATCCTGACAAG	Sequencing
p110γN1-565	TGCTGTGTGAAGTCCTGCAA	Sequencing
p110γN2-423	CCTTCGGATGCTTCAGGCTT	Sequencing
p110γN3-501	CCACACATTCCAGAGTACCT	Sequencing
p110γN4-453	CTTCTTGGCCATCTTGGTGA	Sequencing
p110γnestA	CTCCTGTGCAGGCTACTGTG	Sequencing
p110γnestb	GCTTGATATGTGGTGCTAGG	Sequencing
p110γnestc	GGCACTGAACACAAGCTCTG	Sequencing
T3	AATTAACCCTCACTAAAGGG	Sequencing
T7	GTAATACGACTCACTATAGGGC	Sequencing
p110γ-2157F	TGGCCAGATTCCTGCTGAAG	Sequencing
p110γ-2645R	GGCGCAGATCATCACCATGT	Sequencing
p110γ-1F	CGGAATTCGCCGCCGCATGGAGCTGG	RT-PCR
p110γ-1R	GGCACAGGTCCAGAGATTCA	RT-PCR
p110γ-2F	CTATCAGCAGCAGGTTCACA	RT-PCR
p110γ-2R	ACTCCAGCCACACATTCCAG	RT-PCR
p110γ2889F	GACTTCGGACACATTCTTGG	RT-PCR
p110γ3150R	GGCATTCCTGTCATCAGCAT	RT-PCR
p110-KRF	TCATCTTTAGACATGGTGATGATCTGCGC C	Mutagenesis
p110-KRR	GGCGCAGATCATCACCATGTCTAAAGATG	Mutagenesis

2.1.22 DNA Constructs

pBS (SK)::clone 1 - generated from phage excision of a positive clone from the λ zap murine macrophage cDNA library.

pBS (SK)::clone 2 - generated from phage excision of a positive clone from the λ zap murine macrophage cDNA library

pBS (SK)::clone 3- generated from phage excision of a positive clone from the λ zap murine macrophage cDNA library

pBS (SK)::clone 5- generated from phage excision of a positive clone from the λ zap murine macrophage cDNA library

pBS (SK)::clone 6- generated from phage excision of a positive clone from the λ zap murine macrophage cDNA library

pcDNA3::MmPI3kγ1100 – kindly provided by Matthias Wymann (Fribourg, Switzerland) (Hirsch *et al.*, 2000b). Consists of the coding region of muPI3kγ from nucleotides 360 to 3300.

pcDNA3::MmPI3kγ1111– generated by PCR amplifying the coding region of MmPI3kγ1111 with the engineered restrictions sites, *Bam*HI and *Xba*I, for subcloning into pcDNA3 (Invitrogen).

pcDNA3::MmPI3kγKR - generated by the site-directed mutagenesis of pcDNA3::muPI3kγ1111 at amino acid position 833, changing a lysine (K) residue to and arginine (R).

2.1.23 Molecular weight markers

Spp1 bacteriophage, *Eco*RI digested, and 100 bp molecular weight markers (125 ng; Geneworks, Australia) used in agarose gel electrophoresis. Fragment sizes of Spp1 markers are listed below.

FRAGMENT NUMBER	FRAGMENT SIZE (base pairs)
1.	8557
2.	7427
3.	6106
4.	4899
5.	3639
6.	2799
7.	1953
8.	1882
9.	1515
10.	1412
11.	1164
12.	992
13.	710
14.	492
15.	359
16.	81

2.1.24 Molecular Analysis Programs

All nucleotide and amino acid sequences were obtained from the GenBank Database at the National Centre for Biotechnological Information (NCBI). DNA formatting and translations were carried out using DNASIS (version 7.0). Mutiple alignments were generated using CLUSTAL W (www.microbiology.adelaide.edu.au/learn/index.htm). All restriction analysis was conducted using the Webcutter Program version 2.0.

2.2 *IN VITRO*/CELLULAR TECHNIQUES

2.2.1 Agonists

Recombinant human MIP-3α was a generous gift from Dr Ian Clark-Lewis, (The Biomedical Research Center, University of British Columbia, Vancouver, Canada). Stock was maintained at 1mg/mL and further diluted prior to use in *in vitro* and *in vivo* techniques.

2.2.2 Maintenance of cell lines

Cell lines were routinely maintained in sterile plastic flasks (Falcon, Becton Dickinson Labware, England, UK), in either RPMI or DMEM (Gibco BRL), as indicated in the table below, at 37°C in a humidified atmosphere containing 5% CO_2.

The B300.19-huCCR6 cell line was a kind gift from Bernhard Moser (Theodor-Kocher Institute, Bern, Switzerland).

CELL LINE	CULTURE MEDIUM
J774 - murine macrophages	RPMI, 10% FBS,100 Units penicillin and gentamycin, 2mM L-glutamine, 20mM Hepes
NIH 3T3 - murine fibroblasts	DMEM, 10%FBS,100 Units penicillin and gentamycin, 2mM L-glutamine, 10mM Hepes
HEK-293 - human embryonic kidney	DMEM, 10%FBS, 100 Units penicillin and gentamycin, 2mM L-glutamine, 10mM Hepes
EcoPack2-293 - retroviral packaging cells (based on HEK-293 cells)	DMEM, 10%FBS, 100 Units penicillin and gentamycin, 2mM L-glutamine, 10mM Hepes, 5mM sodium pyruvate
B300.19 - B cell lymphoma	RPMI, 10%FBS, 100 Units penicillin and gentamycin, 2mM L-glutamine, 10mM Hepes, 5mM sodium pyruvate, 0.1mM non essential amino acids, 55uM β-mercaptoethanol

2.2.3 Cryopreservation of cell lines

Cells were cryopreserved in the presence of 10% analytical grade dimethyl sulfoxide (DMSO) to prevent the crystallisation and fracturing of cell membranes. Cells were harvested when semi-confluent, and resuspended at 2 x 10^7cells/mL in fresh medium. Immediately prior to freezing, an equal volume of freezing mix (20% DMSO, 30% heat inactivated FBS, 50% appropriate medium, filter sterilised through a 0.22 μm filter) was added dropwise over a period of 5 min. This mixture was aliquoted into cryopreservation ampules (Nunc, Denmark) and control-rate cryopreserved. Frozen vials were stored in liquid nitrogen.

2.2.4 Thawing of cryopreserved cells

The appropriate medium was brought slowly to room temperature. The frozen vial was allowed to thaw at 37°C 5-10 min, after which medium was added in a dropwise fashion until resuspended. This was then transferred to a larger tube and supplemented with more medium and centrifuged at 1,500 rpm for 5 min. The cells were washed twice to ensure complete removal of DMSO, resuspended finally in the appropriate medium at 37°C and placed into culture.

2.2.5 Transient Transfection of Adherent Cell Lines- FuGENE 6 (Boehringer Mannhiem, Germany)

The day prior to transfection, cells were plated out at a density of 2 x 10^5 cells per 35mm dish and 5 x 10^5 per 60mm dish in 3 mL medium. On the day of transfection, 3 µL (35 mm) or 6 µL (60 mm) FuGENE 6 reagent were diluted in 100 µL of serum-free media, and incubated at RT for 5 min. This mixture was then added in a dropwise manner to 1 µg (35 mm) or 2 µg (60 mm) of plasmid DNA and incubated at RT for 15 min. The FuGENE 6/DNA complex was then added dropwise to the cells with gentle mixing. Expression analysis was examined 24-48 hours post transfection.

2.2.6 Electroporation of B300.19 B Lymphocytes

B300.19 cells were washed twice in PBS and resuspended at a concentration of 5 x10^6 cells/370 µl PBS. Cells were incubated on ice with 15-20µg of closed circular plasmid

DNA for 5 min. Cells were electroporated at 250V, 960 μF with a time constant between 38-43msec using a gene pulser (Biorad, CA, USA). Cells were placed on ice for 5-10 min, diluted 50-fold in pre-warmed RPMI/10% FCS and cultured for 48 hr under normal culture conditions. Forty eight hr post electroporation, cells were resuspended at 5 x 10^5 cells/mL in complete RPMI/10%FCS supplemented with 1.2mg/ml G418/Geneticin (Sigma). Cells were cultered under these conditions for 14 days and MmPI3kγ1111KR expression detected by western analysis.

2.2.7 One Colour Labelling for Flow Cytometry

Cells were resuspended to 4 x 10^6 viable cells/mL in PBS containing 1% bovine serum albumin (BSA; Sigma) and 0.04% sodium azide (mouse staining buffer). Fc receptors were blocked by incubating for 30 minutes at RT with 50μg of murine gamma-globulin (Rockland) per million cells, then 50μL of cells aliquoted into round-bottomed tubes. Cells were mixed with saturating concentrations of the mouse anti-CCR6 (clone 53103.111) monoclonal antibody (R&D Systems, Minneapolis, MN, USA) incubated for 30 minutes at RT and washed once with 3ml of mouse staining buffer prior to addition of biotin-conjugated anti-mouse detection antibody (Rockland Immunochemicals, Gilbertsville, PA, USA). Following a 30-minute incubation on ice, cells were washed with mouse staining buffer and the streptavidin:PECy5 conjugate (Caltag Laboratories, Burlingame, CA, USA) was added and incubated for a further 30 minutes on ice. Cells were washed with 3ml of mouse staining buffer followed by 3ml of protein-free staining buffer and fixed in 200μl of paraformaldehyde (1% in PBS; BDH Laboratory Supplies).

2.2.8 One Colour Flow Cytometry

Flow cytometry was conducted using a FACscan (Becton Dickinson, San Jose, CA) equipped with CellQuest Pro software version 3.1. Cell populations were gated on the basis of their forward scatter (FSC) and side scatter (SSC) profiles, and events were collected from the gate containing such cells. At least 10,000 events were collected from the total gated area.

The negative control was used to optimise instrument settings and determine background fluorescence levels. The background fluorescence was defined as that part of the negative peak which contained 98-99% of the recorded events occurring within a chosen gate.

2.2.9 Protein Precipitation

Transfected monolayers were collected for immunoprecipiation 48 hours post transfection.

Monolayers were washed twice with 1x PBS this was followed by the addition of 1 mL of cell lysis buffer (50mM Tris pH 7.4, 150mM NaCl, and 1.0% Triton X-100 and Complete protease inhibitor cocktail (Roche)). Dishes were incubated on ice for 20-30 min with continuous agitation. Lysates were centrifuged at 14,000rpm at 4°C for 10 min. Supernatants were transferred into fresh eppendorfs. Talon (Clontech) charged resin (30 μL) was incubated with the lysate for a minimum of 4 hours at 4°C. The

resin was washed twice in cold lysis buffer without protease inhibitors, followed by two washes in 1x PBS. Precipitated proteins were either heated in 2x sample buffer for SDS-PAGE analysis, alternatively used directly in the lipid kinase assay.

2.2.10 SDS-PAGE and Protein Transfer

Nine % polyacrylamide gels were cast and layered with a 5% stacking gel. Gels were assembled into a Hoefer gel apparatus tank with electrophoresis running buffer (25 mM Tris, 250 mM glycine). Samples were prepared for electrophoresis by the addition of an equal volume of protein loading dye and boiled for 8 min. Samples were immediately cooled on ice and loaded. Gels were electrophoresed at 15 mA through the stacking gel and 25 mA through the resolving gel. Following electrophoresis the gel was prepared for protein transfer. Polyvinylidine difluoride (PVDF; Millipore, MA, USA) and 6 sheets of 3 mm Whatmann paper were cut to the exact size of the gel. The PVDF membrane was pre-soaked in methanol for 30 sec prior to equilibrating in transfer buffer (49 mM Tris, 39 mM glycine, 0.04% SDS and 20% methanol). Whatmann sheets were also equilibrated in transfer buffer. For semi-dry transfer 3 Whatmann sheets were placed on the cathode, followed by the PVDF membrane. The gel was placed in one movement onto the PVDF and followed by the remaining 3 sheets of pre-soaked filter paper. Protein was transferred at 140 mA for 2 hours. The membrane was air-dried prior to western analysis to further fix the transferred proteins.

2.2.11 Western Analysis

PVDF membranes (Millipore) were rehydrated by soaking in methanol for 30 sec, followed by equilibration in 1x PBS. Membranes were blocked using 5% skim milk in PBS for 30 min at RT. Membranes were subsequently washed in 150 mL 1x PBS/0.5% Tween-20 for 5 min, followed by three 15 min washes once again using 150 mL 1x PBS/0.5% Tween-20. All antibodies were diluted in 1x PBS/0.5% Tween-20. The primary mouse anti-PI3kγ monoclonal antibody (Reinhard Wetzker, Germany) was used at a dilution of 1:100. The secondary, anti-mouse HRP antibody (Amersham Pharmacia Biotech) was used at a dilution of 1:1000. Enhanced chemiluminescence (Amersham Pharmacia Biotech), followed by autoradiography using X-OMAT imaging film, (Kodak, NJ, USA) was used to visualise proteins.

2.2.12 Lipid Kinase Assay

2.2.12.1 Preparation of Samples

Proteins were isolated from whole cell lysates as described in section 2.2.9. Proteins immobilised on beads or charged resin were washed three times in ice-cold 1x kinase buffer (20 mM Hepes, pH7.5, 5 mM $MgCl_2$, 1 mM EDTA). All samples were stored in kinase buffer on ice until required.

2.2.12.2 Preparation of Lipid Substrates

The lipid substrates were purchased as sodium salts (Sigma). A mixture of chloroform/methanol (95:5 v/v) was used to dissolve the salts. Stock solutions were made to a concentration of 10 mg/mL. Following reconstitution the stock solutions were stored under nitrogen, at –20°C in the dark.

To prepare lipid solution for the reaction, 20 µL of each lipid was transferred to a fresh eppendorf. The solvent was carefully held under a stream of nitrogen until ~5 µL remained. Lipids were resuspended in lipid resuspension buffer (20 mM Hepes, pH 7.5, 1 mM $MgCl_2$, 1 mM EGTA) with thorough mixing. This mixture was sonicated using a probe sonicator for 1 min on ice. Following sonication the lipid mixture was kept at RT to maintain the formation of micelles for 2 hr.

2.2.12.3 Enzyme Reaction

Samples to be tested were briefly centrifuged and the kinase buffer completely removed. Thirty µL of beads/resin were transferred to a fresh eppendorf. To this 20 µL of 5x kinase buffer, 2 µL of 2.5mM ATP (cold), and 1 µL of γ^{32}P-ATP were added in the precise order. Finally, 50 µL of the sonicated lipid mixture was incorporated to begin the reaction. Reactions were conducted at RT for 20 min.

2.2.12.4 Lipid Extraction

The reaction was terminated by the addition of 100 µL of 1M HCl. In order to extract the lipid products 200 µL of chloroform/methanol were added, followed by 500 µL of 2M KCl (previously saturated with chloroform). This was vortexed briefly and centrifuged at 13,000 rpm for 2 min. The lower, organic phase, was collected carefully to ensure no contamination from the resin interphase or the upper aqueous layer. Lipids were either used for thin layer chromatography immediately or stored at –20°C for a maximum of 48 hr.

2.2.12.5 Thin Layer Chromatography

Twenty four hr preceeding thin layer chromatography, the TLC plates were coated in oxalate. This was carried out by placing the TLC plate in a dish of oxalate dip (1% potassium oxalate, 2mM EDTA, 50% ethanol) for a maximum of 30 sec. The plate was left to air-dry overnight.

Prior to loading the plate, the chromatography chamber was equilibrated for a minimum of 2 hr using the chosen solvent (chloroform/methanol/acetic acid/water 43:38:5:7, v/v). To load the plate, a line of origin was drawn and samples loaded 1 µL at a time, under a stream of nitrogen or hot air for the evaporation of the solvent, until all the extracted lipids were used.

The plate was placed immediately into the chromatography chamber ensuring that the solvent front was below the line of origin. This was run for ~3 hr, or until the solvent front was 2 cm below the top of the plate. The plate was thoroughly air-dried and products visualised by autoradiography (6-16 hour exposure at -70°C).

2.2.13 Protein Kinase Assay

2.2.13.1 Preparation of Samples

Proteins were isolated from whole cell lysates as described in section 2.2.9. Proteins immobilised on beads or charged resin were washed three times in ice-cold 1x kinase buffer (20 mM Hepes, pH7.5, 5 mM $MgCl_2$, 1 mM EDTA). All samples were stored in kinase buffer on ice until required.

2.2.13.2 Enzyme Reaction

Samples to be tested were briefly centrifuged and the kinase buffer completely removed. Thirty µL of beads/resin were transferred to a fresh eppendorf. To this 20 µL of 5x kinase buffer, 2 µL of 2.5mM ATP (cold), and 1 µL of γ^{32}P ATP were added in the precise order. Reactions were conducted at RT for 30 min. Proteins were resolved on 9% SDS-PAGE and phosphorylation observed by autoradiography (exposure 30 min at 4°C).

2.2.14 Chemotaxis

Cells in suspension were incubated with calcein-AM (2μM) for 30 min at 37°C. Cells were washed twice in incomplete RPMI and once in incomplete RPMI/0.5% BSA. Cells were resuspended at a concentration of 1 x 10^7 cells/mL in incomplete RPMI/0.5% BSA. All agonists were diluted in incomplete RPMI/0.5% BSA. Chemotaxis assays were conducted using Transwell Cell Culture Chambers (Costar, MA, USA) consisting of polycarbonate membranes with 5μm pores. Six hundred μL of agonist were added to the lower chamber of transwell trays, and 100 μL of calcein-loaded cells were placed in the upper chamber. Trays were incubated at 37°C for 3 hr after which wells and the underside of each filter rinsed with incomplete RPMI/0.5% BSA. Cells were centrifuged at 7000 rpm for 5 min, and cell pellets resuspended in 100 μL PBS. Fluorescence levels were measured using a Molecular Imager FX (Biorad) with excitation at 488nm and emission at 494nm. Percentage of cells migrated was determined using the following formula

$$(y\text{-}ymin/ymax) \times 100$$

y is the fluorescence of an experimental well

ymin is the fluorescence in response to the diluent

ymax is the fluorescence for 100μl of calcein loaded cells (1 x 10^6 total cells)

2.2.15 Calcium Mobilisation Assay

Intracellular free calcium was measured using the fluorescent probe FURA-2/AM (Molecular Probes, Eugene Oregon, USA). Cells (10^7 cells/mL) were loaded with FURA-2/AM (1 mM, 30 min, 37°C in the dark). The cells were washed free of extracellular probe, resuspended at 5 x 10^6 cells/ml in HBSS (GIBCO, Burlington Ontario, Canada), and allowed to re-equilibrate for 10 min at 37°C. Cells were then transferred to the thermostatted cuvette compartment (37°C) and their fluorescence was monitored in a spectrofluorometer (SLM 8000, SLM-AMINCO, Urbana, IL) (excitation and emission wavelengths of 340 nm and 510 nm, respectively). The internal calcium concentrations were calculated as described by (McColl & Naccache, 1997). Each run was individually calibrated.

2.2.16 Protein A Chromatography

Anti-serum was equilibrated with 1/20 volume of 2M Tris-HCl, pH 8.0. Protein A beads were initially washed with 5 volumes of 100mM Tris-HCl, pH 8.0 prior to the addition of serum. The serum was allowed to pass through beads by gravity, followed by 10 volumes of 100mM Tris-HCl pH 8.0 and 10 volumes of 10mM Tris-HCl, pH 8.0. IgG molecules were eluted from the protein A beads by the addition of 0.1M glycine, pH 3.0. Fractions were collected and immediately neutralized with 50µL 2M Tris-HCl, pH 8.0 per 1mL of eluate. Elution fractions were analysed for protein content using a spectrophotometer (OD280nm), and fractions containing proteins pooled and dialysed against PBS overnight at 4°C. The approximate concentration of IgG was determined by the following formula, and purity confirmed using SDS-PAGE analysis, 1OD unit = 0.75mg/mL

2.3 *IN VIVO* TECHNIQUES

2.3.1 Animals and Animal Care Procedures

All mice were obtained specific pathogen free and housed under clean conventional conditions during the period of experimentation. Standard mouse chow (Ridley Products, South Australia) and water were provided *ad libitum*. All mice were housed and treated in strict accordance with NH&MRC guidelines.

Mice – Balb/C mice were used for *in vivo* expression study in Chapter 4 section 4.2. NIH/swiss outbred mice were used for all air pouch experiments described in Chapter 5.

Rabbits – female New Zealand Rabbit were used in the work aimed at generating a polyclonal antibody against PI3kγ.

2.3.2 Generation of Air Pouches

Air pouches were raised on the shaved dorsum of mice by the subcutaneous injection of 2.5mL of sterile air on days 0 and 3. All experiments were conducted on day 6. On day 6 agonists were injected, in 1mL volumes, into air pouches. At indicated time points, mice were euthanased, and any residual liquid removed from the air pouch. Air pouches were then washed twice with 2 mL of PBS. Cell counts were performed using trypan blue exclusion and remaining cells were labeled for one colour flow cytometry (section 2.2.7).

2.3.3 Intravenous injection of cultured cells

Aspetic treatment, of cells to be injected into mice, were maintained at all times. Cells were washed three times with endotoxin-free PBS and resuspended at 1 $x10^7$cells/700µL in endotoxin-free PBS. Intravenous injections, of cells, were carried out using 27G needles.

2.3.4 Statistical analysis

Unpaired Student t-tests (2-tailed) were carried out using the Graphpad PRISM (version 3.00) program. P values less than 0.05 were considered statistically significant, and indicated using an asterisk on the appropriate figures.

Chapter Three

The cloning of murine phosphatidylinositol 3-kinase gamma

3.1 Introduction

Members of the chemokine gene superfamily play an important role in the development and maintenance of the immune system through the control of leukocyte trafficking. These members have also been implicated in many disorders where the infiltration of leukocytes contributes to the pathogenesis of disease. This creates interest in the possibility that understanding the way in which chemokine receptor activation results in a change in effector function could possibly provide greater specificity with which to control disorders influenced by leukocyte trafficking.

The family of PI3-kinases have been shown to be activated by a variety of cell surface receptors, and hence are implicated in the initiation of various effector functions such as cytoskeletal rearrangement, cell motility (Pan *et al.*, 1999), cellular growth and antigen presentation (Song *et al.*, 1997). One of these well known receptor families is the GPCR superfamily, some of which have as their ligands, chemotactic factors including the chemokines. A deal of experimentation has established the family of PI3-kinases as downstream signalling mediators of GPCR activation. At the time this study began, this had, in most part, been exclusively established through the use of blanket inhibitors such as wortmannin and LY294002 and although this approach had provided a great deal of information regarding the importance of the family in many cellular functions stimulated by chemotactic factors, there was virtually no information regarding the involvement of specific PI3-kinase isoforms of the family in this pathway.

In late 1995, Stoyanov *et al.*, cloned and isolated a new PI3-kinase catalytic subunit that shared many structural similarities with the previously identified p110 subunits. Noted differences in the primary amino acid structure suggested an alternative mechanism of activation and regulation and this PI3-kinase isoform was termed p110γ (herein referred to as PI3kγ) (Stoyanov *et al.*, 1995). In contrast to the well-established tyrosine kinase-dependent pathway of PI3-kinase activation, this novel isoform appeared to be regulated by G proteins. Therefore, PI3kγ was considered to be a potentially unique element in the signal transduction through chemotactic factor receptors.

The major aim of this project was to examine the involvement of PI3kγ signalling in chemokine-induced effector functions *in vitro* and *in vivo*. At the time this study commenced only the human and porcine orthologues of PI3kγ had been isolated and cloned. Since the mouse system is well suited to *in vivo* studies of the immune system, the murine orthologue of PI3kγ had to be isolated and cloned. The results presented in this chapter address the cloning of a mus musculus (Mm)PI3kγ.

3.2 Isolation of putative clones

A high level of identity exists between all Class I PI3-kinases and especially between the orthologues of each particular isoform. In keeping with this, degenerate primers based on the human and porcine PI3kγ sequences were designed to amplify the full length murine PI3kγ cDNA. These primers, p110γ-1F and p110γ-1R, were subjected to PCR using a murine cDNA template prepared from the J774 macrophage cell line. Several attempts involving varying annealing temperatures, and magnesium concentrations were made to amplify MmPI3kγ from this template. Furthermore, the degenerate primers were used in an attempt to enhance the reverse-transcription of PI3kγ–specific transcripts and the subsequent cDNA subjected to PCR. Despite extensive attempts to obtain the appropriate conditions, amplification of a MmPI3kγ open reading frame proved unsuccessful using this approach.

Due to the lack of success with the initial PCR-based approach that was designed to amplify the full-length MmPI3kγ, it was decided to isolate MmPI3kγ by screening a murine cDNA library. Primers that annealed at the C-terminal portion of the human PI3kγ cDNA, the region of greatest identity amongst the PI3-kinase family, were designed (Figure 3.1A) to amplify a smaller fragment of the PI3kγ gene that could subsequently be used in the cDNA library screen. The primers p110γ-2F and p110γ-2R gave rise to an amplicon of 530bp from J774 cDNA (Figure 3.1B). This amplicon was of the predicted size based on the human and porcine orthologues and was subsequently cloned into the vector pGEM-T. Sequencing analysis of the clone revealed 95% and 92% identity at the nucleotide level to the human and porcine PI3kγ

orthologues respectively (Stephens *et al.*, 1997 emb/Y10743; Stoyanov *et al.*, 1995 gi/4505802), followed distantly by 63% identity to PI3kβ, a Class IA enzyme (Figure 3.1C gb/M93252). It was concluded that this amplicon was likely to represent part of a murine orthologue of PI3kγ and was therefore deemed to be appropriate to use as a probe in a cDNA library screen to isolate MmPI3kγ.

A murine peritoneal macrophage cDNA library was then probed using the 530 bp fragment. The primary screen consisted of 100,000 plaques, and gave rise to the isolation of 6 positive clones (Figure 3.2A, B and C). These clones were successfully taken through to tertiary screens where the 6 clones were isolated and 5 of these excised into the vector pBluescript sk. These putative clones were named SC-1, 2, 3, 5 and SC-6. Digestion of the putative clones with PvuII demonstrated two different restriction patterns. Clones SC-1, SC-2 and SC-3 all gave rise to five additional DNA fragments when compared with the pbluescript vector alone. Putative clones SC-5 and SC-6 demonstrated a restriction pattern of three additional DNA fragments when compared with pbluescript. This restriction analysis illustrated that all the clones appeared to be approximately 3.5kb in size (Figure 3.3).

3.3 Sequence analysis of putative clones

All clones were sequenced using the "primer walking" method. Primers based on the promoter sequences of the vector (T7 and T3), were used to initially sequence all 5 clones. The resultant sequence data from the putative clones allowed nested primers to be designed in the forward 5'-3' direction until the entire insert had been sequenced (clones SC-5 and SC-6) or until a region high in adenosine (A) and

thymidine (T) bases was reached (clones SC-1, SC-2 and SC-3). Primers were subsequently designed to sequence the clones in the opposing direction to ensure accuracy of sequencing. Sequencing beyond the AT-rich region of clones SC1-3 proved to be unsuccessful.

Sequence data obtained from all five clones were compared to known sequences in the Genbank database (nucleotide, nonredundant database). Results from these searches revealed that SC-5 and SC-6 displayed a 86% identity to the N-terminus of human and porcine PI3kγ at both the nucleotide and amino acid level. In contrast, clones SC-1, SC-2 and SC-3 showed 87% and 88% identity at the nucleotide and amino acid level with the C-terminus of the human and porcine orthologues respectively. Alignment of these sequences with each other revealed that SC-5 and SC-6 were homologous to each other and that SC-1, SC-2 and SC-3 also appeared to be homologous. Furthermore, the sequence alignments indicated the existence of a 300 bp overlap region between the two groups of clones. Thus, it appeared that two fragments had been successfully isolated from a murine macrophage cDNA library and that these together contained the complete open reading frame of murine PI3kγ.

3.4 Construction of the MmPI3Kγ open-reading frame

In order to create one contiguous sequence, the two fragments were analysed for restrictions sites, particularly for unique restriction sites occurring in the overlap region. Fortuitously, restriction analysis revealed the existence of a unique *BglI* restriction site in the overlap region between the N- and the C-terminal portions. Since, the pBluescript backbone contained mutliple *BglI* restriction sites both portions

of MmPI3kγ had to be ligated to each other prior to ligation into the vector. PCR primers flanking the *BglI* site in MmPI3kγ were designed for both the N- and C-terminal portions. In addition, the forward primer of the N-terminal fragment and the reverse primer of the C-terminal fragment had *EcoR*I and *BamH*I restriction sites engineered, respectively for easy ligation into the mammalian expression vector pEGFP-CI. Representative clones SC-6 and SC-3 were chosen to use as template for the amplification. The rationale behind this approach was to create a single open-reading frame whilst enabling the ligation of the complete open reading frame into an expression vector for cellular analysis (Figure 3.4).

The complete open-reading frame of MmPI3kγ was re-sequenced to ensure no errors had been introduced during the PCR amplification and ligation process. This revealed that murine PI3kγ comprised 3342 bp (Figure 3.5). Translation of this sequence in frame +1 resulted in an open reading frame consisting of 1113 amino acid residues (Figure 3.5). This sequence was submitted to the Genbank database in late 1999 (AF208345, Appendix I). Comparisons of this sequence, using BLAST analysis, revealed 86% identity at the nucleotide and 93% identity at the amino acid levels to both the human and porcine orthologues. Alignment of the predicted amino acid sequences of all three species confirmed the high level of identity between all sequences (Figure 3.6). Moreover, amino acid differences between the three sequences appeared to be conserved as predicted by the ClustalW alignment/comparison program. The most notable region of dissimilarity appeared to occur in the C-terminus where an additional 11 amino acids, starting from position

1010 to amino acid position 1021, was observed in MmPI3kγ, relative to the human and porcine sequences (Figure 3.6).

3.5 Discussion

In the work detailed in this chapter, the successful cloning of a murine homologue of PI3kγ is reported. By screening a murine macrophage cDNA library, several clones were isolated. A high level of identity between these putative clones and the human and porcine orthologues was displayed at both the nucleotide and amino acid level. Moreover, the minimal differences observed at the nucleotide level gave rise to no change or resulted in only conserved changes in the amino acid sequence of MmPI3kγ compared with the human and porcine orthologues. The sole exception was the presence of 11 contiguous amino acids in the C-terminus of MmPI3kγ that were not present in either the human or porcine orthologues. Overall, these data suggest that a murine homologue of PI3kγ had been successfully isolated.

The similarity that MmPI3kγ displayed to porcine PI3kγ enabled the identification of the various domains that have been previously identified by the resolution of the crystal structure of porcine PI3kγ (Walker *et al.*, 1999). By analogy, MmPI3kγ contained all four homology regions (HR1 to HR4) that are found in all Class I PI3-kinases (Fig 3.7). A ras-binding domain extends from amino acid residue 220-311 followed by the C2 domain (residues 357-522). The catalytic domain consisted of an N-terminal and a C-terminal lobe. The N-terminal lobe incorporates amino acids 726-883 whilst the C-terminal lobe is much larger beginning at amino acid 884 to amino acid 1092. The N-terminal lobe contains the conserved lysine at position 833, the residue that has been unequivocally been shown to be critical for the activation of the human and porcine PI3kγs (Stoyanova *et al.*, 1997; Wymann *et al.*,

1996). Within the C-terminal lobe is the activation loop (residues 964-988) of PI3kγ (Fig 3.7). The conservation of these domains, at least at the primary amino acid level, suggests that the regulation of MmPI3kγ would be similar to that of the human and porcine orthologues.

The most notable difference between the MmPI3kγ and the human and porcine orthologues was an additional 33 bp in the C-terminal end of the cDNA. To date this additional region has not been reported for the other members of the Class IB family. The extra 33 bp, translating to 11 amino acids, occurs downstream of the activation site (lysine at 833) and is also downstream of the activation loop (amino acids residues 964-988). However, the 11 amino acids are encompassed in the C-terminal lobe of the catalytic domain. Considering this, it is feasible to assume that the additional region, may in some manner, change or influence the structural conformation of the MmPI3kγ in the catalytic domain, and thus potentially affect the enzymatic activity of the PI3-kinase.

In summary, the results presented in this chapter suggest that a murine PI3kγ has been successfully cloned. The activity and physiological importance of this MmPI3kγ will subsequently be examined *in vitro* and *in vivo*.

Figure 3.1 Generation of a murine PI3kγ probe with which to screen a murine cDNA library

(A) A schematic representation of the annealing sites of primers p110γ-2F and p110γ-2R, based on the human PI3kγ sequence, to amplify a 530bp product from a murine template. (B) The amplicon was generated by RT-PCR using primers p110γ-2F and p110γ-2R on murine cDNA made from the J774 macrophage cell line. Products were analysed on a 1.2% agarose gel, and the amplified DNA was of the expected size of 530bp. M - *Spp*1 molecular weight markers. (C) The PCR product was cloned into the pGEM-T vector and sequenced. The sequence was compared to other known sequences in the Genbank database (nucleotide, non-redundant) and percentage identity to the amplicon are schematically illustrated. HsPI3kγ - gi/4505802; SsPI3kγ - emb/Y10743; MmPI3kβ - gb/M93252

A.

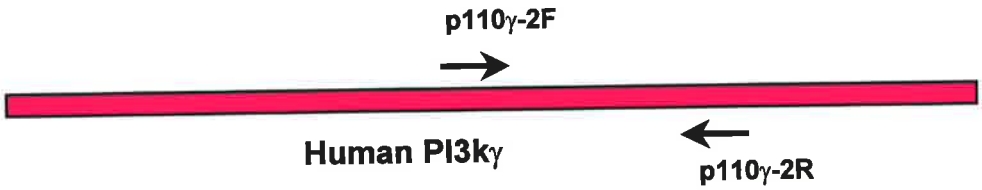
p110γ-2F
Human PI3kγ
p110γ-2R

B.

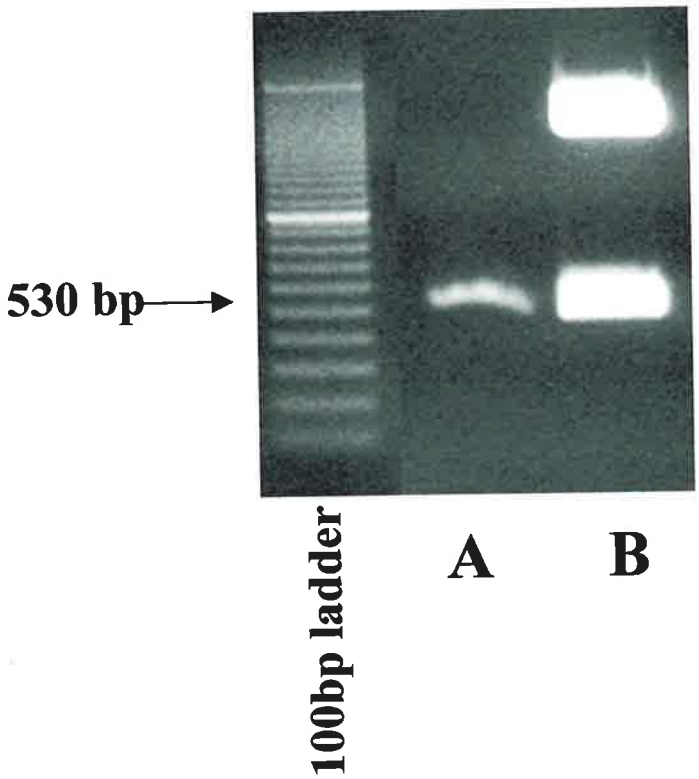
530 bp
100bp ladder
A
B

C.

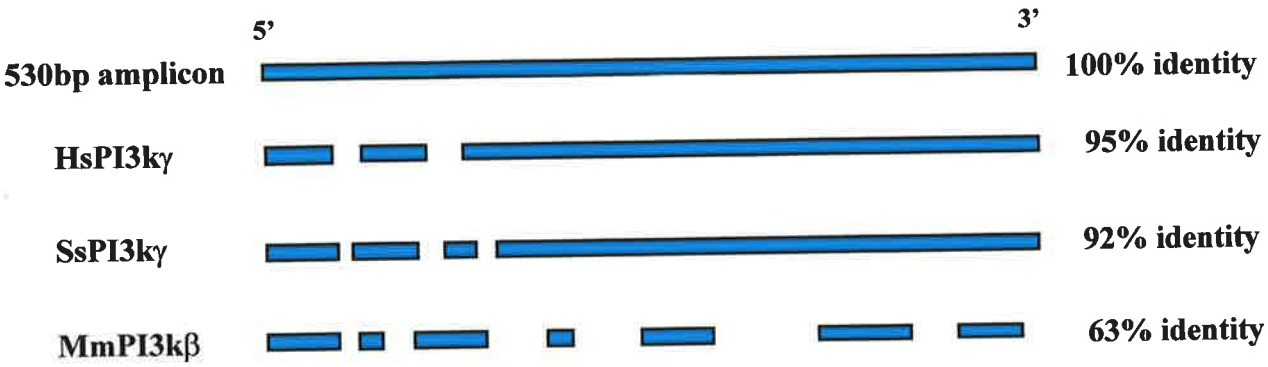
5'
3'
530bp amplicon
100% identity
HsPI3kγ
95% identity
SsPI3kγ
92% identity
MmPI3kβ
63% identity

Figure 3.2 Isolation of putative PI3kγ cDNA clones from a λ zap murine macrophage cDNA library

The 530 bp amplicon was labelled and used to probe a λ zap murine macrophage cDNA library. The primary screen consisted of 100,000 plaques. Filters displaying positive plaques are shown (A, B and C). The clones, indicated by numbers 1-6, were deemed positive by the use of duplicate filters. These 6 positive clones were amplified and successfully taken through to tertiary screens.

A.

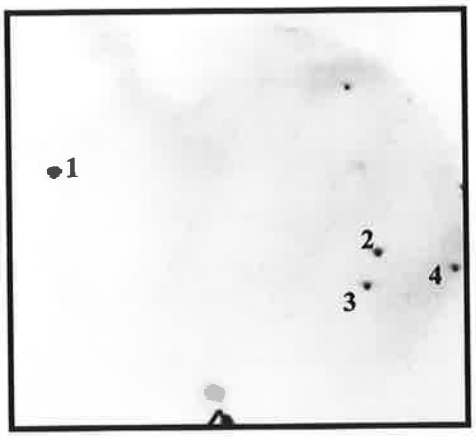

B.

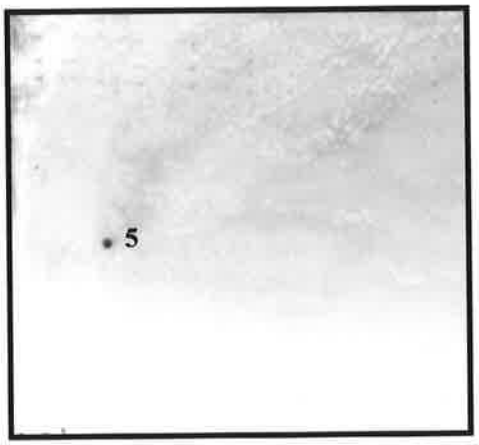

C.

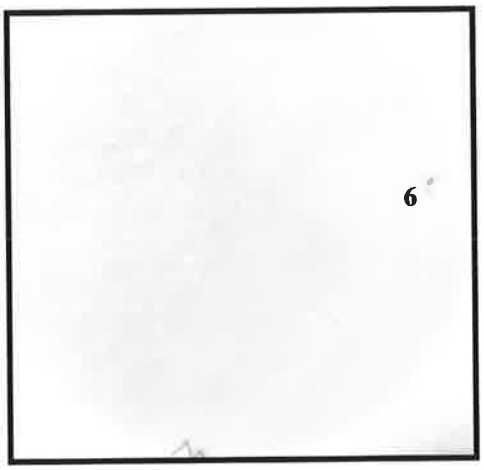

Figure 3.3 Restriction analysis of putative murine PI3kγ clones isolated from a murine macrophage cDNA library

Restriction analysis was conducted on all putative clones (SC-1, SC-2, SC-3, SC-5, and SC-6) and the backbone vector, pbluescript, using the *Pvu*II restriction enzyme. Restricted DNA samples were resolved on a 1.2% agarose gel and visualised using ethidium bromide. The 1kb and 3kb bands of the 100 bp ladder markers are indicated for reference.

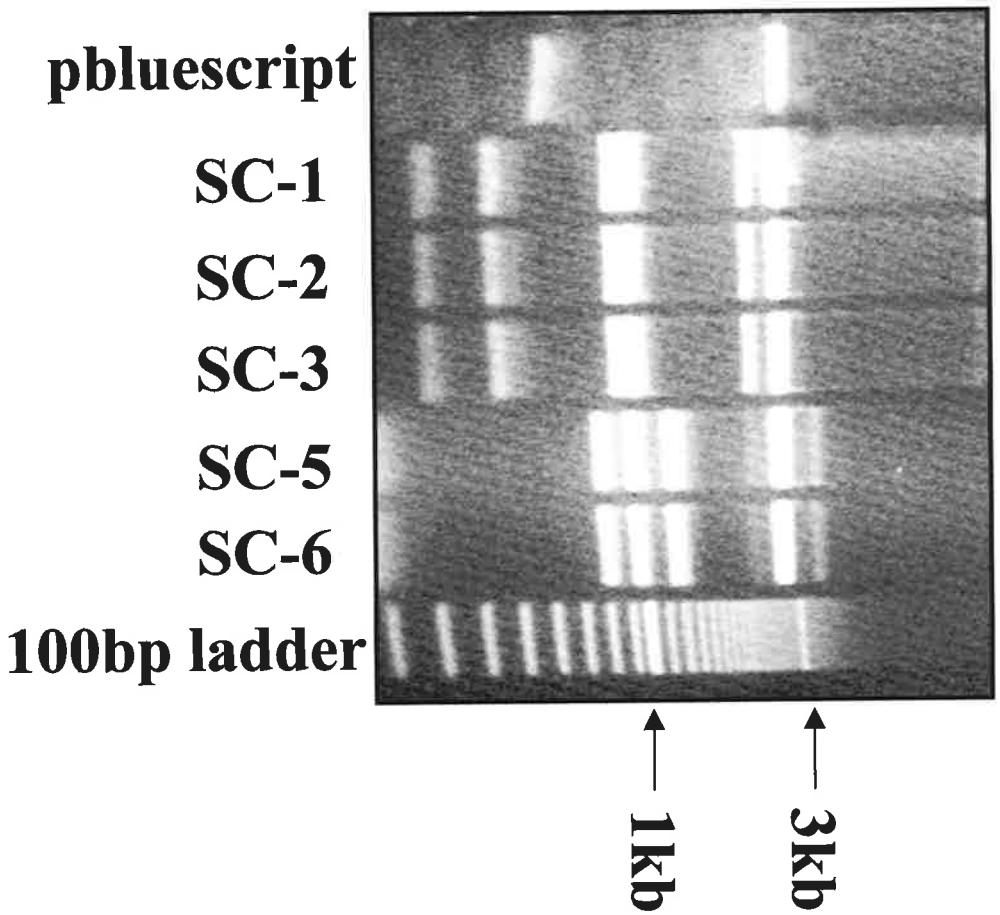
pbluescript
SC-1
SC-2
SC-3
SC-5
SC-6
100bp ladder
1kb
3kb

Figure 3.4 Strategy to obtain the complete MmPI3kγ cDNA

Representative members from the clones that demonstrated the highest identity to the N-terminal (clone SC-6) and the C-terminal portion (clone SC-3) of PI3kγ were used as template for the amplification of the respective portions of the MmPI3kγ cDNA. Primers were designed to flank the common *Bgl*I site in the overlap region of the two representative clones. In addition the forward primer for clone SC-6 and the reverse primer for clone SC-3 were designed to contain appropriate restriction sites to enable ligation of full-length cDNA into the mammalian expression vector pEGFP-CI.

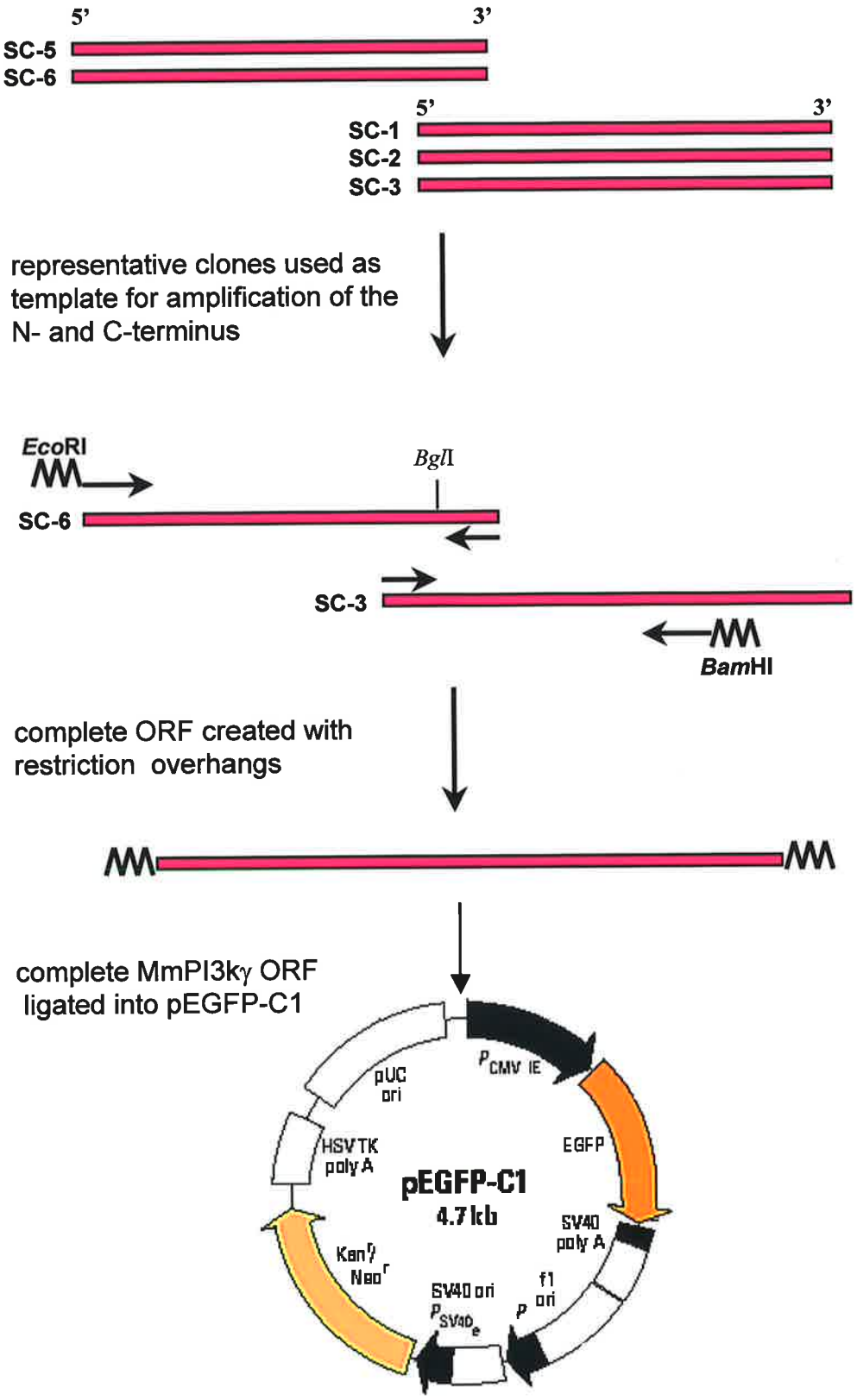
5'
3'
SC-5
SC-6
5'
3'
SC-1
SC-2
SC-3
representative clones used as template for amplification of the N- and C-terminus
EcoRI
BglI
SC-6
SC-3
BamHI
complete ORF created with restriction overhangs
complete MmPI3kγ ORF ligated into pEGFP-C1
pUC ori
P CMV IE
EGFP
HSV TK poly A
pEGFP-C1
4.7 kb
SV40 poly A
Kan^r Neo^r
SV40 ori
P SV40
f1 ori
P

Figure 3.5 The complete nucleotide and predicted amino acid sequence of MmPI3kγ

The full length cDNA of MmPI3kγ was sequenced in both directions using the primers designed for "primer walking" of the isolated clones. Translation of the 3342 nucleotides in frame +1 gave rise to the largest open reading frame of 1113 amino acids. The nucleotide sequence is presented with the encoded amino acids below (Genbank AF208345).

```
  1 ATG GAG CTG GAG AAC TAT GAA CAA CCG GTG GTT CTA AGA GAG GAC AAC 48
  1  M   E   L   E   N   Y   E   Q   P   V   V   L   R   E   D   N  16

 49 CTC CGC CGG CGC CGG AGG ATG AAG CCA CGC AGC GCA GCA GGC AGC CTG 96
 17  L   R   R   R   R   R   M   K   P   R   S   A   A   G   S   L  32

 97 TCT TCC ATG GAG CTC ATC CCC ATT GAG TTC GTA CTG CCC ACC AGC CAG 144
 33  S   S   M   E   L   I   P   I   E   F   V   L   P   T   S   Q  48

145 CGC ATC AGC AAG ACT CCA GAA ACA GCG CTG CTG CAT GTG GCT GGC CAT 192
 49  R   I   S   K   T   P   E   T   A   L   L   H   V   A   G   H  64

193 GGC AAT GTG GAA CAG ATG AAA GCT CAG GTG TGG CTG CGC GCA CTG GAG 240
 65  G   N   V   E   Q   M   K   A   Q   V   W   L   R   A   L   E  80

241 ACC AGT GTG GCT GCG GAG TTC TAC CAC CGA TTG GGC CCG GAC CAA TTC 288
 81  T   S   V   A   A   E   F   Y   H   R   L   G   P   D   Q   F  96

289 CTC CTG CTC TAC CAG AAG AAA GGA CAA TGG TAT GAG ATC TAT GAC AGG 336
 97  L   L   L   Y   Q   K   K   G   Q   W   Y   E   I   Y   D   R 112

337 TAC CAA GTG GTG CAG ACC CTA GAC TGC CTG CAT TAC TGG AAG TTG ATG 384
113  Y   Q   V   V   Q   T   L   D   C   L   H   Y   W   K   L   M 128

385 CAC AAG AGC CCT GGC CAG ATC CAC GTG GTA CAG CGA CAC GTA CCT TCT 432
129  H   K   S   P   G   Q   I   H   V   V   Q   R   H   V   P   S 144

433 GAG GAG ACC TTG GCT TTC CAG AAG CAG CTC ACC TCC CTG ATT GGC TAT 480
145  E   E   T   L   A   F   Q   K   Q   L   T   S   L   I   G   Y 160

481 GAC GTC ACT GAC ATC AGC AAT GTG CAC GAT GAT GAG CTA GAG TTC ACT 528
161  D   V   T   D   I   S   N   V   H   D   D   E   L   E   F   T 176

529 CGC CGC CGT CTG GTT ACG CCC CGC ATG GCT GAA GTG GCT GGC CGG GAT 576
177  R   R   R   L   V   T   P   R   M   A   E   V   A   G   R   D 192

577 GCC AAA CTC TAT GCT ATG CAC CCT TGG GTA ACG TCC AAA CCT CTC CCA 624
193  A   K   L   Y   A   M   H   P   W   V   T   S   K   P   L   P 208

625 GAC TAC CTG TCA AAA AAA ATT GCC AAC AAC TGC ATC TTC ATC GTC ATC 672
209  D   Y   L   S   K   K   I   A   N   N   C   I   F   I   V   I 224

673 CAC CGC GGT ACC ACC AGC CAA ACC ATC AAG GTC TCC GCA GAT GAT ACT 720
225  H   R   G   T   T   S   Q   T   I   K   V   S   A   D   D   T 240

721 CCT GGT ACC ATC CTC CAG AGC TTC TTC ACC AAG ATG GCC AAG AAG AAG 768
241  P   G   T   I   L   Q   S   F   F   T   K   M   A   K   K   K 256

769 TCC CTA ATG AAT ATC TCA GAA AGT CAA AGT GAG CAG GAT TTT GTA TTG 816
257  S   L   M   N   I   S   E   S   Q   S   E   Q   D   F   V   L 272

817 CGG GTT TGT GGC CGC GAT GAG TAC CTG GTG GGT GAA ACA CCC CTC AAA 864
273  R   V   C   G   R   D   E   Y   L   V   G   E   T   P   L   K 288

865 AAT TTC CAG TGG GTG AGG CAG TGC CTC AAG AAC GGA GAT GAA ATA CAC 912
289  N   F   Q   W   V   R   Q   C   L   K   N   G   D   E   I   H 304

913 CTG GTG CTC GAC ACG CCT CCA GAC CCA GCC CTT GAT GAG GTG AGG AAG 960
305  L   V   L   D   T   P   P   D   P   A   L   D   E   V   R   K 320

961 GAA GAA TGG CCG CTG GTG GAT GAC TGC ACT GGA GTC ACC GGC TAC CAC 1008
321  E   E   W   P   L   V   D   D   C   T   G   V   T   G   Y   H 336
```

```
1009 GAG CAG CTG ACC ATC CAT GGC AAG GAC CAC GAG AGT GTG TTC ACA GTG 1056
 337  E   Q   L   T   I   H   G   K   D   H   E   S   V   F   T   V  352

1057 TCT TTG TGG GAC TGC GAC CGA AAG TTC AGG GTC AAG ATC AGA GGC ATT 1104
 353  S   L   W   D   C   D   R   K   F   R   V   K   I   R   G   I  368

1105 GAT ATC CCT GTC CTG CCT CGG AAC ACC GAC CTC ACT GTG TTT GTG GAA 1152
 369  D   I   P   V   L   P   R   N   T   D   L   T   V   F   V   E  384

1153 GCG AAC ATC CAG CAC GGG CAA CAA GTC CTC TGC CAA AGG AGA ACC AGC 1200
 385  A   N   I   Q   H   G   Q   Q   V   L   C   Q   R   R   T   S  400

1201 CCT AAG CCC TTC GCA GAA GAG GTA CTC TGG AAT GTG TGG CTG GAG TTT 1248
 401  P   K   P   F   A   E   E   V   L   W   N   V   W   L   E   F  416

1249 GGC ATC AAA ATC AAA GAC TTG CCC AAA GGG GCT CTA TTG AAC CTA CAG 1296
 417  G   I   K   I   K   D   L   P   K   G   A   L   L   N   L   Q  432

1297 ATC TAC TGC TGC AAA ACC CCA TCA CTG TCC AGC AAG GCT TCT GCA GAG 1344
 433  I   Y   C   C   K   T   P   S   L   S   S   K   A   S   A   E  448

1345 ACT CCA GGC TCC GAG TCC AAG GGC AAA GCC CAG CTT CTC TAT TAC GTG 1392
 449  T   P   G   S   E   S   K   G   K   A   Q   L   L   Y   Y   V  464

1393 AAC TTG CTG TTA ATA GAC CAC CGT TTC CTC CTC CGC CAC GGG GAC TAT 1440
 465  N   L   L   L   I   D   H   R   F   L   L   R   H   G   D   Y  480

1441 GTG CTC CAC ATG TGG CAG ATA TCT GGC AAG GCA GAG GAG CAG GGC AGC 1488
 481  V   L   H   M   W   Q   I   S   G   K   A   E   E   Q   G   S  496

1489 TTC AAT GCT GAC AAG CTC ACA TCC GCA ACC AAT CCT GAC AAG GAG AAC 1536
 497  F   N   A   D   K   L   T   S   A   T   N   P   D   K   E   N  512

1537 TCA ATG TCC ATT TCC ATC CTG CTG GAC AAT TAC TGT CAC CCC ATA GCT 1584
 513  S   M   S   I   S   I   L   L   D   N   Y   C   H   P   I   A  528

1585 TTG CCT AAG CAC CGG CCC ACC CCT GAC CCA GAG GGA GAC AGG GTT CGG 1632
 529  L   P   K   H   R   P   T   P   D   P   E   G   D   R   V   R  544

1633 GCT GAA ATG CCC AAT CAG CTT CGA AAG CAA TTG GAG GCG ATC ATA GCC 1680
 545  A   E   M   P   N   Q   L   R   K   Q   L   E   A   I   I   A  560

1681 ACA GAT CCA CTT AAC CCC CTC ACA GCA GAG GAC AAA GAA TTG CTC TGG 1728
 561  T   D   P   L   N   P   L   T   A   E   D   K   E   L   L   W  576

1729 CAT TTT CGA TAT GAA AGC CTG AAG CAT CCG AAG GCT TAC CCT AAG CTA 1776
 577  H   F   R   Y   E   S   L   K   H   P   K   A   Y   P   K   L  592

1777 TTC AGC TCA GTG AAA TGG GGG CAG CAA GAA ATT GTT GCC AAA ACG TAC 1824
 593  F   S   S   V   K   W   G   Q   Q   E   I   V   A   K   T   Y  608

1825 CAG CTG TTA GCC AGA AGG GAG ATC TGG GAT CAA AGT GCT TTG GAC GTT 1872
 609  Q   L   L   A   R   R   E   I   W   D   Q   S   A   L   D   V  624

1873 GGC TTA ACC ATG CAG CTC CTG GAC TGC AAC TTT TCA GAC GAG AAT GTC 1920
 625  G   L   T   M   Q   L   L   D   C   N   F   S   D   E   N   V  640

1921 CGG GCC ATT GCA GTT CAG AAA CTG GAG AGC TTA GAG GAC GAT GAC GTT 1968
 641  R   A   I   A   V   Q   K   L   E   S   L   E   D   D   D   V  656

1969 TTA CAT TAC CTT CTC CAG CTG GTA CAG GCT GTG AAA TTT GAA CCG TAC 2016
 657  L   H   Y   L   L   Q   L   V   Q   A   V   K   F   E   P   Y  672

2017 CAC GAC AGT GCG CTG GCC AGA TTC CTG CTG AAG CGT GGC TTG AGG AAC 2064
 673  H   D   S   A   L   A   R   F   L   L   K   R   G   L   R   N  688
```

```
2065 AAA AGA ATC GGT CAC TTC TTG TTC TGG TTC CTG CGA AGT GAG ATC GCA 2112
 689  K   R   I   G   H   F   L   F   W   F   L   R   S   E   I   A 704

2113 CAG TCC ANA CAC TAT CAG CAG AGG TTC GCT GTG ATC CTG GAG GCG TAC 2160
 705  Q   S   X   H   Y   Q   Q   R   F   A   V   I   L   E   A   Y 720

2161 CTG CGA GGC TGT GGC ACA GCC ATG TTG CAG GAC TTC ACA CAG CAG GTC 2208
 721  L   R   G   C   G   T   A   M   L   Q   D   F   T   Q   Q   V 736

2209 CAT GTG ATT GAG ATG TTA CAG AAA GTC ACC ATT GAT ATT AAA TCG CTC 2256
 737  H   V   I   E   M   L   Q   K   V   T   I   D   I   K   S   L 752

2257 TCG GCA GAG AAG TAT GAC GTC AGT TCC CAA GTT ATT TCA CAG CTT AAG 2304
 753  S   A   E   K   Y   D   V   S   S   Q   V   I   S   Q   L   K 768

2305 CAA AAG CTT GAA AGC CTT CAG AAC TCC AAT CTC CCC GAG AGC TTT AGA 2352
 769  Q   K   L   E   S   L   Q   N   S   N   L   P   E   S   F   R 784

2353 GTT CCC TAT GAT CCT GGA CTA AAA GCC GGT ACC CTG GTG ATC GAG AAA 2400
 785  V   P   Y   D   P   G   L   K   A   G   T   L   V   I   E   K 800

2401 TGC AAA GTG ATG GCC TCC AAG AAG AAG CCC CTG TGG CTT GAG TTT AAG 2448
 801  C   K   V   M   A   S   K   K   K   P   L   W   L   E   F   K 816

2449 TGT GCT GAT CCC ACA GTC CTA TCC AAC GAA ACC ATT GGA ATC ATC TTT 2496
 817  C   A   D   P   T   V   L   S   N   E   T   I   G   I   I   F 832

2497 AAA CAT GGT GAT GAT CTG CGC CAA GAC ATG TTG ATC TTG CAG ATT CTA 2544
 833  K   H   G   D   D   L   R   Q   D   M   L   I   L   Q   I   L 848

2545 CGC ATC ATG GAG TCC ATT TGG GAG ACT GAA TCT CTG GAC CTG TGC CTT 2592
 849  R   I   M   E   S   I   W   E   T   E   S   L   D   L   C   L 864

2593 CTG CCT TAC GGN TGC ATC TCA ACT GGT GAC AAA ATA GGA ATG ATC GAG 2640
 865  L   P   Y   G   C   I   S   T   G   D   K   I   G   M   I   E 880

2641 ATT GTA AAG GAT GCC ACA ACG ATC GCT CAA ATT CAG CAA AGC ACA GTG 2688
 881  I   V   K   D   A   T   T   I   A   Q   I   Q   Q   S   T   V 896

2689 GGT AAC ACG GGG GCA TTC AAA GAT GAA GTC CTG AAT CAC TGG CTC AAG 2736
 897  G   N   T   G   A   F   K   D   E   V   L   N   H   W   L   K 912

2737 GAA AAA TGT CCT ATT GAA GAA AAG TTT CAG GCC GCA GTG GAA AGG TTT 2784
 913  E   K   C   P   I   E   E   K   F   Q   A   A   V   E   R   F 928

2785 GTT TAC TCC TGT GCA GGC TAC TGT GTG GCC ACA TTT GTT CTT GGG ATC 2832
 929  V   Y   S   C   A   G   Y   C   V   A   T   F   V   L   G   I 944

2833 GGT GAC AGG CAC AAC GAC AAC ATT ATG ATC TCA GAG ACA GGA AAC CTA 2880
 945  G   D   R   H   N   D   N   I   M   I   S   E   T   G   N   L 960

2881 TTT CAT ATA GAC TTC GGA CAC ATT CTT GGG AAT TAC AAG AGT TTC CTG 2928
 961  F   H   I   D   F   G   H   I   L   G   N   Y   K   S   F   L 976

2929 GGC ATC AAT AAA GAG AGA GTG CCC TTC GTC CTA ACC CCA GAC TTT TTG 2976
 977  G   I   N   K   E   R   V   P   F   V   L   T   P   D   F   L 992

2977 GTT GTG ATG GGA TCT TCT GGA AAA AAG ACA AGT CCA CAC TTC CAG AAA 3024
 993  V   V   M   G   S   S   G   K   K   T   S   P   H   F   Q   K 1008

3025 TTC CAG GAT TGC TGT GTG TCT ACT TTA CAG TAC TAT GGG GAT GTC TGT 3072
1009  F   Q   D   C   C   V   S   T   L   Q   Y   Y   G   D   V   C 1024
```

```
3073 GTT AGA GCT TAC CTA GCT CTT CGC CAT CAC ACA AAC CTG TTG ATC ATC 3120
1025  V   R   A   Y   L   A   L   R   H   H   T   N   L   L   I   I 1040

3121 TTG TTC TCC ATG ATG CTG ATG ACA GGA ATG CCC CAG CTG ACA AGC AAA 3168
1041  L   F   S   M   M   L   M   T   G   M   P   Q   L   T   S   K 1056

3169 GAG GAC ATT GAA TAT ATC CGG GAT GCC CTC ACC GTG GGA AAA AGC GAG 3216
1057  E   D   I   E   Y   I   R   D   A   L   T   V   G   K   S   E 1072

3217 GAG GAC GCT AAG AAA TAT TTC CTT GAT CAG ATC GAA GTC TGC AGA GAC 3264
1073  E   D   A   K   K   Y   F   L   D   Q   I   E   V   C   R   D 1088

3265 AAA GGA TGG ACT GTG CAG TTT AAC TGG TTC CTA CAT CTT GTT CTT GGC 3312
1089  K   G   W   T   V   Q   F   N   W   F   L   H   L   V   L   G 1104

3313 ATC AAA CAA GGA GAA AAG CAC TCC GCT TGA                         3342
1105  I   K   Q   G   E   K   H   S   A   *                       1114
```

Figure 3.6 Amino acid alignment of MmPI3kγ and the human and porcine PI3kγ

The ClustalW alignment program was used to align human (gi/4505802), porcine (emb/Y10743) and murine (AF208345) PI3kγ at the amino acid level. The dark shaded regions represent amino acids that are identical between sequences. Conserved changes in amino acids are indicated in grey, while non-conserved changes are represented in white. Percentage identity of each PI3kγ sequence is indicated at the extreme 3' end of the alignment.

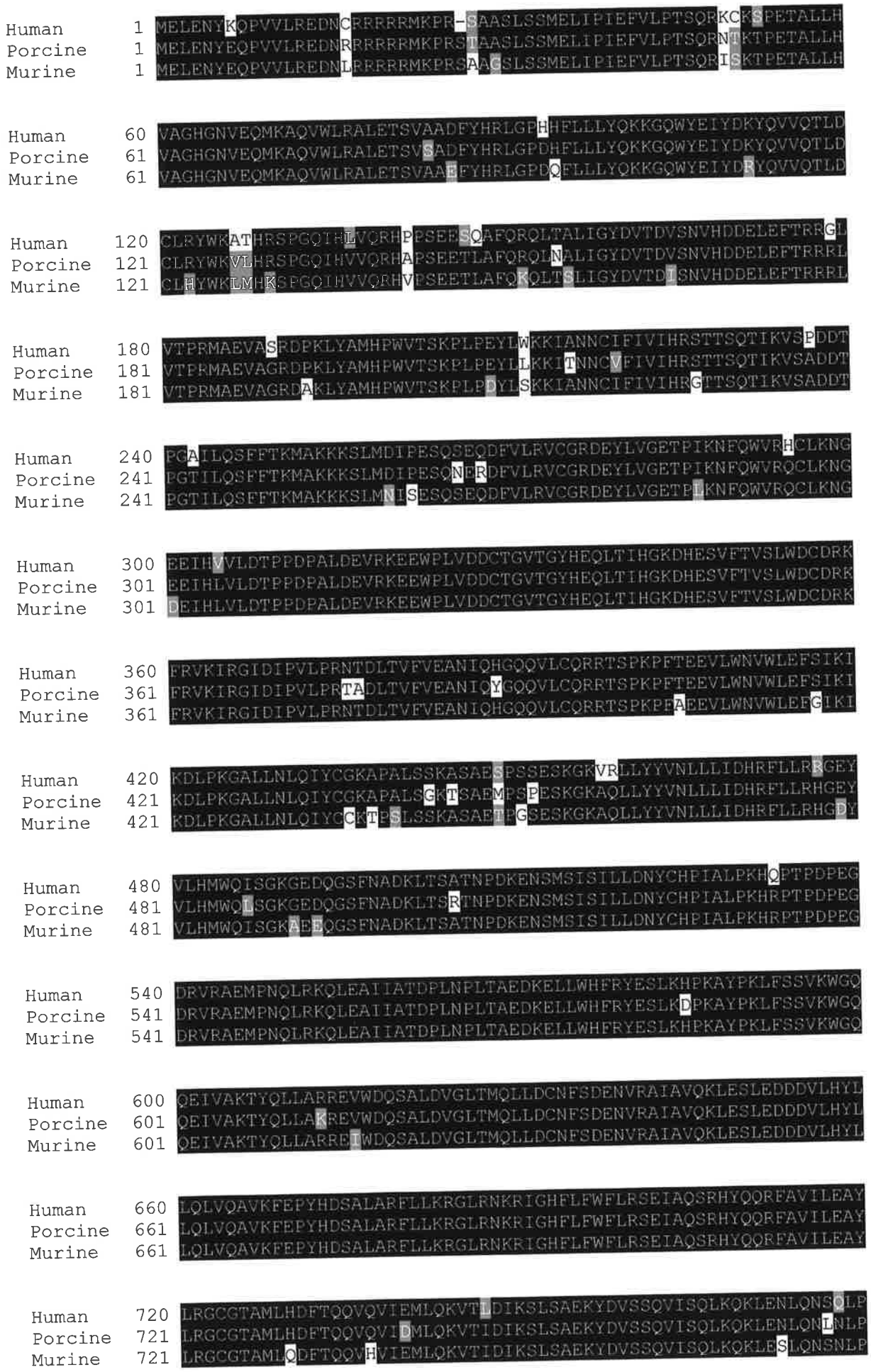
Human 1 MELENYKQPVVLREDNCRRRRRMKPR-SAASLSSMELIPIEFVLPTSQRKCKSPETALLH
Porcine 1 MELENYEQPVVLREDNRRRRRRMKPRSTAASLSSMELIPIEFVLPTSQRNTKTPETALLH
Murine 1 MELENYEQPVVLREDNLRRRRRMKPRSAAGSLSSMELIPIEFVLPTSQRISKTPETALLH
Human 60 VAGHGNVEQMKAQVWLRALETSVAADFYHRLGPHHFLLLYQKKGQWYEIYDKYQVVQTLD
Porcine 61 VAGHGNVEQMKAQVWLRALETSVSADFYHRLGPDHFLLLYQKKGQWYEIYDKYQVVQTLD
Murine 61 VAGHGNVEQMKAQVWLRALETSVAAEFYHRLGPDQFLLLYQKKGQWYEIYDRYQVVQTLD
Human 120 CLRYWKATHRSPCQIHLVQRHPPSEESQAFQRQLTALIGYDVTDVSNVHDDELEFTRRGL
Porcine 121 CLRYWKVLHRSPCQIHVVQRHAPSEETLAFQRQLNALIGYDVTDVSNVHDDELEFTRRRL
Murine 121 CLHYWKLMHKSPGQIHVVQRHVPSEETLAFQKQLTSLIGYDVTDISNVHDDELEFTRRRL
Human 180 VTPRMAEVASRDPKLYAMHPWVTSKPLPEYLWKKIANNCIFIVIHRSTTSQTIKVSPDDT
Porcine 181 VTPRMAEVAGRDPKLYAMHPWVTSKPLPEYLLKKITNNCVFIVIHRSTTSQTIKVSADDT
Murine 181 VTPRMAEVAGRDAKLYAMHPWVTSKPLPDYLSKKIANNCIFIVIHRGTTSQTIKVSADDT
Human 240 PGAILQSFFTKMAKKKSLMDIPESQSEQDFVLRVCGRDEYLVGETPIKNFQWVRHCLKNG
Porcine 241 PGTILQSFFTKMAKKKSLMDIPESQNERDFVLRVCGRDEYLVGETPIKNFQWVRQCLKNG
Murine 241 PGTILQSFFTKMAKKKSLMNISESQSEQDFVLRVCGRDEYLVGETPLKNFQWVRQCLKNG
Human 300 EEIHVVLDTPPDPALDEVRKEEWPLVDDCTGVTGYHEQLTIHGKDHESVFTVSLWDCDRK
Porcine 301 EEIHLVLDTPPDPALDEVRKEEWPLVDDCTGVTGYHEQLTIHGKDHESVFTVSLWDCDRK
Murine 301 DEIHLVLDTPPDPALDEVRKEEWPLVDDCTGVTGYHEQLTIHGKDHESVFTVSLWDCDRK
Human 360 FRVKIRGIDIPVLPRNTDLTVFVEANIQHGQQVLCQRRTSPKPFTEEVLWNVWLEFSIKI
Porcine 361 FRVKIRGIDIPVLPRTADLTVFVEANIQYGQQVLCQRRTSPKPFTEEVLWNVWLEFSIKI
Murine 361 FRVKIRGIDIPVLPRNTDLTVFVEANIQHGQQVLCQRRTSPKPPAEEVLWNVWLEFGIKI
Human 420 KDLPKGALLNLQIYCGKAPALSSKASAESPSSESKGKVRLLYYVNLLLIDHRFLLRRGEY
Porcine 421 KDLPKGALLNLQIYCGKAPALSGKTSAEMPSPESKGKAQLLYYVNLLLIDHRFLLRHGEY
Murine 421 KDLPKGALLNLQIYCCKTPSLSSKASAETPGSESKGKAQLLYYVNLLLIDHRFLLRHGDY
Human 480 VLHMWQISGKGEDQGSFNADKLTSATNPDKENSMSISILLDNYCHPIALPKHQPTPDPEG
Porcine 481 VLHMWQLSGKGEDQGSFNADKLTSRTNPDKENSMSISILLDNYCHPIALPKHRPTPDPEG
Murine 481 VLHMWQISGKAEEQGSFNADKLTSATNPDKENSMSISILLDNYCHPIALPKHRPTPDPEG
Human 540 DRVRAEMPNQLRKQLEAIIATDPLNPLTAEDKELLWHFRYESLKHPKAYPKLFSSVKWGQ
Porcine 541 DRVRAEMPNQLRKQLEAIIATDPLNPLTAEDKELLWHFRYESLKDPKAYPKLFSSVKWGQ
Murine 541 DRVRAEMPNQLRKQLEAIIATDPLNPLTAEDKELLWHFRYESLKHPKAYPKLFSSVKWGQ
Human 600 QEIVAKTYQLLARREVWDQSALDVGLTMQLLDCNFSDENVRAIAVQKLESLEDDDVLHYL
Porcine 601 QEIVAKTYQLLAKREVWDQSALDVGLTMQLLDCNFSDENVRAIAVQKLESLEDDDVLHYL
Murine 601 QEIVAKTYQLLARREIWDQSALDVGLTMQLLDCNFSDENVRAIAVQKLESLEDDDVLHYL
Human 660 LQLVQAVKFEPYHDSALARFLLKRGLRNKRIGHFLFWFLRSEIAQSRHYQQRFAVILEAY
Porcine 661 LQLVQAVKFEPYHDSALARFLLKRGLRNKRIGHFLFWFLRSEIAQSRHYQQRFAVILEAY
Murine 661 LQLVQAVKFEPYHDSALARFLLKRGLRNKRIGHFLFWFLRSEIAQSRHYQQRFAVILEAY
Human 720 LRGCGTAMLHDFTQQVQVIEMLQKVTLDIKSLSAEKYDVSSQVISQLKQKLENLQNSQLP
Porcine 721 LRGCGTAMLHDFTQQVQVIDMLQKVTIDIKSLSAEKYDVSSQVISQLKQKLENLQNLNLP
Murine 721 LRGCGTAMLQDFTQQVHVIEMLQKVTIDIKSLSAEKYDVSSQVISQLKQKLESLQNSNLP

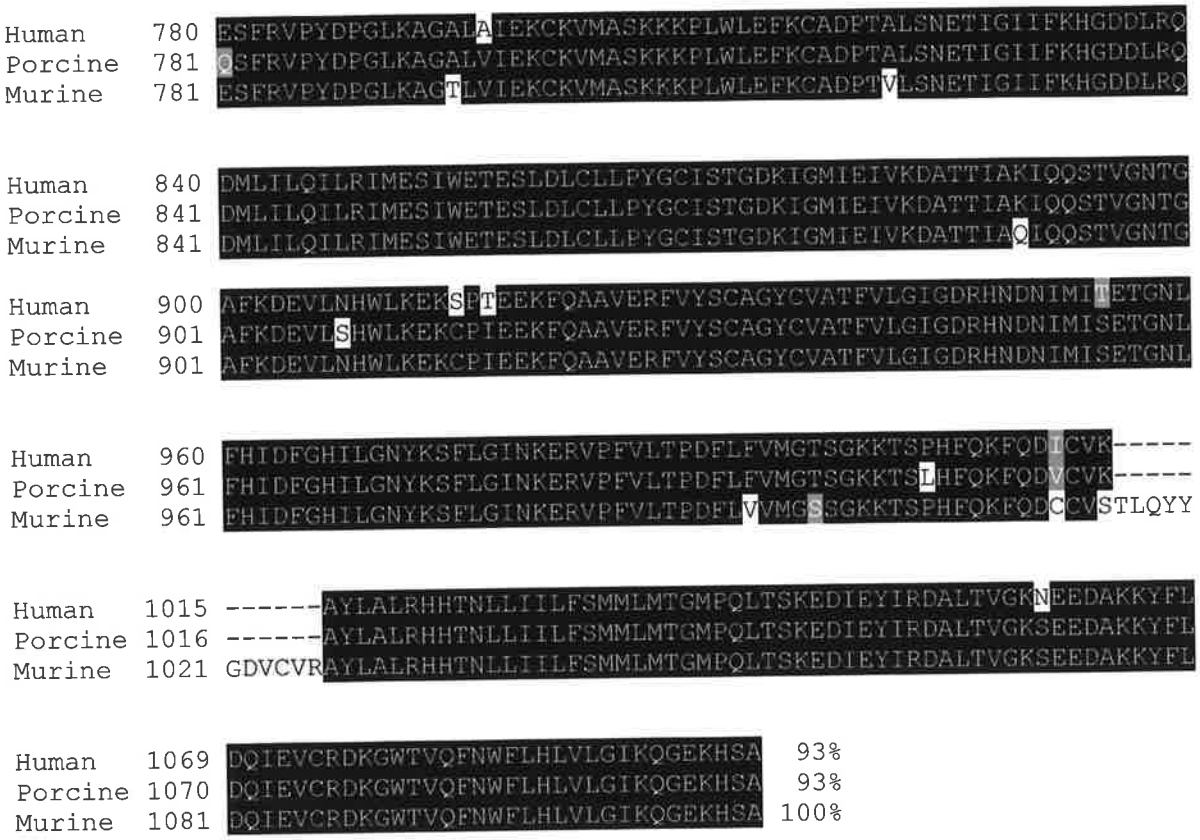
Human 780 ESFRVPYDPGLKAGALAIEKCKVMASKKKPLWLEFKCADPTALSNETIGIIFKHGDDLRQ
Porcine 781 QSFRVPYDPGLKAGALVIEKCKVMASKKKPLWLEFKCADPTALSNETIGIIFKHGDDLRQ
Murine 781 ESFRVPYDPGLKAGTLVIEKCKVMASKKKPLWLEFKCADPTVLSNETIGIIFKHGDDLRQ
Human 840 DMLILQILRIMESIWETESLDLCLLPYGCISTGDKIGMIEIVKDATTIAKIQQSTVGNTG
Porcine 841 DMLILQILRIMESIWETESLDLCLLPYGCISTGDKIGMIEIVKDATTIAKIQQSTVGNTG
Murine 841 DMLILQILRIMESIWETESLDLCLLPYGCISTGDKIGMIEIVKDATTIAQIQQSTVGNTG
Human 900 AFKDEVLNHWLKEKSPTEEKFQAAVERFVYSCAGYCVATFVLGIGDRHNDNIMITETGNL
Porcine 901 AFKDEVLSHWLKEKCPIEEKFQAAVERFVYSCAGYCVATFVLGIGDRHNDNIMISETGNL
Murine 901 AFKDEVLNHWLKEKCPIEEKFQAAVERFVYSCAGYCVATFVLGIGDRHNDNIMISETGNL
Human 960 FHIDFGHILGNYKSFLGINKERVPFVLTPDFLFVMGTSGKKTSPHFQKFQDICVK-----
Porcine 961 FHIDFGHILGNYKSFLGINKERVPFVLTPDFLFVMGTSGKKTSLHFQKFQDVCVK-----
Murine 961 FHIDFGHILGNYKSFLGINKERVPFVLTPDFLVVMGSSGKKTSPHFQKFQDCCVSTLQYY
Human 1015 ------AYLALRHHTNLLIILFSMMLMTGMPQLTSKEDIEYIRDALTVGKNEEDAKKYFL
Porcine 1016 ------AYLALRHHTNLLIILFSMMLMTGMPQLTSKEDIEYIRDALTVGKSEEDAKKYFL
Murine 1021 GDVCVRAYLALRHHTNLLIILFSMMLMTGMPQLTSKEDIEYIRDALTVGKSEEDAKKYFL
Human 1069 DQIEVCRDKGWTVQFNWFLHLVLGIKQGEKHSA 93%
Porcine 1070 DQIEVCRDKGWTVQFNWFLHLVLGIKQGEKHSA 93%
Murine 1081 DQIEVCRDKGWTVQFNWFLHLVLGIKQGEKHSA 100%

Figure 3.7 The conserved domains of MmPI3kγ

By analogy to the crystal structure of porcine PI3kγ (Walker *et al.,* 1999), conserved domains of the Class IB PI3-kinases are illustrated. The ras-binding domain encompasses amino acids 220-311(pink), the C2 domain extends from residues 357-522 (blue). The catalytic domain consists of an N-terminal and C-terminal lobe. The N-terminal lobe is made up of amino acid residues 726-833 (green) while the C-terminal lobe extends from amino acid 834 to 1092 (yellow). The critical residue for activation is located in the N-terminal lobe of the catalytic domain (lysine at position 833; pink), and the activation loop consists of amino acids 964-988.

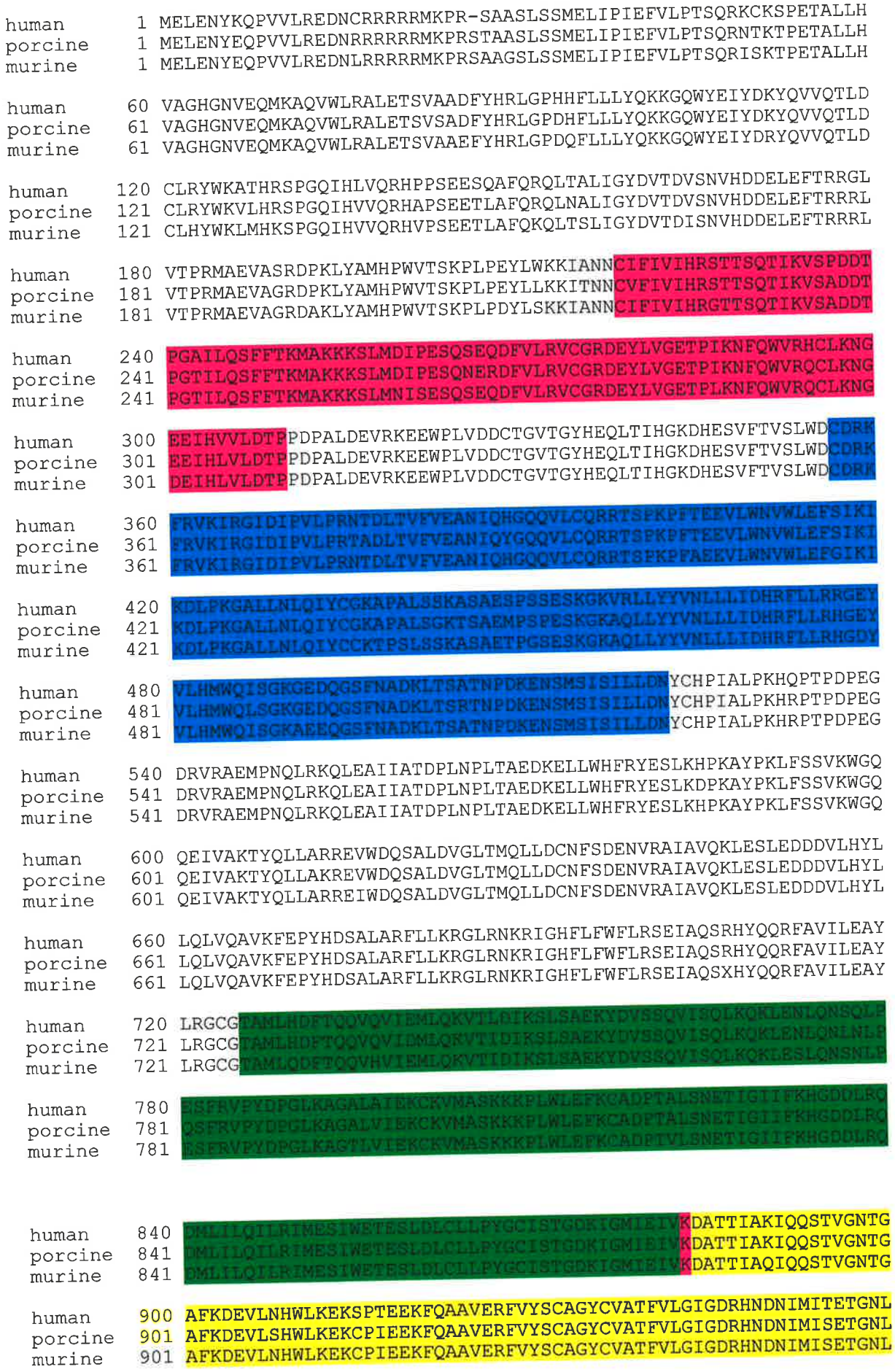
human 1 MELENYKQPVVLREDNCRRRRRMKPR-SAASLSSMELIPIEFVLPTSQRKCKSPETALLH
porcine 1 MELENYEQPVVLREDNRRRRRRMKPRSTAASLSSMELIPIEFVLPTSQRNTKTPETALLH
murine 1 MELENYEQPVVLREDNLRRRRRMKPRSAAGSLSSMELIPIEFVLPTSQRISKTPETALLH
human 60 VAGHGNVEQMKAQVWLRALETSVAADFYHRLGPHHFLLLYQKKGQWYEIYDKYQVVQTLD
porcine 61 VAGHGNVEQMKAQVWLRALETSVSADFYHRLGPDHFLLLYQKKGQWYEIYDKYQVVQTLD
murine 61 VAGHGNVEQMKAQVWLRALETSVAAEFYHRLGPDQFLLLYQKKGQWYEIYDRYQVVQTLD
human 120 CLRYWKATHRSPGQIHLVQRHPPSEESQAFQRQLTALIGYDVTDVSNVHDDELEFTRRGL
porcine 121 CLRYWKVLHRSPGQIHVVQRHAPSEETLAFQRQLNALIGYDVTDVSNVHDDELEFTRRRL
murine 121 CLHYWKLMHKSPGQIHVVQRHVPSEETLAFQKQLTSLIGYDVTDISNVHDDELEFTRRRL
human 180 VTPRMAEVASRDPKLYAMHPWVTSKPLPEYLWKKIANNCIFIVIHRSTTSQTIKVSPDDT
porcine 181 VTPRMAEVAGRDPKLYAMHPWVTSKPLPEYLLKKITNNCVFIVIHRSTTSQTIKVSADDT
murine 181 VTPRMAEVAGRDAKLYAMHPWVTSKPLPDYLSKKIANNCIFIVIHRGTTSQTIKVSADDT
human 240 PGAILQSFFTKMAKKKSLMDIPESQSEQDFVLRVCGRDEYLVGETPIKNFQWVRHCLKNG
porcine 241 PGTILQSFFTKMAKKKSLMDIPESQNERDFVLRVCGRDEYLVGETPIKNFQWVRQCLKNG
murine 241 PGTILQSFFTKMAKKKSLMNISESQSEQDFVLRVCGRDEYLVGETPLKNFQWVRQCLKNG
human 300 EEIHVVLDTPPDPALDEVRKEEWPLVDDCTGVTGYHEQLTIHGKDHESVFTVSLWDCDRK
porcine 301 EEIHLVLDTPPDPALDEVRKEEWPLVDDCTGVTGYHEQLTIHGKDHESVFTVSLWDCDRK
murine 301 DEIHLVLDTPPDPALDEVRKEEWPLVDDCTGVTGYHEQLTIHGKDHESVFTVSLWDCDRK
human 360 FRVKIRGIDIPVLPRNTDLTVFVEANIQHGQQVLCQRRTSPKPFTEEVLWNVWLEFSIKI
porcine 361 FRVKIRGIDIPVLPRTADLTVFVEANIQYGQQVLCQRRTSPKPFTEEVLWNVWLEFSIKI
murine 361 FRVKIRGIDIPVLPRNTDLTVFVEANIQHGQQVLCQRRTSPKPFAEEVLWNVWLEFGIKI
human 420 KDLPKGALLNLQIYCGKAPALSSKASAESPSSESKGKVRLLYYVNLLLIDHRFLLRRGEY
porcine 421 KDLPKGALLNLQIYCGKAPALSGKTSAEMPSPESKGKAQLLYYVNLLLIDHRFLLRHGEY
murine 421 KDLPKGALLNLQIYCCKTPSLSSKASAETPGSESKGKAQLLYYVNLLLIDHRFLLRHGDY
human 480 VLHMWQISGKGEDQGSFNADKLTSATNPDKENSMSISILLDNYCHPIALPKHQPTPDPEG
porcine 481 VLHMWQLSGKGEDQGSFNADKLTSRTNPDKENSMSISILLDNYCHPIALPKHRPTPDPEG
murine 481 VLHMWQISCKAEEQGSFNADKLTSATNPDKENSMSISILLDNYCHPIALPKHRPTPDPEG
human 540 DRVRAEMPNQLRKQLEAIIATDPLNPLTAEDKELLWHFRYESLKHPKAYPKLFSSVKWGQ
porcine 541 DRVRAEMPNQLRKQLEAIIATDPLNPLTAEDKELLWHFRYESLKDPKAYPKLFSSVKWGQ
murine 541 DRVRAEMPNQLRKQLEAIIATDPLNPLTAEDKELLWHFRYESLKHPKAYPKLFSSVKWGQ
human 600 QEIVAKTYQLLARREVWDQSALDVGLTMQLLDCNFSDENVRAIAVQKLESLEDDDVLHYL
porcine 601 QEIVAKTYQLLAKREVWDQSALDVGLTMQLLDCNFSDENVRAIAVQKLESLEDDDVLHYL
murine 601 QEIVAKTYQLLARREIWDQSALDVGLTMQLLDCNFSDENVRAIAVQKLESLEDDDVLHYL
human 660 LQLVQAVKFEPYHDSALARFLLKRGLRNKRIGHFLFWFLRSEIAQSRHYQQRFAVILEAY
porcine 661 LQLVQAVKFEPYHDSALARFLLKRGLRNKRIGHFLFWFLRSEIAQSRHYQQRFAVILEAY
murine 661 LQLVQAVKFEPYHDSALARFLLKRGLRNKRIGHFLFWFLRSEIAQSXHYQQRFAVILEAY
human 720 LRGCGTAMLHDFTQQVQVIEMLQKVTLDIKSLSAEKYDVSSQVISQLKQKLENLQNSQLP
porcine 721 LRGCGTAMLHDFTQQVQVIEMLQKVTIDIKSLSAEKYDVSSQVISQLKQKLENLQNLNLP
murine 721 LRGCGTAMLQDFTQQVHVIEMLQKVTIDIKSLSAEKYDVSSQVISQLKQKLESLQNSNLP
human 780 QSFRVPYDPGLKAGALAIEKCKVMASKKKPLWLEFKCADPTALSNETIGIIFKHGDDLRQ
porcine 781 QSFRVPYDPGLKAGALVIEKCKVMASKKKPLWLEFKCADPTALSNETIGIIFKHGDDLRQ
murine 781 QSFRVPYDPGLKAGTLVIEKCKVMASKKKPLWLEFKCADPTVLSNETIGIIFKHGDDLRQ
human 840 DMLILQILRIMESIWETESLDLCLLPYGCISTGDKIGMIEIVKDATTIAKIQQSTVGNTG
porcine 841 DMLILQILRIMESIWETESLDLCLLPYGCISTGDKIGMIEIVKDATTIAKIQQSTVGNTG
murine 841 DMLILQILRIMESIWETESLDLCLLPYGCISTGDKIGMIEIVKDATTIAQIQQSTVGNTG
human 900 AFKDEVLNHWLKEKSPTEEKFQAAVERFVYSCAGYCVATFVLGIGDRHNDNIMITETGNL
porcine 901 AFKDEVLSHWLKEKCPIEEKFQAAVERFVYSCAGYCVATFVLGIGDRHNDNIMISETGNL
murine 901 AFKDEVLNHWLKEKCPIEEKFQAAVERFVYSCAGYCVATFVLGIGDRHNDNIMISETGNL

```
human     960 FHIDFGHILGNYKSFLGINKERVPFVLTPDFLFVMGTSGKKTSPHFQKFQ----------
porcine   961 FHIDFGHILGNYKSFLGINKERVPFVLTPDFLFVMGTSGKKTSLHFQKFQ----------
murine    961 FHIDFGHILGNYKSFLGINKERVPFVLTPDFLVVMGSSGKKTSPHFQKFQDCCVSTLQYY

human    1015 -DICVKAYLALRHHTNLLIILFSMMLMTGMPQLTSKEDIEYIRDALTVGKNEEDAKKYFL
porcine  1016 -DVCVKAYLALRHHTNLLIILFSMMLMTGMPQLTSKEDIEYIRDALTVGKSEEDAKKYFL
murine   1021 GDVCVRAYLALRHHTNLLIILFSMMLMTGMPQLTSKEDIEYIRDALTVGKSEEDAKKYFL

human    1069 DQIEVCRDKGWTVQFNWFLHLVLGIKQGEKHSA
porcine  1070 DQIEVCRDKGWTVQFNWFLHLVLGIKQGEKHSA
murine   1081 DQIEVCRDKGWTVQFNWFLHLVLGIKQGEKHSA
```

Chapter Four

In vitro characterisation of MmPI3kγ1111

4.1 Introduction

Over the past decade studies examining the characteristics of the PI3-kinase family, and their role in various cellular systems, have centred round the use of *in vitro* expression models. This relatively limited approach taken mostly reflects a lack of availability of reagents that specifically recognise the individual members of the PI3-kinase family, a situation that still exists for PI3kγ.

In the early 1990's, the baculovirus expression system was used to produce large quantities of recombinant Class I PI3-kinases. These were subsequently used to examine functional characteristics using *in vitro* kinase assays. The assays primarily involved reconstitution of known, as well as putative signalling components of hypothesised pathways (Dhand *et al.*, 1994a; Hiles *et al.*, 1992; Otsu *et al.*, 1991). In spite of the limitations in creating an *in vitro* system, these approaches have provided a great deal of information regarding the functional capabilities of the PI3-kinase family. More recently, mammalian over-expression systems that take advantage of the ability to epitope-tag the expressed protein, have been employed (Ma & Abrams, 1999). This allows detection and purification of the recombinant protein, in the absence of specific antibodies, whilst maintaining a true cell-based system. In the experiments presented in this chapter this latter approach has been adopted to examine the *in vitro* characteristics of the cloned PI3kγ.

Results presented in the previous chapter regarding the isolation of a clone with high identity to human and porcine PI3kγ suggested that a murine PI3kγ homologue had been successfully isolated. In the work presented in this chapter,

experiments were conducted firstly, to determine whether the cloned gene is expressed *in vivo*; secondly, to determine the pattern of expression, and finally, to determine whether the gene product displays lipid and protein kinase activity. During the *in vitro* characterisation of MmPI3kγ1111, the independent cloning and characterisation of another MmPI3kγ was reported (Hirsch *et al.*, 2000b). This recently-identified murine orthologue lacked the 33 nucleotides identified (3030-3063 bp) in the clone isolated in the present study and thus exhibited a greater degree of homology to both the human and porcine orthologues already cloned. This particular cDNA (here after referred to as MmPI3kγ1100) was obtained from Matthias Wymann in order to compare its *in vitro* characteristics with those of the PI3kγ cloned in the present study (here after referred to as MmPI3kγ1111).

4.2 *In vivo* expression of MmPI3kγ1111

An RT-PCR based approach was taken to assess MmPI3kγ1111 transcripts in a range of murine tissues. In addition, it was decided to investigate further the presence of the 33 nucleotides (3030-3063 bp) found in MmPI3kγ1111. Therefore, primers p110γ2889 and p110γ3150, were designed to flank the region containing the additional 33 base pairs (Figure 4.1A). These primers were predicted to give a 261 bp product if the additional region was present (MmPI3kγ1111), and a 228 bp product if the additional region was absent (MmPI3kγ1100). RNA was extracted from several organs from Balb/c mice and equivalent amounts of RNA were reverse-transcribed. The PCR was conducted on these samples and the amplicons analysed by agarose gel electrophoresis. MmPI3kγ1111 transcripts appeared to be ubiquitously expressed throughout murine tissues with products of approximately 260 bp identified in the testes, liver, lung, kidney, skin, small and large intestines and brain (Figure 4.1B). Two additional products, of approximate sizes 300 and 230 bp, were also amplified in the spleen (Figure 4.1B).

To unequivocally identify all amplicons, each of the three products amplified in the spleen was cloned into the pGEMT-easy vector. These products were sequenced using primers based on the promoter sequences, T7 and T3, of the vector. Sequence analysis indicated that the 261 bp product was identical to MmPI3kγ1111, including, the additional 33 bp. The smaller amplicon (228 bp in size) shared the greatest level of identity with MmPI3kγ1111 however it appeared not to contain the extra 33 bp and was identical to MmPI3kγ1100 (Figure 4.2). Analysis of the largest amplicon of 294

bp indicated that the product was of non-specific origin, namely a B-galactosidase (data not shown). Further investigation of the ability of the primers p110γ2889 and p110γ3150 to anneal to template corresponding to such a product, revealed 70% identity between the regions. Overall, these results illustrated that MmPI3kγ1111 is not only expressed *in vivo* but also appears to be the dominant product expressed in the mouse.

4.3 Generation of polyclonal antibodies specific for PI3kγ

At the onset of this study, specific antibodies against PI3kγ were commercially unavailable and the murine PI3kγ had not been cloned. Under the assumption that a high degree of homology existed between the human and murine orthologues a peptide based on the C-terminal portion of human PI3kγ was designed and used to generate polyclonal antibodies. The choice of peptide for immunisation was based on the original work conducted by Stoyanov and colleagues (Stoyanov *et al.*, 1995). Rabbits were immunised with a 15 amino acid peptide corresponding to residues 742 to 756 of the original PI3kγ sequence (Stoyanov *et al.*, 1995), gi/4505802). The peptide was coupled to keyhole limpet haemocyanin (KLH) in complete Freund's adjuvant and standard immunisation protocols were followed to generate antibodies. Antiserum was collected and shown in direct ELISA to recognise the immunising peptide (data not shown).

Multiple attempts were made using the resultant antiserum to detect the PI3kγ protein by western analysis with little success. Immunoblots on whole cell lysates

from the human U937 pre-monocytic cell line and the murine macrophage cell line, J774, demonstrated the general lack of sole specificity to PI3kγ (data not shown). In an effort to purify the antibody the polyclonal antiserum was subjected to Protein A chromatography. Results presented in Figure 4.3A demonstrate a decrease in protein concentration with wash fractions, followed by a sharp increase in protein concentration in the second elution fraction. Selected fractions were subsequently analysed by SDS-PAGE and coomassie blue staining to verify the recovery of antibody molecules. As seen in figure 4.3B, fractions corresponding to column elution show the presence of proteins corresponding to the heavy chain (~55-60kD) and light chain (~20-25kD). Wash fractions did not appear to contain these proteins. Following successful purification the antibody was again used to examine PI3kγ protein in whole cell lysates by western analysis. Once again this proved unsuccessful (data not shown).

During the mid-stages of the present study, a sample of a monoclonal antibody (hybridoma supernatant) against the N-terminal portion of HsPI3kγ was generously provided by Professor Reinhard Wetzker (Jena, Germany) (Stoyanova *et al.*, 1997). This antibody was highly-specific in western analysis for the human PI3kγ protein and was established to cross react with the murine orthologue (Hirsch *et al.*, 2000a; Stoyanova *et al.*, 1997). The antibody was not suitable for use in immunoprecitpitation (personal communication Reinhard Wetzker). This monoclonal antibody was subsequently used for all western analysis in the present study.

4.4 Over-expression of MmPI3kγ

In order to examine the function of MmPI3kγ1111 an efficient system for the expression and purification of MmPI3kγ was required. Studies by Stoyanova and colleagues characterised the lipid and protein activities of human PI3kγ by use of cytomegalovirus (CMV) promoter based mammalian expression system (Stoyanova *et al.*, 1997). Similarly, the examination of the bifurcation of signalling pathways downstream of either the lipid or protein kinase activities, were conducted using transient transfections of mammalian cells by CMV-based expression systems (Bondeva *et al.*, 1998). As mentioned in section 4.1, constructs of the independently cloned MmPI3kγ1100 were obtained for comparison from Matthias Wymann. These constructs consisted of the CMV promoter-based eukaryotic expression plasmid pcDNA3, with a His-6 tag at the N-terminus of MmPI3kγ1100. The use of a tag was essential considering the unavailability of specific monoclonal and polyclonal antibodies for immunoprecipitation and hence purification of the protein prior to conducting kinase assays. In order to maintain consistency in the examination and comparison of MmPI3kγ1111 activity, the ORF was similarly sub-cloned into pcDNA3 to result in the over-expression of the His-6 tagged MmPI3kγ1111 protein (Figure 4.4A).

HEK 293 cells were transiently transfected with the pcDNA3 constructs containing either MmPI3kγ1111 or MmPI3kγ1100. Cells were collected and lysed 48 hours post-transfection. To ensure efficient expression of full-length protein occurred, whole cell lysates were subjected to SDS-PAGE and western analysis. Both constructs

efficiently expressed proteins of ~116kD in size (Figure 4.4B). Following confirmation of protein expression, lysates were subjected to protein precipitation using Talon charged resin. Immobilised proteins were denatured and separated by SDS-PAGE and the purification of MmPI3kγ proteins verified by western analysis (Figure 4.4C). In both Figure 4.4B and 4.4C the protein bands detected at approximately 60kD and 33kD are background bands detected by the goat anti-mouse secondary antibody. Successful protein expression and purification of full-length MmPI3kγ1111 and MmPI3kγ1100 were observed using pcDNA3 expression of histidine-tagged proteins and Talon resin based purification. This over-expression system was deemed suitable for the analysis of the *in vitro* characteristics of MmPI3kγ1111.

4.5 Lipid kinase activity MmPI3kγ1111

All Class I PI3-kinases are reported to be able to phosphorylate the lipids PI, PI 4 P and PI 4,5 P_2 *in vitro* (reviewed in (Vanhaesebroeck *et al.*, 2001). Due to the presence of the additional 11 amino acids in the catalytic domain of MmPI3kγ1111, there was a possibility that the catalytic activity of MmPI3kγ1111 would be affected. Therefore, in order to examine the *in vitro* ability of MmPI3kγ1111 to phosphorylate the 3-hydroxyl position of inositol lipids, a lipid kinase assay was utilised.

HEK 293 cells were transfected with the established pcDNA3 constructs containing either MmPI3kγ1100 or MmPI3kγ1111. Proteins were purified 48 hours post-transfection and lipid kinase assays conducted on the immobilised proteins. Due

to the high cost of purified inositol lipids, phosphoinositide was the only lipid used in the assays to determine the lipid kinase activity of MmPI3kγ1111 in comparison to the independently cloned MmPI3kγ1100. Thin layer chromatography of extracted lipid products illustrated the presence of a phosphorylated product of MmPI3kγ1111 migrating at the same distance as the phosphorylated product of MmPI3kγ1100 (Figure 4.5 bottom panel). The results from these experiments indicate that MmPI3kγ1111 does possess lipid kinase activity, similar to that observed with MmPI3kγ1100, a murine orthologue that does not contain the additional 11 amino acids in the catalytic domain.

4.6 Protein kinase activity of MmPI3kγ1111

A novel characteristic of the Class IB PI3-kinases is their dual kinase activity (Stoyanova *et al.*, 1997). Both the human and porcine PI3kγ orthologues display the ability to autophosphorylate, in addition to the ability to phosphorylate lipids (Stoyanova *et al.*, 1997). This characteristic has been well established for MmPI3kγ1100.

In order to determine whether MmPI3kγ1111 was phosphorylated, in a similar fashion to other Class IB PI3-kinase orthologues, HEK 293 cells were transfected with pcDNA3 constructs containing either MmPI3kγ1100 or MmPI3kγ1111 and the proteins purified using Talon charged resin. The immobilised proteins were subjected to a protein kinase assay. This essentially involved the incubation of the over-expressed proteins with ^{32}P-ATP. These proteins were analysed by SDS-PAGE and

autoradiography. The results of this assay clearly indicate that MmPI3kγ1111 was phosphorylated *in vitro* to a similar extent as MmPI3kγ1100 (Figure 4.6 bottom panel).

4.7 The relationship between phosphorylation status of MmPI3kγ and its lipid kinase activity

Studies by Bondeva *et al.*, illustrated a bifurcation in the activity of the PI3kγ. Using hybrid molecules possessing either lipid or protein kinase activity, they demonstrated that the lipid kinase activity mediated activation of the downstream messenger PKB/Akt. In contrast, the recombinant molecules possessing only protein kinase activity mediated activation of the MAP kinase pathway. In addition, it was suggested that the PI3kγ was not able to possess both activities simultaneously (Bondeva *et al.*, 1998). Although it has been shown that PI3kγ acts either as a lipid kinase or a protein kinase, the mechanism that regulates one activity over the other has not been elucidated. Work carried out by Vanhaesebroeck and colleagues with PI3kδ (a class IA PI3-kinase) has shown that a phosphorylated form of PI3kδ is unable to act as a lipid kinase and vice versa for the un-phosphorylated version (Vanhaesebroeck *et al.*, 1999).

In order to examine the influence that phosphorylation of PI3kγ has on its lipid kinase activity MmPI3kγ1111 MmPI3kγ1100 were expressed in HEK 293 cells. Proteins were purified from whole cell lysates and analysed by coomassie blue staining (Figure 4.7A) and western analysis using the anti-PI3kγ mAb (Figure 4.7B) to

ensure equal levels of protein purification were observed for each construct. Equal quantities of MmPI3kγ1100 and MmPI3kγ1111 were either pre-phosphorylated (Figure 4.7 2C and 4C) or left in an unphosphorylated state (Figure 4.7 1C and 3C). These proteins were subsequently subjected to lipid kinase assays and, the production of the 3-phosphorylated lipid, PI 3 P was examined by TLC (Figure 4.7D). The results demonstrate that the phosphorylation of MmPI3kγ1100 and MmPI3kγ1111 (Figure 4.7 2C and 4C) prior to exposure to lipids resulted in a significant decrease in the quantity of PI 3 P production (Figure 4.7 2D and 4D) where little lipid kinase activity was observed. Conversely, immobilised MmPI3kγ1111 and MmPI3kγ1100 were subjected to lipid kinase assays, and subsequently analysed for phosphorylation by SDS-PAGE and autoradiography. During the lipid kinase activity of the immobilised MmPI3kγ1100 and MmPI3kγ1111 proteins Figure 4.7 1D and 3D there was no phosphorylation observed (Figure 4.7 1C and 3C). Taken together these results suggest that either the lipid or protein kinase activity of PI3kγ dominates at one time, and that phosphorylation of PI3kγ is able to downregulate lipid kinase activity.

4.8 Discussion

At the time sequence data was obtained for MmPI3kγ1111 no other murine orthologue had been identified, and the presence of 33 nucleotides in the catalytic domain of PI3kγ had not been previously reported in either the human and porcine orthologues. Although MmPI3kγ1111 shared a high level of identity with the human and porcine PI3kγs, it was important to determine whether MmPI3kγ1111 was expressed *in vivo* and to determine the functional characteristics of the cloned product.

RT-PCR and sequence analysis of amplicons illustrated the presence of MmPI3kγ1111 transcripts in various murine tissues, with two additional transcripts identified in the spleen, the larger product being non-specific. Sequence analysis determined that the smaller 228 bp product was also PI3kγ. This 228 bp amplicon was highly homologous to MmPI3kγ1111 (equivalent amplified region), however, interestingly it lacked the additional 33 bp. In late 2000, another murine orthologue of PI3kγ was cloned (MmPI3kγ1100) (Hirsch *et al.*, 2000b). The MmPI3kγ1100 ORF shared over 95% identity at both the nucleotide and amino acid level with the human and porcine orthologues, did not contain the 33 bp insert observed for MmPI3kγ1111 and was identical to the 228 bp product in that region. During the isolation and cloning of the porcine PI3kγ orthologue and its putative adaptor p101, Stephens *et al.*, reported the identification of two peaks of Gβγ-activated PI3-kinase activity (Stephens *et al.*, 1997). Following purification, these activities were established to consist of a p117/p101, or a p120/p101 heterodimer (names being representative of their molecular weight). The heterodimers were indistinguishable on the basis of their lipid

kinase activity (Stephens *et al.*, 1997). The cDNA putatively encoding p117 has yet to be isolated. Although the work by Stephens *et al.*, indicated the possibility of other members of Class IB PI3-kinases, the present study is the first example where cDNA cloning has pointed to the existence of two forms of PI3kγ.

At the outset, three possibilities were considered: first, the possibility that genomic DNA was the source of MmPI3kγ1111 transcripts detected; second, that MmPI3kγ1111 was the product of an independent gene; and finally, that MmPI3kγ1111 was an alternatively spliced product of one gene encoding PI3kγ.

To ensure that the observed MmPI3kγ1111 transcript was not an artefact of genomic DNA contamination, all RNA samples were treated with RNase-free DNase prior to reverse transcription and subsequent PCR. Moreover, the availability of some details of the genomic organization of MmPI3kγ gene (accession no. AJ249413 – AJ249420) also indicated that the forward and reverse primer designed for the PCR, were located in separate exons (exon 10 and exon 11, respectively) separated by a partially characterised 15 kb intron, suggesting that genomic contamination would be detected by the existence of a larger difference in amplicon sizes than the 33 bp observed.

Fluorescence in-situ hybridisation (FISH) has been used to examine the chromosomal location of the PI3kγ gene. These studies indicated that MmPI3kγ was located on chromosome 12 band B and that the human orthologue is positioned on chromosome 7 (segment 7q22.2-22.3.) (Hirsch *et al.*, 2000b). Although the resolution

of FISH is arguably not high enough to show the presence of two genes in close proximity, it was thought to be unlikely that a second gene was present. Consistent with these studies, three independent groups published data using mice in which PI3kγ had been disrupted by homologous recombination (Hirsch *et al.*, 2000; Li *et al*, 2000; Sasaki *et al.*, 2000). The reliance that this technique has on homologous recombination would make it highly unlikely that if there were two independent genes encoding two functional PI3kγ proteins, the generation of knockout mice would be successful.

The genomic organization also demonstrated that the additional 33 nucleotides occurred precisely at the boundary of two exons (exon 10 and exon 11). Boundaries between exons have been well established to be the region where splice donor and acceptor sites are located, suggesting that MmPI3kγ1111 is an alternatively-spliced gene product. Subsequently, efforts were concentrated towards the amplification of the intervening intron (intron 10) to examine the possibility of MmPI3kγ1111 being an alternatively-spliced product of the gene. Several attempts aimed at the amplification of the intron, and subsequent attempts to obtain the detailed sequence from colleagues who had published the genomic organisation of the gene (Hirsch *et al.*, 2000b), proved unsuccessful (intron 10 has only been partially sequenced). Although the present study has not been able to conclusively prove that MmPI3kγ1111 is an alternatively-spliced product rather than a product of an independent gene, indications from the literature suggest that the former is more probable. Future work, using the Celera database should resolve this issue.

Expression analysis suggested that MmPI3kγ1111 was expressed ubiquitously throughout murine tissues, including peripheral blood leukocytes, from the Balb/c mouse. Studies by Stoyanov et al., during the initial cloning of the human PI3kγ orthologue detected mRNA transcripts in the pancreas, skeletal muscle, liver and heart, by northern analysis (Stoyanov *et al.*, 1995). Now it is more widely appreciated that PI3kγ expression is limited to the leukocyte compartment in eukaryotes (reviewed in (Vanhaesebroeck *et al.*, 2001). This suggested that the mRNA detected in the Northern blots (Stoyanov *et al.*, 1995) may have been due to the presence of leukocytes in the vasculature of the organs from which the RNA was extracted. It is important to note that there is some inconsistency with the work presented here and the current literature in that the smaller amplicon, presumably MmPI3kγ1100, was only detected in the spleen and not in any of the other tissues examined. Surprisingly, the results presented in this study suggest that MmPI3kγ1111 is the predominant form of PI3kγ expressed in the mouse. The potential biological significance of two PI3kγ isoforms is discussed in further detail in Chapter 6.

The 11 amino acid insert in the catalytic domain of MmPI3kγ1111 raised the possibility that the native conformation of the protein might be different from PI3kγ1100, and as a consequence this may have affected the functional capacity of the kinase. This could be manifested by increased activity, reduced activity, or no activity, the latter raising the interesting possibility that MmPI3kγ1111 may function as a dominant-negative kinase. Therefore, having determined that MmPI3kγ1111 was expressed *in vivo*, the functional characteristics of the MmPI3kγ1111 in comparison to MmPI3kγ1100 were examined. Although, the additional region was downstream of

the ATP transfer site, the *in vitro* lipid and protein kinase activities of MmPI3kγ1111 were initially examined. These experiments were conducted on histidine-tagged PI3kγ proteins, which were easily purified using charged resin. MmPI3kγ1111 displayed the ability to phosphorylate the lipid PI as efficiently as MmPI3kγ1100. At this stage, it is difficult to unequivocally prove that the product observed by TLC is the 3-hydroxy phosphorylated lipid, PI 3 P, due to the lack of commercial standards for phosphorylated lipids, and the inability in the present study to conduct appropriate HPLC analysis. However, the use of purified PI as a substrate and the separation of lipid products in the presence of oxalate, a reagent described as being able to distinguish between different phosphorylated hydroxyl groups and in the presence of the positive control MmPI3kγ1100, strongly suggests that the observed lipid product is PI 3 P. The *in vitro* results presented in this chapter therefore demonstrate that MmPI3kγ1111 is a functional lipid kinase and that the presence of the additional 11 amino acids has little or no effect on the lipid kinase activity of the enzyme.

Bifunctional kinase activity of Class I PI3-kinases has been well established (Carpenter *et al.*, 1993; Vanhaesebroeck *et al.*, 1999). Most Class IA PI3-kinase catalytic subunits are able to phosphorylate serine residues in their cognate regulatory subunit and subsequently downregulate their lipid kinase activity (Carpenter *et al.*, 1993). One exception to this general pattern is with the Class IA kinase PI3kδ. Vanhaesebroeck and colleagues demonstrated that the catalytic subunit of PI3kδ was able to autophosphorylate and that this phosphorylation of the PI3kδ catalytic subunit also resulted in a downregulation of its lipid kinase activity (Vanhaesebroeck *et al.*, 1999). To date, autophosphorylation has been demonstrated for all identified PI3kγ

orthologues (Bondeva *et al.*, 1998; Stoyanova *et al.*, 1997). This is believed to involve serine phosphorylation, however, the precise residues involved are yet to be mapped. In order to determine whether MmPI3kγ1111 was phosphorylated, the purified proteins were incubated in the presence of ^{32}P-ATP, resolved by SDS-PAGE and analysed by autoradiography. MmPI3kγ1111 and MmPI3kγ1100 demonstrated phosphorylation. However, the results presented in this chapter do not distinguish between whether this is due to autophosphorylation or phosphorylation by an associated kinase present in the protein extracts. In order to determine whether the phosphorylation observed is autophosphorylation, a catalytically-inactive mutant of MmPI3kγ1111 will have to be made and examined. This particular aspect is addressed in Chapter 5.

Analysis of both the human and murine (MmPI3kγ1100) orthologues of PI3kγ has demonstrated that either the lipid or protein kinase activity of the enzyme dominates at one time (Bondeva *et al.*, 1998; Stoyanova *et al.*, 1997). This similar concept was examined for MmPI3kγ1111. Consistent with the literature, the results presented in this study clearly demonstrate that during lipid kinase activity there is little or no protein kinase activity and phosphorylated PI3kγ displays little lipid kinase activity. Similarly to all Class I PI3-kinases, these results demonstrate that phosphorylation of MmPI3kγ1111 downregulates its ability to act as a lipid kinase. It is still not known what signals trigger the activation of one kinase activity over the other, however these results indicate that elucidation of agonists that generate phosphorylation of PI3kγ may be involved in the mechanisms behind the regulation of Class IB PI3-kinases.

In summary, the focus of this chapter was to establish the *in vivo* expression and functional characteristics of the PI3kγ clone (MmPI3kγ1111) isolated in Chapter 3. The use of mammalian over-expression systems in this study illustrated that MmPI3kγ1111, consistent with other Class IB enzymes, was functional as both a lipid and protein kinase. Moreover, phosphorylation of MmPI3kγ1111 appeared to significantly downregulate the lipid kinase activity of the protein providing further support for the concept that phosphorylation might be involved in regulating one activity over the other. At present, the significance of the additional 11 amino acids in the catalytic domain of MmPI3kγ1111 is unclear. However, the results presented in this chapter unequivocally demonstrate that MmPI3kγ1111 is a murine orthologue of PI3kγ.

Figure 4.1 *In vivo* expression of MmPI3kγ1111 in murine tissue

A. A schematic representation showing the positioning of primers p110γ2889 and P110γ3150 which were designed to flank the 33 base pair insert (green) of MmPI3kγ1111 for use in RT-PCR.

B. PCR was carried out using the primers p110γ3030 and P110γ3290 on cDNA samples generated from various murine tissues (as indicated on the figure). Amplicons were separated on a 3.0% agarose gel, and visualised by ethidium bromide staining. Arrow indicates 260bp product.

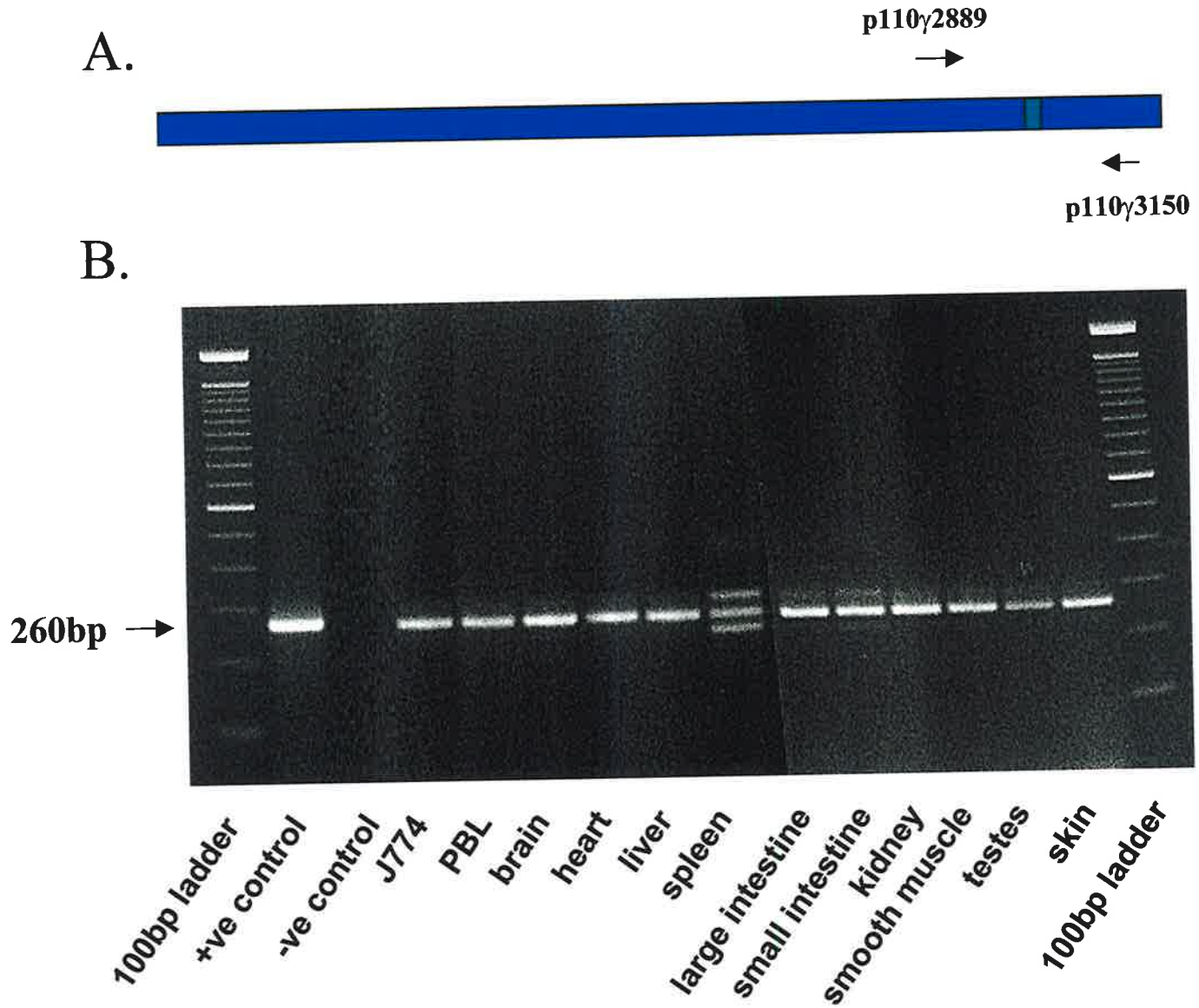
A.
p110γ2889
p110γ3150
B.
260bp
100bp ladder
+ve control
-ve control
J774
PBL
brain
heart
liver
spleen
large intestine
small intestine
kidney
smooth muscle
testes
skin
100bp ladder

Figure 4.2 Sequence analysis of MmPI3kγ primer specific PCR products

The three products amplified from spleen cDNA, and the single product from J774 cDNA were cloned into the pGEM-T easy vector and sequenced (only shown for the J774, 260 bp and 227 bp products). Sequences were translated using the raw translation program and amino acid sequences aligned using the CLUSTAL W program (www.microbiology.adelaide.edu.au/learn/index.htm). The additional 11 amino acids are represented in pink and deviation from the J774 cloned PCR product is labelled "-".

```
J774    FHIDFGHILGNYKSF LGINKERVPFVLTPD FLVVMGSSGKKTSPH FQKFQ DCCVSTLQYY
260bp   FHIDFGHILGNYKSF LGINKERVPFVLTPD FLVVMGSSGKKTSPH FQKFQ DCCVSTLQYY
227bp   FHIDFGHILGNYKSF LGINKERVPFVLTPD FLFVMGTSGKKTSLH FQKFQ ----------

J774    GDVCVRAYLALRHHT NLLIILFSMMLMTGM
260bp   GDVCVRAYLALRHHT NLLIILFSMMLMTGM
227bp   -DVCVKAYLALRHHT NLLIILFSMMLMTGM
```

Figure 4.3 Protein A purification of polyclonal rabbit anti-PI3kγ antibody

A. One mL fractions from the Protein A column were collected (samples 1-10 represent wash fractions, samples 10-31 represent elution fractions) and samples analysed for the presence of protein by optical density at 280nm (OD_{280nm}).

B. Five μL of selected fractions (as indicated on figure) were electrophoretically separated and analysed for IgG purity by 12.0% SDS-PAGE, and visualised by coomassie blue staining.

MW – broad range molecular weight markers (Biorad)

A.

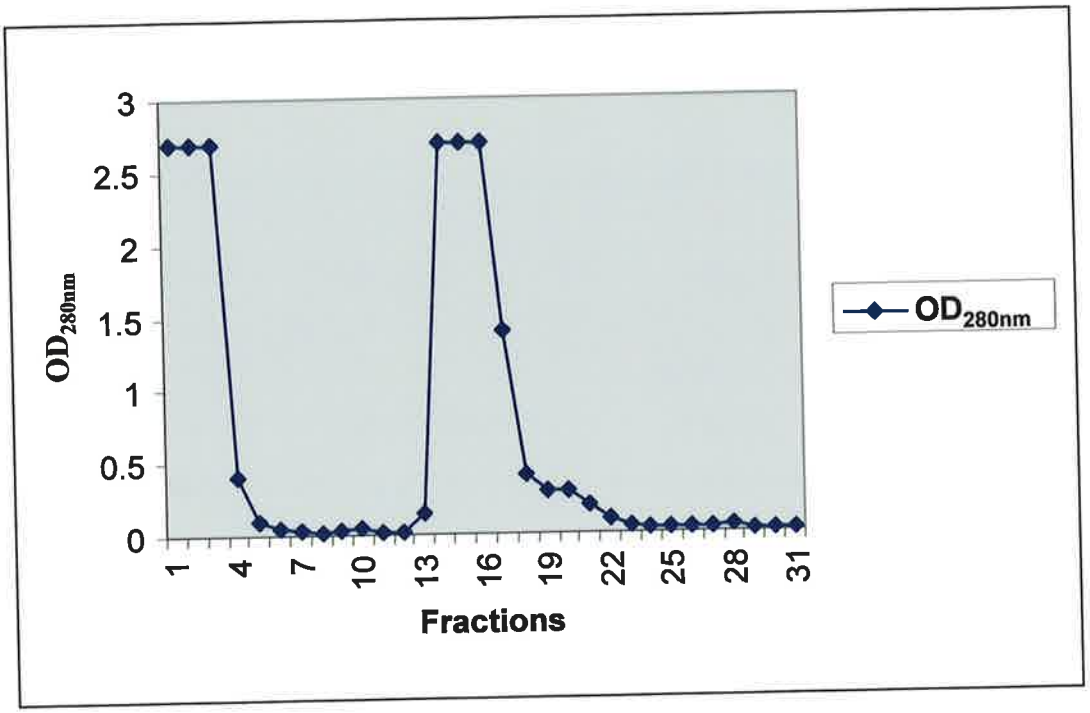
3
2.5
2
1.5
1
0.5
0
OD280nm
1
4
7
10
13
16
19
22
25
28
31
Fractions
OD280nm

B.

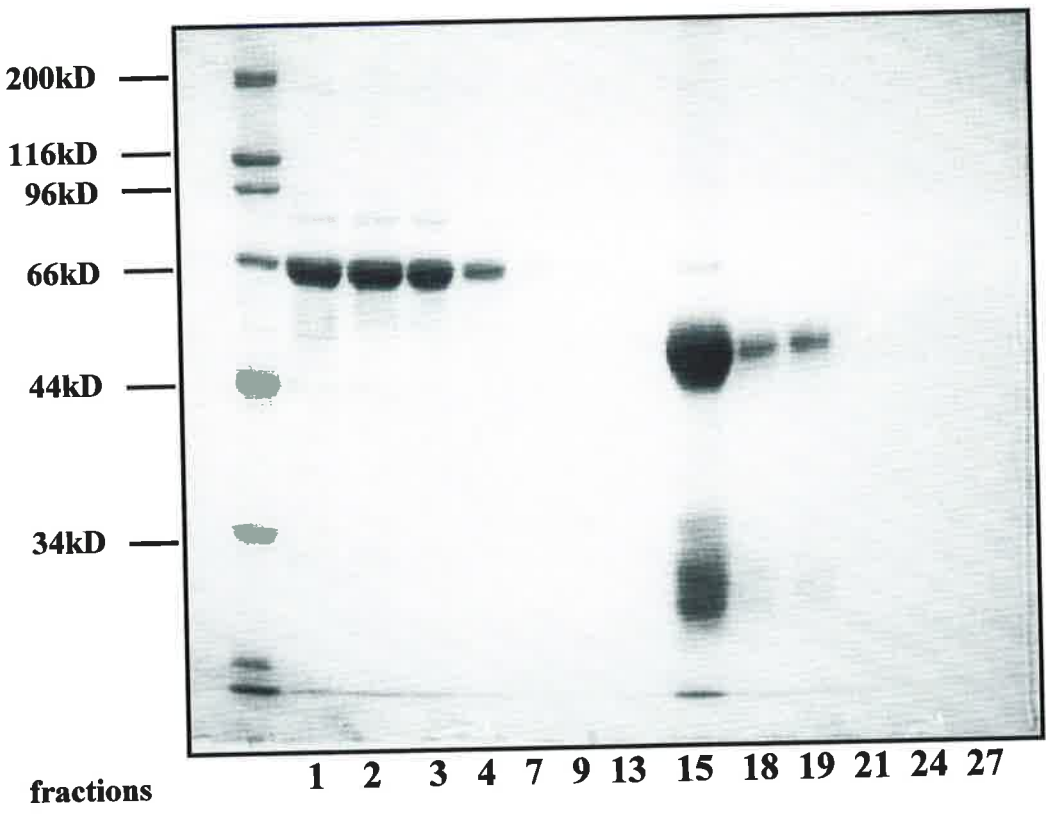
200kD
116kD
96kD
66kD
44kD
34kD
fractions
1 2 3 4 7 9 13 15 18 19 21 24 27

Figure 4.4 Over-expression and purification of MmPI3kγ1100 and MmPI3kγ1111

A. Schematic representation of pcDNA3 constructs made for the over-expression of MmPI3kγ1111 and MmPI3kγ1100 in mammalian cells.

B. HEK 293 cells were transiently transfected with either pcDNA3::MmPI3kγ1100 or the pcDNA3::MmPI3kγ1111 construct (3μg). Forty eight hours post transfection, cells were lysed and membrane fractions removed by centrifugation. Samples of whole cell lysates were resolved by 9.0% SDS-PAGE and PI3kγ protein detected by western analysis using a mouse anti-PI3kγ monoclonal antibody. MmPI3kγ proteins are indicated by the arrow. MmPI3kγ1100 (lane 1), MmPI3kγ1111 (lane 2) and mock transfected (lane 3).

C. HEK 293 cells were transiently transfected with either pcDNA3::MmPI3kγ1100 or the pcDNA3::MmPI3kγ1111 construct (3μg). Forty eight hours post transfection, cells were lysed and membrane fractions removed by centrifugation. Over-expressed proteins were purified using Talon charged resin, and immobilised proteins were resolved by 9.0% SDS-PAGE and PI3kγ protein detected by western analysis using a mouse anti-PI3kγ monoclonal antibody. MmPI3kγ proteins are indicated by the arrow. MmPI3kγ1100 (lane 1), MmPI3kγ1111 (lane 2) and mock transfected (lane 3).

MW – broad range molecular weight standards (Biorad)

A.

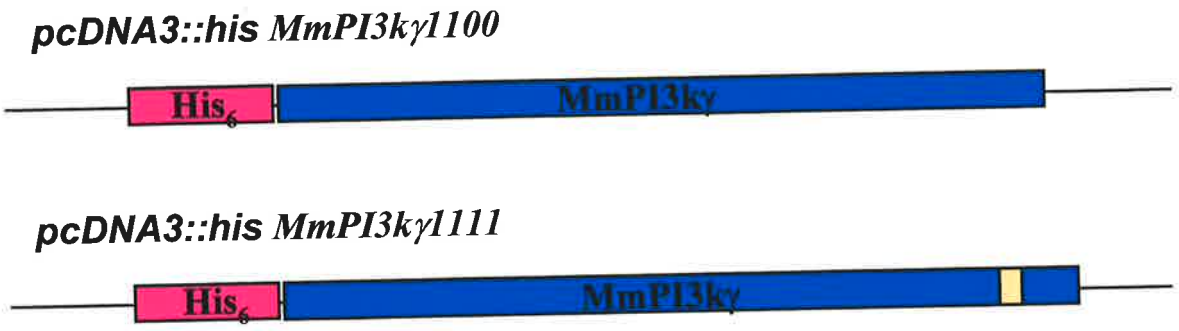
pcDNA3::his MmPI3kγ1100
His6
MmPI3kγ
pcDNA3::his MmPI3kγ1111
His6
MmPI3kγ

B.

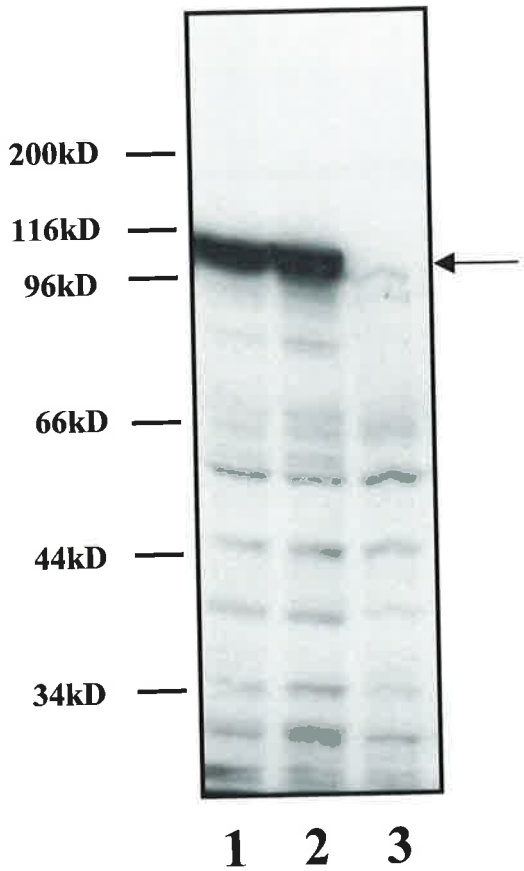
200kD
116kD
96kD
66kD
44kD
34kD
1 2 3

C.

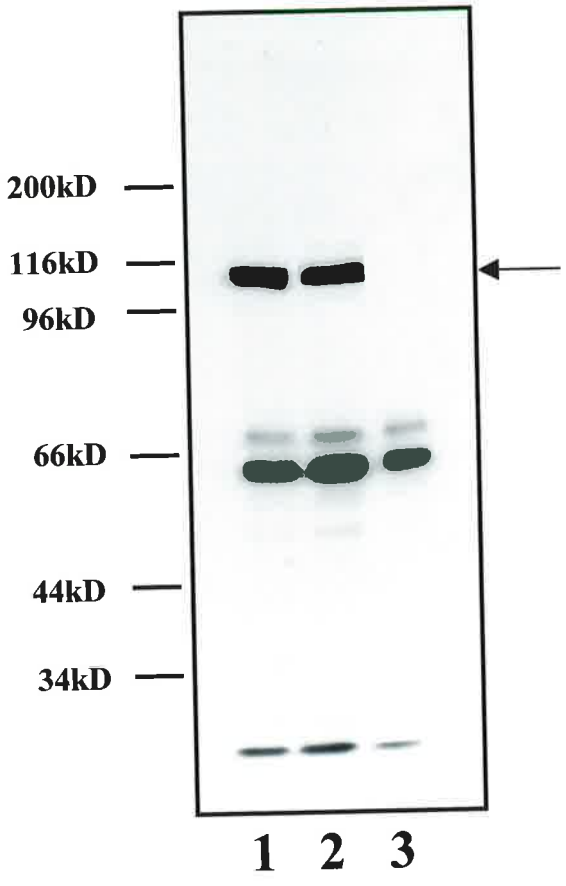
200kD
116kD
96kD
66kD
44kD
34kD
1 2 3

Figure 4.5 Lipid kinase activity of MmPI3kγ1100 and MmPI3kγ1111

HEK 293 cells were transiently transfected with either the pcDNA3::MmPI3kγ1100 or the pcDNA3::MmPI3kγ1111 construct (3μg). Over-expressed proteins were purified using Talon resin.

Top panel - Western analysis of the purified proteins MmPI3kγ1111 and MmPI3kγ1100. One third of purified proteins were separated by 9.0% SDS-PAGE and examined by western analysis using a mouse anti-PI3kγ monoclonal antibody.

Bottom panel - Immobilised proteins were resuspended in kinase buffer and incubated with the lipid substrate, PI, and ^{32}Pγ-ATP for 20 min at RT. Lipids were extracted and analysed by TLC. Products were visualised by autoradiography.

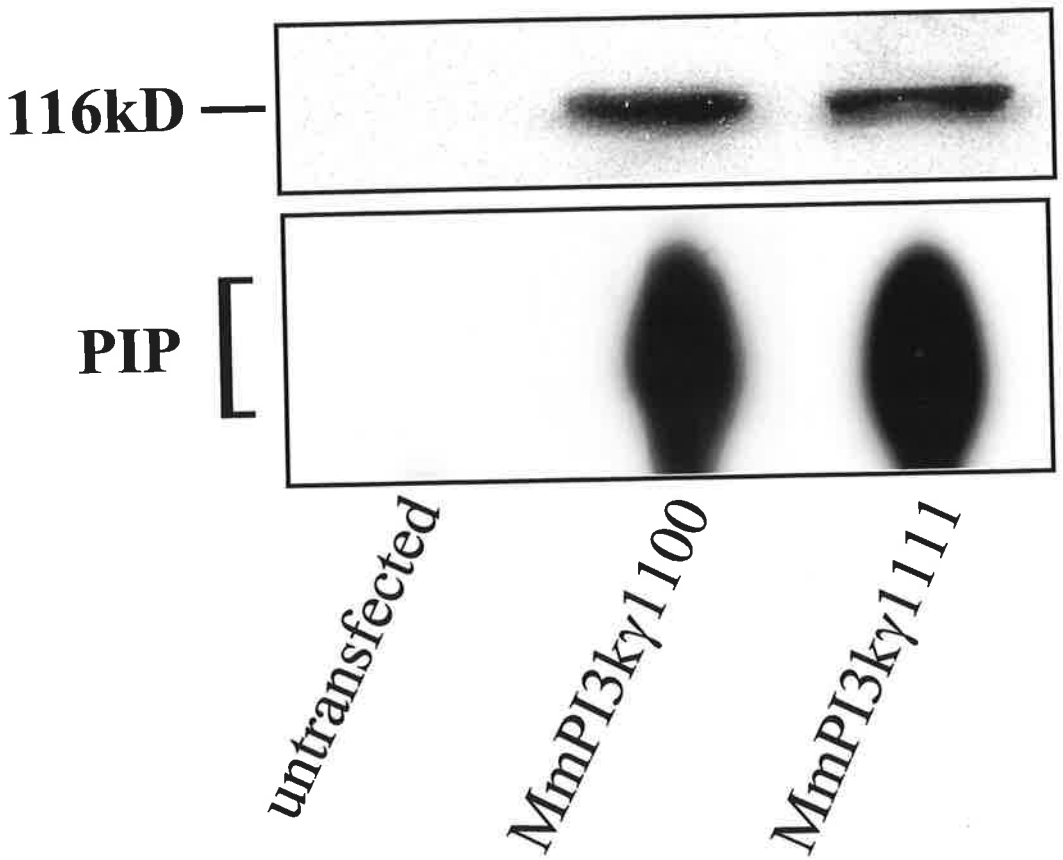
116kD
PIP
untransfected
MmPI3kγ1100
MmPI3kγ1111

Figure 4.6 Phosphorylation of MmPI3kγ1100 and MmPI3kγ1111

HEK 293 cells were transiently transfected with either the pcDNA3::MmPI3kγ1100 or the pcDNA3::MmPI3kγ1111 construct (3μg). Over-expressed proteins were purified using Talon resin.

Top panel - Western analysis of the purified proteins MmPI3kγ1111 and MmPI3kγ1100. One third of purified proteins were separated by 9.0% SDS-PAGE and examined by western analysis using a mouse anti-PI3kγ monoclonal antibody.

Bottom panel - Immobilised proteins were resuspended in kinase buffer and incubated with γ^{32}P-ATP for 20 min at RT. Proteins were analysed by 9.0% SDS-PAGE and autoradiography.

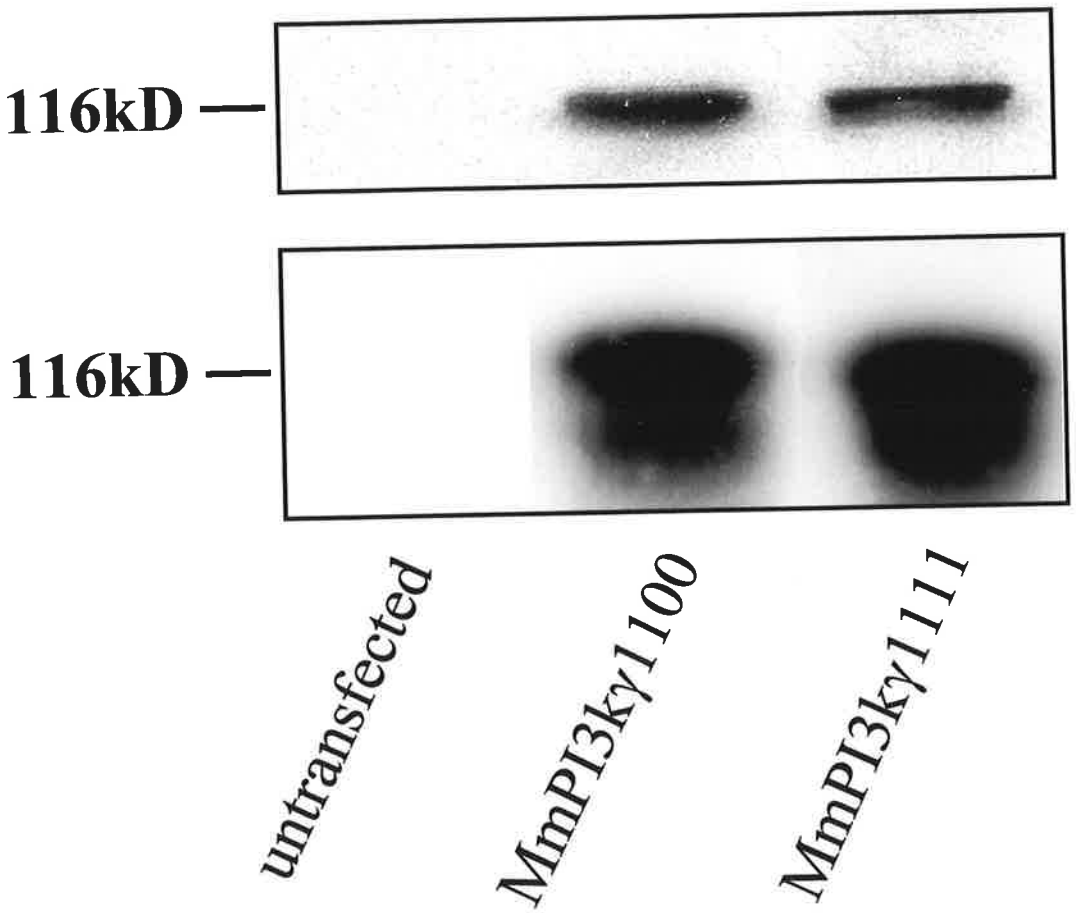
116kD
116kD
untransfected
MmPI3kγ1100
MmPI3kγ1111

Figure 4.7 Phosphorylation of MmPI3kγ downregulates lipid kinase activity

HEK 293 cells were transiently transfected with either the pcDNA3::MmPI3kγ1100 or the pcDNA3::MmPI3kγ1111 construct (3μg). Over-expressed proteins were purified using Talon resin.

A. Five μL of immobilised proteins were separated by 9.0% SDS-PAGE and proteins visualised by coomasssie blue staining.

B. Five μL of immobilised proteins were separated by 9.0% SDS-PAGE and western analysis conducted using mouse anti-PI3kγ monoclonal antibody.

C. Five μL of immobilised proteins were incubated with γ^{32}P-ATP for phosphorylation (panels 2C and 4C) and compared to 5ul of immobilised proteins without γ^{32}P-ATP (panels 1C and 3C).

D. Five μL of immobilised proteins were examined for lipid kinase activity of phosphorylated proteins was examined. Panels 1D and 3D represent unphosphorylated proteins, and panels 2D and 4D represent the lipid kinase activity of phosphorylated proteins.

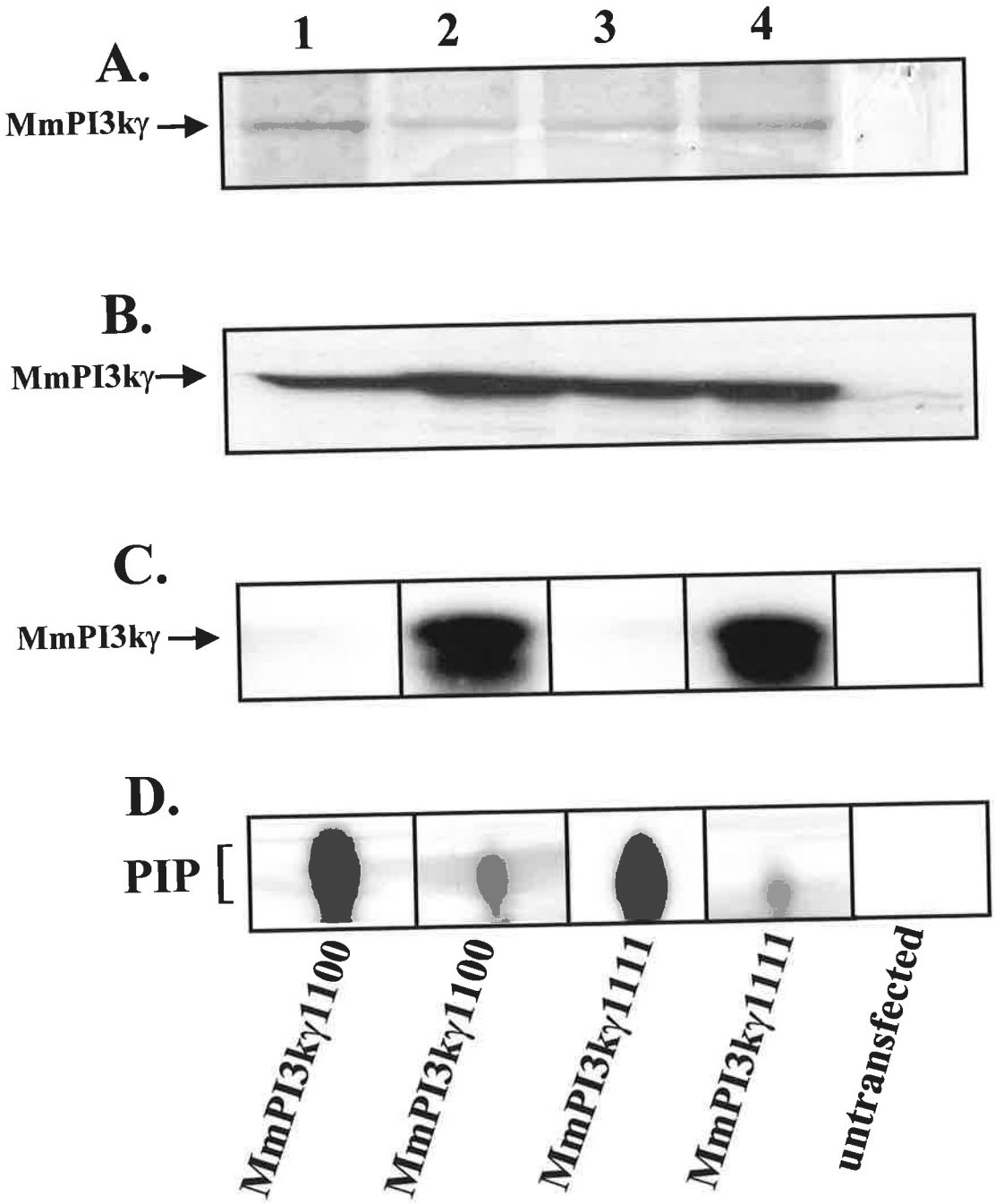
A.
1
2
3
4
MmPI3kγ
B.
MmPI3kγ
C.
MmPI3kγ
D.
PIP
MmPI3kγ1100
MmPI3kγ1100
MmPI3kγ1111
MmPI3kγ1111
untransfected

Chapter Five

The role of MmPI3kγ1111 in lymphocyte migration *in vitro* and *in vivo*

5.1 Introduction

The PI3-kinase family has been implicated in signalling pathways controlling a range of effector functions such as cell cycle regulation, cell survival (Kumar *et al.*, 2001), cytokine production, antigen presentation (Song *et al.*, 1997) and cytoskeletal rearrangement (Ma & Abrams, 1999). Much of the work to establish the importance of this family in such effector functions was initially conducted using the two structurally unrelated inhibitors of PI3-kinase activity, wortmannin and LY294002. In the mid to late 1990's, with discovery of an increasing number of PI3-kinase members and isoforms, and the finding that wortmannin and LY294002 were not specific PI3-kinase inhibitors attention focussed on techniques that would enable the dissection of the individual functions of each member and their respective signalling pathways. Arguably, one of the most definitive approaches to examine the role of an individual member of the PI3-kinase family is through the generation of mice in which the gene encoding the PI3-kinase has been disrupted. This approach has been used extensively to examine the functions of particular Class IA family members (Bi *et al.*, 1999; Fruman *et al.*, 1999), and more recently the Class IB family member PI3kγ (Hirsch *et al.*, 2000a; Li *et al.*, 2000; Sasaki *et al.*, 2000). A major outcome that has resulted from these studies has been the demonstration of developmental defects in mice during embryonic development (in the cases of p110α, p85α, p110β) and in the maturation/development of cellular components of the immune system in adult mice (PI3kγ). Neutrophils from mice deficient in PI3kγ have demonstrated a loss of the migratory ability in response to chemotactic factors such as fMLP, C5α and IL-8 and, murine models of peritonitis in these mice demonstrate a reduced infiltration of

granulocyte populations (Hirsch *et al.*, 2000a; Sasaki *et al.*, 2000). These observations confirm the postulated role of PI3kγ in chemotactic factor-mediated migration of granulocytes. Some researchers have also examined the functional capacity of the lymphocyte compartment in PI3kγ$^{-/-}$ mice concluding that adaptive immunity involving T cells is hampered, whereas functional responses of B cells appear to be independent of PI3kγ (Sasaki *et al.*, 2000). However, the mice in which these studies were conducted clearly demonstrated defects in lymphocyte development calling into question the validity of the data obtained.

The aim of the experiments described in this chapter was to attempt to examine the role of MmPI3kγ1111 in chemotactic responses of mature lymphocytes *in vitro* and *in vivo*. To avoid the developmental problems encountered with the gene knockout approach, an approach using a dominant-negative over-expression system involving a catalytically inactive mutant of MmPI3kγ1111 was adopted.

5.2 Mutagenesis of MmPI3kγ1111

When comparing the structural traits of the PI3-kinase family, the most conserved domain is the C-terminal catalytic domain. Studies examining the regions essential for the kinase activity of these enzymes highlight the importance of the ATP transfer site, and in particular, a highly conserved lysine residue. In the Class IA PI3-kinases this lysine is mapped to position 802 (Dhand *et al.*, 1994b). Mutation of this residue renders the members of the Class IA family kinase inactive and over-expression of this mutant in COS cells results in inhibition of endogenous PI3-kinase activity (Dhand *et al.*, 1994a; Dhand *et al.*, 1994b). PI3kγ has an equivalent lysine residue that has been mapped to 833. Studies mutating this residue in the human orthologue have also resulted in a loss of lipid and protein kinase activity (Stoyanova *et al.*, 1997).

In order to examine the cellular role of the murine orthologue MmPI3kγ1111 using a dominant-negative expression system, the murine PI3kγ was mutated to abolish protein and lipid kinase activities. Site-directed mutagenesis using the 'quikchange' method was used to mutate the lysine residue at 833 (Figure 5.1). This approach takes advantage of the methylated state of the parental plasmid DNA construct. Mutagenic primers are designed to anneal to both the sense and anti-sense strands of the DNA template. Extension from these primers incorporates the changes in a non-methylated product. Finally, *Dpn*I is used to restrict the methylated parental strands, whilst maintaining the mutagenised (non-methylated) extension products (Figure 5.2).

In order to abolish enzymatic activity of MmPI3kγ1111, the lysine residue was mutated to encode for an arginine residue (Figure 5.1). Investigation of the MmPI3kγ1111 nucleotide sequence demonstrated that the lysine at position 833 is encoded by the codon AAA. To minimise the extent of the mutagenesis, primers incorporating a single base pair change to AGA (Figure 5.1) were designed. The minor change of codon form AAA to AGA was predicted to result in a change from a lysine to an arginine residue (Figure 5.1). In addition, this particular nucleotide change also resulted in a loss of a *Dra*I restriction enzyme site thereby enabling restriction analysis to be used to identify constructs positive for the mutation prior to sequencing.

Putative clones obtained after the site-directed mutagenesis of MmPI3kγ1111 (in pcDNA3) were analysed by *Dra*I restriction. Products were resolved on a 1.2% agarose gel and visualised by ethidium bromide staining. Of 5 putative clones, 2 resulted in a restriction pattern consistent with the parental construct, whilst three gave rise to a restriction pattern indicating the loss of a *Dra*I restriction site (Figure 5.3A). Sequence analysis was carried out on all five clones. Consistent with the restriction patterns, clones 2, 3 and 5 all demonstrated a change from the AAA codon to the AGA codon, representing a change from a lysine to an arginine in the translated product (Figure 5.3B). Proteins carrying this mutation are here after referred to as MmPI3kγKR

5.3 Lipid Kinase activity of MmPI3kγKR

HEK 293 cells were transfected with the pcDNA3 construct containing either MmPI3kγ1111 or MmPI3kγKR. The PI3kγ proteins were purified using Talon charged resin 48 hours post-transfection and either western blots or lipid kinase assays were conducted. Western blot analysis of the purified proteins indicated extraction of approximately equivalent amounts in each of the 2 transfected populations (Figure 5.4 upper panel). Thin layer chromatography of extracted lipid products revealed the presence of a 3-phosphorylated lipid product of MmPI3kγ1111 (Figure 5.4 bottom panel). In contrast, no 3-phosphorylated lipid was detectable in the lipid kinase assays of the MmPI3kγKR protein (Figure 5.4 bottom panel). The results from these experiments indicate that the site-directed mutagenesis to alter lysine 833 to an arginine had removed the lipid kinase activity of MmPI3kγ1111.

5.4 Protein kinase activity of MmPI3kγKR

Mutagenesis studies of the family of PI3-kinases have illustrated that both the protein and lipid kinase activities of Class I PI3kinases are dependent on the ATP transfer site. Having determined above that mutation of the lysine residue had resulted in a loss of lipid kinase activity, the protein kinase activity of MmPI3kγKR was then examined.

HEK 293 cells were transfected with pcDNA3 constructs containing either MmPI3kγ1111or MmPI3kγKR, and proteins purified using Talon charged resin. The

purified proteins were then subjected to a protein kinase assay. The western blot presented in Figure 5.4 (upper panel) demonstrating equal levels of protein purification is duplicated for reference in Figure 5.5 (upper panel) as the proteins subjected to a protein kinase assay were a sample from the purification of those resolved on the SDS-PAGE. Following incubation with γ^{32}P-ATP, proteins were resolved on a SDS-PAGE and analysed by autoradiography. In contrast to the phosphorylation observed by MmPI3kγ1111, MmPI3kγKR demonstrated a lack of phosphorylation (Figure 5.5 bottom panel). The results of this assay clearly indicate that the phosphorylation of MmPI3kγ1111 is a result of autophosphorylation, and not due to the presence of other kinases in the protein extracts. Taken together with the Section 5.3, the results confirm that MmPI3kγKR is catalytically inactive.

5.5 Development of a retroviral dominant-negative expression system

In order to address the role of MmPI3kγ1111 in chemotactic factor-induced lymphocyte migration *in vivo*, a mammalian expression system was required. According to the literature, the most efficient technique for the over-expression of proteins in primary lymphocytes are retroviral expression systems (Parijs *et al.*, 1999a; Parijs *et al.*, 1999b; Pear *et al.*, 1998). These systems are likely to permit the constitutive expression of the MmPI3kγKR protein at a level that is able to compete with the endogenous kinase and its associated signalling partners. However, perhaps more importantly, the retroviral system has been reported to enable expression of exogenous proteins in primary lymphocytes to allow the examination of their cellular

function, a process not yet consistently achieved using standard plasmid-based expression systems.

The retroviral vector pMIG was obtained from David Baltimore (CA, USA). This vector was based on the murine stem cell virus with a unique internal ribosome entry site that enables use of the enhanced green fluorescent protein (EGFP) as a reporter gene (Figure 5.6A) (Parijs *et al.*, 1999a; Parijs *et al.*, 1999b). The utility of this system is based on the ability to identify and select for cells expressing the candidate gene through the concomitant expression of EGFP. This is achieved by fluorescence activated cell sorting. The general process of a retroviral expression system is schematically illustrated in Figure 5.6B. The cDNA of interest is cloned into the poly-linker of the retroviral vector and the construct is subsequently transfected into a packaging cell line. The long terminal repeats engineered into the construct enable the packaging of the cDNA into viral particles which are subsequently released into the growth medium of the cells. The supernatant is harvested and incubated with the target cells to facilitate viral infection and resultant integration into the target cell chromosome.

In order to use the retroviral system several variables had to be optimised. Virus production in this system was deemed to be a direct reflection of the efficiency of transfection of the packaging cell line. In turn, efficiency of transfection was dependent upon the construct and the cell density used. The ectotropic Ecopack2 cell line was purchased from Clontech (CA, USA) for this approach. Guided by manufacturer's instructions two cell densities ($5x10^5$ and $1x10^6$) were transfected each with 2 concentrations of pMIG plasmid DNA (0.5μg and 3μg) using the FuGENE 6

reagent (Boerhinger Mannheim). Approximately 50 hours post-transfection supernatants were harvested and incubated with target cells, NIH 3T3 murine fibroblasts. Target cells were harvested and examined for EGFP expression using a FACScan (Beckton Dickinson). To determine the level of autofluorescence of the NIH 3T3 population, cells were incubated with the supernatant of untransfected Ecopack 2 cells. Cells expressing a higher level of fluorescence than these cells were deemed to be positive for EGFP expression. When comparing the EcoPack2 cell densities used for transfection and the two quantities of DNA, the number of EGFP-positive NIH 3T3 cells was greater when using a cell density of 10^6 cells/dish and 3μg of plasmid DNA (Figure 5.7). Using these conditions approximately 8.0% of the target cell population was positive for viral uptake and gene expression.

Based on these results, efforts focussed on further increasing the efficiency of transfection of the packaging cells and therefore increasing the target cell viral infection. In order to do this, a wider range of DNA quantity, and quality, and alternative transfection protocols were examined. Successful transfection of cell lines is reported to resemble a bell shaped curve in which increasing concentrations of DNA are used. For every DNA construct and cell line there is an optimum concentration of DNA to use in order to obtain high transfection efficiencies. The use of DNA concentrations higher or lower than this, result in sub-optimal transfections. To determine the optimum concentration for the transfection of EcoPack2 cells with pMIG, increasing levels of plasmid DNA were used for transfection of 10^6 packaging cells. The results demonstrated an initial dose-dependent increase in NIH 3T3 cells positive for EGFP expression using 0.5-3ug of plasmid DNA. The level of EGFP expression for 3 and 6ug of DNA were both ~8%. These results indicated that the

optimum concentration of DNA was between 3 and 6ug of DNA (Figure 5.9). Alternative DNA qualities were subsequently examined. Five μg of pMIG DNA prepared by various methods ranging from traditional alkaline lysis midi-preps to various column purification kits, were used to transfect 10^6 EcoPack2 cells. On analysis of target NIH 3T3 cells the highest level of viral infection (~10%) was observed using DNA purified by traditional alkaline lysis and a column DNA purification kit obtained from Geneworks, Australia. Finally, various transfection protocols/reagents were tested using 5μg of pMIG on 10^6 Ecopack2 cells. The reagents examined were FuGENE 6, Effectene (Qiagen, Germany), Lipofectamine 2000 (Clontech, USA) and $CaCl_2$-based transfection (Pear *et al.*, 1998). Once again the highest level of expression of NIH 3T3 cells was ~ 8-10%. During the latter stages, viral supernatant was incubated with proliferating primary T lymphocytes. Experiments using these primary target cells for viral infection resulted in less than 5% of the population expressing EGFP, a level insufficient for the planned experiments to be completed successfully. Although further parameters could have been examined it was deemed at this stage that sufficient time had been spent in developing this method. It was therefore decided to conduct further experimentation using plasmid-based transfection of a lymphocytic cell line.

5.6 Generation of B lymphocytes stably-transfected with pcDNA3::MmPI3kγKR

The pcDNA3 constructs were next transfected into the murine B lymphocyte cell line (B300.19) expressing the human CCR6 chemokine receptor. To generate stable B300.19 cells expressing MmPI3kγKR, the B cell line was electroporated with

either pcDNA3 vector alone or with the dominant-negative construct, pcDNA3::MmPI3kγKR. Forty eight hours post-electroporation, the antibiotic G418 (geneticin; 1.2mg/mL) was used to begin selection for transfectants. Following 2 weeks of selection, cells were analysed for protein expression by western analysis of whole cell lysates. Figure 5.8 (top panel) illustrates the presence of endogenous MmPI3kγ protein in the lysates of untransfected cells, and in cells transfected with pcDNA3 or pcDNA::MmPI3kγKR. Due to the presence of endogenous MmPI3kγ it was impossible to distinguish between this and MmPI3kγKR in a simple western blot. In order to specifically demonstrate expression of MmPI3kγKR, whole cell lysates were incubated with Talon-charged resin and the purified proteins subjected to western analysis (Figure 5.8 bottom panel). Protein precipitation followed by western analysis clearly demonstrated the presence of MmPI3kγKR (Figure 5.8 bottom panel) in comparison to the untransfected and the mock-transfected B300.19 cells, indicating that MmPI3kγKR was being expressed in these cells.

5.7 Protein and lipid kinase activity of the MmPI3kγKR

To ensure that the stably-transfected cells were expressing the catalytically-inactive form of MmPI3kγ1111, lipid and protein kinase assays were conducted. Transfected cells were lysed and proteins purified using Talon resin. In comparison to the production of the 3-phosphorylated lipids by the wild type MmPI3kγ1111, the proteins purified from the MmPI3kγKR transfected B cells demonstrated little lipid kinase activity (Figure 5.9 middle panel). Similarly, autophosphorylation was not

observed for MmPI3kγKR protein purified from transfected B cells (Figure 5.9 bottom panel).

5.8 Effect of transfection with MmPI3kγKR on *in vitro* chemotaxis of B300.19-huCCR6 cells in response to human MIP-3α

In order to determine whether MmPI3kγ1111 is involved in the CCR6 signal transduction pathway that regulates the directed recruitment of the B300.19-huCCR6 cell line, *in vitro* transwell chemotaxis assays were employed. B300.19-huCCR6 cells stably-transfected with pcDNA3 alone and those transfected with MmPI3kγKR were loaded with the fluorophore calcein-AM. Calcein-AM loaded cells were exposed to a range of concentrations of human MIP-3α, the ligand for the human CCR6 receptor, and their migration examined using transwell chemotaxis chambers. Cells were allowed to migrate for 3 hr at 37°C, after which they were collected and the level of fluorescence measured in the lower chambers. The percentage of migrated cells for the various concentrations of human MIP-3α, are depicted for B300.19-huCCR6 cells transfected with either MmPI3kγKR or the vector alone (Figure 5.10). B300.19-huCCR6 cells transfected with pcDNA3 alone demonstrate a typical bell shaped dose-response curve, where the increasing levels of migration are observed from 3ng/ml to 300ng/ml of huMIP-3α, the latter being the concentration for which the greatest migration is observed. The percentage of migrated pcDNA3 transfected cells declined at 1μg/ml huMIP-3α. Upon examination of the MmPI3kγKR-transfected B300.19-huCCR6 cells in *in vitro* chemotaxis, using the same range of huMIP-3α concentrations, a significantly lower level of migration was observed (Figure 5.10).

Approximately 30% - 50% reduction in migration was observed for all doses from 3ng/ml to 300ng/ml. These results suggest an important role for MmPI3kγ1111 in the chemotactic function of B300.19-huCCR6 cells in response to huMIP-3α.

5.9 CCR6 expression on B300.19-huCCR6::MmPI3kγKR cells

In view that transfection of B300.19 cells significantly reduced *in vitro* chemotaxis in response to MIP-3α it was imperative to ensure that the over-expression of MmPI3kγKR did not alter the level of expression of the chemokine receptor CCR6, in comparison to the wild type cells.

In order to evaluate the effect of over-expression of MmPI3kγKR on the level of CCR6 receptor expression flow cytometric analyses were conducted. Cells transfected with pcDNA3 alone, or with MmPI3kγKR were labelled using a monoclonal antibody against the human CCR6 receptor, followed by a mouse biotin conjugate and finally a PECy5 streptavidin conjugate. Gates were set based on the forward- and side-scatter profiles and background autofluorescence determined using an isotype-matched control primary antibody. The mean fluorescence intensities for both populations are shown in Figure 5.11. B300.19 cells transfected with pcDNA3 alone demonstrate a mean fluorescence intensity of 7.67 in comparison to a mean fluorescence intensity of 2.99 for pcDNA3- transfected cells stained with a control antibody (Figure 5.11 A and B). The mean fluorescence levels of the MmPI3kγKR transfected cells were approximately 8.45 (Figure 5.11 C). These data indicate that neither the transfection and the selection processes nor the over-expression of MmPI3kγKR, appears to significantly influence the level of CCR6 expression on the

B300.19 lymphocytes, and the inhibitory effect of MmPI3kγKR overexpression on *in vitro* chemotaxis is not due to alterations in CCR6 expression.

5.10 Calcium mobilisation of B300.19-huCCR6 cells stably-tranfected with pcDNA3::MmPI3kγKR

The results of the previous experiments demonstrated that over-expression of the MmPI3kγKR did not affect the level of expression of CCR6 on the cell surface. However, it was still important to demonstrate that the inhibition of *in vitro* chemotaxis observed was not the result of a general non-specific inhibitory effect on B300.19 function. Therefore, a second assay of chemokine function was investigated. Chemokines are capable of mobilising intracellular calcium upon ligation of their cognate receptors, and this increase in the level of intracellular calcium is presently known to be independent of PI3kγ activity (Thelen, 2001). Over-expression of MmPI3kγKR should therefore not inhibit MIP-3α-induced calcium mobilisation.

A calcium mobilisation assay was carried out on both the B300.19 cells transfected with pcDNA alone and those transfected with the MmPI3kγKR construct. Cells were loaded with Fura-2-AM, and exposed to various concentrations of the CCR6 ligand, MIP-3α. The level of intracellular calcium in response to MIP-3α, was then calculated for each transfected cell line. Figure 5.12 depicts a representative time trace of intracellular calcium mobilisation of B300.19-huCCR6 cells transfected with pcDNA3 alone (Figure 5.12A) or MmPI3kγKR (Figure 5.12B), in response to 30ng/mL of human MIP-3α. No significant difference was observed in the level of

calcium mobilised in the MmPI3kγKR-transfected cells, in response to human MIP-3α, when compared with the cells transfected with the vector alone. Upon examination of various concentrations of huMIP-3α ranging from 1ng/ml to 1μg/mL no detectable difference was observed between the cell lines in their ability to release intracellular calcium stores upon huCCR6 receptor ligation (data not shown). These results demonstrate that receptor ligation of huCCR6, by huMIP-3α, is able to mediate the mobilisation of intracellular calcium equally well, independently of the presence or absence of MmPI3kγKR.

5.11 *In vivo* recruitment of B300.19-huCCR6 cells

In order to investigate the impact of MmPI3kγ1111 on lymphocyte migration *in vivo*, a mouse model examining the directed migratory patterns of the B300.19 cells was developed. A well-established technique in the laboratory to observe directed movement of cells *in vivo* is the murine subcutaneous air-pouch model. This technique creates a vascularized cavity on the dorsum of mice in which reagents can be injected and cellular infiltrates easily collected and measured (Coates & McColl, 2001). Experiments were therefore conducted to determine whether recruitment of passively transferred B300.19-huCCR6 cells could be measured in the subcutaneous air-pouches in response to huMIP-3α.

The B300.19 B lymphocytic cell line was generated from NIH/Swiss outbred mice. Therefore, to minimise potential problems with host recognition of the B300.19 cells as foreign, Swiss outbred mice were used for all of these in vivo experiments.

Air-pouches were raised on the dorsum of mice on day 0 and reinflated on day 3. On day 6, 10^7 B300.19-huCCR6 cells were intravenously injected into each mouse, followed by injection of either PBS or huMIP-3α (3 or 10μg) into the air pouch. The cellular infiltrates were collected from the air pouches either 4 hr or 24 hr later. Total recovered cells were determined and compared for each of the chosen concentrations and time points. In addition, a fraction of the collected cells were labelled with the anti-human CCR6 monoclonal antibody for analysis by flow cytometry to determine the number of huCCR6-positive cells recruited into the air pouch at each dose and time point.

The total number of cells recovered at 4 hr from the air pouches of mice, was clearly dose-dependent (Figure 5.13A). The total number of cells recovered from the air pouches of mice injected with 3μg and 10μg was significantly higher than in the diluent control (PBS). Furthermore, administration of 10μg of huMIP-3α resulted in a significant increase in cellular recruitment as compared with 3μg of huMIP-3α. At 24 hr post-injection, a greater number of total cells were recovered from the air pouches of mice injected with 10μg when compared with PBS or 3μg of huMIP-3α. In contrast to the observations at 4 hr, injection of 3μg of huMIP-3α for 24 hr did not result in a significant increase of cellular recruitment compared with the diluent control (Figure 5.13A). When comparing the total number of cells recruited at 4 hr verses 24 hr it was evident that the number of cells accumulating in the air pouches had begun to decline by 24 hr post agonist injection.

Flow cytometric analysis of cellular infiltrates to determine the number of huCCR6-positive B300.19 cells recovered from the air pouches demonstrated results consistent with the data obtained for total cell counts. Ten μg of huMIP-3α stimulated recruitment of a significantly greater number of huCCR6-positive cells than either PBS or 3μg huMIP-3α at both 4 hr and 24 hr post-injection. At 4 hr post-injection, 3μg of huMIP-3α also stimulated recruitment of a greater number of huCCR6-positive cells. However, at 24 hr post-injection no significant increase was observed (Figure 5.13B). Once again, more CCR6-positive cells were observed at 4 hr than at 24 hr post-injection at each of the concentrations of agonist used.

Taken together, these results demonstrate that directed recruitment of B300.19-huCCR6 cells, in response to huMIP-3α is measurable using the murine air pouch model. In addition, 10μg of huMIP-3α and examination of the cellular infiltrate 4 hr post agonist injection appear to be suitable parameters for use in further experiments to examine the effect of MmPI3kγKR over-expression on the recruitment of B300.19 cells *in vivo*.

5.12 The effect of transfection with MmPI3kγ1111 on *in vivo* migration of B300.19-huCCR6 cells

To determine the *in vivo* role of MmPI3kγ1111 in the recruitment of B300.19 cells in response to MIP-3α, subcutaneous air pouches were raised on the backs of mice on day 0 and reinflated on day 3. Three days post reinflation, 10^7 B300.19-huCCR6 cells transfected with pcDNA3 or pcDNA3::MmPI3kγKR were injected

intravenously into the mouse. The air pouches were subsequently injected with either 10μg huMIP-3α or PBS. Four hr post-agonist injection, cellular infiltrates were collected and total cell counts determined using trypan blue exclusion. A portion of the cells were labelled using an anti-human CCR6 monoclonal antibody for flow cytometric analysis in order to specifically quantify the number of B300.19-huCCR6 cells recruited.

Examination of total recovered cells demonstrated a significant increase in infiltration of leukocytes in response to 10μg huMIP-3α in comparison to the diluent control for mice intravenously injected with B300.19-huCCR6 cells transfected with the vector alone (Figure 5.14A). These results were consistent with those obtained in Section 5.10. Similarly, mice injected with B300.19-huCCR6 cells expressing MmPI3kγKR, the catalytically-inactive form of MmPI3kγ1111, also demonstrated a significant increase in cellular infiltration in response to huMIP-3α, as compared with the diluent control. There was no significant difference observed in the total number of cells recruited into the pouch in response to huMIP-3α, between mice injected with B300.19-huCCR6 cells transfected with vector alone and those with MmPI3kγKR (Figure 5.14A).

Upon examination of the total number of CCR6-positive cells present in air pouches following agonist injection, a similar pattern was observed. Mice injected with either cells transfected with pcDNA3 alone or MmPI3kγKR demonstrated a significant increase in the number of CCR6-positive cells recruited in response to 10μg of huMIP-3α, when compared with the diluent control. However, no significant

difference was observed in the number of CCR6-positive cells obtained from air pouches, in response to huMIP-3α when comparing cells transfected with vector alone or the dominant-negative construct (Figure 5.14B).

5.13 Discussion

The broad aim of the present study was to clone the murine orthologue of PI3kγ, and examine its cellular role in lymphocyte migration *in vitro* and *in vivo*. The work presented in this chapter focussed on the generation of a catalytically-inactive form of MmPI3kγ1111, termed MmPI3kγKR, in order to examine the importance of this molecule in the generation of lymphocyte chemotaxis downstream of chemokine receptor ligation using of a dominant-negative expression system.

The level of identity that exists between all PI3-kinases and some PI4-kinases in the catalytic domain has enabled the adoption of information gained regarding essential residues required for activation, from one isoform to another. The catalytic activity of the PI3-kinases resides in a lysine residue that is essential for the transfer of the ATP to activate the kinase (reviewed in Wymann & Pirola, 1998)). In the Class IA PI3-kinases, this lysine residue is mapped to position 802 (Carpenter *et al.*, 1993), and in the Class IB PI3-kinases the lysine residue is mapped to position 833 (Stoyanova *et al.*, 1997). Previous studies have demonstrated that mutagenesis of the lysine residue results in the loss of both protein and lipid kinase activity and sequence analysis of MmPI3kγ1111 indicated the presence of the same lysine at position 833. Using the quikchange mutagenesis method, the lysine residue at 833 was mutated by a single base pair resulting in a change to an arginine residue. The resultant protein product was referred to as MmPI3kγKR. Consistent with other Class IB orthologues, examination of lipid kinase activity demonstrated that site-directed mutagenesis of the lysine residue resulted in the loss of PI 3 P production. Moreover, this was also

accompanied by a loss of protein phosphorylation of the PI3kγ. The loss of protein phosphorylation not only demonstrated that the phosphorylation of MmPI3kγ observed in chapter 4 was due to the inherent protein kinase activity of MmPI3kγ1111, but that mutagenesis of the lysine residue was integral for both the lipid and protein kinase activities.

Because disruption of Class IA PI3-kinase catalytic subunits is embryonic lethal and disruption of the Class IB PI3-kinase catalytic subunit leads to developmental defects observed in the lymphocyte compartment, it was decided to take an alternative approach to examine the role of PI3kγ in lymphocyte trafficking *in vitro* and *in vivo*. Using the catalytically-inactive form of PI3kγ was used to generate a dominant-negative expression system. This system relies on the ability to express higher levels of the MmPI3kγKR protein than endogenous levels of the wild-type protein. This enables the catalytically-inactive protein to competitively bind any endogenous signalling partners or molecules required for correct spatial arrangement, thereby preventing the activation of the wild-type protein. Hence effector functions dependent on the activation of MmPI3kγ are inhibited. The advantage of such a system is that it avoids developmental defects that may result from the lack of PI3kγ action during embryogenesis and therefore allows examination of the function PI3kγ in mature cells.

In the present study initial attempts were made to utilise a retroviral system to express the dominant-negative construct. This approach was initially chosen because, according to the literature, it was the only consistent way to express exogenous

proteins in primary lymphocytes, the cell type of interest (Parijs *et al.*, 1999a; Parijs *et al.*, 1999b; Pear *et al.*, 1998). However, a lack of successful viral production led to the adoption of an alternative approach involving plasmid-based transfection of a lymphocytic cell line. The B300.19 cell line was obtained for the generation of these particular cells. This B cell line was initially derived from the bone marrow of NIH/Swiss outbred mice for the examination of gene rearrangements involved in the production of variable regions of the immunoglobulin heavy chain during B cell development (Reth *et al.*, 1985; Reth *et al.*, 1986). The particular B300.19 cell line used in the present study, referred to as B300.19-huCCR6 was developed to express the human CCR6 chemokine receptor, enabling the downstream analysis of activation induced by MIP-3α, the chemokine ligand for CCR6. B300.19-huCCR6 cell lines stably-transfected with either pcDNA3 alone or pcDNA3::MmPI3kγKR were generated and to ensure the over-expressed proteins maintained the catalytically-inactive phenotype, the MmPI3kγKR protein was purified and examined in a lipid kinase and protein kinase assay. Consistent with the *in vitro* analysis in Chapter 4, the over-expressed protein demonstrated no kinase activity in B300::huCCR6 cells.

Chemokines were initially identified on the basis of their ability to direct migration of various leukocyte populations both *in vitro* and *in vivo*. In order to determine the role of MmPI3kγ1111 downstream of chemokine signalling, the stably transfected cells were examined for their ability to migrate in response to MIP-3α. Chemotaxis of B300.19-huCCR6 cells transfected with pcDNA3 alone demonstrated a standard "bell shaped response curve" upon exposure to increasing concentrations of huMIP-3α. B300.19-huCCR6 cells expressing MmPI3kγKR exhibited a marked

decrease in the percent of cells migrating in response to the same doses of huMIP-3α. These results suggested that the chemotactic response of B300.19 cells in response to huMIP-3α is dependent on MmPI3kγKR.

To ensure that the decrease in migration of the cells transfected with MmPI3kγKR observed was not due to a decrease in huCCR6 receptor expression on the cell surface, flow cytometric analysis was conducted. No significant difference was observed in the levels of huCCR6 expression between the B300.19-huCCR6 MmPI3kγKR cells and the cells transfected with vector alone. Further to this, the ability of these cells to signal through the huCCR6 receptor was examined. Activation of the majority of GPCRs by chemotactic factors leads to the mobilisation of intracellular stores of calcium resulting in a transient increase in the level of intracellular calcium (Thelen, 2001). This is directly due to the activation of PLC by GPCRs. PLC is known to metabolise PIP_2 into DAG and IP_3. It is the production of IP_3 that results in the mobilisation of calcium from intracellular stores. The increase in intracellular calcium in conjunction with DAG is subsequently able to mediate the activation of other second messengers and resulting in the activation of a range of effector functions (Berridge & Irvine, 1989). This particular pathway to the release of calcium stores is, to date, known to be independent of PI3-kinase activation (Thelen, 2001). In order to ensure that signal transduction downstream of CCR6 ligation was not generally suppressed by the over-expression of MmPI3kγKR thereby resulting in the inhibition of cell migration, calcium mobilisation assays were conducted. The results obtained from these assays confirmed that both the control B300.19 cells and B300.19 cells expressing MmPI3kγKR were able to mobilise calcium with equal

efficiency. Taken together these results indicate that the loss of MmPI3kγ1111 activity results in the downregulation of *in vitro* migration in response to huMIP-3α and that this is not due to non-specific inhibition of GPCR-dependent lymphocyte activation.

To extend these findings to an *in vivo* model of migration the subcutaneous air pouch model was employed. This model creates a vascularized cavity on the dorsum of mice where the enumeration and manipulation of cellular infiltrates in response to agonists are easily examined (Coates & McColl, 2001). Air pouches were generated on the dorsum of NIH/Swiss outbred mice. Untransfected B300.19 cells were intravenously injected into these mice, followed immediately by an injection of huMIP-3α into the air pouches. A significant accumulation of total cells and huCC6-positive cells was demonstrated 4 hr later, in response to 10μg of MIP-3α. This is the first time the *in vivo* recruitment of passively transferred lymphoid cells expressing a specific chemokine receptor has been demonstrated in response to a chemokine.

This model was subsequently utilised to determine the role of MmPI3kγ1111 in the *in vivo* migration of B300.19-huCCR6 cells in response to huMIP-3α. B300.19-huCCR6 cells transfected with either MmPI3kγKR or with pcDNA3 alone were passively transferred into NIH/Swiss outbred mice prior to the injection of PBS or huMIP-3α. B330.19::huCCR6 cells transfected with vector alone or pcDNA3::MmPI3kγKR both demonstrated the significant accumulation of total cells and CCR6-positive cells in response to MIP-3α. No difference was observed between the two cell lines in their *in vivo* response to huMIP-3α using the subcutaneous air pouch model. These data suggest that, in contrast to the *in vitro* data obtained,

MmPI3kγ1111 is not essential for the migration of B300.19 cells into the air pouch in response to huMIP-3α.

It is possible that the discrepancy between the *in vitro* and *in vivo* data is due to inherent differences between the assays used. The transwell chemotaxis assay relies on cellular migration through a porous polycarbonate membrane whereas, *in vivo*, leukocyte extravasation involves the coordinated action of a range of expression molecules that control the movement of cells from the circulation, through the endothelium into peripheral tissues (Vaday *et al.*, 2001). The simplistic *in vitro* system does not encompass the various factors present in the *in vivo* system and it is possible that PI3kγ signalling is redundant during chemotaxis *in vivo*. It is therefore possible that the use of these two different assays accounts for the inconsistency observed.

It is also possible that further development of the *in vivo* migration model used in the present study to provide more optimal conditions for the recruitment of passively-transferred cells will reveal dependence of the assay on MmPI3kγ1111. Particular parameters may involve examination of the number of cells transferred per animal, and the examination of alternative mammalian expression systems for use in the B300.19 B lymphocyte cell line to enhance MmPI3kγKR expression.

Finally, in keeping with the complexity of leukocyte extravasation *in vivo*, the results obtained in the present study may represent an accurate account of the role of PI3kγ in *in vivo* recruitment of B300.19-huCCR6 cells in response to MIP-3α. It is

still possible that MmPI3kγ1111 has a role in the migration of lymphocytes in response to chemokines *in vivo*, however future experiments may need to employ alternative *in vivo* migratory models to confirm or eliminate a role for PI3kγ in leukocyte recruitment.

In summary, the results presented in this chapter demonstrate the importance of lysine residue 833 for the activation of both the protein and lipid kinase activities. Generation of a catalytically-inactive form of MmPI3kγ1111, and its over expression in a B lymphocyte cell line enabled the examination of the role of MmPI3kγ1111 in the chemotactic response of these cells to MIP-3α. *In vitro* data suggest a critical role for MmPI3kγ1111 in the chemotactic response. However, in using the air pouch model to assess *in vivo* migration, no role could be attributed to MmPI3kγ1111 in the migratory response of the B cell line in response to chemokines. Alternative approaches to examine the role of MmPI3kγ1111 in lymphocyte migration *in vivo* and the implications of the data generated in the present study are addressed in Chapter 6.

Figure 5.1 A diagrammatic representation of the ATP transfer site in the catalytic domain of MmPI3kγ1111

The amino acid conservation in the region of ATP transfer between the human (Hs), the porcine (Ss) and MmPI3kγ1111 are represented. The lysine residue integral for the ATP transfer and activation of the kinases is illustrated in green. In order to mutate the lysine residue a single base pair change was created resulting in a change from lysine to arginine.

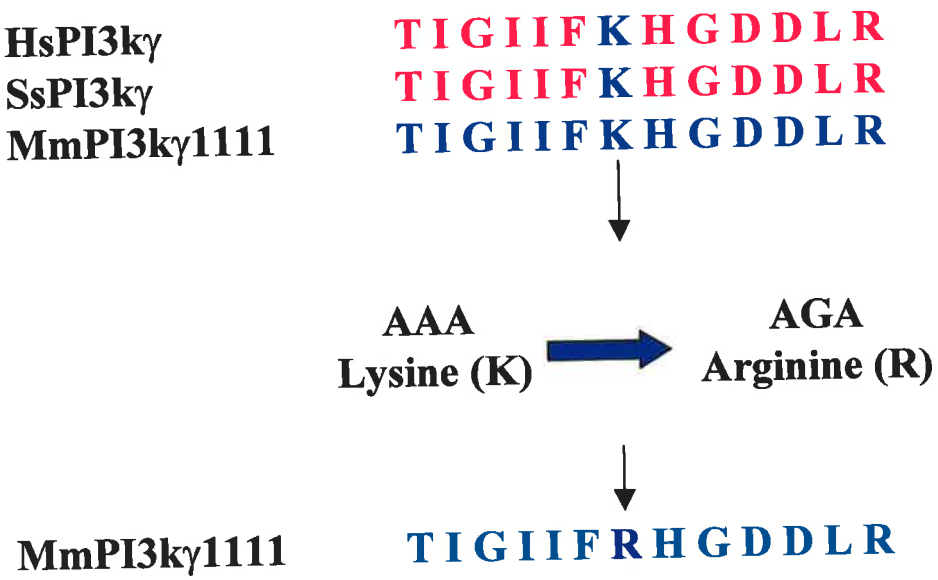
HsPI3kγ
SsPI3kγ
MmPI3kγ1111
T I G I I F K H G D D L R
T I G I I F K H G D D L R
T I G I I F K H G D D L R
AAA
Lysine (K)
AGA
Arginine (R)
MmPI3kγ1111
T I G I I F R H G D D L R

Figure 5.2 Schematic representation of the 'quikchange' mutagenesis technique used to generate a catalytically-inactive MmPI3kγ1111

Mutagenic primers anneal to the methylated parental DNA template, and enable the primer extension incorporating base changes. *Dpn*I restriction endonuclease cleaves methylated DNA. Because of the methylated state of the parental DNA, and the non-methylated state of the mutagenised extension products, restriction digestion using *Dpn*I only degrades the parental template. The restricted reaction is transformed into bacterial cells giving rise to mutagenised clones.

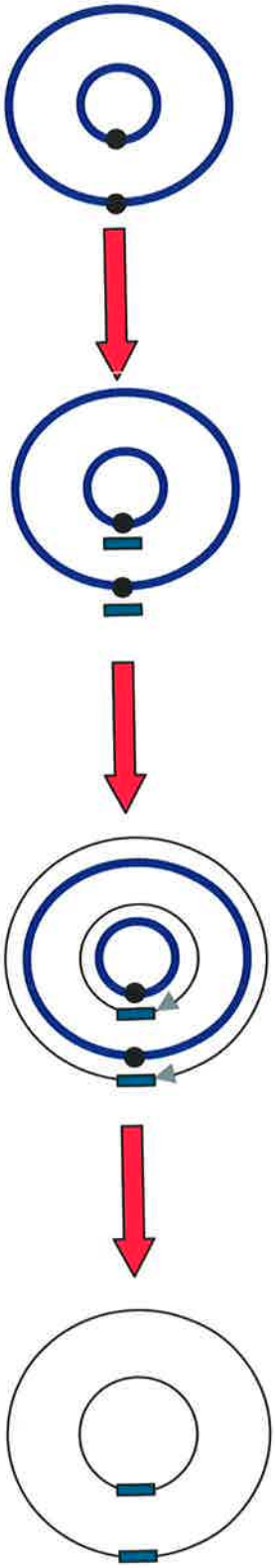

Gene in methylated plasmid with target site (●) for mutation

Plasmid is denatured and mutagenic primers (▬) anneal to parental DNA

Primer extension to incorporate the mutagenic primers

Dpn I digestion of the methylated, non-mutated parental DNA template and transformation into bacteria

Figure 5.3 Restriction and sequence analysis of putative MmPI3kγKR clones

A. Site-directed mutagenesis was performed using the pcDNA3::MmPI3kγ1111 construct as template. Primers incorporating the desired base change were used to generate mutated extension products, and the parental DNA was digested using *Dpn*I. Following bacterial transformation, putative clones were analysed by *Dra*I restriction. Restricted products were resolved on a 1.2% agarose gel and visualised by ethidium bromide staining.

B. All putative clones of MmPI3kγKR were sequenced using the primer p110γ2157F and p110γ2890R. Sequences were aligned against the wild-type MmPI3kγ1111 and examined for a base pair change, from the base adenosine to guanine, at base pair position 2500. Clones harbouring the change at nucleotide position 2500 are illustrated with the guanine base highlighted in green.

A.

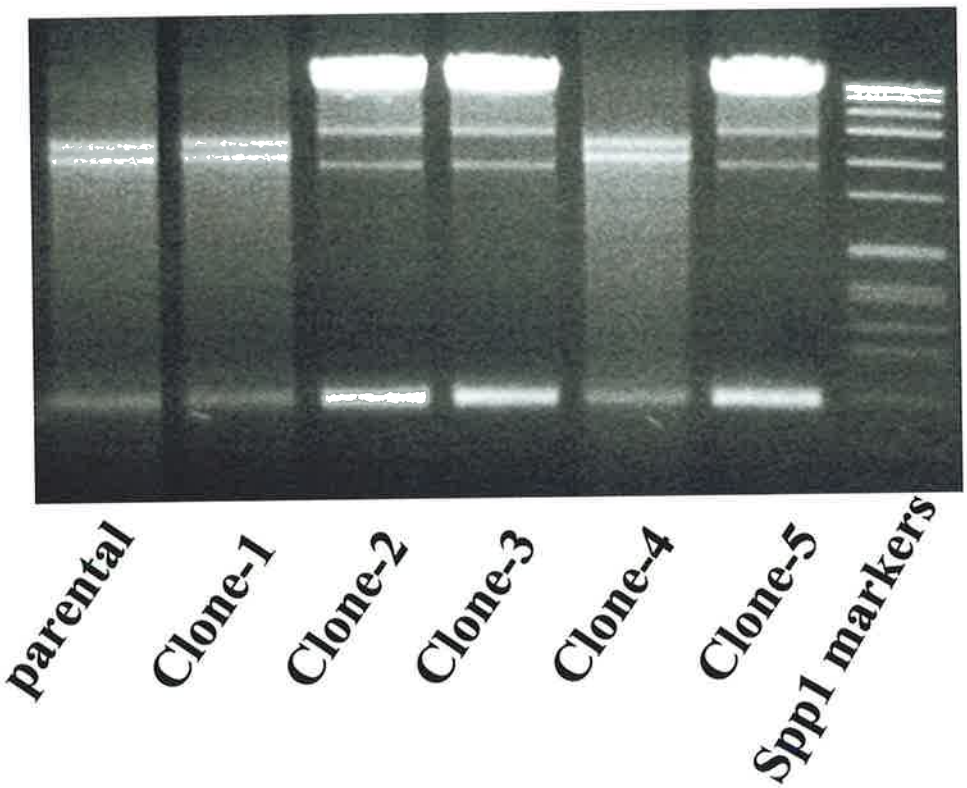

B.

parental	ATT GGA ATC ATC TTT AAA CAT GGT GAT GAT CTG
Clone-1	ATT GGA ATC ATC TTT AAA CAT GGT GAT GAT CTG
Clone-2	ATT GGA ATC ATC TTT AGA CAT GGT GAT GAT CTG
Clone-3	ATT GGA ATC ATC TTT AGA CAT GGT GAT GAT CTG
Clone-4	ATT GGA ATC ATC TTT AAA CAT GGT GAT GAT CTG
Clone-5	ATT GGA ATC ATC TTT AGA CAT GGT GAT GAT CTG

Figure 5.4 Lack of lipid kinase activity of MmPI3kγKR

HEK 293 cells were transiently transfected with either the pcDNA3::MmPI3kγ1111 or the pcDNA3::MmPI3kγKR construct (3μg). Over-expressed proteins were purified using Talon resin.

Top panel - Western analysis of the purified proteins MmPI3kγ1111 and MmPI3kγKR. One third of purified proteins were separated by 9% SDS-PAGE and examined by western analysis using a mouse anti-PI3kγ monoclonal antibody.

Bottom panel - Immobilised proteins were resuspended in kinase buffer and incubated with the lipid substrate, PI, and γ^{32}P-ATP for 20 min at RT. Lipids were extracted and analysed by TLC. Products were visualised by autoradiography.

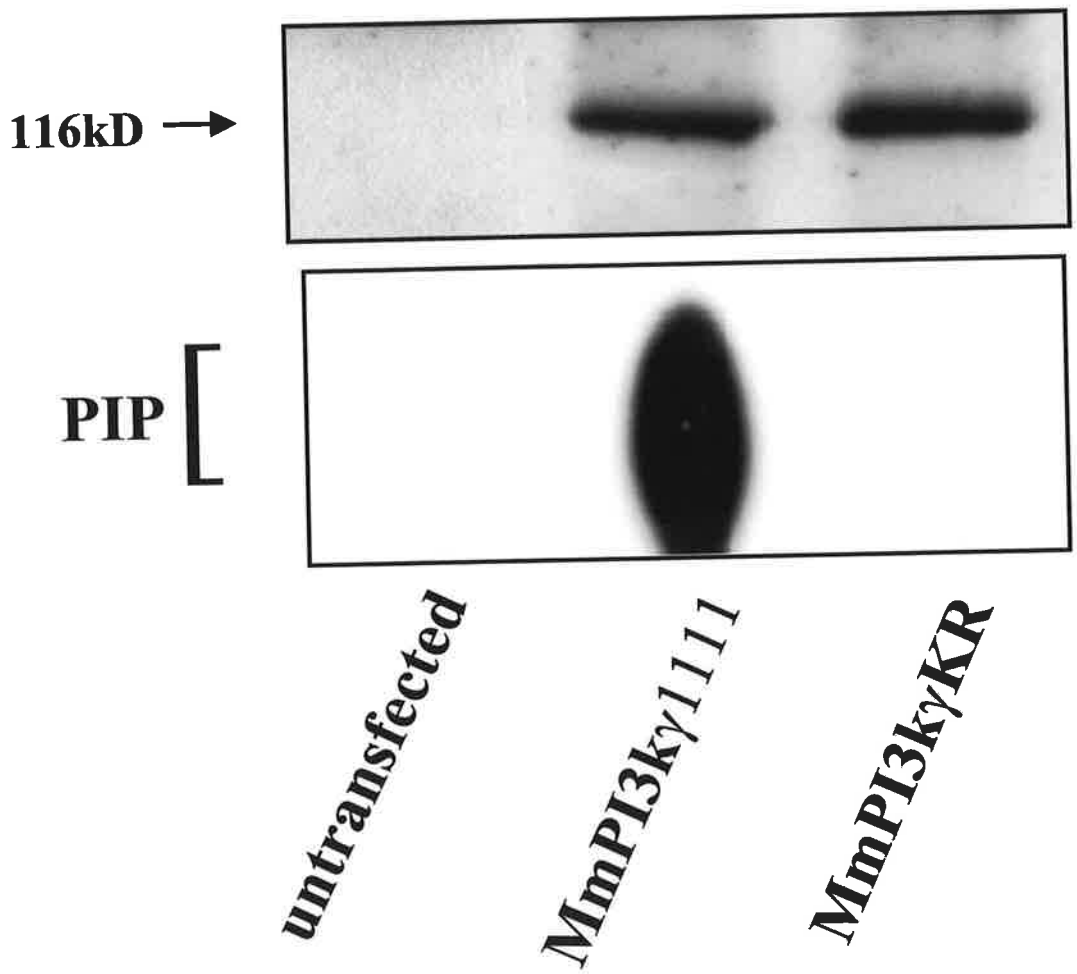
116kD
PIP
untransfected
MmPI3kγ1111
MmPI3kγKR

Figure 5.5 Lack of phosphorylation of MmPI3kγKR

HEK 293 cells were transiently transfected with either the pcDNA3::MmPI3kγ1111 or the pcDNA3::MmPI3kγKR construct (3μg). Over-expressed proteins were purified using Talon resin.

Top panel - Western analysis of the purified proteins MmPI3kγ1111 and MmPI3kγKR. One third of purified proteins were separated by 9% SDS-PAGE and examined by western analysis using a mouse anti-PI3kγ monoclonal antibody. Same data as Figure 5.3 upper panel.

Bottom panel - Immobilised proteins were resuspended in kinase buffer and incubated with γ^{32}P-ATP for 20 min at RT. Proteins were analysed by 9% SDS-PAGE and autoradiography.

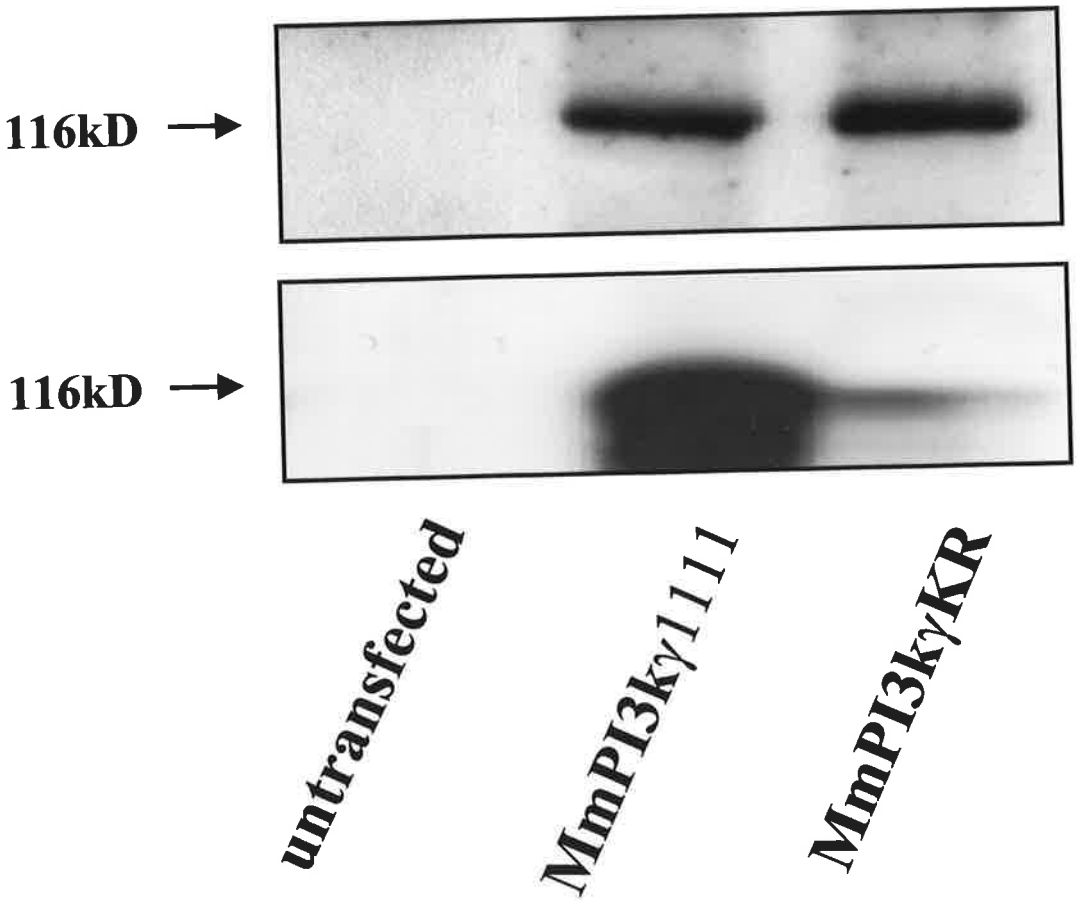
116kD
116kD
untransfected
MmPI3kγ1111
MmPI3kγKR

Figure 5.6 pMIG retroviral expression system

A. The pMIG retroviral vector obtained from D. Baltimore (CA, USA) for the expression of MmPI3kγKR. The expression vector is comprised of long terminal repeats (LTR) flanking a multiple cloning site (MCS), an internal ribosome entry site (IRES) and the enhanced green fluorescent protein (EGFP) gene.

B. A diagrammatic representation of the retroviral expression system. The retroviral vector containing the gene of interest is transfected into a packaging cell line. Approximately 48 to 72 hr later the supernatants from the transfected packaging cells are harvested and incubated with the target cells. Approximately 48 hr post-viral infection, target cells are harvested and sorted based on EGFP expression. These cells can then be used to address cellular function using *in vitro* assays and *in vivo* models.

A.


LTR
MCS
IRES
EGFP
LTR

B.

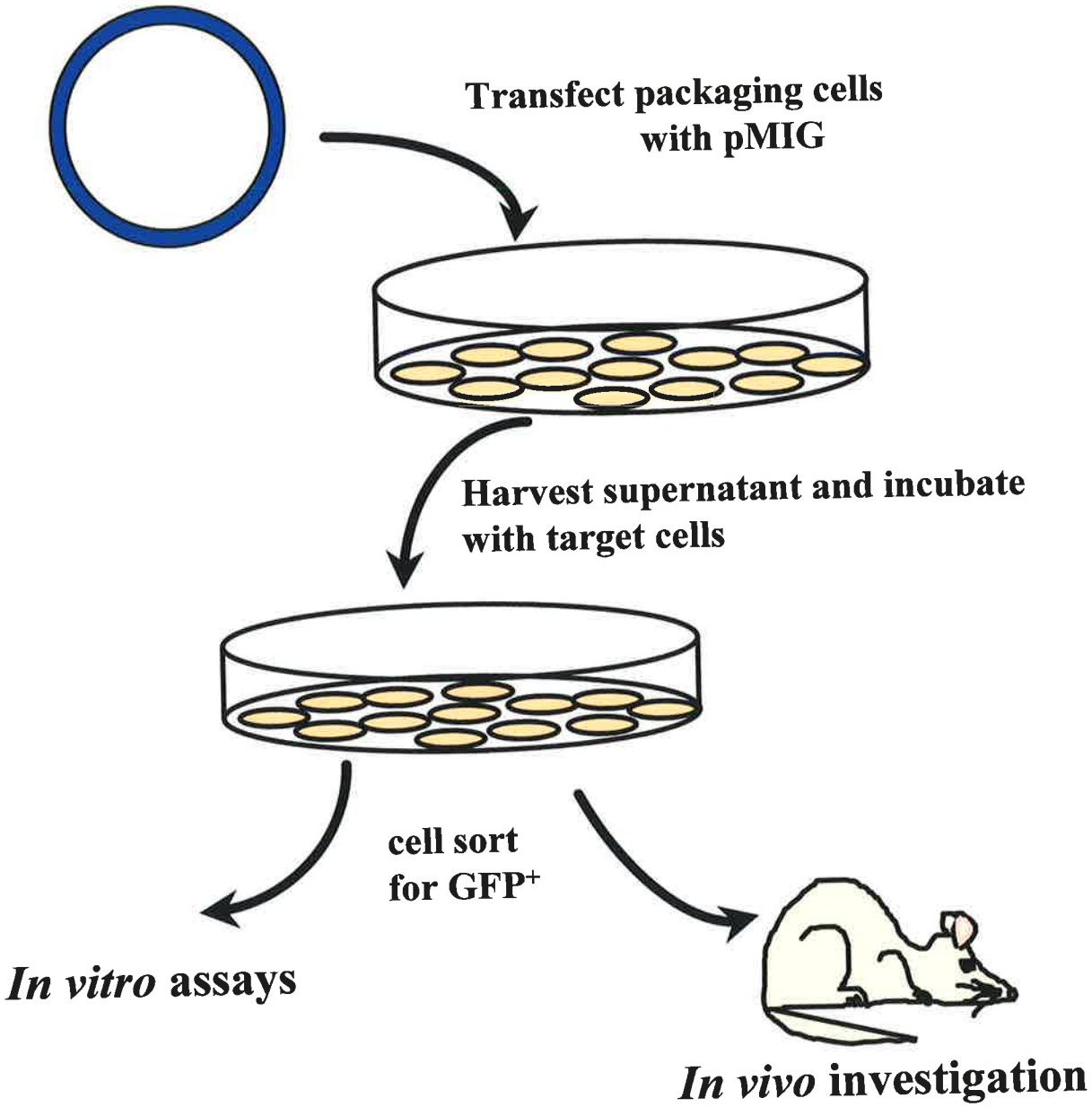
Transfect packaging cells with pMIG
Harvest supernatant and incubate with target cells
cell sort for GFP+
In vitro assays
In vivo investigation

Figure 5.7 Optimisation of the pMIG retroviral expression system

A. The EcoPack2 cell line was plated at either $5x10^5$cells/35mm dish or $1x10^6$cells/35mm dish. Cells were transiently transfected with 0.5μg pMIG, and 3.0μg pMIG at both cell densities. Fifty hr post-transfection supernatants were harvested and incubated with $5x10^5$ NIH 3T3 murine fibroblasts. Forty eight hr later cells were examined for EGFP expression using a FACScan. The percent of NIH 3T3 cells positive for EGFP expression are indicated for each cell density. Representative values from 2 independent experiments are indicated.

B. The EcoPack2 cell line was plated at $1x10^6$ cells/35mm dish. Cells were transiently transfected with a range of concentrations of pMIG DNA (as indicated). Fifty hr post-transfection supernatants were harvested and incubated with $5x10^5$ NIH 3T3 murine fibroblasts. Forty eight hr later cells were examined for EGFP expression using a FACScan. The percent of NIH 3T3 cells positive for EGFP expression are indicated for each cell density. Representative values from 2 independent experiments are indicated.

A.

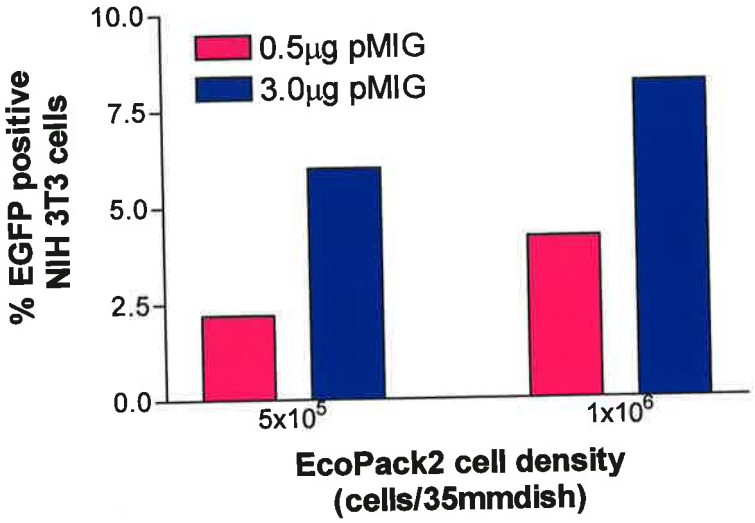
10.0
7.5
5.0
2.5
0.0
0.5μg pMIG
3.0μg pMIG
% EGFP positive NIH 3T3 cells
5x10^5
1x10^6
EcoPack2 cell density (cells/35mmdish)

B.

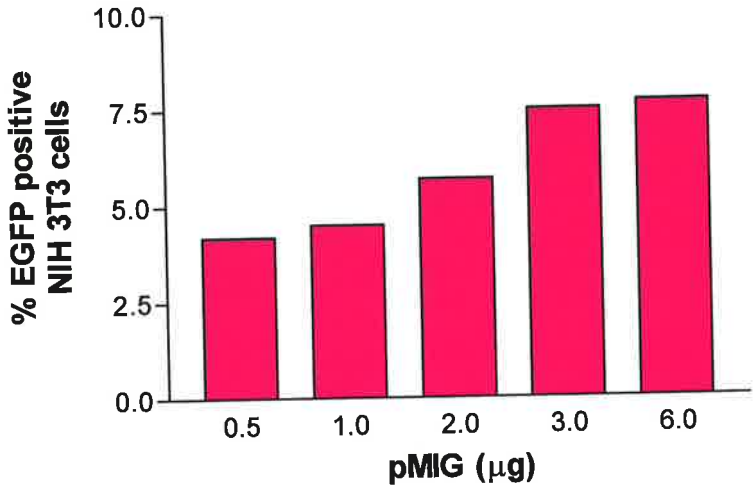
10.0
7.5
5.0
2.5
0.0
% EGFP positive NIH 3T3 cells
0.5
1.0
2.0
3.0
6.0
pMIG (μg)

Figure 5.8 MmPI3kγKR expression in B300.19-huCCR6 cells

Murine B300.19 B lymphocytes were electroporated with either the pcDNA3::MmPI3kγKR construct or pcDNA3 alone. Forty-eight hr post-electroporation cells were cultured in the presence of the antibiotic, G418 (geneticin). Following this, cells were always cultured in the presence of G418.

Top panel - Following 15 days of selection, cells were lysed and membrane fractions removed by centrifugation. Samples of whole cell lysates were resolved by 9% SDS-PAGE and PI3kγ protein detected by western analysis using a mouse anti-PI3kγ monoclonal antibody.

Bottom panel - Following 15 days of selection, cells were lysed and membrane fractions removed by centrifugation. Over-expressed proteins were purified using Talon-charged resin, immobilised proteins were resolved by 9% SDS-PAGE and PI3kγ protein detected by western analysis using a mouse anti-PI3kγ monoclonal antibody.

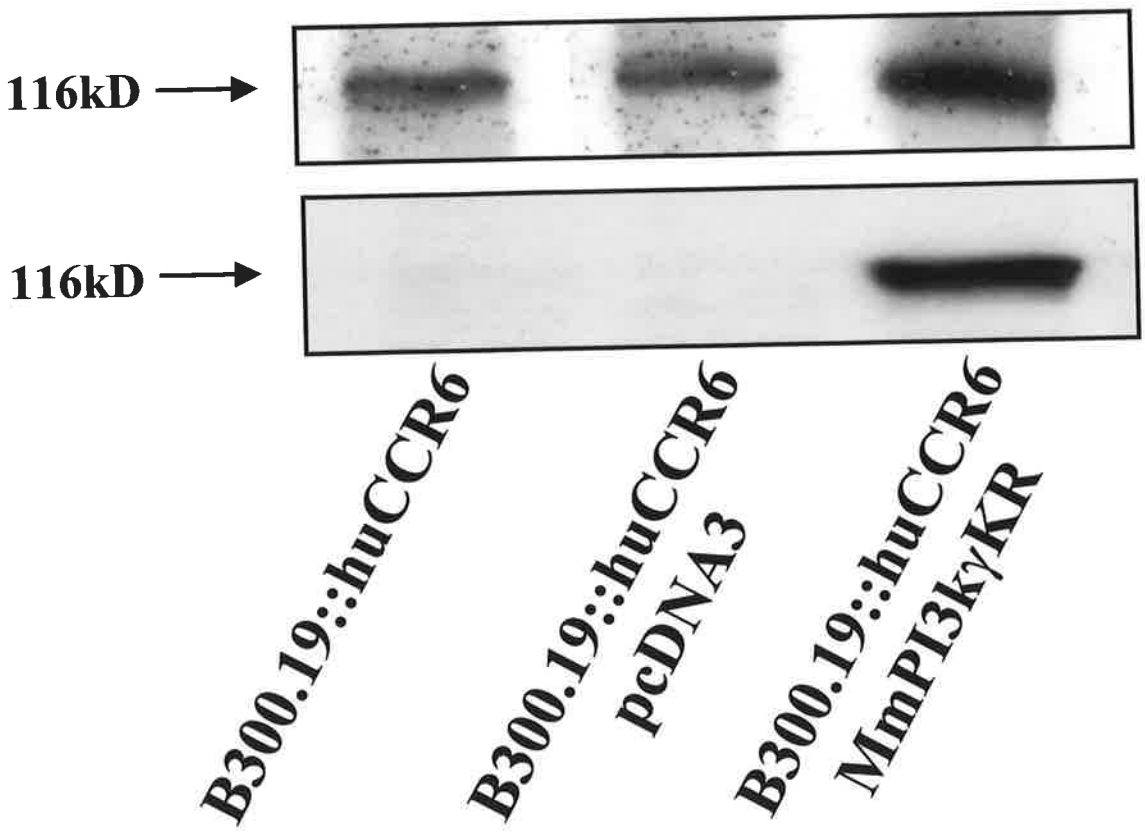
116kD
116kD
B300.19::huCCR6
B300.19::huCCR6 pcDNA3
B300.19::huCCR6 MmPI3kγKR

Figure 5.9 Lipid and protein kinase activities of MmPI3kγKR purified from stably-transfected B300.19-huCCR6 cells

Top panel - Western analysis of the purified proteins, MmPI3kγKR (from the transfected B300.19-huCCR6 cell line) and MmPI3kγ1111 from transiently-transfected HEK 293 cells as reference. One third of purified proteins were separated by 9% SDS-PAGE and examined by western analysis using a mouse anti-PI3kγ monoclonal antibody.

Middle panel - Immobilised proteins were resuspended in kinase buffer and incubated with the lipid substrate PI, and γ^{32}P-ATP for 20 min at RT. Lipids were extracted and analysed by TLC. Products were visualised by autoradiography.

Bottom panel - Immobilised proteins were resuspended in kinase buffer and incubated with γ^{32}P-ATP for 20 min at RT. Proteins were analysed by 9% SDS-PAGE and autoradiography.

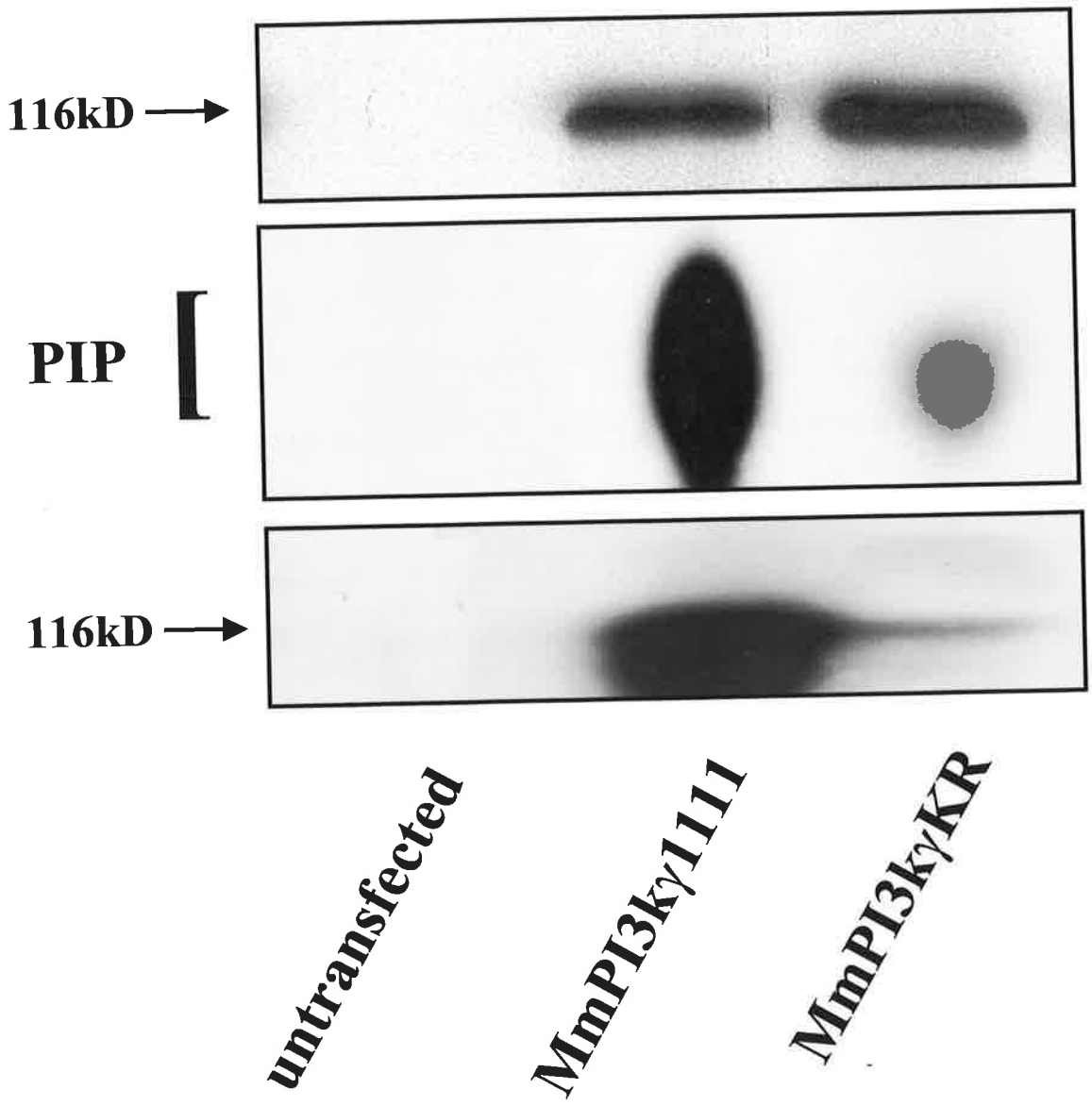
116kD
PIP
116kD
untransfected
MmPI3kγ1111
MmPI3kγKR

Figure 5.10 Chemotactic response of B300.19-huCCR6 cells transfected with either MmPI3kγKR or the vector control, in response to human MIP-3α

B300.19-huCCR6 cells transfected with either pcDNA3 alone or MmPI3kγKR were loaded with calcein-AM. Six hundred µl of the indicated concentration of human MIP-3α added into the lower chamber of transwell chambers, and 100 µL of a cell suspension (10^7cells/mL) were added to the upper compartment, and. Chemotaxis assays were conducted at 37°C for 3hr, after which the level of fluorescence in the lower chambers was determined. The data are depicted as the percentage of cells migrating in response to the various concentrations of human MIP-3α. Values are represented as mean +/- S.E.M. n = 4.

* - significantly different from control at $p<0.05$ (2-tailed Students t-test)

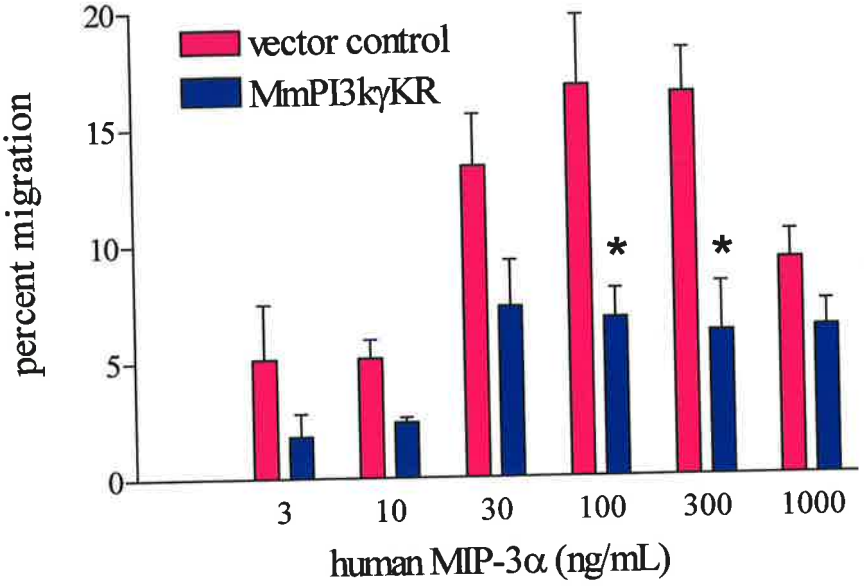
vector control
MmPI3kγKR
percent migration
20
15
10
5
0
*
*
3
10
30
100
300
1000
human MIP-3α (ng/mL)

Figure 5.11 Expression levels of the human CCR6 receptor on transfected B300.19-huCCR6 cells

B300.19-huCCR6 cells transfected with either pcDNA3 alone or pcDNA3::MmPI3kγKR were labelled with the mouse anti-human CCR6 monoclonal antibody, followed by a anti-mouse biotin conjugate and finally a PECy5 streptavidin conjugate. Gates were set based on the forward and side scatter profiles of the cells. (A) Autofluorescence of the cell population was determined using an isotype-matched control antibody. The mean fluorescence intensity is indicated, in the lower right corner of the FACs plots, for cells stably transfected with either pcDNA3 alone (B) or pcDNA3::MmPI3kγKR (C).

A.

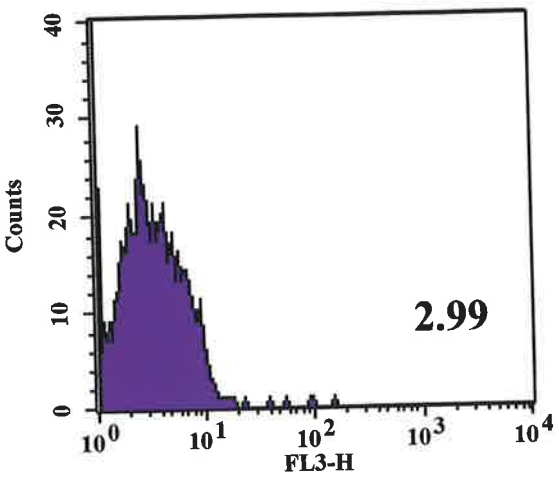
Counts
0
10
20
30
40
2.99
10^0
10^1
10^2
10^3
10^4
FL3-H

B.

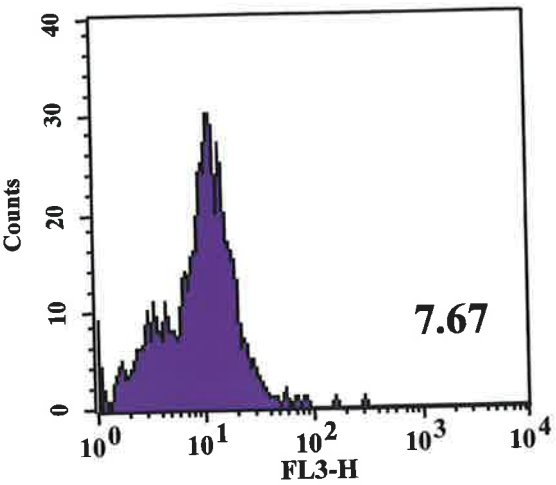
Counts
0
10
20
30
40
7.67
10^0
10^1
10^2
10^3
10^4
FL3-H

C.

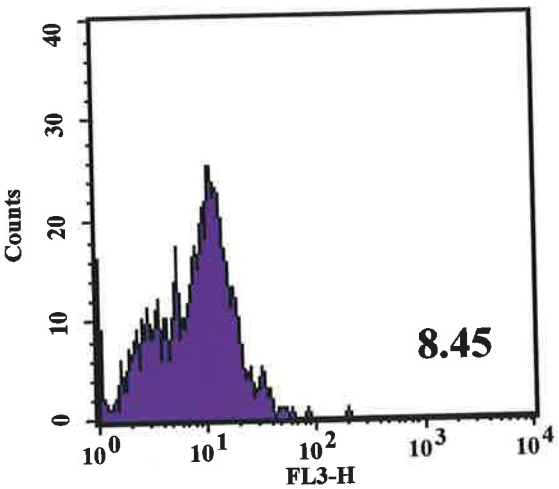
Counts
0
10
20
30
40
8.45
10^0
10^1
10^2
10^3
10^4
FL3-H

Figure 5.12 Intracellular Calcium mobilisation in B300.19-huCCR6 cells expressing MmPI3kγKR

B300.19-huCCR6 cells, transfected with pcDNA3 alone (A) or MmPI3kγKR (B), were loaded with the fluorescent probe Fura-2/AM. Cells were then transferred to the thermostatted cuvette compartment (37°C) of an SLM Aminco AB2 luminescence spectrophotometer. The fluorescence was monitored in response to human MIP-3α, (excitation and emission wavelengths of 340 nm and 510 nm, respectively). Intracellular calcium mobilisation in response to human MIP-3α is represented over time. Data are representative of 2 independent experiments. Arrows indicate addition of MIP-3α to cells.

A.

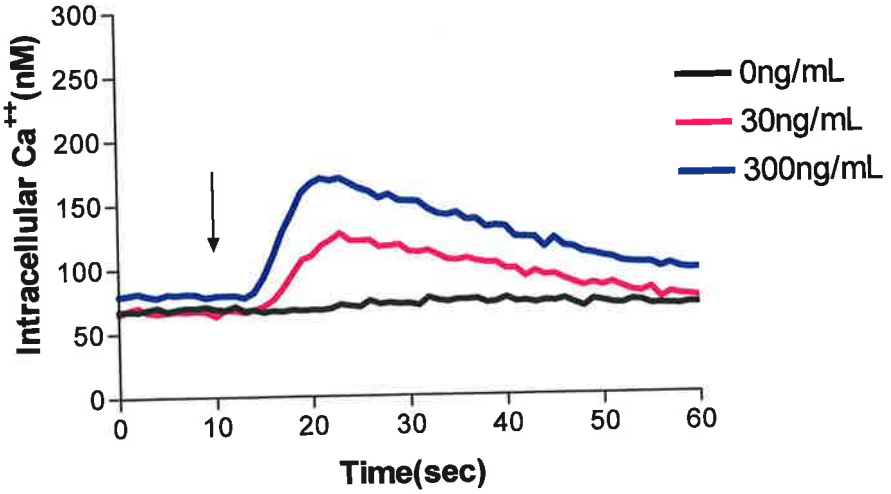
Intracellular Ca++(nM)
300
250
200
150
100
50
0
0
10
20
30
40
50
60
Time(sec)
0ng/mL
30ng/mL
300ng/mL

B.

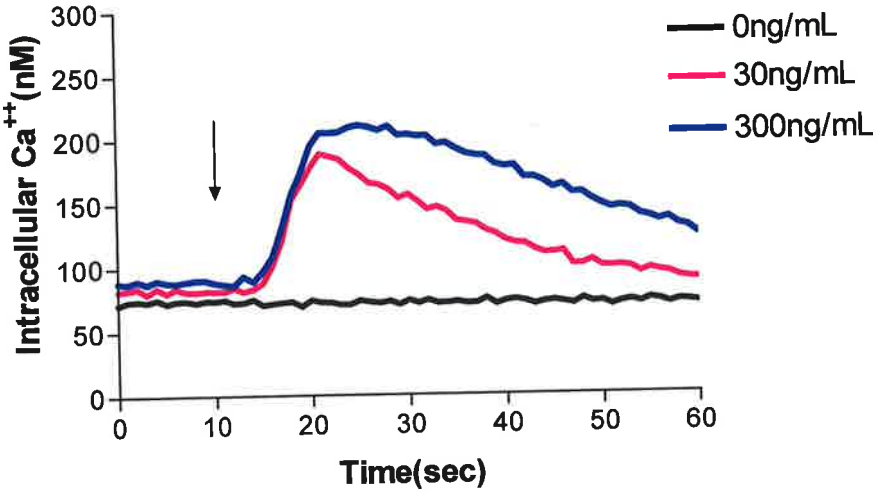
Intracellular Ca++(nM)
300
250
200
150
100
50
0
0
10
20
30
40
50
60
Time(sec)
0ng/mL
30ng/mL
300ng/mL

5.13 *In vivo* recruitment of B300.19-huCCR6 cells in response to human MIP-3α – a time course and dose response.

Air pouches were raised on the dorsum of NIH/Swiss outbred mice. B300.19-huCCR6 cells (10^7) were intravenously injected into each mouse, followed immediately by an injection of either PBS, 3μg, 10μg human MIP-3α into the subcutaneous air pouch. At either 4 hr or 24 hr post-agonist injection, cellular infiltrates were recovered from the air pouches. Cellular infiltrates were either counted using a haemocytometer to determine the total number of cells accumulating, or labelled for flow cytometry using a mouse anti-human CCR6 monoclonal antibody. Autofluorescence of the population was determined by using an isotype-matched primary antibody. (A) Total leukocytes recovered at 4 hr and 24 hr are indicated for each concentration of human MIP-3α. (B) The total number of huCCR6-positive cells recovered at 4 hr and 24 hr are indicated for each concentration of human MIP-3α. Values are represented as mean +/- S.E.M. n = 6 mice.

* - significantly different from control at $p<0.05$ (2-tailed Students t-test)

A.

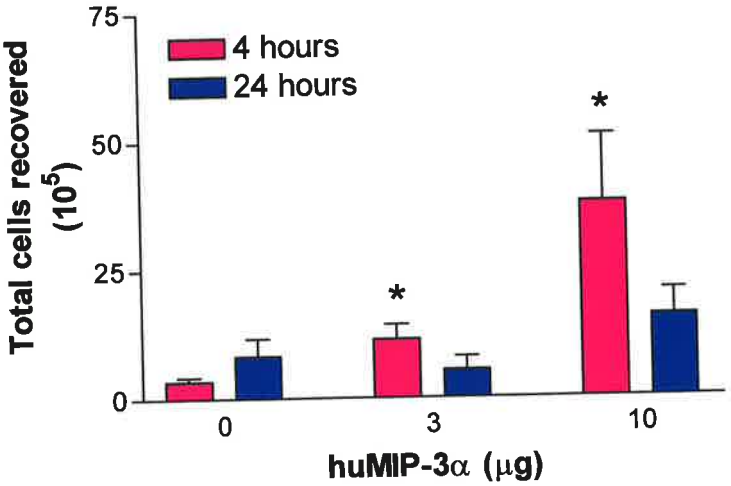
75
50
25
0
4 hours
24 hours
Total cells recovered (10^5)
*
*
0
3
10
huMIP-3α (μg)

B.

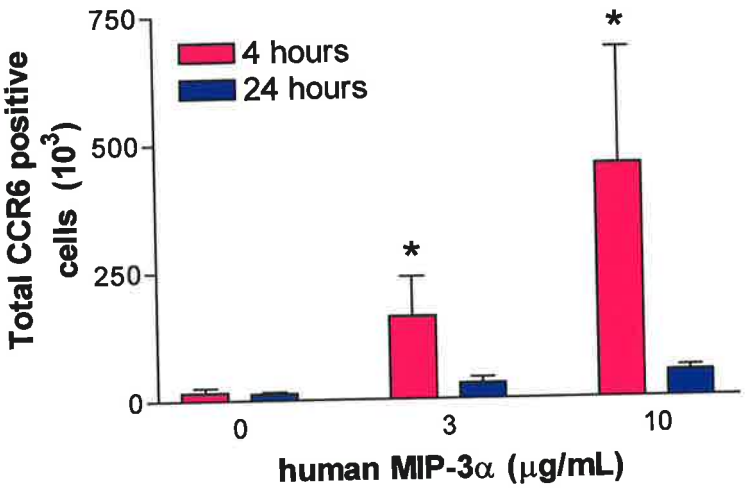
750
500
250
0
4 hours
24 hours
Total CCR6 positive cells (10^3)
*
*
0
3
10
human MIP-3α (μg/mL)

Figure 5.14 *In vivo* recruitment of B300.19-huCCR6 cells, transfected with MmPI3kγKR, in response to human MIP-3α

Subcutaneous air pouches were raised on the dorsum of NIH/Swiss outbred mice. B300.19-huCCR6 cells (10^7) transfected with either pcDNA3 alone or MmPI3kγKR, were intravenously injected into each mouse, immediately followed by an injection of either PBS, or 10μg human MIP-3α. Four hr post agonist injection cellular infiltrates were recovered. (A) Total leukocytes recovered at 4 hr as determined using a haematocytometer. (B) The total number of CCR6-positive cells recovered at 4 hr as determined by flow cytometry. Values are represented as mean +/- S.E.M. n = 8 mice. * - significantly different from PBS value at $p<0.05$ (2-tailed Students t-test); **- significantly different from PBS value at $p<0.05$ (2-tailed Students t-test)

A.

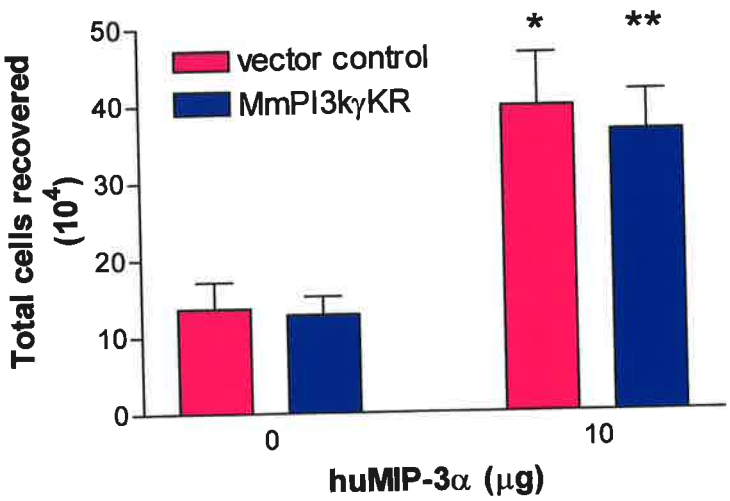
Total cells recovered (10^4)
50
40
30
20
10
0
vector control
MmPI3kγKR
*
**
0
10
huMIP-3α (μg)

B.

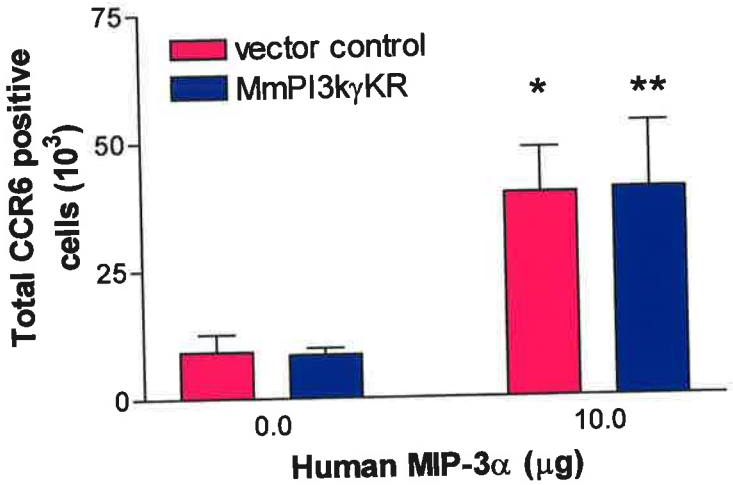
Total CCR6 positive cells (10^3)
75
50
25
0
vector control
MmPI3kγKR
*
**
0.0
10.0
Human MIP-3α (μg)

Chapter Six

General Discussion

6.1 Discussion

Signals triggered by extracellular messengers are required for cells to sense their environment. This is a critical component of cellular physiology that controls diverse cellular processes including cell differentiation and proliferation, cell survival, as well as the generation of effector functions as is particularly the case with leukocytes. These signals begin at the receptor ligation level and lead to the activation of many downstream intracellular messengers. A plethora of protein kinases have been established as important signalling molecules in these pathways. During the last decade the role of lipid kinases in the transmission of signals throughout the cell has gained considerable prominence and the family of PI3-kinases are an important group of lipid kinases involved in this cellular signalling. All members of this family are able to phosphorylate the 3-OH position of the inositol headgroup in phosphoinositides. The structure and substrate specificities of the PI3-kinase members enable their catergorisation into three distinct classes, the Class I, II and III PI3-kinases. The Class I kinases were the first identified members and are therefore the best-characterised PI3-kinases in terms of their structure and cellular function. The Class I subfamily are further divided into the Class IA and IB groups based on the mechansims of their activation and regulation. The class IA PI3-kinases are recruited through the activation of receptors that have inherent tyrosine kinase activity, alternatively through receptors that are able to recruit tyrosine kinase activation immediately downstream of receptor ligation (reviewed in Vanhaesebroeck *et al.*, 2001). In contrast, the Class IB kinases are dependent on heterotrimeric G protein subunits for their activation and appear to be independent of cellular tyrosine

phosphorylation (reviewed in Vanhaesebroeck *et al.*, 2001). It is with the only Class IB member, PI3kγ, that the present study is concerned.

The chemokines are a large family of chemotactic cytokines that play an important role in the maintenance and regulation of immune responses via their ability to control migration of leukocytes. These chemotactic factors signal through G protein-coupled receptors and this stimulates an increase in the production of 3-phosphorylated lipids in a tyrosine phosphorylation-independent manner (Stephens *et al.*, 1993a; Stephens *et al.*, 1991; Stephens *et al.*, 1993b). More recently, studies have demonstrated that this increase in 3-phosphorylated lipids is most likely due to the activation of PI3kγ, the Class IB PI3-kinase dependent on G proteins for activation (Hirsch *et al.*, 2000a; Li *et al.*, 2000; Naccache *et al.*, 2000; Sasaki *et al.*, 2000).

To date, most of the reliable studies examining the role of PI3kγ in leukocyte function have been carried out using cells of the innate immune system, such as neutrophils and monocytes. Stimulation of human neutrophils with the chemotactic factors IL-8 and fMLP resulted in activation of PI3kγ and furthermore this activity was abrogated with either wortmannin or pertussis toxin (Naccache *et al.*, 2000). In the absence of PI3kγ expression (for example in PI3kγ$^{-/-}$ mice), both neutrophil and monocytes demonstrate a reduced ability to migrate *in vitro* as well as towards inflammatory sites *in vivo* (Hirsch *et al.*, 2000a; Sasaki *et al.*, 2000). Neutralisation of PI3kγ activity *in situ* by the microinjection of polyclonal anti-huPI3kγ antibodies led to reduced migration of natural killer cells in response to the chemokines RANTES, MCP-1, IP-10 and SDF-1α (al-Aoukaty *et al.*, 1999). However, in comparison to cells of the innate immune system, there is considerably less understood regarding the role

of PI3kγ in lymphocyte migration occurring as a result of chemotactic factor signalling. To date, the only studies that examine this question have been conducted using mice deficient in PI3kγ expression (Sasaki *et al.*, 2000). These mice, although overtly phenotypically normal, exhibit major developmental/maturation defects in the lymphocyte compartment. The data generated from these mice with respect to the adaptive immune response is therefore difficult to interpret due to the inability to distinguish between the functional consequences observed solely due to the absence of PI3kγ function in the mature cell and those occurring as a result of developmental defects (Sasaki *et al.*, 2000).

In view this previous literature, the broad aim of the current study was to investigate the importance of PI3kγ signal transduction in chemokine-induced lymphocyte migration *in vivo*. Several novel pieces of information were generated over the course of this study. The present study reports the cloning of a novel Class IB PI3-kinase isoform, MmPI3kγ1111, that is expressed in peripheral blood leukocytes with ubiquitous expression throughout all murine tissues tested. Consistent with the human and porcine orthologues, the novel isoform exhibits both protein and lipid kinase activities, with autophosphorylation downregulating its ability to phosphorylate lipids. The overexpression of a catalytically-inactive form of the PI3kγ reduced the ability of a B lymphocyte cell line to migrate, *in vitro*, in response to the chemokine huMIP-3α.

At the commencement of this study only the human and porcine orthologues of PI3kγ had been cloned (Stephens *et al.*, 1997; Stoyanov *et al.*, 1995). Sequence comparisons between MmPI3kγ1111 and the human and porcine PI3kγs illustrated an

extremely high degree of conservation across all domains. The presence of an additional 11 amino acids in the catalytic domain of MmPI3kγ1111 was the only area departing from the conservation observed elsewhere in the protein. During the latter stages of this project, the cloning of a MmPI3kγ, termed MmPI3kγ1100 isolated from murine 32Dcl3 cells, was published (Hirsch *et al.*, 2000a). This isoform shared the same high degree of conservation when compared with the human and porcine orthologues, and in contrast to the MmPI3kγ1111 cloned in the present study, it did not contain the additional 11 amino acids in the catalytic domain. A survey of a range of murine tissues indicated that the MmPI3kγ1111 was more ubiquitously expressed than MmPI3kγ1100, however attempts in the present study to compare the origins of the two isoforms proved unsuccessful. The two major possibilities are that the two forms are products of separate genes or that they arise as a result of alternative splicing of a single gene. FISH has not revealed the presence of a second PI3kγ gene in the mouse (Hirsch *et al.*, 2000a), effectively eliminating the first possibility. However, it is presently unclear whether MmPI3kγ1111 is a splice variant of MmPI3kγ1100 or vice versa. Examination of the Celera database and /or amplification and sequence analysis of the intronic sequence bordered by exons 10 and 11 would confirm the validity of the suggestion.

Comparison of the 11 amino acids demonstrated no identity with domains in other protein and lipid kinases and other putative signalling molecules. Due to the presence of several cysteine residues in the 11 amino acid segment, the possibility of conformational changes in the quaternary structure of MmPI3kγ1111, and the possibility of this affecting the activity of the protein had to be considered. *In vitro*

expression and assays of kinase activity of the protein demonstrated that the additional 11 amino acids did not affect either expression or the activity of the kinase. More recently, several studies have investigated the interactions between lipid substrates and the PI3-kinase catalytic domain of Class IA PI3-kinases (Pirola *et al.*, 2001). Pirola *et al.*, demonstrated that sequences downstream of the ATP-binding site determine the substrate specificity of PI3kα (Pirola *et al.*, 2001). All Class I PI3-kinases demonstrate the ability to phosphorylate the three lipid substrates PI, PI 4 P and PI 4,5 P_2 *in vitro*. However, these kinases demonstrate an *in vivo* preference for PI 4,5 P_2. Taken together, it is possible that the additional amino acids that lie downstream of the ATP-binding site, alter the substrate specificity of MmPI3kγ1111 *in vivo* and may consequently mediate the coupling of MmPI3kγ1111 to alternative second messenger systems. Further studies using HPLC and highly purified phosphorylated inositol products as standards will be required to address this issue. These reagents were not available at the time of preparation of this thesis.

The biological significance of two MmPI3kγ isoforms that display very similar *in vitro* characteristics is presently unclear. Upon examination of the tissue distribution of MmPI3kγ1111, it is clear that MmPI3kγ1100 transcripts were only detectable in the spleen, in contrast to a ubiquitous pattern of expression of MmPI3kγ1111 transcripts throughout all murine tissues examined. The specificity of their functions may lie in the particular tissues and cells in which they are expressed. It is known that distinct cell populations demonstrate distinct G protein subunits expression patterns (McColl & Neote, 1996). Although both isoforms appear to be expressed in peripheral leukocytes, the coupling of either PI3kγs to various G protein

isoforms may dictate the signalling pathways activated and the resultant effector functions stimulated. More recently, a G protein activated isoform of PI3-kinase was detected in murine smooth muscle cells (Bacqueville *et al.*, 2001). The functional importance of this isoform in smooth muscle cells is yet to be established and at this stage, it is not known whether it is the MmPI3kγ1100, the MmPI3kγ1111, or another isoform. However, the finding supports the existence of mutiple isoforms of Class IB PI3-kinases in distinct cell populations with the potential for specialised functions.

The ability of MmPI3kγ1111 to autophosphorylate was consistent with other Class IB PI3-kinases. The autophosphorylation of PI3kδ has been shown to downregulate its lipid kinase activity (Vanhaesebroeck *et al.*, 1999), and similarly, the phosphorylation of adaptor subunits in other Class IA PI3-kinases also downregulates lipid kinase activity (Carpenter *et al.*, 1993). Upon examination of the lipid kinase activity of the pre-phosphorylated MmPI3kγ1111, a similar outcome was observed. The dual kinase function of PI3kγ raises several important questions, especially considering that the activities appear to negatively cross-regulate each other. Of relevance, work by Bondeva *et al.*, demonstrated using an over-expression system in COS cells, demonstrated stimulation of the lipid kinase activity results in the activation of PKB, whereas stimulation of the protein kinase activity results in the activation of the MAP kinase pathway (Bondeva *et al.*, 1998). This bifurcation generates an interesting question regarding the mechanism that regulates this decision to activate one PI3kγ activity over the other. Not all chemotactic factors appear to stimulate an increase in the level of cellular PI 3,4,5 P_3 (B. Vanhaesebroeck personal communication). It may be possible that some ligands stimulate the phosphorylation

of PI3kγ downstream of GPCR ligation and hence activate the MAP kinase pathway, while others result in lipid kinase activity and activate PKB. Traditionally, the examination of cellular levels of PI 3,4,5 P_3 have dictated whether a ligand is thought to activate PI3-kinase, however concomitant investigation of the phosphorylation status of PI3kγ downstream of various ligands may also provide a more complete understanding of the agonists of phosphorylation versus those of lipid kinase activation. Over-expression of a permanently phosphorylated form of PI3kγ may provide greater understanding of the importance of phosphorylated lipid production in the generation of leukocyte effector functions downstream of GPCR stimulation.

While studies using blanket PI3-kinase inhibitors (wortmannin and LY294002) have demonstrated that migration of lymphocytes in response to chemokines involves the PI3-kinase family (Rumsey *et al.*, 2001) the particular isoforms involved in this signalling pathway are yet to be determined. In the present study, over-expression of a catalytically-inactive form of MmPI3kγ1111 resulted in a reduced capacity of the B lymphocyte cell line B300.19, expressing huCCR6 to migrate towards huMIP-3α *in vitro*. This is the first study to directly demonstrate that PI3kγ plays a role in the migration of B lymphocytes towards a chemotactic factor. Furthermore, the results indicate the involvement of PI3kγ in the CCR6 signal transduction pathway activated by the chemokine MIP-3α. In the present study, however, no proof for a role of PI3kγ in lymphocyte migration *in vivo* was obtained. While it is possible that PI3kγ does not play a role in migration of lymphocytes in response to chemokines *in vivo*, further experimentation is required before making this conclusion. The use of alternative over expression systems and additional *in vivo*

migratory models may provide another picture. The use of the retroviral expression system still remains as potentially the most powerful system because it will allow examination of the function of PI3kγ in primary lymphocytes and the extension to a true *in vivo* based immune response. Mice deficient in the chemokines BLC/BCA1 and the cognate receptor CXCR5 show a marked defect in the movement of B cells towards follicles in secondary lymphoid tissues (Ansel *et al.*, 1999; Ansel *et al.*, 2000; Forster *et al.*, 1996). Expression of a catalytically-inactive form of PI3kγ in primary B cells may therefore provide an insight into the involvement of PI3kγ in the migratory patterns of quiescent B cells, downstream of CXCR5 signalling. Mice deficient in CCR6 expression demonstrate a decrease in antibody responses when compared with the wild-type littermates (Cook *et al.*, 2000; Varona *et al.*, 2001) as CCR6 expression is also thought to be important in the migration of plasma cells to mucosal sites. Since data in the present study show that PI3kγ plays an important role in CCR6-mediated chemotaxis of B lymphocytes (at least *in vitro*), expression of a catalytically-inactive form of MmPI3kγ1111 in activated primary B lymphocytes and investigation of their migratory pattern could provide an insight into the importance of PI3kγ in generation of a humoral immune response.

To date, there is very little understood regarding the function of PI3kγ in lymphocyte function. The role of PI3kγ can be examined in various aspects of T cell biology however, the role of chemokines appears to be critical in the movement of activated T cells from secondary lymphoid tissues to peripheral sites and the correct positioning of B cells in specialised compartments within secondary lymphoid tissues. Two murine immune disorders established in the laboratory could be used to further

characterise PI3kγ function in lymphocyte migration *in vivo*. These are the murine model of multiple sclerosis, known as experimental autoimmune encephalomyelitis, EAE, and a murine model of delayed type hypersensitivity (DTH). In both these models, passive transfer of activated T cells results in the manifestation of CNS based peripheral paralysis (EAE), and significant inflammation of challenged peripheral sites (DTH) respectively. It is postulated that chemokine driven signals are imperative for the movement of these activated T cells towards peripheral sites where disease pathogenesis is observed. In order, to examine the role of PI3kγ signalling in the migration of activated primary T cells *in vivo*, the retroviral expression system could be employed in both the models described above. Integration of a catalytically inactive form of MmPI3kγ1111 could be carried out during the *in vitro* re-stimulation of sensitised T cells obtained from donor animals. Following incubation with viral particles, activated T cells positive for DNA integration could be separated by FACS, based on EGFP expression, and subsequently injected intravenously into recipient animals. Onset and severity of disease pathogenesis could be determined phenotypically, as well as at the cellular level utilising fluorescent microscopy of tissue sections, in both the EAE and DTH models. If PI3kγ plays an important role in migration of effector T cells to sites of inflammation, then EAE and DTH should be inhibited when PI3kγKR-expressing T cells are passively transferred into the recipients.

In summary, the work presented in this thesis describes the cloning of MmPI3kγ1111, a novel isoform of PI3kγ. The structural and functional characteristics of this protein *in vitro* support its catergorisation as a Class IB PI3-kinase. The

employment of a dominant-negative based approach demonstrates for the first time the importance of MmPI3kγ1111 signalling in B lymphocyte migration downstream of CCR6 receptor signaling. Further studies will be required to determine whether MmPI3kγ1111 plays and important role in T and B lymphocyte migration *in vivo*.

Chapter Seven

Bibliography

Adema G. J., Hartgers F., Verstraten R., de Vries E., Marland G., Menon S., Foster J., Xu Y., Nooyen P., McClanahan T., Bacon K. B., and Figdor C. G. (1997). A dendritic-cell-derived C-C chemokine that preferentially attracts naive T cells. *Nature* **387:** 713-7.

Ahmed S., Lee J., Wen L., Zhao Z., Ho J., Best A., Kozma R., and Lim L. (1994). Breakpoint cluster region gene product-related domain of n-chimaerin. Discrimination between Rac-binding and GTPase-activating residues by mutational analysis. *J Biol Chem* **269:** 17642-8.

al-Aoukaty A., Rolstad B., and Maghazachi A. A. (1999). Recruitment of pleckstrin and phosphoinositide 3-kinase gamma into the cell membranes, and their association with G beta gamma after activation of NK cells with chemokines. *J Immunol* **162:** 3249-55.

Alessi D. R., Andjelkovic M., Caudwell B., Cron P., Morrice N., Cohen P., and Hemmings B. A. (1996). Mechanism of activation of protein kinase B by insulin and IGF-1. *Embo J* **15:** 6541-51.

Ansel K. M., McHeyzer-Williams L. J., Ngo V. N., McHeyzer-Williams M. G., and Cyster J. G. (1999). In vivo-activated CD4 T cells upregulate CXC chemokine receptor 5 and reprogram their response to lymphoid chemokines. *J Exp Med* **190:** 1123-34.

Ansel K. M., Ngo V. N., Hyman P. L., Luther S. A., Forster R., Sedgwick J. D., Browning J. L., Lipp M., and Cyster J. G. (2000). A chemokine-driven positive feedback loop organizes lymphoid follicles. *Nature* **406:** 309-14.

Auger K. R., Carpenter C. L., Cantley L. C., and Varticovski L. (1989). Phosphatidylinositol 3-kinase and its novel product, phosphatidylinositol 3-

phosphate, are present in Saccharomyces cerevisiae. *J Biol Chem* **264:** 20181-4.

Bacqueville D., Deleris P., Mendre C., Pieraggi M., Chap H., Guillon G., Perret B., and Breton-Douillon. M. (2001). Characterization of a G protein-activated phosphoinositide 3-kinase in vascular smooth muscle cell nuclei. *J Biol Chem.* **276:** 22170-6.

Baggiolini M. (1998). Chemokines and leukocyte traffic. *Nature* **392:** 565-8.

Balashov K. E., Rottman J. B., Weiner H. L., and Hancock W. W. (1999). CCR5(+) and CXCR3(+) T cells are increased in multiple sclerosis and their ligands MIP-1alpha and IP-10 are expressed in demyelinating brain lesions. *Proc Natl Acad Sci U S A* **96:** 6873-8.

Berridge M., and Irvine R. (1989). Inositol phosphates and cell signalling. *Nature* **341:** 197-205.

Bi L., Okabe I., Bernard D., Wynshaw-Boris A., and Nussbaum (1999). Proliferative defect and embryonic lethality in mice homozygous for a deletion in the p110alpha subunit of phosphoinositide 3-kinase. *J Biol Chem.* **274:** 10963-8.

Birnbaumer. L. (1992). Receptor-to-effector signaling through G proteins: roles for beta gamma dimers as well as alpha subunits. *Cell.* **71:** 1069-72.

Bjorge J., Chan T., Antczak M., Kung H., and Fujita D. (1990). Activated type I phosphatidylinositol kinase is associated with the epidermal growth factor (EGF) receptor following EGF stimulation. *Proc Natl Acad Sci U S A* **87:** 3816-20.

Bleul C. C., Fuhlbrigge R. C., Casasnovas J. M., Aiuti A., and Springer T. A. (1996). A highly efficacious lymphocyte chemoattractant, stromal cell-derived factor 1 (SDF-1). *J Exp Med* **184:** 1101-9.

Bondev A., Rubio I., and Wetzker R. (1999). Differential regulation of lipid and protein kinase activities of phosphoinositide 3-kinase gamma in vitro. *Biol Chem* **380:** 1337-40.

Bondeva T., Pirola L., Bulgarelli-Leva G., Rubio I., Wetzker R., and Wymann M. (1998). Bifurcation of lipid and protein kinase signals of PI3Kgamma to the protein kinases PKB and MAPK. *Science* **282:** 293-6.

Bonecchi R., Bianchi G., Bordignon P. P., D'Ambrosio D., Lang R., Borsatti A., Sozzani S., Allavena P., Gray P. A., Mantovani A., and Sinigaglia F. (1998). Differential expression of chemokine receptors and chemotactic responsiveness of type 1 T helper cells (Th1s) and Th2s. *J Exp Med* **187:** 129-34.

Bourne H., Sanders D., and McCormick F. (1991). The GTPase superfamily: conserved structure and molecular mechanism. *Nature* **349:** 117-27.

Brandt S., Dougherty R., Lapetina E., and Niedel J. (1985). Pertussis toxin inhibits chemotactic peptide-stimulated generation of inositol phosphates and lysosomal enzyme secretion in human leukemic (HL-60) cells. *Proc Natl Acad Sci U S A* **82:** 3277-80.

Carpenter C., Auger K., Duckworth B., Hou W., Schaffhausen B., and Cantley. L. (1993). A tightly associated serine/threonine protein kinase regulates phosphoinositide 3-kinase activity. *Mol Cell Biol.* **13:** 1657-65.

Chensue S., Lukacs N., Yang T., Shang X., Frait K., Kunkel S., Kung T., Wiekowski M., Hedrick J., Cook D., Zingoni A., Narula S., Zlotnik A., Barrat F., O'Garra A., Napolitano M., and Lira S. (2001). Aberrant in vivo T helper type 2 cell response and impaired eosinophil recruitment in CC chemokine receptor 8 knockout mice. *J Exp Med* **193:** 573-84.

Chvatchko Y., Hoogewerf A. J., Meyer A., Alouani S., Juillard P., Buser R., Conquet F., Proudfoot A. E., Wells T. N., and Power C. A. (2000). A key role for CC chemokine receptor 4 in lipopolysaccharide-induced endotoxic shock. *J Exp Med* **191:** 1755-64.

Cicchetti P., Mayer B., Thiel G., and Baltimore D. (1992). Identification of a protein that binds to the SH3 region of Abl and is similar to Bcr and GAP-rho. *Science* **257:** 803-6.

Coates N. J., and McColl S. R. (2001). Production of chemokines in vivo in response to microbial stimulation. *J Immunol* **166:** 5176-82.

Cochet C., Filhol O., Payrastre B., Hunter T., and Gill G. (1991). Interaction between the epidermal growth factor receptor and phosphoinositide kinases. *J Biol Chem.* **266:** 637-44.

Cohen B., Liu Y., Druker B., Roberts T., and Schaffhausen B. (1990a). Characterization of pp85, a target of oncogenes and growth factor receptors. *Mol Cell Biol.* **10:** 2909-15.

Cohen B., Yoakim M., Piwnica-Worms H., Roberts T., and Schaffhausen B. (1990b). Tyrosine phosphorylation is a signal for the trafficking of pp85, an 85-kDa phosphorylated polypeptide associated with phosphatidylinositol kinase activity. *Proc Natl Acad Sci U S A* **87:** 4458-62.

Cohen G., Ren R., and Baltimore D. (1995). Modular binding domains in signal transduction proteins. *Cell* **80:** 237-48.

Cole K. E., Strick C. A., Paradis T. J., Ogborne K. T., Loetscher M., Gladue R. P., Lin W., Boyd J. G., Moser B., Wood D. E., Sahagan B. G., and Neote K. (1998). Interferon-inducible T cell alpha chemoattractant (I-TAC): a novel non-ELR

CXC chemokine with potent activity on activated T cells through selective high affinity binding to CXCR3. *J Exp Med* **187:** 2009-21.

Cook D., Prosser D., Forster R., Zhang J., Kuklin N., Abbondanzo S., Niu X., Chen S., Manfra D., Wiekowski M., Sullivan L., Smith S., Greenberg H., Narula S., Lipp M., and . S. L. (2000). CCR6 mediates dendritic cell localization, lymphocyte homeostasis, and immune responses in mucosal tissue. *Immunity.* **12:** 495-503.

Coughlin S. R., Escobedo J. A., and Williams L. T. (1989). Role of phosphatidylinositol kinase in PDGF receptor signal transduction. *Science* **243:** 1191-4.

Cross M. J., Stewart A., Hodgkin M. N., Kerr D. J., and Wakelam M. J. (1995). Wortmannin and its structural analogue demethoxyviridin inhibit stimulated phospholipase A2 activity in Swiss 3T3 cells. Wortmannin is not a specific inhibitor of phosphatidylinositol 3-kinase. *J Biol Chem* **270:** 25352-5.

Dey B., Furlanetto R., and Nissley S. (1998). Cloning of human p55 gamma, a regulatory subunit of phosphatidylinositol 3-kinase, by a yeast two-hybrid library screen with the insulin-like growth factor-I receptor [published erratum appears in Gene 1998 May 28;212(1):155]. *Gene* **209:** 175-83.

Dhand R., Hara K., Hiles I., Bax B., Gout I., Panayotou G., Fry M. J., Yonezawa K., Kasuga M., and Waterfield M. D. (1994a). PI 3-kinase: structural and functional analysis of intersubunit interactions. *Embo J* **13:** 511-21.

Dhand R., Hiles I., Panayotou G., Roche S., Fry M. J., Gout I., Totty N. F., Truong O., Vicendo P., Yonezawa K., and et al. (1994b). PI 3-kinase is a dual specificity enzyme: autoregulation by an intrinsic protein-serine kinase activity. *Embo J* **13:** 522-33.

Diekmann D., Brill S., Garrett M., Totty N., Hsuan J., Monfries C., Hall C., Lim L., and Hall A. (1991). Bcr encodes a GTPase-activating protein for p21rac. *Nature* **351:** 400-2.

Dieu M. C., Vanbervliet B., Vicari A., Bridon J. M., Oldham E., Ait-Yahia S., Briere F., Zlotnik A., Lebecque S., and Caux C. (1998). Selective recruitment of immature and mature dendritic cells by distinct chemokines expressed in different anatomic sites. *J Exp Med* **188:** 373-86.

End P., Gout I., Fry M. J., Panayotou G., Dhand R., Yonezawa K., Kasuga M., and Waterfield M. D. (1993). A biosensor approach to probe the structure and function of the p85 alpha subunit of the phosphatidylinositol 3-kinase complex. *J Biol Chem* **268:** 10066-75.

Escobedo J. A., Kaplan D. R., Kavanaugh W. M., Turck C. W., and Williams L. T. (1991a). A phosphatidylinositol-3 kinase binds to platelet-derived growth factor receptors through a specific receptor sequence containing phosphotyrosine. *Mol Cell Biol* **11:** 1125-32.

Escobedo J. A., Navankasattusas S., Kavanaugh W. M., Milfay D., Fried V. A., and Williams L. T. (1991b). cDNA cloning of a novel 85 kd protein that has SH2 domains and regulates binding of PI3-kinase to the PDGF beta-receptor. *Cell* **65:** 75-82.

Farber J. M. (1997). Mig and IP-10: CXC chemokines that target lymphocytes. *J Leukoc Biol* **61:** 246-57.

Forster R., Mattis A., Kremmer E., Wolf E., Brem G., and Lipp M. (1996). A putative chemokine receptor, BLR1, directs B cell migration to defined lymphoid organs and specific anatomic compartments of the spleen. *Cell* **87:** 1037-47.

Forster R., Schubel A., Breitfeld D., Kremmer E., Renner-Muller I., Wolf E., and Lipp M. (1999). CCR7 coordinates the primary immune response by establishing functional microenvironments in secondary lymphoid organs. *Cell* **99:** 23-33.

Franke T. F., Kaplan D. R., and Cantley L. C. (1997). PI3K: downstream AKTion blocks apoptosis. *Cell* **88:** 435-7.

Frech M., Andjelkovic M., Ingley E., Reddy K., Falck J., and Hemmings B. (1997). High affinity binding of inositol phosphates and phosphoinositides to the pleckstrin homology domain of RAC/protein kinase B and their influence on kinase activity. *J Biol Chem.* **272:** 8474-81.

Fruman D. A., Snapper S. B., Yballe C. M., Davidson L., Yu J. Y., Alt F. W., and Cantley L. C. (1999). Impaired B cell development and proliferation in absence of phosphoinositide 3-kinase p85alpha. *Science* **283:** 393-7.

Fry M. J., Panayotou G., Booker G. W., and Waterfield M. D. (1993). New insights into protein-tyrosine kinase receptor signaling complexes. *Protein Sci* **2:** 1785-97.

Gale L. M., and McColl S. R. (1999). Chemokines: extracellular messengers for all occasions? *Bioessays* **21:** 17-28.

Garside P., Ingulli E., Merica R., Johnson J., Noelle R., and Jenkins M. (1998). Visualization of specific B and T lymphocyte interactions in the lymph node. *Science* **281:** 96-9.

Gerard C., and Gerard N. (1994). C5A anaphylatoxin and its seven transmembrane-segment receptor. *Annu Rev Immunol* **12:** 775-808.

Gerard C., and Rollins B. J. (2001). Chemokines and disease. *Nat Immunol* **2:** 108-15.

Godiska R., Chantry D., Dietsch G. N., and Gray P. W. (1995). Chemokine expression in murine experimental allergic encephalomyelitis. *J Neuroimmunol* **58:** 167-76.

Gout I., Middleton G., Adu J., Ninkina N., Drobot L., Filonenko V., Matsuka G., Davies A., Waterfield M., and Buchman V. (2000). Negative regulation of PI 3-kinase by Ruk, a novel adaptor protein. *EMBO J.* **19:** 4015-25.

Gunn M. D., Kyuwa S., Tam C., Kakiuchi T., Matsuzawa A., Williams L. T., and Nakano H. (1999). Mice lacking expression of secondary lymphoid organ chemokine have defects in lymphocyte homing and dendritic cell localization. *J Exp Med* **189:** 451-60.

Gutierrez-Ramos J., Lloyd C., and Gonzalo J. (1999). Eotaxin: from an eosinophilic chemokine to a major regulator of allergic reactions. *Immunol Today* **20:** 500-4.

Hancock W. W., Gao W., Faia K. L., and Csizmadia V. (2000a). Chemokines and their receptors in allograft rejection. *Curr Opin Immunol* **12:** 511-6.

Hancock W. W., Lu B., Gao W., Csizmadia V., Faia K., King J. A., Smiley S. T., Ling M., Gerard N. P., and Gerard C. (2000b). Requirement of the chemokine receptor CXCR3 for acute allograft rejection. *J Exp Med* **192:** 1515-20.

Hawkins P., Jackson T., and Stephens L. (1992). Platelet-derived growth factor stimulates synthesis of PtdIns(3,4,5)P3 by activating a PtdIns(4,5)P2 3-OH kinase. *Nature* **358:** 157-9.

Hieshima K., Imai T., Opdenakker G., Van Damme J., Kusuda J., Tei H., Sakaki Y., Takatsuki K., Miura R., Yoshie O., and Nomiyama H. (1997). Molecular cloning of a novel human CC chemokine liver and activation-regulated

chemokine (LARC) expressed in liver. Chemotactic activity for lymphocytes and gene localization on chromosome 2. *J Biol Chem* **272:** 5846-53.

Hiles I. D., Otsu M., Volinia S., Fry M. J., Gout I., Dhand R., Panayotou G., Ruiz Larrea F., Thompson A., Totty N. F., and et al. (1992). Phosphatidylinositol 3-kinase: structure and expression of the 110 kd catalytic subunit. *Cell* **70:** 419-29.

Hirsch E., Katanaev V., Garlanda C., Azzolino O., Pirola L., Silengo L., Sozzani S., Mantovani A., Altruda F., and Wymann M. (2000a). Central role for G protein-coupled phosphoinositide 3-kinase gamma in inflammation. *Science* **287:** 1049-53.

Hirsch E., Wymann M., Patrucco E., Tolosano E., Bulgarelli-Leva G., Marengo S., Rocchi M., and Altruda F. (2000b). Analysis of the murine phosphoinositide 3-kinase gamma gene. *Gene* **256:** 69-81.

Kapeller R., Prasad K. V., Janssen O., Hou W., Schaffhausen B. S., Rudd C. E., and Cantley L. C. (1994). Identification of two SH3-binding motifs in the regulatory subunit of phosphatidylinositol 3-kinase. *J Biol Chem* **269:** 1927-33.

Kaplan D., Whitman M., Schaffhausen B., Pallas D., White M., Cantley L., and Roberts. T. (1987). Common elements in growth factor stimulation and oncogenic transformation: 85 kD phosphoprotein and phosphatidylinositol kinase activity. *Cell* **50:** 1021-9.

Karpus W. J., and Kennedy K. J. (1997). MIP-1alpha and MCP-1 differentially regulate acute and relapsing autoimmune encephalomyelitis as well as Th1/Th2 lymphocyte differentiation. *J Leukoc Biol* **62:** 681-7.

Klippel A., Escobedo J. A., Fantl W. J., and Williams L. T. (1992). The C-terminal SH2 domain of p85 accounts for the high affinity and specificity of the binding of phosphatidylinositol 3-kinase to phosphorylated platelet-derived growth factor beta receptor. *Mol Cell Biol* **12:** 1451-9.

Koch A., Kunkel S., Harlow L., Johnson B., Evanoff H., Haines G., Burdick M., Pope R., and Strieter R. (1992). Enhanced production of monocyte chemoattractant protein-1 in rheumatoid arthritis. *J Clin Invest* **90:** 772-9.

Koch C., Anderson D., Moran M., Ellis C., and Pawson T. (1991). SH2 and SH3 domains: elements that control interactions of cytoplasmic signaling proteins. *Science* **252:** 668-74.

Kodaki T., Woscholski R., Hallberg B., Rodriguez Viciana P., Downward J., and Parker P. J. (1994). The activation of phosphatidylinositol 3-kinase by Ras. *Curr Biol* **4:** 798-806.

Krugmann S., Hawkins P., Pryer N., and Braselmann S. (1999). Characterizing the interactions between the two subunits of the p101/p110gamma phosphoinositide 3-kinase and their role in the activation of this enzyme by G beta gamma subunits. *J Biol Chem* **274:** 17152-8.

Kumar C., Diao R., Yin Z., Liu Y., Samatar A., Madison V., and Xiao L. (2001). Expression, purification, characterization and homology modeling of active Akt/PKB, a key enzyme involved in cell survival signaling. *Biochim Biophys Acta.* **1526:** 257-68.

Leopoldt D., Hanck T., Exner T., Maier U., Wetzker R., and Nurnberg. B. (1998). Gbetagamma stimulates phosphoinositide 3-kinase-gamma by direct interaction with two domains of the catalytic p110 subunit. *J Biol Chem.* **273:** 7024-9.

Li Z., Jiang H., Xie W., Zhang Z., Smrcka A., and Wu. D. (2000). Roles of PLC-beta2 and -beta3 and PI3Kgamma in chemoattractant-mediated signal transduction. *Science* **287:** 1046-9.

Liu X., Marengere L. E., Koch C. A., and Pawson T. (1993). The v-Src SH3 domain binds phosphatidylinositol 3'-kinase. *Mol Cell Biol* **13:** 5225-32.

Luster A., and Rothenberg M. (1997). Role of the monocyte chemoattractant protein and eotaxin subfamily of chemokines in allergic inflammation. *J Leukoc Biol.* **62:** 620-33.

Ma A. D., and Abrams C. S. (1999). Pleckstrin induces cytoskeletal reorganization via a Rac-dependent pathway. *J Biol Chem* **274:** 28730-5.

Matter W. F., Brown R. F., and Vlahos C. J. (1992). The inhibition of phosphatidylinositol 3-kinase by quercetin and analogs. *Biochem Biophys Res Commun* **186:** 624-31.

Mayer B., Hamaguchi M., and Hanafusa H. (1988). A novel viral oncogene with structural similarity to phospholipase C. *Nature* **332:** 272-5.

McColl S., and Naccache P. (1997). "Calcium transient assays: An evaluation of their usefulness in studying chemokine receptor signal transduction.," Academic press.

McColl S., and Neote K. (1996). "Chemoattractant ligands and their receptors," CRC press.

McColl S. R., and Clark-Lewis I. (1999). Inhibition of murine neutrophil recruitment in vivo by CXC chemokine receptor antagonists. *J Immunol* **163:** 2829-35.

McColl S. R., Krump E., Naccache P. H., Poubelle P. E., Braquet P., Braquet M., and Borgeat P. (1991). Granulocyte-macrophage colony-stimulating factor increases the synthesis of leukotriene B4 by human neutrophils in response to

platelet-activating factor. Enhancement of both arachidonic acid availability and 5-lipoxygenase activation. *J Immunol* **146:** 1204-11.

McDonald P. P., Pouliot M., Borgeat P., and McColl S. R. (1993). Induction by chemokines of lipid mediator synthesis in granulocyte-macrophage colony-stimulating factor-treated human neutrophils. *J Immunol* **151:** 6399-409.

Molendijk A. J., and Irvine R. F. (1998). Inositide signalling in Chlamydomonas: characterization of a phosphatidylinositol 3-kinase gene. *Plant Mol Biol* **37:** 53-66.

Moser B., and Loetscher P. (2001). Lymphocyte traffic control by chemokines. *Nat Immunol* **2:** 123-8.

Murphy P. (1994). The molecular biology of leukocyte chemoattractant receptors. *Annu Rev Immunol* **12:** 593-633.

Musacchio A., Cantley L. C., and Harrison S. C. (1996). Crystal structure of the breakpoint cluster region-homology domain from phosphoinositide 3-kinase p85 alpha subunit. *Proc Natl Acad Sci U S A* **93:** 14373-8.

Naccache P. H., Levasseur S., Lachance G., Chakravarti S., Bourgoin S. G., and McColl S. R. (2000). Stimulation of human neutrophils by chemotactic factors is associated with the activation of phosphatidylinositol 3-kinase gamma. *J Biol Chem* **275:** 23636-41.

Nagasawa T., Hirota S., Tachibana K., Takakura N., Nishikawa S., Kitamura Y., Yoshida N., Kikutani H., and Kishimoto T. (1996). Defects of B-cell lymphopoiesis and bone-marrow myelopoiesis in mice lacking the CXC chemokine PBSF/SDF-1. *Nature* **382:** 635-8.

Napolitano M., and Santoni A. (1999). Structure and function of the CC chemokine receptor (CCR) 8. *Forum (Genova)* **9:** 315-24.

Ngo V. N., Korner H., Gunn M. D., Schmidt K. N., Riminton D. S., Cooper M. D., Browning J. L., Sedgwick J. D., and Cyster J. G. (1999). Lymphotoxin alpha/beta and tumor necrosis factor are required for stromal cell expression of homing chemokines in B and T cell areas of the spleen. *J Exp Med* **189:** 403-12.

Oberlin E., Amara A., Bachelerie F., Bessia C., Virelizier J. L., Arenzana-Seisdedos F., Schwartz O., Heard J. M., Clark-Lewis I., Legler D. F., Loetscher M., Baggiolini M., and Moser B. (1996). The CXC chemokine SDF-1 is the ligand for LESTR/fusin and prevents infection by T-cell-line-adapted HIV-1. *Nature* **382:** 833-5.

Otsu M., Hiles I., Gout I., Fry M. J., Ruiz Larrea F., Panayotou G., Thompson A., Dhand R., Hsuan J., Totty N., and et al. (1991). Characterization of two 85 kd proteins that associate with receptor tyrosine kinases, middle-T/pp60c-src complexes, and PI3-kinase. *Cell* **65:** 91-104.

Pan Z. K., Christiansen S. C., Ptasznik A., and Zuraw B. L. (1999). Requirement of phosphatidylinositol 3-kinase activity for bradykinin stimulation of NF-kappaB activation in cultured human epithelial cells. *J Biol Chem* **274:** 9918-22.

Panayotou G., Gish G., End P., Truong O., Gout I., Dhand R., Fry M. J., Hiles I., Pawson T., and Waterfield M. D. (1993). Interactions between SH2 domains and tyrosine-phosphorylated platelet-derived growth factor beta-receptor sequences: analysis of kinetic parameters by a novel biosensor-based approach. *Mol Cell Biol* **13:** 3567-76.

Parijs L., Refaeli Y., Abbas A., and Baltimore. D. (1999a). Autoimmunity as a consequence of retrovirus-mediated expression of C-FLIP in lymphocytes. *Immunity.* **11:** 763-70.

Parijs L., Refaeli Y., Lord J., Nelson B., Abbas A., and Baltimore D. (1999b). Uncoupling IL-2 signals that regulate T cell proliferation, survival, and Fas-mediated activation-induced cell death. *Immunity.* **11:** 281-8.

Pawson T., and Gish G. (1992). SH2 and SH3 domains: from structure to function. *Cell* **71:** 359-62.

Pear W., Miller J., Xu L., Pui J., Soffer B., Quackenbush R., Pendergast A., Bronson R., Aster J., Scott M., and Baltimore. D. (1998). Efficient and rapid induction of a chronic myelogenous leukemia-like myeloproliferative disease in mice receiving P210 bcr/abl-transduced bone marrow. *Blood* **92:** 3780-92.

Pirola L., Zvelebil M., Bulgarelli-Leva G., Obberghen E. V., Waterfield M., and Wymann M. (2001). Activation loop sequences confer substrate specificity to phosphoinositide 3-kinase alpha (PI3Kalpha). Functions of lipid kinase-deficient PI3Kalpha in signaling. *J Biol Chem.* **276:** 21544-54.

Pleiman C. M., Clark M. R., Gauen L. K., Winitz S., Coggeshall K. M., Johnson G. L., Shaw A. S., and Cambier J. C. (1993). Mapping of sites on the Src family protein tyrosine kinases p55blk, p59fyn, and p56lyn which interact with the effector molecules phospholipase C-gamma 2, microtubule-associated protein kinase, GTPase-activating protein, and phosphatidylinositol 3-kinase. *Mol Cell Biol* **13:** 5877-87.

Pons S., Asano T., Glasheen E., Miralpeix M., Zhang Y., Fisher T. L., Myers M. G., Jr., Sun X. J., and White M. F. (1995). The structure and function of p55PIK

reveal a new regulatory subunit for phosphatidylinositol 3-kinase. *Mol Cell Biol* **15:** 4453-65.

Ponzetto C., Bardelli A., Maina F., Longati P., Panayotou G., Dhand R., Waterfield M. D., and Comoglio P. M. (1993). A novel recognition motif for phosphatidylinositol 3-kinase binding mediates its association with the hepatocyte growth factor/scatter factor receptor. *Mol Cell Biol* **13:** 4600-8.

Prasad K. V., Janssen O., Kapeller R., Raab M., Cantley L. C., and Rudd C. E. (1993). Src-homology 3 domain of protein kinase p59fyn mediates binding to phosphatidylinositol 3-kinase in T cells. *Proc Natl Acad Sci U S A* **90:** 7366-70.

Rameh L., Tolias K., Duckworth B., and Cantley. L. (1997). A new pathway for synthesis of phosphatidylinositol-4,5-bisphosphate. *Nature* **390:** 192-6.

Reth M., Ammirati P., Jackson S., and Alt F. (1985). Regulated progression of a cultured pre-B-cell line to the B-cell stage. *Nature* **317:** 353-5.

Reth M., Jackson S., and Alt F. (1986). VHDJH formation and DJH replacement during pre-B differentiation: non-random usage of gene segments. *EMBO J.* **5:** 2131-8.

Rodriguez Viciana P., Warne P. H., Dhand R., Vanhaesebroeck B., Gout I., Fry M. J., Waterfield M. D., and Downward J. (1994). Phosphatidylinositol-3-OH kinase as a direct target of Ras [see comments]. *Nature* **370:** 527-32.

Rumsey L., Teague R., Benedict S., and Chan. M. (2001). MIP-1alpha induces activation of phosphatidylinositol-3 kinase that associates with Pyk-2 and is necessary for B-cell migration. *Exp Cell Res.* **268:** 77-83.

Sadowski I., Stone J., and . T. P. (1986). A noncatalytic domain conserved among cytoplasmic protein-tyrosine kinases modifies the kinase function and

transforming activity of Fujinami sarcoma virus P130gag-fps. *Mol Cell Biol.* **6:** 4396-408.

Sallusto F., Lanzavecchia A., and Mackay C. R. (1998a). Chemokines and chemokine receptors in T-cell priming and Th1/Th2-mediated responses. *Immunol Today* **19:** 568-74.

Sallusto F., Lenig D., Mackay C. R., and Lanzavecchia A. (1998b). Flexible programs of chemokine receptor expression on human polarized T helper 1 and 2 lymphocytes. *J Exp Med* **187:** 875-83.

Sasaki T., Irie-Sasaki J., Jones R., Oliveira-dos-Santos A., Stanford W., Bolon B., Wakeham A., Itie A., Bouchard D., Kozieradzki I., Joza N., Mak T., Ohashi P., Suzuki A., and Penninger. J. (2000). Function of PI3Kgamma in thymocyte development, T cell activation, and neutrophil migration. *Science* **287:** 1040-6.

Schon M. P., and Ruzicka T. (2001). Psoriasis: the plot thickens. *Nat Immunol* **2:** 91.

Sekido N., Mukaida N., Harada A., Nakanishi I., Watanabe Y., and Matsushima K. (1993). Prevention of lung reperfusion injury in rabbits by a monoclonal antibody against interleukin-8. *Nature* **365:** 654-7.

Simpson J., Rezaie P., Newcombe J., Cuzner M. L., Male D., and Woodroofe M. N. (2000). Expression of the beta-chemokine receptors CCR2, CCR3 and CCR5 in multiple sclerosis central nervous system tissue. *J Neuroimmunol* **108:** 192-200.

Skolnik E. Y., Margolis B., Mohammadi M., Lowenstein E., Fischer R., Drepps A., Ullrich A., and Schlessinger J. (1991). Cloning of PI3 kinase-associated p85 utilizing a novel method for expression/cloning of target proteins for receptor tyrosine kinases. *Cell* **65:** 83-90.

Song W., Wagle N. M., Banh T., Whiteford C. C., Ulug E., and Pierce S. K. (1997). Wortmannin, a phosphatidylinositol 3-kinase inhibitor, blocks the assembly of peptide-MHC class II complexes. *Int Immunol* **9:** 1709-22.

Songyang Z., Shoelson S., Chaudhuri M., Gish G., Pawson T., Haser W., King F., Roberts T., Ratnofsky S., and Lechleider R. (1993). SH2 domains recognize specific phosphopeptide sequences. *Cell* **72:** 767-78.

Stephens L., Cooke F. T., Walters R., Jackson T., Volinia S., Gout I., Waterfield M. D., and Hawkins P. T. (1994a). Characterization of a phosphatidylinositol-specific phosphoinositide 3-kinase from mammalian cells. *Curr Biol* **4:** 203-14.

Stephens L., Eguinoa A., Corey S., Jackson T., and Hawkins P. T. (1993a). Receptor stimulated accumulation of phosphatidylinositol (3,4,5)-trisphosphate by G-protein mediated pathways in human myeloid derived cells. *Embo J* **12:** 2265-73.

Stephens L., Hawkins P. T., Eguinoa A., and Cooke F. (1996). A heterotrimeric GTPase-regulated isoform of PI3K and the regulation of its potential effectors. *Philos Trans R Soc Lond B Biol Sci* **351:** 211-5.

Stephens L., Hughes K., and Irvine R. (1991). Pathway of phosphatidylinositol(3,4,5)-trisphosphate synthesis in activated neutrophils. *Nature* **351:** 33-9.

Stephens L., Jackson T., and Hawkins P. T. (1993b). Synthesis of phosphatidylinositol 3,4,5-trisphosphate in permeabilized neutrophils regulated by receptors and G-proteins. *J Biol Chem* **268:** 17162-72.

Stephens L., Smrcka A., Cooke F. T., Jackson T. R., Sternweis P. C., and Hawkins P. T. (1994b). A novel phosphoinositide 3 kinase activity in myeloid-derived cells is activated by G protein beta gamma subunits. *Cell* **77:** 83-93.

Stephens L. R., Eguinoa A., Erdjument Bromage H., Lui M., Cooke F., Coadwell J., Smrcka A. S., Thelen M., Cadwallader K., Tempst P., and Hawkins P. T. (1997). The G beta gamma sensitivity of a PI3K is dependent upon a tightly associated adaptor, p101. *Cell* **89:** 105-14.

Stoyanov B., Volinia S., Hanck T., Rubio I., Loubtchenkov M., Malek D., Stoyanova S., Vanhaesebroeck B., Dhand R., Nurnberg B., and et al. (1995). Cloning and characterization of a G protein-activated human phosphoinositide-3 kinase. *Science* **269:** 690-3.

Stoyanova S., Bulgarelli Leva G., Kirsch C., Hanck T., Klinger R., Wetzker R., and Wymann M. P. (1997). Lipid kinase and protein kinase activities of G-protein-coupled phosphoinositide 3-kinase gamma: structure-activity analysis and interactions with wortmannin. *Biochem J* **324:** 489-95.

Sun X. J., Rothenberg P., Kahn C. R., Backer J. M., Araki E., Wilden P. A., Cahill D. A., Goldstein B. J., and White M. F. (1991). Structure of the insulin receptor substrate IRS-1 defines a unique signal transduction protein. *Nature* **352:** 73-7.

Susa M., Keeler M., and Varticovski L. (1992). Platelet-derived growth factor activates membrane-associated phosphatidylinositol 3-kinase and mediates its translocation from the cytosol. Detection of enzyme activity in detergent-solubilized cell extracts. *J Biol Chem* **267:** 22951-6.

Terauchi Y., Tsuji Y., Satoh S., Minoura H., Murakami K., Okuno A., Inukai K., Asano T., Kaburagi Y., Ueki K., Nakajima H., Hanafusa T., Matsuzawa Y., Sekihara H., Yin Y., Barrett J. C., Oda H., Ishikawa T., Akanuma Y., Komuro I., Suzuki M., Yamamura K., Kodama T., Suzuki H., Kadowaki T., and et al. (1999). Increased insulin sensitivity and hypoglycaemia in mice lacking the p85 alpha subunit of phosphoinositide 3-kinase. *Nat Genet* **21:** 230-5.

Tessier P. A., Naccache P. H., Clark-Lewis I., Gladue R. P., Neote K. S., and McColl S. R. (1997). Chemokine networks in vivo: involvement of C-X-C and C-C chemokines in neutrophil extravasation in vivo in response to TNF-alpha. *J Immunol* **159:** 3595-602.

Tessier P. A., Naccache P. H., Diener K. R., Gladue R. P., Neote K. S., Clark-Lewis I., and McColl S. R. (1998). Induction of acute inflammation in vivo by staphylococcal superantigens. II. Critical role for chemokines, ICAM-1, and TNF-alpha. *J Immunol* **161:** 1204-11.

Thelen M. (2001). Dancing to the tune of chemokines. *Nat Immunol* **2:** 129-34.

Toker A., and Cantley. L. (1997). Signalling through the lipid products of phosphoinositide-3-OH kinase. *Nature* **387:** 673-6.

Tolias K., Cantley L., and Carpenter C. (1995). Rho family GTPases bind to phosphoinositide kinases. *J Biol Chem* **270:** 17656-9.

Tolias K., Rameh L., Ishihara H., Shibasaki Y., Chen J., Prestwich G., Cantley L., and Carpenter C. (1998). Type I phosphatidylinositol-4-phosphate 5-kinases synthesize the novel lipids phosphatidylinositol 3,5-bisphosphate and phosphatidylinositol 5-phosphate. *J Biol Chem* **273:** 18040-6.

Traynor-Kaplan A., BLThompson, Harris A., Taylor P., Omann G., and Sklar L. (1989). Transient increase in phosphatidylinositol 3,4-bisphosphate and phosphatidylinositol trisphosphate during activation of human neutrophils. *J Biol Chem.* **264:** 15668-73.

Vaday G. G., Franitza S., Schor H., Hecht I., Brill A., Cahalon L., Hershkoviz R., and Lider O. (2001). Combinatorial signals by inflammatory cytokines and chemokines mediate leukocyte interactions with extracellular matrix. *J Leukoc Biol* **69:** 885-92.

Vanhaesebroeck B., Higashi K., Raven C., Welham M., Anderson S., Brennan P., Ward S. G., and Waterfield M. D. (1999). Autophosphorylation of p110delta phosphoinositide 3-kinase: a new paradigm for the regulation of lipid kinases in vitro and in vivo. *Embo J* **18:** 1292-302.

Vanhaesebroeck B., Leevers S., Ahmadi K., Timms J., Katso R., Driscoll P., Woscholski R., Parker P., and . M. W. (2001). Synthesis and function of 3-phosphorylated inositol lipids. *Annu Rev Biochem.* **70:** 535-602.

Vanhaesebroeck B., Leevers S. J., Panayotou G., and Waterfield M. D. (1997a). Phosphoinositide 3-kinases: a conserved family of signal transducers. *Trends Biochem Sci* **22:** 267-72.

Vanhaesebroeck B., Welham M. J., Kotani K., Stein R., Warne P. H., Zvelebil M. J., Higashi K., Volinia S., Downward J., and Waterfield M. D. (1997b). P110delta, a novel phosphoinositide 3-kinase in leukocytes. *Proc Natl Acad Sci U S A* **94:** 4330-5.

Varona R., Villares R., Carramolino L., Goya I., Zaballos A., Gutierrez J., Torres M., Martinez-A C., and Marquez. G. (2001). CCR6-deficient mice have impaired leukocyte homeostasis and altered contact hypersensitivity and delayed-type hypersensitivity responses. *J Clin Invest.* **107:** R37-45.

Vlahos C. J., Matter W. F., Brown R. F., Traynor Kaplan A. E., Heyworth P. G., Prossnitz E. R., Ye R. D., Marder P., Schelm J. A., Rothfuss K. J., and et al. (1995). Investigation of neutrophil signal transduction using a specific inhibitor of phosphatidylinositol 3-kinase. *J Immunol* **154:** 2413-22.

Vlahos C. J., Matter W. F., Hui K. Y., and Brown R. F. (1994). A specific inhibitor of phosphatidylinositol 3-kinase, 2-(4-morpholinyl)-8-phenyl-4H-1-benzopyran-4-one (LY294002). *J Biol Chem* **269:** 5241-8.

Waksman G., Kominos D., Robertson S., Pant N., Baltimore D., Birge R., Cowburn D., Hanafusa H., Mayer B., and Overduin M. (1992). Crystal structure of the phosphotyrosine recognition domain SH2 of v-src complexed with tyrosine-phosphorylated peptides. *Nature* **358:** 646-53.

Waksman G., Shoelson S., Pant N., Cowburn D., and Kuriyan J. (1993). Binding of a high affinity phosphotyrosyl peptide to the Src SH2 domain: crystal structures of the complexed and peptide-free forms. *Cell.* **72:** 779-90.

Walker E. H., Perisic O., Ried C., Stephens L., and Williams R. L. (1999). Structural insights into phosphoinositide 3-kinase catalysis and signalling. *Nature* **402:** 313-20.

Walz A., Peveri P., Aschauer H., Thelen M., Kernen P., Dewald B., and Baggiolini M. (1989). Structure and properties of a novel neutrophil-activating factor (NAF) produced by human monocytes. *Agents Actions.* **26:** 148-50.

Whitman M., Downes C. P., Keeler M., Keller T., and Cantley L. (1988). Type I phosphatidylinositol kinase makes a novel inositol phospholipid, phosphatidylinositol-3-phosphate. *Nature* **332:** 644-6.

Whitman M., Kaplan D. R., Schaffhausen B., Cantley L., and Roberts T. M. (1985). Association of phosphatidylinositol kinase activity with polyoma middle-T competent for transformation. *Nature* **315:** 239-42.

Wymann M. P., Bulgarelli Leva G., Zvelebil M. J., Pirola L., Vanhaesebroeck B., Waterfield M. D., and Panayotou G. (1996). Wortmannin inactivates phosphoinositide 3-kinase by covalent modification of Lys-802, a residue involved in the phosphate transfer reaction. *Mol Cell Biol* **16:** 1722-33.

Wymann M. P., and Pirola L. (1998). Structure and function of phosphoinositide 3-kinases. *Biochim Biophys Acta* **1436:** 127-50.

Yoshimura T., Usami E., Kurita C., Watanabe S., Nakao T., Kobayashi J., Yamazaki F., and Nagai H. (1995). Effect of theophylline on the production of interleukin-1 beta, tumor necrosis factor-alpha, and interleukin-8 by human peripheral blood mononuclear cells. *Biol Pharm Bull* **18:** 1405-8.

Yu H., Chen J. K., Feng S., Dalgarno D. C., Brauer A. W., and Schreiber S. L. (1994). Structural basis for the binding of proline-rich peptides to SH3 domains. *Cell* **76:** 933-45.

Zhang J., Banfic H., Straforini F., Tosi L., Volinia S., and Rittenhouse S. E. (1998). A type II phosphoinositide 3-kinase is stimulated via activated integrin in platelets. A source of phosphatidylinositol 3-phosphate. *J Biol Chem* **273:** 14081-4.

Zhang Y., Liou G. I., Gulati A. K., and Akhtar R. A. (1999). Expression of phosphatidylinositol 3-kinase during EGF-stimulated wound repair in rabbit corneal epithelium. *Invest Ophthalmol Vis Sci* **40:** 2819-26.

Appendix I

LOCUS AF208345 3342 bp mRNA ROD 19-DEC-2000
DEFINITION Mus musculus phosphatidylinositol 3-kinase gamma isoform (Pik3cg) mRNA, complete cds.
ACCESSION AF208345
VERSION AF208345.1 GI:11890407
KEYWORDS .
SOURCE house mouse.
ORGANISM Mus musculus
Eukaryota; Metazoa; Chordata; Craniata; Vertebrata; Euteleostomi; Mammalia; Eutheria; Rodentia; Sciurognathi; Muridae; Murinae; Mus.
REFERENCE 1 (bases 1 to 3342)
AUTHORS Chakravarti,S. and McColl,S.R.
TITLE Cloning of a murine ortholog of PI 3-kinase gamma
JOURNAL Unpublished
REFERENCE 2 (bases 1 to 3342)
AUTHORS Chakravarti,S. and McColl,S.R.
TITLE Direct Submission
JOURNAL Submitted (25-NOV-1999) Microbiology & Immunology, University of Adelaide, Frome Road, Adelaide, SA 5005, Australia
FEATURES Location/Qualifiers
source 1..3342
/organism="Mus musculus"
/strain="BALB/c"
/db_xref="taxon:10090"
/cell_type="macrophage"
gene 1..3342
/gene="Pik3cg"
/note="PI3Kgamma; p110 gamma"
CDS 1..3342
/gene="Pik3cg"
/codon_start=1
/product="phosphatidylinositol 3-kinase gamma isoform"
/protein_id="AAG41122.1"
/db_xref="GI:11890408"
/translation="MELENYEQPVVLREDNLRRRRRMKPRSAAGSLSSMELIPIEFVL
PTSQRISKTPETALLHVAGHGNVEQMKAQVWLRALETSVAAEFYHRLGPDQFLLLYQK
KGQWYEIYDRYQVVQTLDCLHYWKLMHKSPGQIHVVQRHVPSEETLAFQKQLTSLIGY
DVTDISNVHDDELEFTRRRLVTPRMAEVAGRDAKLYAMHPWVTSKPLPDYLSKKIANN
CIFIVIHRGTTSQTIKVSADDTPGTILQSFFTKMAKKKSLMNISESQSEQDFVLRVCG
RDEYLVGETPLKNFQWVRQCLKNGDEIHLVLDTPPDPALDEVRKEEWPLVDDCTGVTG
YHEQLTIHGKDHESVFTVSLWDCDRKFRVKIRGIDIPVLPRNTDLTVFVEANIQHGQQ
VLCQRRTSPKPFAEEVLWNVWLEFGIKIKDLPKGALLNLQIYCCKTPSLSSKASAETP
GSESKGKAQLLYYVNLLLIDHRFLLRHGDYVLHMWQISGKAEEQGSFNADKLTSATNP
DKENSMSISILLDNYCHPIALPKHRPTPDPEGDRVRAEMPNQLRKQLEAIIATDPLNP
LTAEDKELLWHFRYESLKHPKAYPKLFSSVKWGQQEIVAKTYQLLARREIWDQSALDV
GLTMQLLDCNFSDENVRAIAVQKLESLEDDDVLHYLLQLVQAVKFEPYHDSALARFLL
KRGLRNKRIGHFLFWFLRSEIAQSXHYQQRFAVILEAYLRGCGTAMLQDFTQQVHVIE
MLQKVTIDIKSLSAEKYDVSSQVISQLKQKLESLQNSNLPESFRVPYDPGLKAGTLVI
EKCKVMASKKKPLWLEFKCADPTVLSNETIGIIFKHGDDLRQDMLILQILRIMESIWE
TESLDLCLLPYGCISTGDKIGMIEIVKDATTIAQIQQSTVGNTGAFKDEVLNHWLKEK
CPIEEKFQAAVERFVYSCAGYCVATFVLGIGDRHNDNIMISETGNLFHIDFGHILGNY

KSFLGINKERVPFVLTPDFLVVMGSSGKKTSPHFQKFQDCCVSTLQYYGDVCVRAYLA
LRHHTNLLIILFSMMLMTGMPQLTSKEDIEYIRDALTVGKSEEDAKKYFLDQIEVCRD
KGWTVQFNWFLHLVLGIKQGEKHSA"

BASE COUNT 900 a 853 c 837 g 750 t 2 others

ORIGIN

```
       1 atggagctgg agaactatga acaaccggtg gttctaagag aggacaacct ccgccggcgc
      61 cggaggatga agccacgcag cgcagcaggc agcctgtctt ccatggagct catccccatt
     121 gagttcgtac tgcccaccag ccagcgcatc agcaagactc cagaaacagc gctgctgcat
     181 gtggctggcc atggcaatgt ggaacagatg aaagctcagg tgtggctgcg cgcactggag
     241 accagtgtgg ctgcggagtt ctaccaccga ttgggcccgg accaattcct cctgctctac
     301 cagaagaaag gacaatggta tgagatctat gacaggtacc aagtggtgca gaccctagac
     361 tgcctgcatt actggaagtt gatgcacaag agccctggcc agatccacgt ggtacagcga
     421 cacgtacctt ctgaggagac cttggctttc cagaagcagc tcacctccct gattggctat
     481 gacgtcactg acatcagcaa tgtgcacgat gatgagctag agttcactcg ccgccgtctg
     541 gttacgcccc gcatggctga agtggctggc cgggatgcca aactctatgc tatgcaccct
     601 tgggtaacgt ccaaacctct cccagactac ctgtcaaaaa aaattgccaa caactgcatc
     661 ttcatcgtca tccaccgcgg taccaccagc caaaccatca aggtctccgc agatgatact
     721 cctggtacca tcctccagag cttcttcacc aagatggcca agaagaagtc cctaatgaat
     781 atctcagaaa gtcaaagtga gcaggatttt gtattgcggg tttgtggccg cgatgagtac
     841 ctggtgggtg aaacacccct caaaaatttc agtgggtga ggcagtgcct caagaacgga
     901 gatgaaatac acctggtgct cgacacgcct ccagacccag cccttgatga ggtgaggaag
     961 gaagaatggc cgctggtgga tgactgcact ggagtcaccg gctaccacga gcagctgacc
    1021 atccatggca aggaccacga gagtgtgttc acagtgtctt tgtgggactg cgaccgaaag
    1081 ttcagggtca agatcagagg cattgatatc cctgtcctgc ctcggaacac cgacctcact
    1141 gtgtttgtgg aagcgaacat ccagcacggg caacaagtcc tctgccaaag gagaaccagc
    1201 cctaagccct tcgcagaaga ggtactctgg aatgtgtggc tggagtttgg catcaaaatc
    1261 aaagacttgc ccaaaggggc tctattgaac ctacagatct actgctgcaa aaccccatca
    1321 ctgtccagca aggcttctgc agagactcca ggctccgagt ccaagggcaa agcccagctt
    1381 ctctattacg tgaacttgct gttaatagac caccgtttcc tcctccgcca cggggactat
    1441 gtgctccaca tgtggcagat atctggcaag gcagaggagc agggcagctt caatgctgac
    1501 aagctcacat ccgcaaccaa tcctgacaag gagaactcaa tgtccatttc catcctgctg
    1561 gacaattact gtcaccccat agctttgcct aagcaccggc ccacccctga cccagaggga
    1621 gacagggttc gggctgaaat gcccaatcag cttcgaaagc aattggaggc gatcatagcc
    1681 acagatccac ttaacccccc cacagcagag gacaaagaat tgctctggca ttttcgatat
    1741 gaaagcctga agcatccgaa ggcttaccct aagctattca gctcagtgaa atgggggcag
    1801 caagaaattg ttgccaaaac gtaccagctg ttagccagaa gggagatctg ggatcaaagt
    1861 gctttggacg ttggcttaac catgcagctc ctggactgca acttttcaga cgagaatgtc
    1921 cgggccattg cagttcagaa actggagagc ttagaggacg atgacgtttt acattacctt
    1981 ctccagctgg tacaggctgt gaaatttgaa ccgtaccacg acagtgcgct ggccagattc
    2041 ctgctgaagc gtggcttgag gaacaaaaga atcggtcact tcttgttctg gttcctgcga
    2101 agtgagatcg cacagtccan acactatcag cagaggttcg ctgtgatcct ggaggcgtac
    2161 ctgcgaggct gtggcacagc catgttgcag gacttcacac agcaggtcca tgtgattgag
    2221 atgttacaga aagtcaccat tgatattaaa tcgctctcgg cagagaagta tgacgtcagt
    2281 tcccaagtta tttcacagct taagcaaaag cttgaaagcc ttcagaactc caatctcccc
    2341 gagagcttta gagttcccta tgatcctgga ctaaaagccg gtaccctggt gatcgagaaa
    2401 tgcaaagtga tggcctccaa gaagaagccc ctgtggcttg agtttaagtg tgctgatccc
    2461 acagtcctat ccaacgaaac cattggaatc atctttaaac atggtgatga tctgcgccaa
    2521 gacatgttga tcttgcagat tctacgcatc atggagtcca tttgggagac tgaatctctg
    2581 gacctgtgcc ttctgcctta cggntgcatc tcaactggtg acaaaatagg aatgatcgag
    2641 attgtaaagg atgccacaac gatcgctcaa attcagcaaa gcacagtggg taacacgggg
    2701 gcattcaaag atgaagtcct gaatcactgg ctcaaggaaa aatgtcctat tgaagaaaag
    2761 tttcaggccg cagtggaaag gtttgtttac tcctgtgcag gctactgtgt ggccacattt
    2821 gttcttggga tcggtgacag gcacaacgac aacattatga tctcagagac aggaaaccta
    2881 tttcatatag acttcggaca cattcttggg aattacaaga gtttcctggg catcaataaa
    2941 gagagagtgc ccttcgtcct aaccccagac tttttggttg tgatgggatc ttctggaaaa
    3001 aagacaagtc cacacttcca gaaattccag gattgctgtg tgtctacttt acagtactat
    3061 ggggatgtct gtgttagagc ttacctagct cttcgccatc acacaaacct gttgatcatc
    3121 ttgttctcca tgatgctgat gacaggaatg ccccagctga caagcaaaga ggacattgaa
    3181 tatatccggg atgccctcac cgtgggaaaa agcgaggagg acgctaagaa atatttcctt
    3241 gatcagatcg aagtctgcag agacaaagga tggactgtgc agtttaactg gttcctacat
    3301 cttgttcttg gcatcaaaca aggagaaaag cactccgctt ga
//
```

Appendix II

P.H. Naccache, S. Levasseur, G. Lachance, S. Chakravarti, S.G. Bourgoin and S.R. McColl (2000) Stimulation of Human Neutrophils by Chemotactic Factors Is Associated with the Activation of Phosphatidylinositol 3-Kinase γ*.
Journal of Biological Chemistry, v. 275 (31), pp. 23636-23641, August 2000

AMENDMENT

Cellular Migration and the PI3-kinase family

Preliminary studies using the inhibitors, wortmannin and LY294002 led to a proposed role for the PI3-kinase family in the directed movement of cells. Treatment of cells with these inhibitors resulted in a reduced migratory capacity of a variety of leukocytes, including monocytes and neutrophils, in response to inflammatory stimuli (as reviewed in Rickert *et al.,* 2001). More recently it has been demonstrated that cytoskeletal rearrangement, a process essential for directed cellular migration, is influenced by the production of PI 3,4,5 P_3, the major lipid product of the Class I PI3-kinases (reviewed in Blomberg *et al.,* 1999). Over-expression of PTEN, a phosphatase responsible for the 3-OH dephosphorylation of PI 3,4,5 P_3, in fibroblasts resulted in reduced motility toward inflammatory stimuli (Tamura *et al.,* 1998). Furthermore myeloid cells from PTEN-deficient mice exhibited enhanced motility (Lilental *et al.,* 2000). Work carried out by Sanchez-Madrid and del Pozo in the late 1990's implicated the family of Rho GTPases in the increase of cytoskeletal molecules such as F-actin, at the leading edge of a migrating cell (Sanchez-madrid and del Pozo, 1999). The importance of the Rho GTPase family members, Rac and Cdc42, in cellular motility was demonstrated by the expression of dominant-negative forms of each in macrophage chemotaxis (Allen *et al.,* 1998). Moreover, the importance of PI3-kinase lipid products, particularly PI 3,4,5 P_3, in the stimulation of Rac and Cdc42 was also demonstrated in PTEN-deficient mice (Lilental *et al.,* 2000). It is proposed that the lipid products of PI3-kinases influence the activities of cytoplasmic tyrosine kinases, most likely through the preferential binding of these lipid products to PH domains. In turn specific GDP-GTP exchange factors are activated to influence Rho GTPase activity, and the rearrangement of the cytoskeleton thus affecting the migratory capacity of the cell.

Given that the use of catalytically inactive subunits, of both the Class IA and IB PI3-kinases, has illustrated a resultant defect in the migration of cells (reviewed in Rickert *et al.,* 2001), it is presently unclear as to the specific subfamilies and/or isoforms involved in this particular pathway. In addition, given that both subfamilies of Class I PI3-kinases produce PI 3,4,5 P_3 it is likely that the specificity of signalling lies upstream of these lipid products (eg: receptor ligation). The ability of these lipids to bind to PH domain containing-proteins (Blomberg *et al.,* 1999) has the potential to create a vast repertoire of cytoplasmic binding partners, and hence various signalling cascades downstream of PI3-kinase activation. Although it is presently unclear as to the specific components of the signalling cascade resulting in cell migration, studies using different cell types quite clearly demonstrate the involvement of uniform signalling families such as the PI3-kinases, Rho GTPases and PH domain containing-proteins.